Transmission of bacterial symbionts in the gutless oligochaete *Olavius algarvensis*

Dissertation

zu Erlangung des Grades eines

Doktors der Naturwissenschaften

- Dr. rer. Nat -

dem Fachbereich Biologie / Chemie der

Universität Bremen

vorgelegt von

Mario-Philip Schimak

Bremen

Dezember 2015

SYMBIOMICS

MARIE CURIE ACTIONS

Die vorgelegte Doktorarbeit wurde von Oktober 2011 bis Dezember 2015 in der Abteilung Symbiose am Max Planck Institute für Marine Mikrobiologie in Bremen angefertigt.

Universität Bremen

Max Planck Institute for Marine Microbiology

1. Gutachterin: Prof. Dr. Nicole Dubilier

2. Gutachterin: Prof. Dr. Monika Bright

Tag des Promotionskolloquiums: 27.1.2016

Cover

Front: Multi-labelled fluorescence *in situ* hybridisation (MiL-FISH) of the γ1 symbiont (red) associated to a developing juvenile *Olavius algarvensis* in its cocoon. The symbionts are situated between cuticle and developing epidermal cells (Green).

Back: Simultaneous Multi-labelled fluorescence *in situ* hybridisation (MiL-FISH) of six bacterial strains and one archaea in a mock consortium. Combinatorial labelling of 16S rRNA probes with the three RGB colours red, blue and green creates up to seven colours for simultaneous targeting of organisms (See Chapter III).

“Your pain is the breaking of the shell that encloses your understanding. It is the bitter potion by which the physician within you heals your sick self. Therefore, trust the physician and drink his remedy in silence and tranquillity”

- Khalil Gibran -

“…. dictated but not read …. “

- Steve Zissou -

Table of Contents

Summary

The essential role that symbioses between bacteria and animals play for life on earth has been a major topic of scientific research for the past fifty years. We now understand that eukaryotic life could not have evolved without the intricate influence of bacteria, which impact physiological, metabolic, nutritional, developmental and evolutionary processes in many eukaryotic phlya.
One model system for such associations is the well-studied symbiosis between the gutless oligochaete *Olavius algarvensis*, from the island of Elba, Italy, and its obligate consortium of chemoautotrophic sulphide-oxidizing γ -proteobacteria and sulphate-reducing δ -proteobacteria. The complete nutritional dependency of the host to its symbionts has led to the reduction of the digestive tract and the excretory system. The aim of this thesis is to investigate how this symbiosis is maintained over consecutive generations. In particular I examine whether symbionts are transmitted into the next host generation vertically – by smearing from the parent worm during oviposition, horizontally – by uptake from the environment, or by both these modes. To answer this question further initial investigation of worm ecology and the development of new methods was required as outlined below:

i) A deeper understanding of worm physiology, ecology and the habitat is required in order to determine factors needed for embryos to complete development and, thus, to obtain all relevant developmental stages. For the symbiotic consortium to drive sulphur metabolism both aerobic and anaerobic conditions are required. Additionally carbon monoxide (CO) and hydrogen (H_2) can be utilised in anaerobic conditions. In the environment worms must shuttle between stratified sediment layers to provide these conditions to their symbionts. It was unclear to date if immobile eggs of gutless oligochaetes also require the same conditions for development and if so how these conditions are provided to them. With the use of planar optodes, time lapse photography and newly developed imaging algorithms I aimed to correlate worm distribution in the sediment with chemical gradients in order to gain insight into the conditions required for optimal embryo development. Adult worms actively followed oxic gradients in search for substrate rich zones by chemotaxis. Periodic shuttling between oxic and anoxic sediment layers was observed and high levels of H_2 and CO were tolerated for prolonged periods of time. Overall a chemocline transition zone was found to be favoured, which provides symbionts with both oxygen and reduced substrates that they require.
ii) To clarify the origin and location of symbiont cells as well as their potential influence on host development, identification with phylotype specific markers is needed. Fluorescence *in situ* hybridisation (FISH) targeting the 16S rRNA of bacterial cells was used to achieved this. Current FISH techniques however, presented several challenges in achieving this task. To overcome these work was conducted on the development of a novel multi-labelled FISH (MiL-FISH) technique. Further, an expansion of the method for its applicability to single cell genomics was conducted paving the way future research on gutless oligochaete developmental biology.
iii) The transmission mode itself was determined by stable isotope tracing with ^{15}N. Sexually mature worms were exposed to ^{15}N-ammonium and incubated in

aquaria until eggs were deposited. Any isotope-enriched bacteria found inside the cocoons should therefore originate from the parent worm. MiL-FISH, for cell identification, and nano-scale-secondary-ion-mass-spectrometry (nanoSIMS), for detection of ^{15}N enrichment, were applied in parallel. Results revealed that all symbionts originate from the parent worm and that the main mode of transmission is therefore vertical. As a long-term evolutionary strategy however, I do not however exclude occasional horizontal transmission and use this hypothesis as a basis for in depth discussion at the end of the chapter.

This thesis provides understanding of the roles that bacterial symbionts play for the development and evolution of a metazoan host. We have gained insight into the ecology and distribution of a symbiont regulated animal system and made several methodical advancements on the way.

Zusammenfassung

Symbiosen zwischen Bakterien und Tieren und deren wesentliche Rolle für das Leben auf der Erde sind seit über fünfzig Jahren ein essentielles Thema der naturwissenschaftlichen Forschung. Mittlerweile verstehen wir, dass eukaryotische Organismen ohne den Einfluss von Bakterien sich nicht entwickeln hätten können und dass diese Interaktionen physiologische, metabolische, Nahrungs-, Entwicklungs- und Evolutionsprozesse in vielen Eukaryonten beeinflussen.

Als Modellsystem für solche Interaktionen dient der darmlose Oligochät *Olavius algarvensis*, der gemeinsam mit einem obligaten Konsortium von chemoautotrophen Sulfid-oxidierenden γ-Proteobakterien und Sulfat-reduzierenden δ-Proteobakterien in den marinen Sedimenten vor der Insel Elba, Italien vorkommt. Der Wirt ist für seine Ernährung auf Symbionten angewiesen, was zu einer kompletten Reduktion des Verdauungstraktes und des Ausscheidungssystems geführt hat. Ziel dieser Arbeit ist die Erforschung der Frage, wie eine solche Symbiose über mehrere Generationen aufrechterhalten werden kann. Hierbei untersuche ich die Weitergabe von obligaten chemosynthetischen, Symbionten an die nächste Generation des Wirtes. Dies kann durch vertikale Übertragung der Symbionten, zum Beispiel durch Schmierprozesse vom Muttertier auf das Ei während dessen Ablage, durch horizontale Übertragung in Form der Aufnahme von Bakterien aus der Umwelt, oder durch beide dieser Mechanismen geschehen.

Um die Frage nach dem Transmissionsmechanismus beantworten zu können bedarf es weiterer Einblicke in die Ökologie der Würmer, sowie der Entwicklung neuer Methoden wie nachstehend beschrieben:

i) Um Eier aller relevanten ontogenetischen Stadien zu sammeln und zu kultivieren, ist ein besseres Verständnis des Lebensraums, der Ökologie und der Physiologie des Wurmes waren erforderlich. Das symbiontische Konsortium gewinnt Energie durch Atmen von hoch giftigen Schwefelwasserstoff und Sulfat und benötigt daher sowohl aerobe als auch anaeroben Umweltbedingungen. Zusätzlich kann zur Energiegewinnung auch Kohlenmonoxid (CO) und Wasserstoff (H_2) benutzt werden. Würmer müssen daher zwischen aeroben und anaeroben Sedimentschichten wandern. Es war bislang unklar ob die unbeweglichen Eier der darmlosen Oligochäten die gleichen Bedingungen für ihre Entwicklung brauchen, und wenn ja, wie sie zu diesen Bedingungen kommen. Mit dem Einsatz von Optoden, Zeitraffer-Fotografie und neu entwickelten Bildbearbeitungsalgorithmen konnte ich in das Verhalten und die Verteilung von Würmern anhand von chemischen Gradienten feststellen. Dieser Einblick erlaubt, die optimalen Bedingungen für die Entwicklung der Embryonen zu schaffen. Adulte Würmer folgen aktiv sowohl Sauerstoff als auch chemischen Substratgradienten mittels Chemotaxis. Periodische Pendelbewegungen zwischen oxischen und anoxischen Sedimentschichten wurden beobachtet und hohe Konzentrationen von H_2 und dem toxischen CO wurden für längere Zeit von den Würmern toleriert. Insgesamt wurde die Übergangszone, in der die Symbionten mit Sauerstoff und reduzierten chemischen Substanzen versorgt werden, bevorzugt.

ii) Um die Position und Herkunft der Symbionten, sowie deren Einfluss auf die Wirtsentwicklung zu verstehen, müssen die Bakterien innerhalb des

Wurmkokons mittels artspezifischer Sonden identifiziert und markiert werden. Fluoreszenz-in-situ-Hybridisierung (FISH) wird in vielen biologischen Disziplinen für die Identifikation von Bakterienzellen eingesetzt. Da aktuelle FISH-Techniken jedoch unzureichend für die Analyse der Kokons waren, musste diese Methode weiterentwickelt werden. Das Ergebnis war eine neuartige Mehrfachmarkierte FISH Methode (MiL-FISH) die sämtliche dieser Probleme überwindet. Zusätzlich wurde dieses Verfahren für die Anwendung in Einzelzellengenomanalysen optimiert, um zukünftig weitere Forschung an verschiedenen Entwicklungsbiologischen Stadien der darmlosen Oligochäten durchzuführen.

iii) Der Übertragungsmodus selbst wurde unter Verwendung von stabilen ^{15}N-Isotopen bestimmt. Geschlechtsreife Würmer wurden in Aquarien mit ^{15}N-Ammoniak ausgesetzt und die abgelegten Eier gesammelt. Falls Bakterien in den Kokons ein ^{15}N-Isotop Signal aufweisen, müssten diese daher von dem Muttertier stammen. Mittels MiL-FISH wurden Zellen identifiziert und anschließend mittels nano-skalaren-Sekundärionen-Massenspektrometrie (nanoSIMS) auf ^{15}N-Anreicherung untersucht. Die Ergebnisse zeigten, dass alle Symbionten vom Muttertier stammen und dass daher der Hauptübertragungsweg der Bakterien vertikal ist. Als langfristige Evolutionsstrategie jedoch schließe ich horizontale Übertragung nicht aus und benütze diese Hypothese als Grundlage für weitere theoretische Diskussion am Ende dieses Kapitels.

Die vorliegende Arbeit hat zu unserem Verständnis über die Rollen, die bakterielle Symbionten für die Entwicklung und Evolution eines mehrzelligen Wirtes spielen, beigetragen. Wir haben einen Einblick in die Verbreitung und Ökologie eines durch seine Symbionten regulierten Tieres gewonnen und auf diesen Weg mehrere methodische Fortschritte gemacht.

List of abbreviations

α, γ, δ	alpha, gamma, delta
AprAB	adenylylphosphosulfate (APS) reductase
CARD	catalysed reporter deposition
CBB	Calvin-Benson-Bassham cycle
CO	carbon monoxide
CuAAC	copper(I)-catalysed alkyne-azide cycloaddition
DsrAB	reversely operating sulphite reductase
FA	formamide
FACS	fluorescence activated cell sorting
FISH	fluorescence *in situ* hybridisation
MiL	multi-labelled
PBS	phosphate-buffered saline
PHA	polyhydroxyalkanoate
rRNA	ribosomal ribonucleic acid
Sat	ATP sulfurylase
SEM	scanning electron microscopy
SIMS	secondary ion mass spectrometry
SNP's	single nucleotide polymorphism
TEM	transmission electron microscopy

Chapter I

Introduction

1.1 Symbiosis

Transient or permanent interaction between organisms throughout the biosphere and from all three kingdoms is a necessity for life on earth. These interactions shape ecological and evolutionary processes on individual and population levels and are in sum termed as "Symbiosis" (Gilbert *et al*., 2015).

1.1.1 General definition

The interaction of two reproductively isolated, taxonomically defined organisms, was first described as the general definition of symbiosis by Anton de Bary in 1879 (de Bary, 1879). The word 'symbiosis' originates from Greek and literally means "with" (sym-) "living" (biosis). Although often interpreted as beneficial, the original definition includes beneficial, neutral and detrimental associations termed as "mutualism", "commensalism" and "parasitism", respectively (Sapp, 2010). The use of this definition has broad applicability because the nature of an association between organisms can change over time. For example, a change in environmental condition or resource availability can lead to a shift in the benefit a partner may gain. This can result in once mutualistic associations becoming exploitative parasitic ones (Sapp, 2010). Further, the molecular mechanisms involved in pathogenic infections are in many cases the same as, or similar to, the mechanisms found in the establishment of beneficial symbiosis and it is therefore often difficult to differentiate between the two (Dale and Moran, 2006). Short-term transient associations may be challenging to allocate into one of the three categories

that define symbiosis and the effect of the association on the individual partners involved is often not clear. It has therefore been proposed that symbioses should be defined as "a long-term association of two or more organisms of different species that are integrated at the behavioural, metabolic or genetic level" (Moya *et al*., 2008). This definition will be adopted for the following thesis.

Lynn Margulis termed the association between reproductively isolated individuals over significant proportions of the individuals live history as a "symbiosis" whereby individuals are named "bionts" and the sum of individuals the "holobiont" (Margulis, 1993). The term "holobiont" itself was first coined to describe the "macrobe" and its primary "microbe" symbiont (Mindell, 1992) and later expanded to include all microbial symbionts including viruses (Rohwer *et al*., 2002). In this thesis I differentiate between the partners, the "bionts", by size after Starr (1975) and adopt the nomenclature whereby the larger, taxonomic name-giving organism is termed the "macrobe" and the smaller, on an organisational level lower, the "microbe". Further, the localisation of the associated microbe to the macrobe host is a question of morphology and is for the purpose of this thesis differentiated and defined as follows: an "endosymbiont" is contained within a living host tissue layer within or underneath epithermal cells, either intra- or extra cellular. An "ectosymbiont" lives on the surface epithelium of a host, not contained within a living tissue layer, and often in host mucus, this includes body cavities and the digestive tract.

1.1.2 Mutualism: Partner cost and benefits

The terms mutualism, commensalism and parasitism have their roots in economics and describe the perceived benefit or harm between two or more partners in a give-and-take relationship (Gordon *et al*., 2010). Indeed, evolutionary biologists have long puzzled over how cooperation between species can be viable in the long term. Darwin already noted that a trait that solely benefits one species cannot be favoured in the other, as it will be removed by deleterious natural selection over time (Sachs *et al*., 2004). Within the holobiont definition, a macrobe is simply one of many individual partners that comprise the functional unit – the holobiont. Each of the partners must benefit the "greater good" and find an equilibrium to the cost / benefit they contribute. If the cost outweighs the benefit offered, a partner will be termed as parasitic and be faced with the possible consequence of exclusion from the holobiont unless mechanisms are in place to prevent this (i.e. (Sachs *et al*., 2010)). The maintenance of prevention mechanisms however also costs energy and cooperation is therefore likely to be a viable, energetically "cheaper", strategy than parasitism in the long term.

To unify both partner strategies for the maintenance of any given holobiont system, I have coined the phrase "Cooperate or (be) eliminate(ed)!". From the macrobe's perspective "cooperate or be eliminated" is applicable for any given microbe partner that costs more than it supplies to the system. From the microbes perspective "cooperate or eliminate" applies, because either a strategy of mutualism or parasitism can be employed in an association.

To help resolve the paradox that cooperative behaviour poses for evolutionary theory much attention has been given to economic market theory and its applicability to biological systems in recent years (i.e. (Tasoff *et al.,* 2015) (Werner *et al.,* 2014) (Johnstone and Bshary, 2002). In the following thesis I will consider the economic market

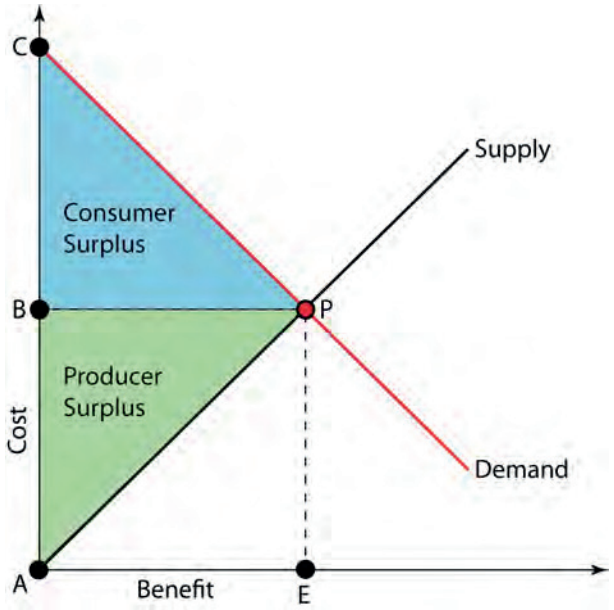

Figure 1: Mutualistic interactions explained along an economic cost / benefit model of supply and demand, which determines the price of goods (Marshall, 1898). This price will vary, due to market competition, until equilibrium is found in which the demand equals the supply (P). In any trade association, the amount an organism actually pays (B) for benefits gained (E) is given by the area B, P, E, A. The maximum cost an organism is potentially willing to pay is given by (C). There is a net benefit gain because the actual cost is less than the organism can potentially afford to pay i.e. the area C, P, E, A is larger than B, P, E, A. In economics this area is defined as "consumer surplus" and is defined as the total benefit minus the amount spent (C, P, E, A - B, P, E, A = C, P, B) This represents the surplus of resources not invested by the consumer which still yield the same benefit gained. "Producer surplus" (P, A, B) is the benefit to the supplier of a resource defined by selling at a price higher than the minimum cost of production (A). This is equal to profit gained thought the trade interaction. Market equilibrium (P), in the context of mutualistic association, can be further explained by use of the Pareto-optimal model (Figure 2).

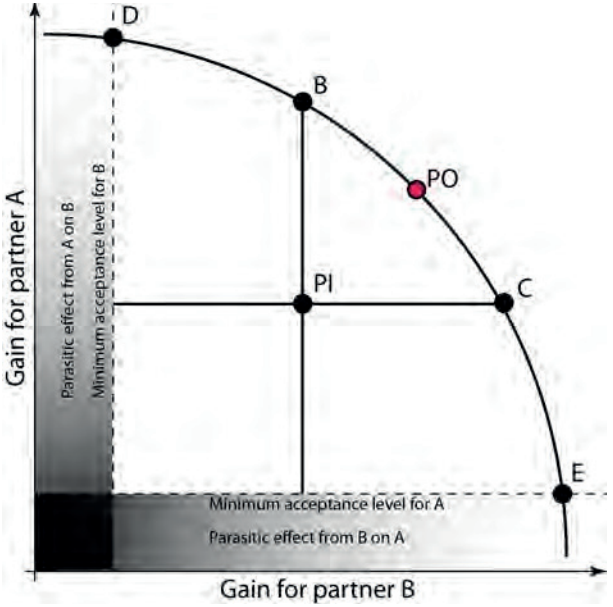

Figure 2: The Pareto-optimal (PO) may be used to explain resource distribution between organisms and is defined as the point at which any redistribution of resources beneficial for one organism will have negative effect on another organism in the trade association. At PO the gain for both partners is equal. The point PI is a Pareto-inefficiency whereby Pareto-improvements can still be made to benefit both partners without negative effect to any one individual. Points B and C are slightly detrimental for one of the two partners but still within an acceptable boundary because a small loss of benefit can be buffered before fitness is affected negatively. Points D and E are the limit off acceptance for a loss of gain. Bellow this point an organism can be seen as exploitative or even parasitic towards another individual in the association. If this is the case the definition of mutualism is no longer applicable for a trade association.

theory framework as the basis for mutualistic symbiotic interaction and apply its concept to the evolutionary implications that it may have for the symbiotic system presented in this study.

The economic market framework is a useful tool to explain evolutionary dynamics between organisms by characterising investment of partners in an association (Werner *et al*., 2014): if both partners have a choice in cooperation then trade (leverage) outweighs the benefits gained over force (coercion), by beneficially controlling the level of influence on fitness that partners have on each other. Indeed, it was stated that one of the mayor variables in any mutualistic association is the degree to which fitness is controlled for either partner. In the long term the control of fitness has big implications for the evolution, ecology and development of both partners and can be generalised in a basic economic cost / benefit model (Figure 1). For long term functioning of an association between two or more organisms, the value of goods and services rendered must remain high enough if refrainment of trade is to be avoided. The level of benefit for any given partner may vary over time, e.g. with change in environmental conditions or resource availability. In a world of constantly changing conditions the maintenance of mutualistic viability is therefore dependant on inter-changeability of partners. If, however, conditions can be kept stable, as for example a microbe in an intracellular endosymbiosis, inter-changeability of partners falls redundant and the symbiosis between two partners is permanently established and may become obligate (e.g. the endosymbiosis theory). Six market model strategies have been reported to be of fundamental importance for maintenance of mutualistic associations (Table 1). These strategies are interchangeable and several may be adopted simultaneously in any association. I propose that the number of strategies applicable to any given association can be used as a proxy for the strength of the mutualistic relationship. For example, the association between a client fish and a

cleaner wrasse is not obligate for either of the partners and strategies one, two and three apply (see Table 1). The association between the gutless deep-sea giant tubeworm *Riftia pachyptila* and intracellular sulphur-oxidising symbionts is essential for the host and strategies one to six apply (i.e. (Felbeck, 1981; Robidart *et al.,* 2008). Further, it must be noted that organisms act in self-interest, to benefit themselves, and not to serve the market for the greater good.

Table 1: Adapted from Werner 2014 (Werner *et al.,* 2014). The table lists strategies employed by symbiotic partners for the maintenance of mutualistic associations.

Strategy	Effect	Biological example	Reference
Avoid bad trading partners	Will reduce the cost for services rendered	Switching of cleaner fish if cheating events increase	(Bshary and Grutter, 2002)
Building local business ties	The environment determines with whom to trade	Aggregation between hydrogen-fermenters and methanogens	(Wintermute and Silver, 2010)
Diversify or specialise	Diversification reduces costs if a particular commodity becomes limited	Actinobacteria protect the nutrition source of leaf-cutter ants and ants themselves from pathogenic fungus by production of antibiotics	(Little *et al.*, 2006) (Mattoso *et al.*, 2012)
Become indispensible	Providing a vital function but restricting choice in attaining it elsewhere results in a high market value and is rewarded with high benefit	Endosymbiotic associations i.e. cysteine synthesis capability in lost by corals. Symbionts fulfil this function	(Shinzato *et al.*, 2011)
Saving for a rainy day	Storage of a commodity will in times of scarcity increase its value to the trading partner	Mycorrhizal fungus store phosphorus in an inaccessible form to the plant host releasing it only when soil nutrient levels sink	(Kiers *et al.*, 2011)
Eliminate the competition	Elimination or outcompeting of other organisms capable of establishing a mutualistic association with one of the two primary partners	Toxins produced by bacteria to inhibit other strains competing for a resource	(Cascales *et al.,* 2007)

There is no intent in evolution and it has been postulated by theoretical population biologists that mutualism evolved from parasitism, over commensalism, due to the self interest of a pathogen to reduce its virulence and not to kill its host, therefore ensuring its own survival (Yamamura, 1993). It is therefore plausible that mutualistic associations between partners in a naturally changing environment are a function of the Pareto-optimal (Figure 2). That is, any reallocation of resources (or benefits) by one individual will negatively influence another individual in a trade association. Indeed, I postulate that this concept is applicable to all symbiotic associations which is for example especially well demonstrated in the resource management strategies between plants and mycorrhizal fungi (Kiers *et al.,* 2011). Here, fungi ensure cooperative behaviour toward plans by offering more nutrients only if rewarded with an increase in carbohydrates (i.e. moving from PI to PO on a Pareto-optimal curve).

1.1.3 Mutualism as a driving force in evolution

Mutualistic interactions drive the evolution of all partners involved. Through beneficial interaction each partner in an association gains selective advantages over their individual parts. This concept is for example emphasised well with the hydrogen hypothesis postulated by William F. Martin and Miklos Müller in 1998 (Martin and Muller, 1998). Based on Lynn Margulis endosymbiont hypothesis, which states that mitochondria and plastids originate from free living bacteria that fused with a primitive eukaryotic cell to build the first eukaryotes (Margulis, 1970), the hydrogen hypothesis states that the host which acquired the prokaryote was in itself a hydrogen dependant archaeon which makes use of hydrogen (H_2) and carbon dioxide (CO_2) for methane (CH_4) production ($4H_2 + CO_2 \rightarrow CH_4 + 2H_2O$). Indeed this metabolic pathway is still found today in methanogenic archaea. The prokaryote destined to become the mitochondrion or

plastid was a facultative anaerobe producing hydrogen and carbon dioxide as waste products during anaerobic respiration ($CH_4 + 2H_2O \rightarrow 4H_2 + CO_2$). Unlike the original endosymbiont hypothesis, the hydrogen hypothesis excludes the possibility for the existence of a primitive eukaryotic cell lacking mitochondria. Based on this idea it can be said that the third branch in the tree of life, the eukaryotes, came into existence as a by-product of a mutualistic symbiotic nutritional dependant association between members of the other two branches on the tree of life, the bacteria and the archaea. This idea bases its foundation in market theory as discussed in 1.1.2 and emphasises nutritionally dependent mutualism as a driving force in the evolution of multicellular life on earth.

Mutualistic interactions can also result in congruent evolution (co-speciation) for both symbiotic partners and seems to be restricted to obligate mutualists, with the oldest known example being ~ 500 million years old (Gruber-Vodicka 2011). In an ecological sense, a mutualistic holobiont may show a high degree of plasticity by adapting to environmental change and exploiting novel resources when and if they become available. This is made possible by the exploitation of novel metabolic pathways and physical or behavioural adaptations that would otherwise not be available to the individual parts. Further, optimal adaptation of the macrobe to new environmental conditions or a newly available resource can be made possible by exchange of microbe partners and / or by reorganising the relative abundance of these partners (Gordon *et al*., 2010). This will result in an increase of fitness for both partners due to the adaptive capability of the holobiont. Ultimately, the outcome will be directional selection favouring allele frequency shifts towards the phenotype best adapted to a new condition (Gordon *et al*., 2010). Exploitation of new niches, even on small spatial scales, may result in niche partitioning which in turn can create an "islanding effect" for a sub group of a given population. The resulting spatial reproductive isolation from other members of the

population may over time result in speciation (Brucker and Bordenstein, 2012) (Kiers and West, 2015).

1.1.4 Symbiotic nutrition and metabolism

Although several kinds of symbiotic associations exist, most are nutritionally based, and in particular microbial-animal associations are rooted in nutritional dependency from one partner to the other. Microorganisms can utilise several electron donors for carbon fixation that are unavailable to eukaryotes. Indeed, chemosynthesis, the use of chemical electron donors as energy source for carbon fixation, is a trait solely exploited by bacteria and archaea (refer to Chapter 1.2). Enzymatic redox reactions yield energy by oxidation of electron donors such as hydrogen sulphide (H_2S) or carbon monoxide (CO) by a terminal electron acceptor such as oxygen (O_2) or sulphate (SO_4^{2-}). The reaction is dependent on substrate availability and differences in redox potential to yield energy for the fixation of C_1 molecules such as carbon dioxide (CO_2) or methane (CH_4). Several metabolic pathways are employed for C_1 fixation and include the Calvin-Benson-Bassham (CBB) cycle, the reductive tricarboxylic acid (TCA) cycle, or the reductive acetyl-CoA pathway (Sato and Atomi, 2010). Symbionts therefore present a potential autotrophic nutrient source, which can be exploited by the macrobe host heterotrophically through either active transfer of metabolites ("milking") or herding and digestion of microbial cells ("farming").

1.1.5 Symbiont transmission

For symbiotic associations to persist over consecutive generations, microbial partners must be transmitted to the macrobe host progeny. Two main transmission modes have been described: vertical and horizontal (for review see (Bright and Bulgheresi, 2010) & (Bulgheresi, 2011)).

1) Vertical transmission (Figure 3b): the microbe is passed on directly to the macrobe progeny either through the germline or by contact transfer such as bacterial smearing or ingestion via coprophagia (Serbus *et al*., 2008) (Kaltenpoth, 2009) (Hosokawa *et al*., 2013). In this instance, the macrobe does not experience a free-living aposymbiotic stage, devoid of a symbiotic partner for any prolonged period of time. Transmission through the germline is in most cases maternal, through the female egg. Examples of paternal transmission via male sperm have been documented and most commonly found amongst the viruses. Examples include the cytoplasmic negative sense RNA sigma virus of *Drosophila melanogaster* found in sperm cells which causes the death of an infected host after exposure to CO_2 (Fleuruet, 1988). However, paternal transmission rarely stand alone and is most commonly coupled with maternal and / or horizontal transmission modes (Ebert, 2013). Paternal transmission is assumed to be scarce in nature due to the low amount of cytoplasm introduced to the zygote by the much smaller sperm cell. This reduces the number of virulent factors passed on to the zygote which can be measured by a low rate of infection in the next generation when compared to viral transmission through eggs (Longdon and Jiggins, 2010).

Strict vertical transmission can be regarded as a closed system for the microbe partner as it is not exposed to the environment for any prolonged period of time. This is especially true for many obligate intracellular symbionts, which show genomic traits for adaptation to a lifestyle entirely dependent on their macrobe host. These genomic alterations result from continuous bottlenecking of the microbe population over many generations and include; a reduction in genome size, as many genes for "free-living" are no longer required (< 1 Mbp) and a high AT bias (> 70% AT), hypothesised to be due to DNA repair mechanisms falling redundant (Moran and Wernegreen, 2000), (Moran *et al*., 2008), (Moya *et al*., 2008), (Moran *et al*., 2009), (Van Leuven and McCutcheon, 2012).

In addition a high degree of transposable elements is sometimes present in symbionts that "have recently transitioned or are transitioning to an obligate, host-associated lifestyle." (Kleiner *et al*., 2013). Generally it can be said that strict vertical transmission modes are quite rare and limited to only a few invertebrate taxa. Fine, 1975, noted that vertical transmission must be beneficial to the host, otherwise the host line, on which symbionts rely obligatorily, would be outcompeted by uninfected hosts (Fine, 1975).

In a population ecology context the rate of vertical transmission is only partially coupled with host population densities. With high population densities, reproductive potential for an individual increases, however, transmission rates depend on reproductive success and this can only be increased if the symbiotic association has a positive influence on fitness in an individual ensuring a higher number of infection events (Lipsitch *et al*., 1996).

2) Horizontal transmission (Figure 3a): an initially aposymbiotic macrobe host is infected by facultatively free-living symbionts, which are taken up from the environment by each host generation anew. The above-mentioned genomic characteristics, such as genome reduction, are most commonly not observed in symbionts with strict horizontal transmission because genomes must encoded the potential for life in a diverse environment. Exceptions have however been noted and include the reduced genomes of methane oxidising symbionts in *Bathymodiolus* mussels (Paul Antony Chakkiath - personal communication). Albeit the potential is given for pathogens or "cheaters" to exploit horizontal transmission modes, associations are very specific and selection of the viable symbiont from the environmental microbiome is crucial for the maintenance of the symbioses. Examples of specific environmental symbiont uptake include the *Euprymna scolopes* and *Vibrio fischeri* symbiotic system (Nyholm and McFall-Ngai, 2004) Here, the host selects strains of *V. fischeri* for colonisation of its light organ from the available

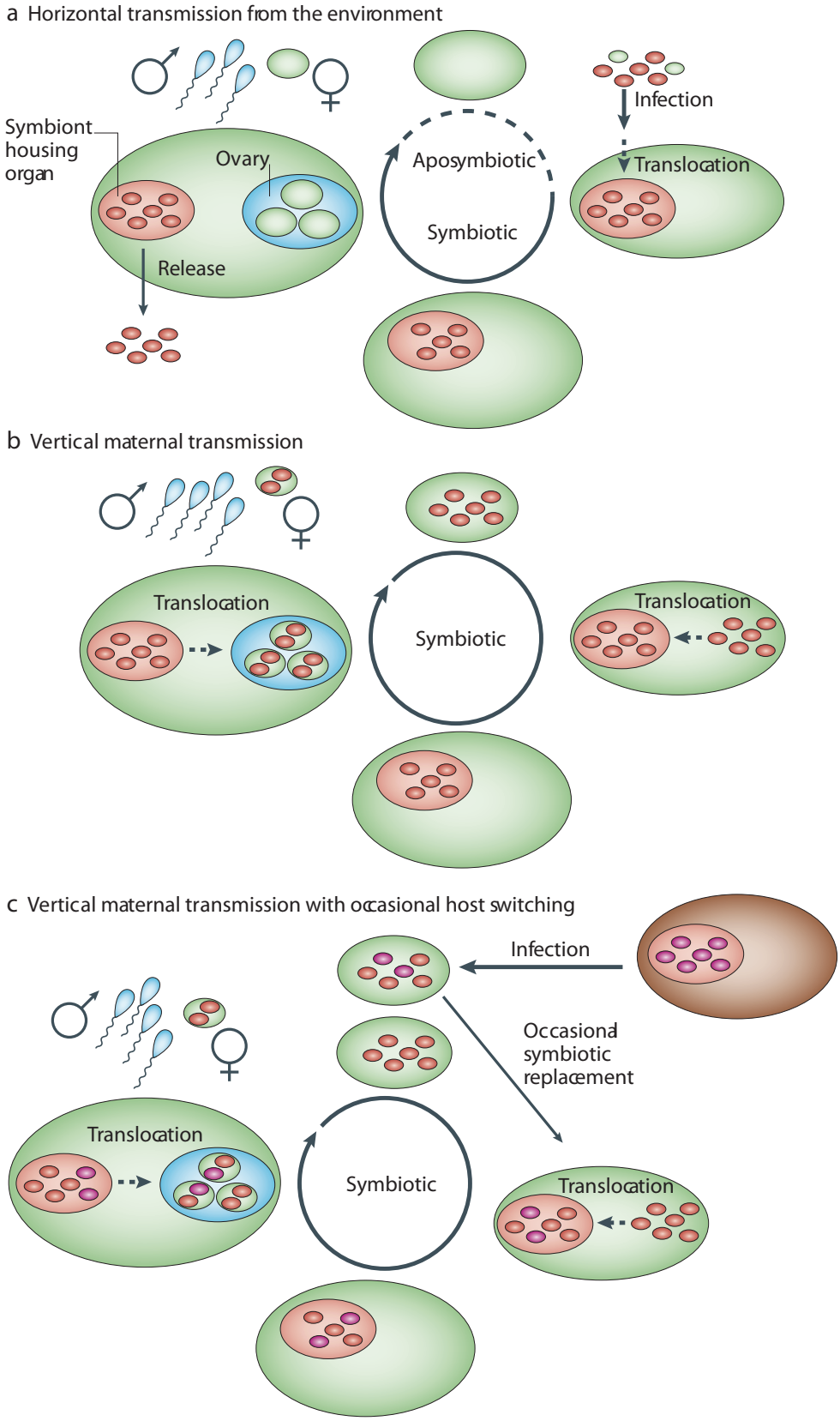

Figure 3 – Schematic depicting a) horizontal, b) vertical and c) mixed transmission modes. Taken from Bright & Bulgheresi 2010. (Bright and Bulgheresi, 2010)

environmental microbiome.

In other systems such as the marine nematode *Laxus oneistus* highly specific protein-lectin recognition systems have been shown to play an important role for the establishment of the symbiosis (e.g. (Bulgheresi *et al*., 2006)). Additionally, a macrobe host can serve as a "brood chamber" for the microbe by providing a stable environment in which proliferation rates increase due to a decrease in competition from the environment. This brings with it selective advantages over obligate free-living microbes. Upon release from the host a re-inoculation of the free-living microbial population is given and has been demonstrated a number of times in the marine system (Nyholm and McFall-Ngai, 2004; Klose *et al*., 2015). Horizontal transmission increases with host population density because a higher rate of potential transmission events are possible (Lipsitch *et al*., 1995).

3) Mixed transmission modes (Figure 3c): a combination of both vertical and horizontal transmission modes whereby a macrobe host takes up microbes from parents as well the environment. For a microbe, mixed transmission is given through the capability to infer an infection through the germline which produces secondary infections even if not in the same host individual (Ebert, 2013). For example, *Toxoplasma gondii* can infect a host by one of three physical routes namely oral uptake of oocytes, carnivory of an infected host and / or maternal infection. Although a number of transmission routes are given for *T. gondii*, which should potentially result in higher infection rates, this particular strategy is not viable in the long term, because maternal vertical transmission will result in death of the offspring before horizontal infection of another host can take place. This brings with it a self-inflicted, antagonistic, reduction of fitness for *T. gondii* caused by a mixed transmission mode. Population density dependant transmission is positively influenced by adoption of a mixed transmission mode. Microbe persistence can be achieved by vertical transmission in low host density populations or even nomadic

species – such as early human hunter-gatherer societies – as well as prevalence through high infection rates by horizontal transmission when host density is high (Ebert, 2013) (i.e. (Dobson and Carper, 1996))

1.1.6 Symbiont influence on host reproductive biology

It has become apparent in recent years that the success of developmental processes for many animal species depends on the presence and activity of symbiotic microbial partners (McFall-Ngai, 2002). Traditionally development was seen as a self-contained, well-regulated program, tightly controlled by specific gene expression at various embryonic stages. Hamdoun & Epel 2007 elegantly reviewed that early development is indeed very robust and has a large buffer to external disturbances such as temperature changes, UV radiation, free radicals, oxygen availability and teratogens (Hamdoun and Epel, 2007). After initial resistance, prolonged exposure to intolerable levels of these disturbances can lead to (a) embryonic diapause, until conditions become favourable, (b) alternate developmental pathways, often resulting in phenotypic plasticity, or (c) death of the embryo (Figure 4). As proposed by McFall-Ngai and Gilbert, eukaryotes evolved in the presence of bacteria which must therefore be considered a permanent environmental factor potentially influencing developmental processes accordingly (Gilbert, 2001), (McFall-Ngai, 2002), (Fraune and Thomas C G Bosch, 2010), (Gilbert, 2012), (McFall-Ngai and Hadfield, 2013). Not only the presence of pathogens but also the absence of beneficial bacteria or changes in the specific composition of an associated bacterial community can potentially have an effect on the developing embryo. Indeed, as reviewed by Gilbert 2012, the early association of microbes to all metazoans questions the concept of “individuality”. There are no sterile animals and bacteria are often required to complete specific metabolic pathways, developmental processes, offer selectable genetic variation for natural selection and are

required for the development of the immune system (Gilbert *et al*., 2012). In light of this, developmental biologists have started to consider bacteria as an ecological factor driving differential gene expression at specific embryonic stages, thus influencing the developmental program itself and ultimately determining phenotypes (Gilbert *et al*., 2015).

The roles that bacteria play in development vary greatly and can be considered as both beneficial and parasitic but rarely neutral. Beneficial roles include the example of the solitary digger wasp genus *Philanthus,* which is in symbiosis with an Actinobacterium that is smeared from specialised glands in the adult's antenna onto freshly lain eggs (Kaltenpoth, 2009). The bacteria protect cocoons from fungal and environmental bacterial infection by presumably producing antibiotics (Kaltenpoth *et al*., 2005). In the cnidarian *Hydra sp.* it is argued that the innate immune system, containing host specific antimicrobial peptides and pattern recognition receptors, is responsible for the control of the resident beneficial microbial population, which in turn initiates developmental processes such as stem cell transcription via environmental cues (TCG Bosch, 2014). Further, the bacterial strain *Pseudoalteromonas luteoviolacea* has been shown to dictate larval settlement and metamorphosis of the polychaete *Hydroides elegans.* Here, it was found that four genes related to cell adhesion and bacterial secretion systems are responsible for metamorphosis of larvae (Hadfield, 2011) & (Huang *et al*., 2012).

Some microbes involved in the developmental processes may have both beneficial and parasitic effects, depending on the host that they occupy. This is highlighted well by example of the maternally transmitted reproductive parasite *Wolbachia* found in many arthropods and some crustaceans. Generally the bacteria control maternal transmission and infection by feminisation of males, male liquidation or clonal production of females to distort sex ratios in a population towards the female. This ensures higher vertical

transmission rates at a cost to the host population and as such is considered parasitic (Rigaud *et al*., 2001) (McFall-Ngai, 2002). Alternatively, the removal of *Wolbachia* in the parasitic wasp *Asobara tabida,* by anti-biotic treatment, resulted in females no longer being able to produce mature oocytes. The inclination is, that the symbiont is required for the proper development of host embryos and therefore has a beneficial effect on the wasps development through its presence (Dedeine *et al*., 2001).

Protective, communicative and parasitic roles of associated bacteria in the development of metazoans have been described above. In some cases, however, fundamental morphological and invasive bauplan alterations are a direct result of symbiont activity. For example, the deep-sea vestimentiferan polychaete tubeworm *Riftia pachyptila* undergoes massive visceral mesoderm apoptosis after infection by its obligate symbionts during its larval stage. With this, the basic bauplan of the polychaete worm is altered as the specialised symbiont housing organ, the trophosome, develops (Nussbaumer *et al*., 2006).

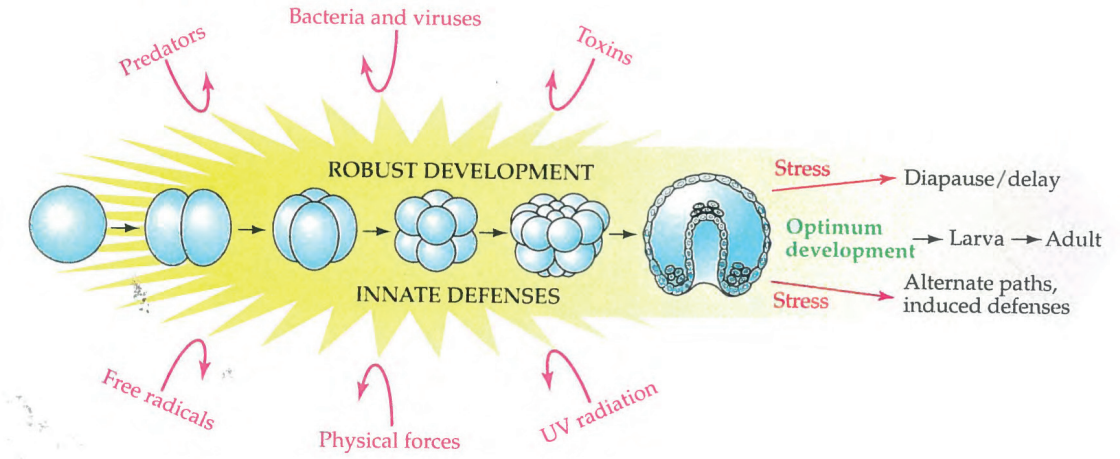

Figure 4: Taken from Gilbert & Epel - Ecological Developmental Biology 1st Edition. Early development to the blastula stage is highly resistant to many environmental disturbance factors such as toxins, UV radiation and bacteria or viruses. If conditions for optimal development are not give then an embryo may enter diapause or adopt alternative developmental pathways often resulting in phenotypic plasticity (Gilbert and Epel, 2009).

1.2 Marine chemosynthetic symbiosis

1.2.1 Discovery, definition and habitat

The Ukrainian microbiologist Sergei Nikolaevich Vinogradskii first defined the process of chemosynthesis in 1890 as the fixation of carbon by oxidation of chemical compounds as energy source. However, only in 1977 did scientists discover its large-scale implications for life on earth with the discovery of the hydrothermal vent systems and the associated macrofauna that these systems support. Analysis of the animals from hydrothermal vents revealed that a large proportion of the invertebrate species found are in symbiosis with chemoautotrophic sulphur oxidising bacteria, which also occur in the surrounding vent fluid in dense numbers (Cavanaugh *et al*., 1981) (Felbeck, 1981) (Jannasch *et al*., 1971) (Ruby *et al*., 1981). Scientists quickly discovered that many other marine invertebrates also harbour chemoautotrophic bacterial symbionts. To date at least seven animal phyla have been described to live in chemosynthetic symbiosis with proteobacterial symbionts (Dubilier *et al*., 2008).

Associations between chemosynthetic bacteria and invertebrate animal hosts are indeed found in almost all reduced marine habitats on earth and include marshes, mangrove sediments, sea grass sediments, coral reef sediments, continental slopes, whale falls, cold seeps and mud volcanoes. The communality of all these habitats is the free availability of reduced compounds as electron donor, which includes a variety of sulphide species (H_2S, HS^- and S^{2-}), carbon monoxide (CO), hydrogen (H_2), methane (CH_4) and ammonia (NH_3) amongst others. Reduced sediments are characterised by aerobic oxygenated top layers and anaerobic reduced bottom layers between which a redox potential discontinuity (RPD) is given. Meio- and infauna in association with chemoautotrophic symbionts such as ciliates, nematodes, oligochaetes and clams, as well as some free living chemosynthetic bacteria such as *Beggiatoa sp.* (i.e. (Schwedt *et al*.,

2011)), reside in the RPD layer and gain simultaneous access to both electron donors and acceptors. In aerobic sediment layers oxygen is used as terminal electron acceptor, which does not necessarily yield more energy per reaction than the use of electron acceptors during anaerobic respiration such as nitrate (NO_3^-) or sulphate (SO_4^{2-}) (Wentrup, 2012).

Hydrothermal vent, cold seep, and mud volcano communities rely on hot fluids or diffuse flow to provide sulphide or methane as electron donors whilst oxygen is used as a terminal electron acceptor from the surrounding seawater. In contrast to popular believe, these systems are therefore not totally independent of photosynthetic primary production because most oxygen in seawater originates from euphotic zones.

Whale falls and sunken wood can also support chemosynthetic symbiotic communities for short time periods by the release of sulphide as they decay. This attracts several specialised organisms, such as *Osedax* or *Sclerolinum,* which have adapted to an opportunistic lifestyle.

1.3 The gutless oligochaetes – symbiosis with a chemosynthetic consortium

1.3.1 Host phylogeny

The annelid subfamily Phallodrilinae (Clitellata, Tubificidae) is comprised of 36 genera and to date a total of 453 known species (Source: http://www.marinespecies.org/). In this study I will focus on two monophyletic genera within the Phallodrilinae, the paraphyletic genus *Olavius,* comprised of 63 known species, and the monophyletic genus *Inanidrilus*, consisting of 26 known species, together commonly termed as the "gutless oligochaetes" (Nylander *et al.,* 1999).

1.3.2 Distribution

Gutless oligochaetes are distributed worldwide from ~ 45° N to ~ 45° S and inhabit reduced siliceous and calcareous sediments from tropical to temperate zones. Most commonly worms are found in shallow water sediments, associated to coral reefs or sea grass meadows, with the exception of a few species discovered on the Peruvian and Californian continental slope at a maximum water depth of ~ 600 m (Ftnogenova, 1986) & (Erseus, 1991). Although no comparative ecological study has targeted worm distribution directly, available data from two species may indicate variance in worm abundance according to latitudes and the corresponding primary production rates that determine nutrient availability. *Inanidrilus leukodermatus* from highly sulphidic nutrient rich coral sediments around Bermuda (32.3° N), in the Sargasso Sea, may be found in abundance of ~ 80,000 individuals per square meter (Giere *et al*., 1982). Mediterranean worms from low sulphide sediments around the island of Elba (42.7° N) in the Tyrrhenian Sea occur in abundances of ~ 25,000 individuals per square meter (C. Lott, unpublished data). Worms are found in both oxic and anoxic sediment zones with the majority occurring in the RPD layer between the two (Giere *et al*., 1991). It was

postulated that worms shuttle between oxic and anoxic zones to supply themselves with oxygen and their symbionts with the conditions and substrates they require to drive their metabolism.

1.3.3 Physiological and metabolic aspects of the *Olavius algarvensis* holobiont

The discovery that gutless Phallodrilinae live in symbiosis with bacteria dates back to 1979 (Erséus, 1979) and coincides with the discovery of chemosynthetic ecosystems in the deep sea. Most morphologically defined species of *Olavius* and *Inanidrilus* live in symbiosis with a consortium of chemoautotrophic bacteria situated under the worms cuticle (Felbeck *et al*., 1983). To date, all worms analysed were found to carry a primary sulphur-oxidising γ-proteobacterial symbiont (γ1 symbiont) belonging to the *Candidatus* Thiosymbion clade (Gruber-Vodicka in prep.), with only one exception - *Inanidrilus exumae* (Bergin, 2009) whose primary γ–symbiont falls into a different clade within the γ-proteobacteria. The characteristic white colour of the worms originates from sulphur globules and polyhydroxyalkanoate (PHA) storage vesicles contained within the highly abundant primary γ1 symbionts. Sulphur storage is built up in anoxic sediment layers and oxidised when worms move into aerobic zones by several pathways including DsrAB, AprAB and Sat (for review see (Dahl *et al.,* 2008)). Oxidation of sulphur storage compounds becomes apparent by discolouration of worms from white to translucent when kept in aerobic conditions. CO_2 fixation in the γ1 symbionts follows the Calvin-Benson-Bassham cycle (CBB) via reduced sulphur as electron donor.

Other, secondary, members of the consortium are transient throughout the genera and include members of the *Alpha -, Gamma -, Deltaproteobacteria* and the *Spirochaetes*. A range of metabolic capabilities are covered by secondary symbionts including sulphur oxidation, sulphate reduction, carbon monoxide oxidation and hydrogen oxidation (Dubilier *et al*., 2001), (Woyke *et al*., 2006), (Kleiner *et al*., 2012), (Kleiner *et al*., 2015).

Of particular interest is the well studied symbiotic system of *Olavius algarvensis* from the Mediterranean sea which displays syntrophic cycling of sulphur species between sulphur oxidising γ-proteobacteria and sulphate reducing δ-proteobacterial symbionts (Dubilier *et al*., 2001). In addition, two studies have recently found the potential for symbionts to utilise carbon monoxide (CO) and hydrogen (H_2) as further electron donors (Kleiner *et al.,* 2012) (Kleiner *et al.,* 2015) (see Chapter II of this thesis). Symbionts are in a mutualistic association with their host, as well as with each other, and all six strategies for the maintenance of such associations apply (Chapter 1.1.2 – Table 1). The association actively contributes to the fitness of the holobiont by offering metabolic pathways for the exploitation of sulphide poor habitats and through recycling of sulphur species between symbionts (see Chapter II – Figure 1). How carbon fixed by symbionts is transferred to the host is still not clear and topic of current research. Either, "milking" of symbionts, by direct transfer of carbohydrates to the host, or "farming" by, lysis of symbiont cells through phago – or pinocytosis, is plausible. Indeed transmission electron microscope images have revealed degraded bacterial cells in lysosomes of host epidermal cells (N. Leisch & J. Wippler unpublished data). Unique to the gutless oligochaetes amongst annelids is the reduction of the waste disposal organs – the nephridia. This poses the obvious question of how host produced waste products are removed from the holobiont. Growing evidence suggests that symbionts have replaced the function of the worms excretory organs by uptake and metabolises of nitrogenous (i.e. urea and ammonium) and non-nitrogenous waste products (i.e. acetate and propionate) (Woyke *et al*., 2006) (Kleiner *et al.,* 2012).

1.3.4 Habitat and ecology – biotic and abiotic

Olavius algarvensis inhabits shallow water Mediterranean sediments and has to date been found in the Portuguese Algarve (Giere and Erseus, 1998), the Island of Elba, Italy (Giere and Erseus, 2002), and the close situated island of Pianosa (42°34'04.6"N 10°05'28.6"E) (C. Lott, unpublished data) (Figure 5). Worms in this study originate from the bay of Sant' Andrea on Elba, from 6-8 meter water depth (42°48'30.0"N 10°08'34.5"E). However, recently worms were found in several other locations on the island including the Bay of Cavoli (42°44'10.0"N 10°11'13.7"E) characterised by large exposed seagrass rhizome mats and in the Bay of Pomonte (42°44'37.0"N 10°07'10.2"E), characterised by methane seepage from the sea floor. At all sites worms are commonly found associated to *Posidonia oceanica* (Linnaeus, 1813) seagrass meadows. Additionally, three further gutless oligochaete species co-occur in these sediments, *Olavius ilvae* (Giere and Erseus, 2002) and two, as of yet, unnamed species (Wentrup *et al*., in prep).

Siliceous sediments of 713 µm median grain size (Nemecky, 2008) and with 0.42 (ϕ) porosity (Kleiner, 2012) around the island of Elba are oligotrophic with low nutrient input and low sulphide concentration measuring a maximum 0.55 µM in 15cm sediment depth. Hydrogen concentration in the sediment were surprisingly high between 438 – 2147 nM compared to < 10 nM for other oligotrophic sediments and < 60 nM for marine sediments in general. Carbon monoxide (CO) concentration was measured at 17 – 51 nM (Kleiner *et al*., 2012) (Kleiner *et al*., 2015). The chemical composition of sediments from the island of Elba therefore provides a large additional nutrient source for the chemosynthetic consortium of *O. algarvensis.* This in turn results in high selection pressure for the holobiont to retain CO and H_2 oxidation pathways for the utilisation of the available substrates.

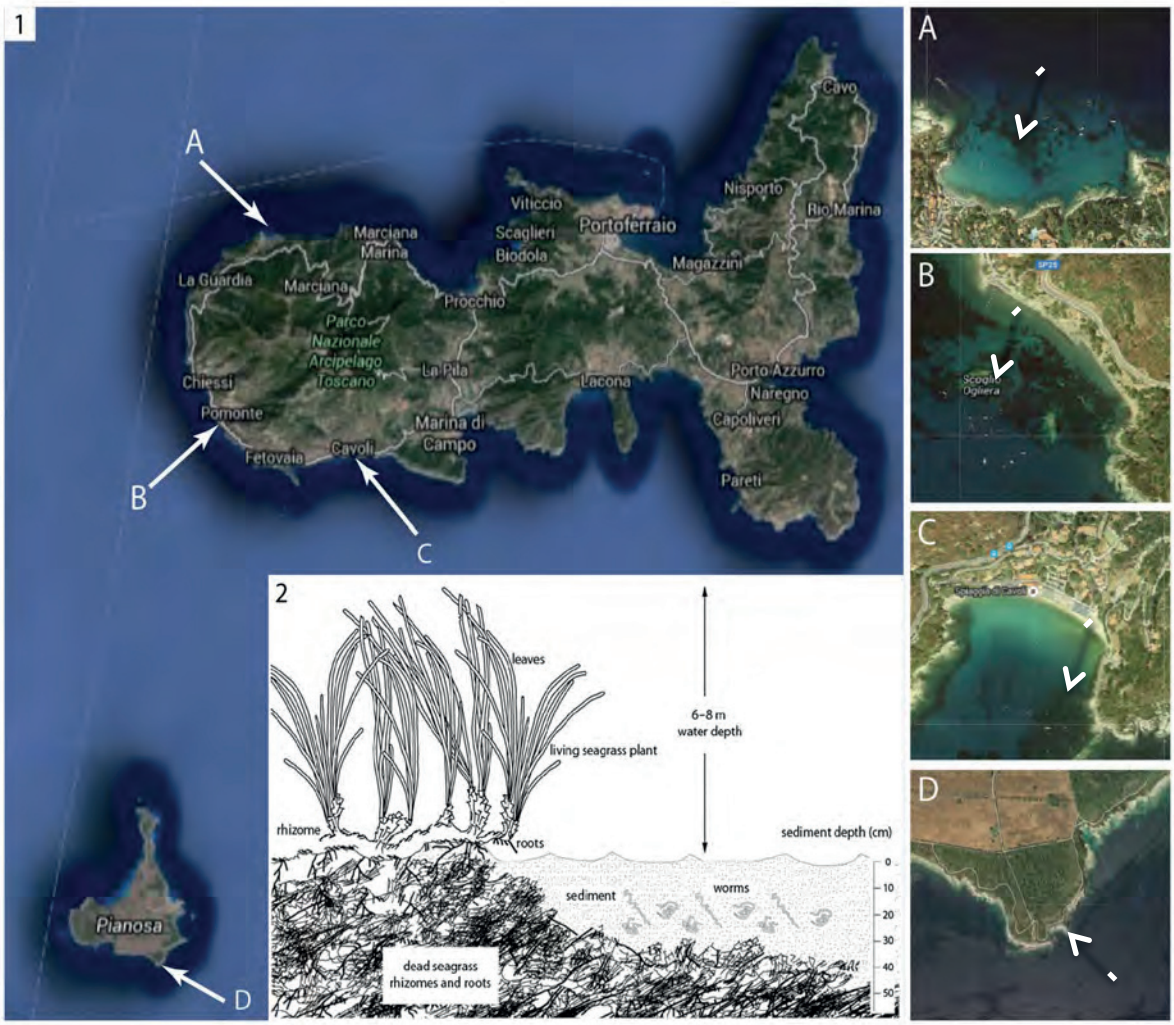

Figure 5: The island of Elba and Pianosa, Italy, where *O. algarvensis* naturally occurs. A) the bay of Sant' Andrea from which worms used in this study were collected. B) the bay of Pomonte, C) the bay of Cavoli and D) the island of Pianosa where worms have also been discovered. Arrows indicate sampling sites. 2) scheme of the underwater habitat of *O. algarvensis* in the bay of Sant' Andrea (taken from Kleiner *et al.,* 2015).

1.3.5 Holobiont morphology

The bauplan of gutless oligochaetes is adapted to life in marine sediments as part of the interstitial meiofaunal community (Figure 6). The segmented worms are between 100 and 300 µm in diameter and up to 4 cm long. As discussed in section 1.3.3, sulphur storage compounds of the primary γ1 symbiont give the worms their distinctive white colour. The anterior of the worm appears translucent because γ1 symbiont abundance is low or missing altogether in this region (A. Gruhl unpublished data).

Oligochaetes are simultaneous hermaphrodites and as such *O. algarvensis* bears both male and female reproductive organs in segment X in segment XI respectively (Figure 8B). Two male pores in segments XI and two female pores in segment XII are situated ventrally. Based on the high degree of morphological variation between species reproductive organs are commonly used as a criteria for taxonomic classification. The clitellum is situated from segment ½ X to segment XII and, like in other oligochaetes, secretes the materials needed for the formation of the egg during oviposition. The eggs themselves are comprised of a cocoon wall, albumen and a membrane bound zygote. The genital pad, a ventral bacteria-filled pouch, lies posterior to the clitellum in segment XII and may vary in appearance between some species. This makes it an additional criterion for morphological identification between species (Figure 6 b & c).

Symbionts are located between the worms cuticle and epidermis posterior to the genital pads and surround the worm for the rest of its length. Annelid cuticle is composed of collagen fibres secreted by epidermal cells and as such is not a living host tissue layer. Based on the definition presented in Chapter 1.1.1 and by strict morphological criteria I do not considered symbionts as endosymbiotic per se. Rather, the cuticle presents a permeable barrier that permanently associates symbionts to their host. The cuticle collagen fibre matrix is permeable for substances up to 70 kDa, (Dubilier *et al.,* 2006) and allows for the passage of substrates required for symbiont metabolism by free diffusion and / or diffusion by current flow produced by worm movement (see Chapter 1.3.3). In contrast to endosymbiotic bacteria located within or underneath host epithelia, symbionts of gutless oligochaetes are freely exposed to size restricted biotic and abiotic environmental factors that do not pass through host cell membrane.

Metagenomic data and clone banks of adult *O. algarvensis* worms have revealed the presence of two γ-proteobacterial phylotypes – γ1 and γ3 - and four δ-proteobacterial

phylotypes – δ1, δ3, δ4 and δ 6 – of which two are generally dominant (δ1 and δ4) (Wippler *et al.,* in prep). Paraformaldehyde fixed specimens measured the primary γ1 symbiont to have a diameter of 2.3 – 3μm, the δ1 symbiont 1 - 1.8 μm and both γ3 and δ4 symbionts 0.9 – 1.2 μm (Ruehland *et al.,* 2008). Symbionts are several orders of magnitude larger than the cuticle pore size and are therefore "trapped" underneath it, presumably for the life history of the host. This makes it highly unlikely that horizontal transmission of environmental symbionts, provided these exist, takes place once the symbiosis has been established.

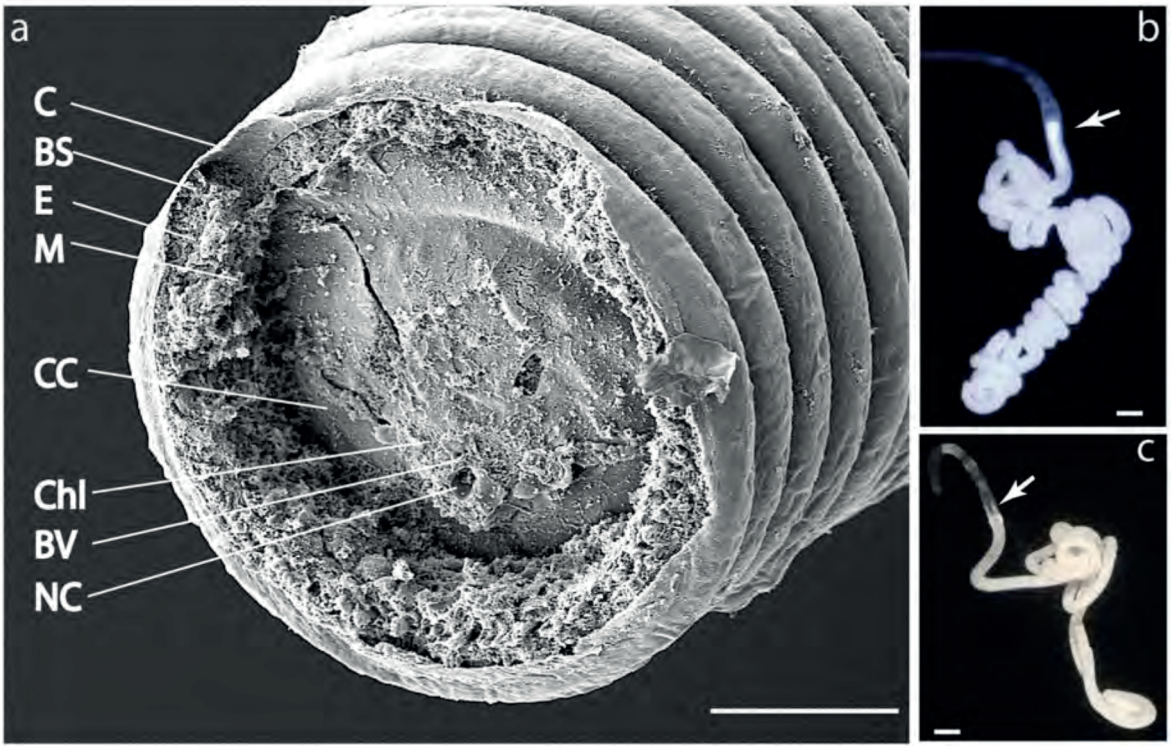

Figure 6: The anatomy of gutless oligochaetes from the island of Elba, Italy. a) scanning electron microscope image of the internal anatomy of *O. algarvensis*. C = cuticle, BS = bacterial symbionts, E = epidermal layer, M = muscle tissue, CC = coelomic cavity, Chl = chloragogen tissue, BV = ventral blood vessel and NC = ventral nerve chord. b) Reproductively mature adult *Olavius algarvensis* individual. Arrow indicates the "diamond" shaped genital pad. Scale bar = 500 μm (image courtesy of A. Gruhl). c) Reproductively mature adult *Olavius ilvae* individual. Arrow indicates a "fork" shaped genital pad. Scale bar = 500 μm.

Lateral and longitudinal muscles situated underneath epidermal cells comprise part of the worm's hydrostatic skeleton. The fluid filled coelom, containing several types

of coelomocytes, comprises the other part of the hydrostatic skeleton (A. Gruhl unpublished data). Enclosed in the coelomic cavity lie the ventral nerve chord, blood vessels of the closed circulatory system and chloragogen tissue. No reminisce of a digestive tract or nephridia have been found to date. Each worm segment is separated by septa through which the nerve chord and blood vessels pass into the adjacent segment.

1.4 Developmental and reproductive biology

1.4.1 Oligochaete development

All oligochaetes are hermaphrodites that cross-fertilise. Much work on development of oligochaetes has been conducted with the common earthworm (*Lubricous*, *Lumbricus terrestris*), which will provide the basis for the following description. Sperm is produced in the testes and released into the coelomic cavity or stored in seminal vesicles (storage sacks) that derive from the septal peritoneum, where they mature. During copulation (Figure 7c) sperm is released from the male posterior paired gonopore whilst simultaneously being received through the anterior spermathecal pores (Figure 7a). The female reproductive system consists of a single pair of ovaries located posterior to the male reproductive system. Ova are released into the coelomic space and in some species stored in an ovisac derived from the septal wall until mature. Next to each ovisac are ciliated funnels that transport the mature ova to the female gonopore. The spermatheca (receptaculum seminis) receives and stores foreign sperm after copulation and can appear in one, two or more pairs. These are located in anterior segments to the ovary and are situated next to the seminal vesicles (Figure 7a).

The clitellum, giving the Class of the Clitellata their name, is a unique glandular tissue that has the appearance of a thick “sleeve” which partially or completely encircles

the worm's body. Its function is to produce materials required for cocoon formation. The clitellum is formed by secretory cells within the epidermis of specific body segments, which may vary between but never within a species and is composed of three types of glandular cells: 1) mucus glands, 2) cells for secretion of cocoon forming material, 3) albumin (plasma proteins – egg white) secreting cells (Figure 7b). Several hours to a few days after copulation a sheet of mucus is produced around the clitellum. An early cocoon sheath is secreted followed by an underlying layer of albumin. The cocoon and albumin sheet move anterior through muscular movement of the worm and pick up the egg, followed by sperm, from the oviduct and spermatheca respectively (Figure 7d). Fertilization occurs within the albumin matrix inside the now congealed, leathery, cocoon. The cocoons seal at both ends as they are deposited building an environmentally stable casing for development of the embryo. This developmental strategy yields a high offspring survival rate balancing the high-energy investment of egg production by the parent worm.

Embryonic development for all annelids follows a spiral cleavage. Polychaete zygotes develop into a non-yolky planktotrophic or yolk rich lecithotrophic trochophore that undergoes metamorphosis into the larvae. Clitellates follow direct development, without a trochophore stage, of the isolecithal (even yolk distribution) ova. Cleavage is holoblastic, meaning that the cleavage furrow extends through the entire egg. The production of the coelomic space and following segments is teloblastic. This is unique to clitellate annelids and encompasses the development and asymmetric proliferation from a large cell (macromere), which divides to form many smaller blast cells that subsequently form segmental tissue. Developmental times can vary greatly within a species and are environmentally dependant. Long developmental times correlate to "severe" environmental conditions, short times to more stable conditions. Sources: (R C Brusca

and G J Brusca, 2003) (Davidson and Stahl, 2008) (Bergter *et al*., 2004) (Wanninger, 2015).

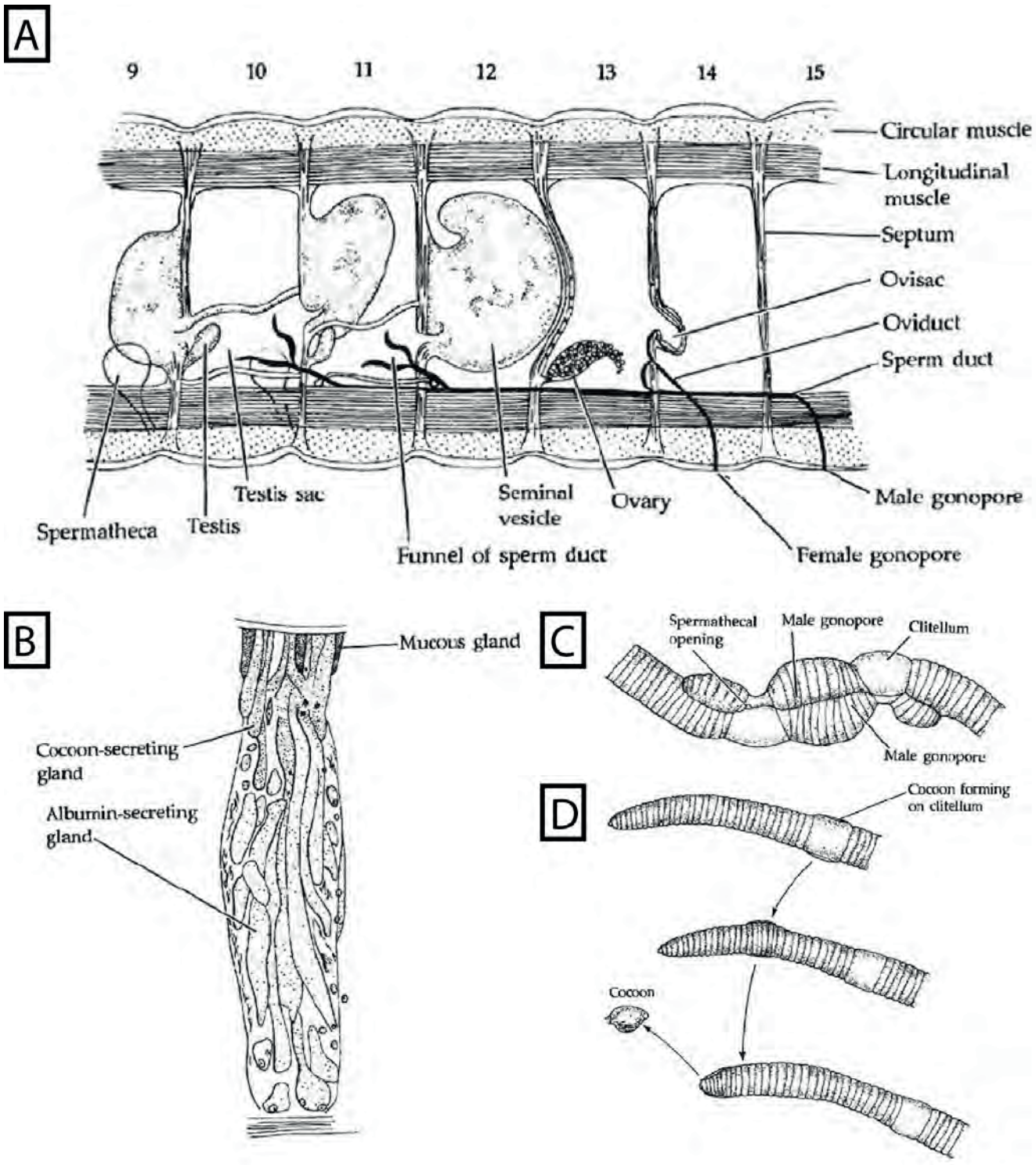

Figure 7: Reproductive anatomy of the common earthworm *Lumbricus terrestris* used as a baseline model for oligochaete reproduction in this thesis. Taken from (R C Brusca and G J Brusca, 2003).

1.4.2 *Olavius algarvensis* reproductive anatomy

The male and female reproductive organs are situated in segment IX, X and XI. An original description of *O. algarvensis* noted that testes are in segment X (Giere and Erseus, 2002) (Figure 8 – schematic region B). Several images attained during preparation of this thesis however, found testes to be situated in segment IX with the spermatheca and sperm funnel in segment X (Figure 8B). Higher resolution electron microscopy analysis will have to be conducted to resolve this morphological issue. The ovaries and prostate 1 & 2 are situated in segment XI. This segment also contains the ventral male pore and associated penal chaetae for copulation (Figure 8B) (refer to Appendix - A - 7.3). The oocyte matures posterior to the clitellum spanning through several worm segments, seen as constrictions along its length as it passes between septa separating the body segments (Figure 8 C & D) (discussed in 6.2 I). Only a single oocyte per worm has been observed at any one time.

1.4.3 Gutless oligochaete oviposition, transmission and development

Surprisingly, relatively little is know about the developmental cycle of gutless oligochaetes. This lies in the inability to culture worms in the laboratory and in the difficulty of finding eggs in the environment. In fact, to my knowledge, eggs have never been found in the environment and thus all studies to date have relied solely on fieldwork and *ex situ* experiments.

Giere & Langheld, 1987, showed that in *Inanidrilus leukodermatus* bacteria were transferred from the worms genital pad to the mucus surrounding the egg during oviposition. Symbionts have never been found in or around oocytes whilst inside the parent worm and transovarial vertical transmission has therefore been ruled out (Krieger, 2000) (Ortega, 2011). During oviposition the clitellum was noted to swell and an oviduct, which does not penetrate the cuticle, formed temporarily in the region of the genital pads

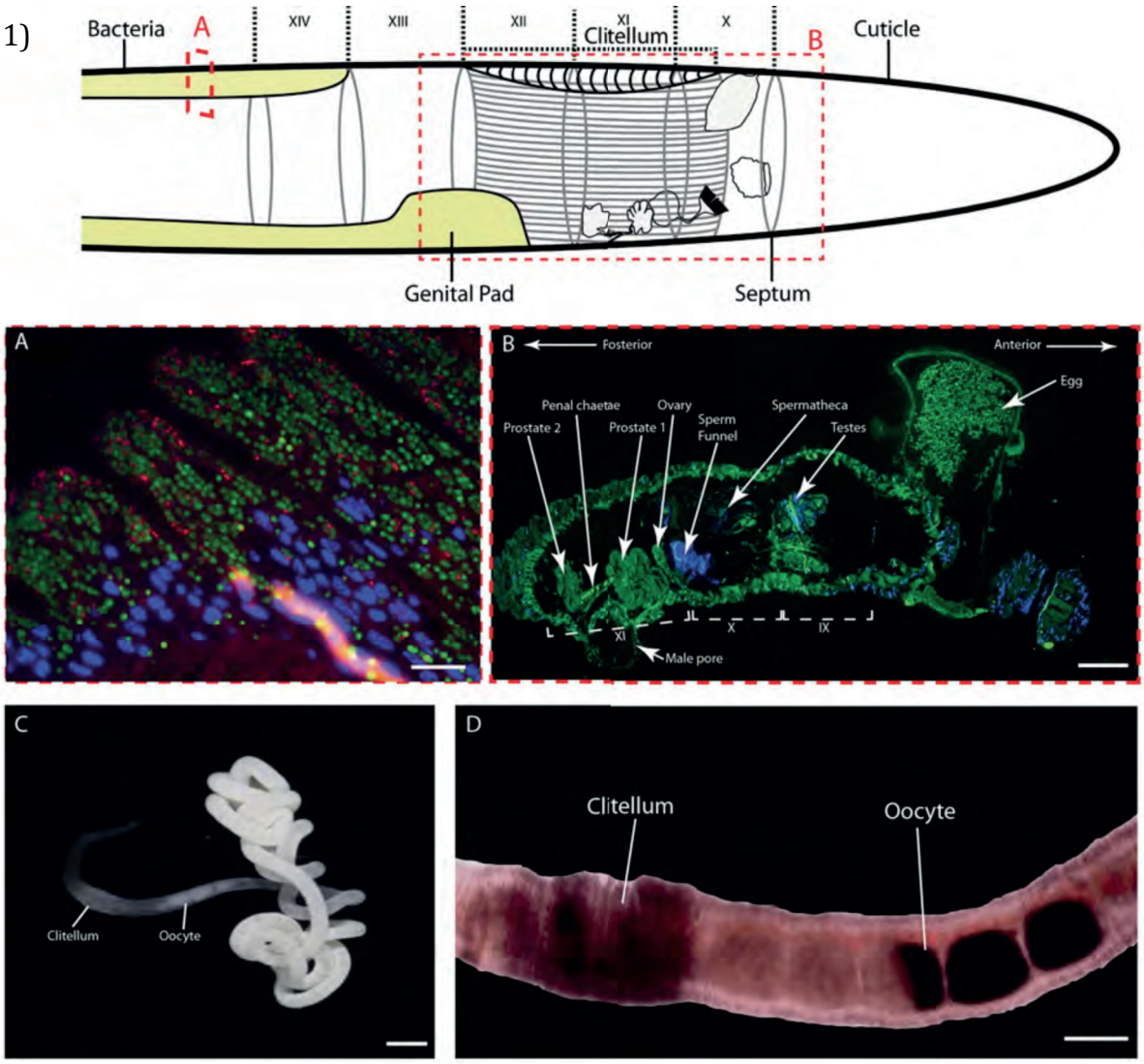

Figure 8: 1) Schematic of *O. algarvensis* reproductive anatomy. A): a cross section through the bacterial coat shows symbionts distribution under the cuticle by application of MiL-FISH with the class specific probes Gam42a for γ- symbionts (Green) and DSS658 for δ-symbionts (red). Scale bar = 10 µm. B): longitudinal section through a DAPI stained (blue) adult worm just after oviposition. Egg still attached. Sperm is visible in the testes, spermatheca and sperm funnel (blue). Scale bar: 50 µm. C): adult *O. algarvensis* carrying an internal oocyte posterior to the clitellum. Scale bar – 500 µm. D): oocyte spanning through several worm segments to segment XVII. Scale bar – 100 µm (Images C & D courtesy of A. Gruhl).

where bacterial cell density increases prior to oviposition. As the oocyte is pressed out the cuticle was noted to rupture. Worms deposited one egg singly and appear to have a low number of offspring per reproductive season. After deposition, bacteria were found in the mucus filament that attaches the egg to the parent worm as well as in the mucus surrounding the egg. Bacteria were subsequently assumed to enter the egg by passing

through the mucus layer into the egg albumen. Although bacterial cells were not identified to phylotype level in this study both large (γ-proteobacterial) and small (α-proteobacterial) morphotypes were found. A later study by Krieger 2000 however, excluded that bacteria pass through the mucus layer into the eggs and stated that these were already present inside the cocoons after oviposition. Immunogold labelling in this study identified γ -proteobacterial symbionts and bacteria of a smaller morphotype between the egg casing and the membrane bound zygote. Four hours after deposition bacteria were noted to aggregate at one pole within the egg.

1.5 Aim of this thesis

The primary aim of this thesis is to resolve the transmission of obligate bacterial symbionts in the gutless oligochaete *Olavius algarvensis* (Chapter V). In addition, the documentation of various ontogenetic stages and the localisation of symbionts associated to these are discussed. The short seasonal reproductive period of this non-cultivable gutless oligochaete is, as far as we know, limited to the months of July and August and as such offers only a limited timeframe for experimental fieldwork. Prior to the start of this thesis no late developmental stages had been attained and the conditions required for egg development were not clear. Experimental work was conducted to shed light on the natural ecology of the worms with the intent to provide evidence for the cultivation conditions required to attain late developmental stages *ex situ* (Chapter II). Further, for the localisation of bacteria within the eggs molecular methods for visualisation and identification of cells to phylotype level had to be applied. This was achieved by fluorescence *in situ* hybridisation (FISH), however high auto-fluorescence of some egg components such as egg yolk and the cocoon casing presented challenges in the identification of individual bacterial cells. We resolved these issues through development

of a novel FISH approach that yields higher probe conferred signal than standard mono-labelled or double-labelled-oligonucleotide-FISH (DOPE FISH) (Chapter III & Chapter IV) (Amann *et al.,* 1990) (Stoecker *et al.,* 2010).

1.5.1 Worm distribution and ecology

It was experimentally determined that gutless oligochaetes reside in both oxidised and reduced sediment layers but take preference to the RPD (Giere *et al.,* 1991). In this manner worms provide their symbiotic consortium with the substrates they require to drive metabolism. What was not clear however was on which environmental basis worms determine specific zones in the sediment. It was hypothesised that geotaxis alone could not drive worm migration because unpredictable shifting chemical gradients in the sediment change on very short time scales to which worms need to adapt to accordingly. Chemotaxis was therefore suspected to play a major role in finding substrates needed for both symbiont metabolism and the oxygen that worms require for their own respiration. Which chemical parameters determine chemotactic behaviour and during which timeframes adjustment to chemical gradients occurs on were unknown and the aim of the study presented in Chapter II. To answer these questions an experimental system was designed to fulfilled the following requirements: i) real-time monitoring of worm movement in the sediment, ii) real-time monitoring of oxygen gradients iii) introduction and manipulation of individual substrates of interest (H_2S, CO and H_2), iv) data analysis tools for the monitoring of worm movement and distribution over time related to corresponding chemical parameters. The knowledge gained from this study was considered a prerequisite for further methodical work in attaining eggs of various developmental stages required for the study presented in Chapter V.

1.5.2 Methods for identification and localisation of microbial cells

Fluorescence *in* situ hybridisation (FISH) is commonly used in microbial ecology to identify and localise individual microbial cells within a community. In this thesis FISH was used to identify and localise symbionts within cocoons of *O. algarvensis*. In order to maximise the analytical yield per specimen and due to the small size of eggs and scarcity of sample material embedding and section in a FISH compatible acrylic resin was applied (Schimak *et al*., 2012). The yolk rich embryos however show high auto fluorescence, which makes the detectability of single microbial cells difficult with standard mono-labelled FISH. An alternative is the use of catalysed reporter deposition – FISH (CARD-FISH), which yields a signal strong enough to overcome autofluorescence. However, due to fluorescence halo formation, a common bias of CARD-FISH, resolution was not sufficient to differentiate between single cells within a bacterial consortium. For the simultaneous identification of phylogenetically distinct cells and visual separation of microbial cells within the consortium a multi-colour FISH approach with high probe conferred signal was required for the study presented in Chapter V. In particular the following aspects had to be resolved with the development of such a method; i) increased signal strength to overcome autofluorescence of embryo yolk, ii) compatibility with, and high resolution of, signal on acrylic resin sections, 3) multi-labelling capabilities for simultaneous identification of several bacterial phylotypes (Chapter III).

In addition, the ability to isolate individual cells from within cocoons and to subsequently conduct single cell genomics is given by the application of FISH and fluorescence activated cell sorting (FACS). A workflow such as this would give insights into the specific role of each phylogenetically distinct symbiotic partner and allow a more targeted testing of hypothesis regarding individual cell niche partitioning and the role that bacteria may play during ontogenesis. The study presented in Chapter IV paves the way

for such analysis and shows that the FISH method presented in Chapter III is applicable in such workflows.

1.5.3 Transmission

The aim of this thesis is to present new insight into the transmission of bacterial symbionts in the well-studied symbiotic system of *Olavius algarvensis*. Past studies on the transmission of gutless oligochaetes were unable to determine which symbiont phylotypes were transmitted vertically and which, if any, taken up from the environment (Giere and Langheld, 1987; Krieger, 2000; Ortega, 2011). To answer this question embryos of various developmental stages were required. Past studies solely relied on the collection of sexually mature worms and incubation of these *ex situ* until eggs were lain (Krieger, 2000). For the Mediterranean gutless oligochaetes, however, this approach yielded a low quantity of eggs most of which were unfertilised or dead (C. Wentrup unpublished data). After initial incubation adjustments it was noted that eggs did not develop past the blastula stage. Considering that developmental times are often environmentally dependant and that embryos may enter a diapause in unfavourable conditions it became clear that our workflow was not optimal for the development of embryos *ex situ* (Hamdoun and Epel, 2007).

The insights gained from Chapter II of this thesis were applied in designing a system to provided conditions for successful rearing of eggs. The identification and localisation of symbiont cells within cocoons alone would not reveal the transmission mode because no further clues are given as to the origin of these cells. To resolve this ^{15}N stable isotope tracing was applied and a combinatorial approach was developed that offers both phylogenetic identification of cells by MiL-FISH and detection of stable isotope enrichment by nano-scale secondary ion mass spectrometer (nanoSIMS) (a similar approach to (Berry *et al.,* 2013) or (McGlynn *et al.,* 2015). Further, the

association of bacterial cells to different ontogenetic stages was to be documented and the establishment of the symbiosis determined. Evolutionary aspects and the implications of our findings are discussed for *O. algarvensis*, and mutualistic interactions in general, at the end of this chapter.

1.6 References – Chapter I

Amann RI, Krumholz L, Stahl DA. (1990). Fluorescent-oligonucleotide probing of whole cells for determinative, phylogenetic, and environmental studies in microbiology. *J Bacteriol* **172**: 762–770.

Bergin C. (2009). Phylogenetic diversity and metabolic versatility of the bacterial endosymbionts in marine gutless oligochaete worms. Deutsche Nationalbibliothek. Doctoral Thesis - University of Bremen, Bremen.

Bergter A, Beck LA, Paululat A. (2004). Embryonic development of the oligochaete Enchytraeus coronatus: an SEM and histological study of embryogenesis from one-cell stage to hatching. *J Morphol* **261**: 26–42.

Berry D, Stecher B, Schintlmeister A, Reichert J, Brugiroux S, Wild B, *et al.,* (2013). Host-compound foraging by intestinal microbiota revealed by single-cell stable isotope probing. *PNAS* **110**: 4720–4725.

Blazejak A, Erseus C, Amann R, Dubilier N. (2005). Coexistence of Bacterial Sulfide Oxidizers, Sulfate Reducers, and Spirochetes in a Gutless Worm (Oligochaeta) from the Peru Margin. *Appl Environ Microbiol* **71**: 1553–1561.

Bosch TCG. (2014). Rethinking the role of immunity: lessons from Hydra. *Trends Immunol* **35**: 495–502.

Bright M, Bulgheresi S. (2010). A complex journey: transmission of microbial symbionts. *Microbiol* **8**: 218–230.

Brucker RM, Bordenstein SR. (2012). Speciation by symbiosis. *Trends Ecol Evol* **27**: 1–9.

Brusca R. Brusca, 2003: Invertebrates 2nd Edition. Sinauer Associated, Inc.

Bshary R, Grutter AS. (2002). Experimental evidence that partner choice is a driving force in the payoff distribution among cooperators or mutualists: the cleaner fish case. *Ecol Letters*. doi:10.1046/j.1461-0248.2002.00295.x.

Bulgheresi S. (2011). Microbial Symbiont Transmission: Basic Principles and Dark Sides. Book chapter in: *Beneficial Microorganisms in Multicellular Life Forms*, Springer Berlin Heidelberg: Berlin, Heidelberg, pp 299–311.

Bulgheresi S, Schabussova I, Chen T, Mullin NP, Maizels RM, Ott JA. (2006). A New C-Type Lectin Similar to the Human Immunoreceptor DC-SIGN Mediates Symbiont Acquisition by a Marine Nematode. *Appl Environ Microbiol* **72**: 2950–2956.

Cascales E, Buchanan SK, Duché D, Kleanthous C, Lloubès R, Postle K, *et al.,* (2007). Colicin biology. *Microb Mol Bio Rev* **71**: 158–229.

Cavanaugh CM, Gardiner SL, Jones ML, Jannasch HW, Waterbury JB. (1981). Prokaryotic Cells in the Hydrothermal Vent Tube Worm Riftia pachyptila Jones: Possible Chemoautotrophic Symbionts. *Science* **213**: 340–342.

Dahl C, Friedrich C, Kletzin A. (2008). Sulfur oxidation in prokaryotes. *eLS*. doi:10.1002/9780470015902.a0021155.

Dale C, Moran NA. (2006). Molecular Interactions between Bacterial Symbionts and Their Hosts. *Cell* **126**: 453–465.

Davidson SK, Stahl DA. (2008). Selective recruitment of bacteria during embryogenesis of an earthworm. *ISME J* **2**: 510–518.

de Bary A. (1879). Die Erscheinung der Symbiose: Vortrag gehalten auf der Versammlung Deutscher Naturforscher und Aerzte zu Cassel. Strassburg, Verlag von Karl J. Trübner.

Dedeine F, Vavre F, Fleury F, Loppin B, Hochberg ME, Bouletreau M. (2001). Removing symbiotic Wolbachia bacteria specifically inhibits oogenesis in a parasitic wasp. *PNAS* **98**: 6247–6252.

Dobson AP, Carper ER. (1996). Infectious diseases and human population history - Throughout history the establishment of disease has been a side effect of the growth of civilization. *BioScience* **46**: 115–126.

Dubilier N, Bergin C, Lott C. (2008). Symbiotic diversity in marine animals: the art of harnessing chemosynthesis. *Microbiol* **6**: 725–740.

Dubilier N, Blazejak A, Ruhland C. (2006). Symbioses between bacteria and gutless marine oligochaetes. Book chapter in: *Molecular Basis of Symbiosis*. J. Overmann, Ed. Berlin Heidelberg, Springer. **41:** 251-275

Dubilier N, Mulders C, Ferdelman T, de Beer D, Pernthaler A, Klein M, *et al.,* (2001). Endosymbiotic sulphate-reducing and sulphide-oxidizing bacteria in an oligochaete worm. *Nature* **411**: 298–302.

Ebert D. (2013). The epidemiology and evolution of symbionts with mixed-mode transmission. Chapter in: *Annu Rev of Ecol Evol S* **44:** 623 - 643

Erséus C. (1979). Taxonomic Revision of the Marine Genus Phallodrilus Pierantoni (Oligochaeta, Tubificidae), with Descriptions of Thirteen New Species1. *Zool Scripta* **8**: 187–208.

Erséus C. (1991). Two new deep-water species of the gutless genus Olavius (Oligochaeta: Tubificidae) from sides of North America. Proceedings of the Biological Society of Washington.

Felbeck H. (1981). Chemoautotrophic Potential of the Hydrothermal Vent Tube Worm, Riftia pachyptila Jones (Vestimentifera). *Science* **213**: 336–338.

Felbeck H, Liebezeit G, Dawson R, Giere O. (1983). CO2 fixation in tissues of marine oligochaetes (Phallodrilus leukodermatus and P. planus) containing symbiotic, chemoautotrophic bacteria. *Mar Biol*. **75**(2-3): 187-191.

Fine P. (1975). Vectors and vertical transmission: an epidemiologic perspective. *Ann NY Acad Sci*. **266:** 173-194

Fleuriet A. (1988). Maintenance of a hereditary virus. *Evol Biol*. **23:** 1-30

Fraune S, Bosch TCG. (2010). Why bacteria matter in animal development and evolution. *Bioessays* **32**: 571–580.

Ftnogenova N. (1986). Six new species of marine Tubificidae (Oligochaeta) from the continental shelf off Peru. *Zool Scripta*. **15**(1): 45-51

Giere O, Conway NM, Gastrock G, Schmidt C. (1991). Regulation" of gutless annelid ecology by endosymbiotic bacteria. *Mar Ecol Prog Ser*. **68:** 287-299

Giere O, Erseus C. (1998). A new species of Olavius (Tubificidae) from the Algarve coast in Portugal, the first East Atlantic gutless oligochaete with symbiotic bacteria. *Zool Anz*. **257**(2-3): 209-214

Giere O, Erseus C. (2002). Taxonomy and new bacterial symbioses of gutless marine Tubificidae (Annelida, Oligochaeta) from the Island of Elba (Italy). *Org Divers Evol* **2**: 289–297.

Giere O, Langheld C. (1987). Structural organisation, transfer and biological fate of endosymbiotic bacteria in gutless oligochaetes. *Mar Biol*. **93:** 641-650

Giere O, Liebezeit G, Dawson R. (1982). Habitat Conditions and Distribution Pattern of the Gutless Oligochaete Phallodrilus-Leukodermatus. *Mar Ecol Prog Ser* **8**: 291–299.

Gilbert SF. (2001). Ecological Developmental Biology: Developmental Biology Meets the Real World. *Dev Biol* **233**: 1–12.

Gilbert SF. (2012). Ecological developmental biology: environmental signals for normal animal development. *Evol Dev* **14**: 20–28.

Gilbert SF, Bosch TCG, Ledón-Rettig C. (2015). Eco-Evo-Devo: developmental symbiosis and developmental plasticity as evolutionary agents. *Nature* **16**: 611–622.

Gilbert SF, Epel D. (2009). Ecological developmental biology: integrating epigenetics, medicine, and evolution. *Yale J Biol Med.* **82**(2): 231-232

Gilbert SF, Sapp J, Tauber AI. (2012). A symbiotic view of life: we have never been

individuals. *Q Rev Biol* **87**: 325–341.

Gordon J, Knowlton N, Relman DA, Rohwer F. (2010). Superorganisms and holobionts. *Issues*. http://www.microbemagazine.org/index.php?option=com_content&view=article&id=6300:superorganisms-and-holobionts&Itemid=1464

Hadfield MG. (2011). Biofilms and marine invertebrate larvae: what bacteria produce that larvae use to choose settlement sites. *Ann Rev Mar Sci* **3**: 453–470.

Hamdoun A, Epel D. (2007). Embryo stability and vulnerability in an always changing world. *PNAS* **104**: 1745–1750.

Hosokawa T, Hironaka M, Inadomi K, Mukai H, Nikoh N, Fukatsu T. (2013). Diverse strategies for vertical symbiont transmission among subsocial stinkbugs. *PLoS ONE* **8**: e65081.

Huang Y, Callahan S, Hadfield MG. (2012). Recruitment in the sea: bacterial genes required for inducing larval settlement in a polychaete worm. *Sci Rep* **2**: 228.

Jannasch HW, Eimhjellen K, Wirsen CO, Farmanfarmaian A. (1971). Microbial degradation of organic matter in the deep sea. *Science* **171**: 672–675.

Johnstone RA, Bshary R. (2002). From parasitism to mutualism: partner control in asymmetric interactions. *Ecol Letters* **5**: 1–6.

Kaltenpoth M. (2009). Actinobacteria as mutualists: general healthcare for insects? *Trends Microbiol* **17**: 529–535.

Kaltenpoth M, Göttler W, Herzner G, Strohm E. (2005). Symbiotic bacteria protect wasp larvae from fungal infestation. *Curr Biol* **15**: 475–479.

Kiers ET, Duhamel M, Beesetty Y, Mensah JA, Franken O, Verbruggen E, *et al.,* (2011). Reciprocal rewards stabilize cooperation in the mycorrhizal symbiosis. *Science* **333**: 880–882.

Kiers ET, West SA. (2015). Evolutionary biology. Evolving new organisms via symbiosis. *Science* **348**: 392–394.

Kleiner M. (2012). Metabolism and Evolutionary Ecology of Chemosynthetic Symbionts from Marine Invertebrates. Deutsche Nationalbibliothek. Doctoral Thesis - University of Bremen, Bremen.

Kleiner M, Wentrup C, Holler T, Lavik G, Harder J, Lott C, *et al.,* (2015). Use of carbon monoxide and hydrogen by a bacteria-animal symbiosis from seagrass sediments. *Environ Microbiol*. doi:10.1111/1462-2920.12912.

Kleiner M, Wentrup C, Lott C. (2012). Metaproteomics of a gutless marine worm and its symbiotic microbial community reveal unusual pathways for carbon and energy use. *PNAS.* **109**(19): E1173-E1182.

Kleiner M, Young JC, Shah M, VerBerkmoes NC, Dubilier N. (2013). Metaproteomics

reveals abundant transposase expression in mutualistic endosymbionts. *MBio* **4**: e00223–13.

Klose J, Polz MF, Wagner M, Schimak MP, Gollner S, Bright M. (2015). Endosymbionts escape dead hydrothermal vent tubeworms to enrich the free-living population. *PNAS* **112**: 11300–11305.

Krieger J. (2000). Funktion und Übertragung endosymbiontischer Bakterien bei darmlosen marinen Oligochaeten. (Function and transmission of endosymbiotic bacteria in gutless marine oligochaetes). Deutsche Nationalbibliothek. Doctoral Thesis - University of Hamburg, Hamburg.

Lipsitch M, Nowak MA, Ebert D, May RM. (1995). The population dynamics of vertically and horizontally transmitted parasites. *P R Soc B* **260**: 321–327.

Lipsitch M, Siller S, Nowak MA. (1996). The evolution of virulence in pathogens with vertical and horizontal transmission. *Evolution* **50**: 1729–1741.

Little AEF, Murakami T, Mueller UG, Currie CR. (2006). Defending against parasites: fungus-growing ants combine specialized behaviours and microbial symbionts to protect their fungus gardens. *Biol Lett* **2**: 12–16.

Longdon B, Jiggins FM. (2010). Paternally transmitted parasites. *Curr Biol* **20**: R695–R696.

Margulis L. (1970). Origin of eukaryotic cells: evidence and research implications for a theory of the origin and evolution of microbial, plant, and animal cells on the Precambrian Earth. XXII u. 349 S., 89 Abb., 49 Tab. New Haven-London 1970: Yale University Press

Margulis L. (1993). Symbiosis in cell evolution: microbial communities in the Archean and Proterozoic eons. WH Freeman & Co

Marshall A. (1898). Principles of economics. Vol. 1. London: Macmillian and Co., Ltd.

Martin W, Muller M. (1998). The hydrogen hypothesis for the first eukaryote. *Nature* **392**: 37–41.

Mattoso TC, Moreira DDO, Samuels RI. (2012). Symbiotic bacteria on the cuticle of the leaf-cutting ant Acromyrmex subterraneus subterraneus protect workers from attack by entomopathogenic fungi. *Biol Lett* **8**: 461–464.

McFall-Ngai M, Hadfield MG. (2013). Animals in a bacterial world, a new imperative for the life sciences. *PNAS.* **110**(9): 3229-36

McFall-Ngai MJ. (2002). Unseen forces: the influence of bacteria on animal development. *Dev Biol* **242**: 1–14.

McGlynn SE, Chadwick GL, Kempes CP, Orphan VJ. (2015). Single cell activity reveals direct electron transfer in methanotrophic consortia. *Nature* **526**: 531–535.

Mindell DP. (1992). Phylogenetic consequences of symbioses: Eukarya and Eubacteria

are not monophyletic taxa. *Biosystems* **27**: 53–62.

Moran NA, McCutcheon JP, Nakabachi A. (2008). Genomics and evolution of heritable bacterial symbionts. *Annu Rev Genet* **42**: 165–190.

Moran NA, McLaughlin HJ, Sorek R. (2009). The dynamics and time scale of ongoing genomic erosion in symbiotic bacteria. *Science* **323**: 379–382.

Moran NA, Wernegreen JJ. (2000). Lifestyle evolution in symbiotic bacteria: insights from genomics. *Trend Eco Evol* **15**: 321–326.

Moya A, Peretó J, Gil R, Latorre A. (2008). Learning how to live together: genomic insights into prokaryote–animal symbioses. *Nat Rev Genet* **9**: 218–229.

Nemecky S. (2008). Benthic degradation rates in shallow subtidal carbonate and silicate sands. Deutsche Nationalbibliothek. Diploma Thesis - University of Bremen, Bremen.

Nussbaumer AD, Fisher CR, Bright M. (2006). Horizontal endosymbiont transmission in hydrothermal vent tubeworms. *Nature* **441**: 345–348.

Nyholm SV, McFall-Ngai MJ. (2004). The winnowing: establishing the squid-vibrio symbiosis. *Microbiol* **2**: 632–642.

Nylander J, Erseus C, Källersjö M. (1999). A test of monophyly of the gutless Phallodrilinae (Oligochaeta, Tubificidae) and the use of a 573-bp region of the mitochondrial cytochrome oxidase I gene in analysis of annelid phylogeny. *Zool Scripta*. **28**(3-4): 305-313

Ortega BEN. (2011). Symbiont transmission in Olavius algarvensis. Deutsche Nationalbibliothek. Bachelor Thesis - University of Bremen, Bremen.

Rigaud T, Pennings PS, Juchault P. (2001). Wolbachia bacteria effects after experimental interspecific transfers in terrestrial isopods. *J Invertebr Pathol* **77**: 251–257.

Robidart JC, Bench SR, Feldman RA, Novoradovsky A, Podell SB, Gaasterland T, *et al.,* (2008). Metabolic versatility of the Riftia pachyptila endosymbiont revealed through metagenomics. *Environ Microbiol* **10**: 727–737.

Rohwer F, Seguritan V, Azam F, Knowlton N. (2002). Diversity and distribution of coral-associated bacteria. *Mar Ecol Prog Ser* **243**: 1–10.

Ruby EG, Wirsen CO, Jannasch HW. (1981). Chemolithotrophic Sulfur-Oxidizing Bacteria From the Galapagos Rift Hydrothermal Vents. *Appl Environ Microbiol* **42**: 317–324.

Ruehland C, Blazejak A, Lott C, Loy A, Erséus C, Dubilier N. (2008). Multiple bacterial symbionts in two species of co-occurring gutless oligochaete worms from Mediterranean sea grass sediments. *Environ Microbiol* **10**: 3404–3416.

Sachs JL, Mueller UG, Wilcox TP, Bull JJ. (2004). The evolution of cooperation. *Q Rev Biol* **79**: 135–160.

Sachs JL, Russel JE, Lll YE, Black KC, Lopez G, Patil AS. (2010). Host control over infection and proliferation of a cheater symbiont. *J Evolution Biol* **23**: 1919–1927.

Sapp J. (2010). On the Origin of Symbiosis. Book Chapter: *Symbioses and Stress* **17**: 3–18. In Cellular Origin, Life in Extreme Habitats and Astobiology. Springer & Business Media.

Sato T, Atomi H. (2010). Microbial inorganic carbon fixation. *eLS*. doi:10.1002/9780470015902.a0021153.

Schimak MP, Toenshoff ER, Bright M. (2012). Simultaneous 16S and 18S rRNA fluorescence in situ hybridization (FISH) on LR White sections demonstrated in Vestimentifera (Siboglinidae) tubeworms. *Acta Histochem* **114**: 122–130.

Schwedt A, Kreutzmann AC, Polerecky L. (2011). Sulfur respiration in a marine chemolithoautotrophic Beggiatoa strain. *Front Microbiol* **2**: 276.

Serbus LR, Casper-Lindley C, Landmann F, Sullivan W. (2008). The Genetics and Cell Biology of Wolbachia-Host Interactions. *Annu Rev Genet* **42**: 683–707.

Shinzato C, Shoguchi E, Kawashima T, Hamada M, Hisata K, Tanaka M, *et al.,* (2011). Using the Acropora digitifera genome to understand coral responses to environmental change. *Nature* **476**: 320–323.

Stoecker K, Dorninger C, Daims H, Wagner M. (2010). Double labeling of oligonucleotide probes for fluorescence in situ hybridization (DOPE-FISH) improves signal intensity and increases rRNA accessibility. *Appl Environ Microbiol* **76**: 922–926.

Tasoff J, Mee MT, Wang HH. (2015). An Economic Framework of Microbial Trade. Huerta-Quintanilla, R (ed). *PLoS ONE* **10**: e0132907.

Van Leuven JT, McCutcheon JP. (2012). An AT mutational bias in the tiny GC-rich endosymbiont genome of Hodgkinia. *Genome Biol Evol* doi:10.1093/gbe/evr125.

Wanninger A. (2015). Evolutionary Developmental Biology of Invertebrates 6. Springer-Verlag, Wien.

Wentrup C. (2012). Acquisition and activity of bacterial symbionts in marine invertebrates. Deutsche Nationalbibliothek. Doctoral Thesis - University of Bremen, Bremen.

Werner GDA, Strassmann JE, Ivens ABF, Engelmoer DJP, Verbruggen E, Queller DC, *et al.,* (2014). Evolution of microbial markets. *PNAS* **111**: 1237–1244.

Wintermute EH, Silver PA. (2010). Dynamics in the mixed microbial concourse. *Genes Dev* **24**: 2603–2614.

Woyke T, Teeling H, Ivanova NN, Huntemann M, Richter M, Gloeckner FO, *et al.,* (2006). Symbiosis insights through metagenomic analysis of a microbial consortium. *Nature* **443**: 950–955.

Yamamura N. (1993). Vertical transmission and evolution of mutualism from parasitism.

Theor Popul Biol **44**: 95–109.

Chapter II

Substrate dependent chemotactic behaviour in the gutless oligochaete *Olavius algarvensis*

Mario P. Schimak[1], Nikolaus Leisch[1,2], Lubos Polerecky[3], Arne Kreutzmann[4], Alexander Gruhl[1], Manuel Liebeke[1], Charles R. Fischer[5], Nicole Dubilier[1]

[1]Max Planck Institute for Marine Microbiology, Celsiusstrasse 1, D-28359 Bremen, Germany
[2]Department Ecogenomics and Systems Biology, University of Vienna, Althanstrasse 14, A-1090 Vienna, Austria
[3]University of Utrecht, Bestuursgebouw, Heidelberglaan 8, 3584 CS Utrecht, Holland
[4] University of Bremen, SFB/TR 8 Spatial cognition, Enrique-Schmidt Strasse 5, 28359, Bremen, Germany
[5] Pennsylvania State University, University Park, PA 16801, U.S.A

Manuscript in preparation

Corresponding author

Mario Schimak: mschimak@mpi-bremen.de

Author contributions

N.D. was project supervisor, C.R.F. for scientific input throughout the project, A.K. for writing of image analysis algorithms, L.P. for Mollie systems, A.G. image analysis, M.L. scientific input throughout the project, N.L. designed project and experiments, conducted experiments and gave scientific input throughout the project M.P.S. designed project and experiments, conducted experiments and wrote the manuscript.

Abstract

Marine chemosynthetic bacteria can use reduced substrates from the environment to drive their metabolism. The sediments that these bacteria inhabit and the corresponding chemical gradients that they require are however subjected to fast shifts in chemical composition due to constantly changing environmental conditions. Bacteria must therefore keep up with moving chemical gradients to ensure access to the substrates they require. One evolutionary strategy to compensate for these shifts has been the association of bacteria with motile invertebrate animal hosts. The animal host profits from a nutritional benefit provided by the symbionts, which may become so profitable that in some cases the association becomes obligate. A host must therefore provide a mechanism to ensure access to the required substrates needed for symbiont metabolism. Geotaxis alone may not be sufficient in environments with non-directional changes in chemical gradients and chemotaxis therefore also plays an essential role in finding substrate. However, it is not clear how some reduced substrates can be detected in animal host or how these are sought out in the environment. The gutless oligochaete *Olavius algarvensis* harbours a consortium of chemosynthetic bacteria that can make use of hydrogen sulphide (H_2S), sulphate (SO_4^{-3}), carbon monoxide (CO) and hydrogen (H_2) as energy source. Our findings indicated that worms could identify and actively seek out each of these substrates independently, which is surprising as there are no known chemoreceptors for CO or H_2 in animal metazoans. These finding give the first clues to possible signalling pathways between symbiont and host and the role that symbionts play in regulating worm distribution and ecology in the sediment.

Introduction

Symbiosis between metazoan hosts and chemosynthetic bacteria are wide spread and found in virtually all marine benthic ecosystems (Dubilier *et al.,* 2008). Together, as a unit, each partner of the association has a selective advantage over its individual parts. Through exploitation of newly available ecological niches an increase of fitness results for both partners (Gordon *et al.,* 2010). Therefore, the sum of individuals, the holobiont, has a very specific role in the ecosystem (Rohwer *et al.,* 2002).

Chemosynthetic associations are nutritionally based and as such the distribution of the chemosynthetic holobiont is closely coupled with the availability of the required substrates and the biogeochemical processes related to them. Hosts must occupy a niche that provides substrate for the metabolic requirements of symbionts without neglecting their own. This can be achieved by adopting one of two strategies: 1) Sedentary organisms must position themselves in a stable environment to access both electron donors, such as hydrogen sulphide, and terminal electron acceptors, such as oxygen. This commonly leads to physiological and / or morphological adaptations of the host, to actively facilitate access to substrate for its symbionts. Examples of this include the deep-sea giant tubeworm *Riftia pachyptila,* binding reduced sulphur species to specially adapted haemoglobin for transfer via the vascular system to the symbiont housing organ, the trophosome (Felbeck, 1981). For such a strategy to be viable, guarantee must be given that stable and constant fluxes of reduced substrates are available time frames long enough for an animal to reproduce and colonise new sites. 2) Motile organisms can actively seek out and position themselves in zones in which electron donors and or reduced substrates are available. Motile chemosynthetic meiofauna such as nematodes, vesicomyid clams and gutless oligochaetes use chemical gradients and the redox potential discontinuity (RPD) to provide symbionts with the substrates and conditions needed to

drive their metabolism (Ott and Novak, 1989) (Giere *et al.,* 1991) (Ott *et al.,* 1991). A host must therefore either detect chemically favourable gradients, using a chemotactic pathway, or symbionts themselves may potentially signal their host to communicate the presence of favourable conditions once they have been detected (Hay, 2009) (Wadhams and Armitage, 2004).

One of the main factors that govern the distribution of meiofauna animals in symbiosis with chemoautotrophic bacteria inhabiting reduced sediments is therefore substrate availability and the chemical gradients such as oxygen and / or reduced electron donors. Which partner in the association determines distribution of the holobiont in the sediment and which gradients are followed has for the best part remained unanswered. Giere *et al.,* 1991 demonstrated that the behavioural distribution of the Caribbean gutless oligochaete *Inanidrilus leukodermatus,* from sulphide rich sediments (max. 200 µm in 15 cm sediment depth), is coupled with its sulphur oxidising γ -proteobacterial symbiont physiology. Endpoint measurements of sediment cores revealed that worms were primarily found in the chemocline where access to reduced sulphur and microoxic conditions is given. It was indeed the position of the chemocline in the sediment that determines distribution of gutless oligochaetes rather than depth alone. Worms were also found in oxic zones above and the highly sulphuric zones below the chemocline and a migratory behaviour of worms between these zones was postulated (Giere *et al.,* 1991). Further it was postulated that the uptake of sulphide occurs in reduced anoxic sediment layers, which are later oxidised in upper oxygenated zones after a storage phase. This has indeed been reported for several other chemoautotrophic symbiotic systems and it has been stated that most thiobiotic species drive their metabolism in reduced environments and that migratory behaviour is necessary to supply oxygen for sulphur oxidation (Meyers *et al.,* 1987).

Similarly, Ott *et al.,* 1991 showed that *Stilbonematinae* nematodes, living in association with sulphur oxidising symbiotic bacteria, migrate between oxic and highly reduced sediment layers (Ott *et al.,* 1991). The mechanisms that dictate migration, such as following the sulphide gradient, were not resolved and the question that remained open was: "(do) hosts adjust their behaviour to the need of their symbionts i.e., migrating downward when the bacteria require a fresh supply of reduced sulphur compounds." (Ott *et al.,* 1991).

The Mediterranean gutless oligochaete *Olavius algarvensis* harbours a consortium of γ -proteobacterial sulphur oxidisers and δ -proteobacterial sulphate reducing chemoautotrophic symbionts (Dubilier Nature 2001). In addition to sulphur metabolism two studies have recently shown that carbon monoxide (CO) and hydrogen (H_2) can also be used as electron donors (Figure 1). The two γ -proteobacterial phylotypes in the consortium can oxidise H_2S and CO. The δ-proteobacterial phylotypes are able to utilise SO_4, CO and H_2. (Dubilier *et al.,* 2001) (Kleiner *et al.,* 2013) (Kleiner *et al.,* 2015). Mediterranean siliceous sediments in which worms occur are oligotrophic with sulphide concentrations up to a hundred fold lower than the Caribbean sediments of the 1991 study by Giere *et al* (max. 0.55 µm in 15 cm sediment depth - (Kleiner, 2012)). The utilisation of additional electron donors presumably facilitates the worms to inhabit oligotrophic sediments. Indeed, *in situ* H_2 concentrations of 89 - 2147 nM were the highest ever measured for any known shallow water marine sediments and CO concentrations were found to be in the range of 17 – 51 nM. Although CO is known to act as a signalling molecule between cells there is no evidence to date that metazoan animals can actively sense neither CO nor H_2 via chemoreceptors (Morse *et al.,* 2002).

In this study we investigate the response of the host *Olavius algarvensis* to the individual substrates that can be metabolised by its symbionts. Through a variety of experimental conditions, in flat aquaria, and the use of planar optodes we aim to elucidate the role that chemotaxis plays for worms in finding the substrates required for symbiont metabolism. Newly developed imaging algorithms are used to shed light on the influence that O_2, H_2S, CO and H_2 have on the ecological behaviour of worms and if these substrates are actively sought out. Real-time distribution, adaptation to changes in gradients and shuttling between the RPD were monitored and visualised with the use of a 3D projection of worm migratory movement over time. This helps give insight into the ecological and physiological implications that symbionts have for their hosts in the natural environment.

Material and Methods

Sample collection: Field experiments were carried out in June 2014 at the Hydra field station, Elba, Italy. Siliceous sediment from the Bay of Sant' Andrea (42°48'30''N, 10° 8'33''E), was collected into buckets by SCUBA divers from a depth of 7 meters adjacent to *Posidonia oceanica* sea grass meadows. The sediment samples were transported back to the field station and worms retrieved by decantation as they were needed for experiments. *Olavius algarvensis*, one of the three co-occurring gutless oligochaetes found at the sampling site, was visually sorted under a standard dissection microscope.

Aquarium setup: Two rubber ring sealed flat aquaria of 200 x 150 x 3 mm (h x w x d), internal dimension, were used for all experiments. A 240 x 240 x 15 mm (h x w x d) rectangular Acrylic plate with two 5 mm thick Plexiglas sheets on either side, one fixed and one removable, made up the main body of the aquarium. Two glass panes of 6 mm

thickness were attached to the inside of the Plexiglas, with silicon, resulting in 3 mm spacing between them (SI Figure 1). Four vertical and four horizontal transparent planar optode stripes (Holst and Grunwald, 2014) were fixed to the glass panes with silicon. A groove was cut into the Acrylic plate to accommodate a single rubber ring, sealing the removable pane watertight by use of 11 stainless steel bolts. Two holes were drilled at 4 cm and 16 cm from the top of the aquarium on one side to the internal chamber. Two surgical needles, with lure locks, where fixed in place permanently at these positions with silicon in order to take for pore water samples, or to introduce substrates via a syringe. The chamber of the aquarium was filled with laboratory standard chemically inert 1.25 – 1.65 mm glass beads (Carl Roth, Karlsruhe, Germany) to replace the sediment worms reside in. To keep temperature constant during all experiments the flat migration aquaria were immersed in a larger tank filled with fresh seawater (salinity 39 ‰) and cooled to a constant temperature of 20 °C by a cooling aggregate (Titan-150, Aqua Medic, Bissendorf, Germany).

Imaging acquisition: Image acquisition followed by time-laps photography using the modular luminescent lifetime imaging system (MOLLI) after (Holst *et al.,* 1998) & (Polerecky 2005). Two MOLLI systems were set up, one to record photo images of worm movement every 15 seconds and one to measure oxygen concentrations via planar optodes every 300 seconds (integration time 800ms). For each system a cooled CCD camera (Sensicam, PCO, Kelheim, Germany) and two blue-light emitting diodes (LED's; λ_{max} = 455nm, LXHL-LR5C, Lumileds, Philips), connected to heat sinks, were used.

Optode settings: The rapid lifetime determination method (RLD) was chosen to measure oxygen concentrations from 100% – 0% air saturation (AS). At a temperature of 20 °C, 1 ATM and a salinity of 39‰, 100% AS equals 222 µM oxygen (Naqvi *et al.,* 2010). Hypoxia was defined as 30% AS or bellow (< 62.5 µM O_2) (Levin *et al.,* 2009) .

Migration experimental procedure: per experiment 4 freshly picked adult *Olavius algarvensis* were used for the conditions listed in Figure 2. Experiments were run for either 180 minutes or 300 minutes. Oxic and hypoxic seawater of 39‰ salinity was prepared and introduced into the flat aquaria as follows:

For oxygenated medium, 0.22 µm sterile-filtered seawater (Nalgene Rapid Flow Filter Units, Nalge Nunc, Rochester, New York) was aerated with an air stone and aquarium air pump for at least 30 minutes. Flat aquaria were assembled, filled with oxygenated seawater to the desired amount, and glass beads added. For experiments with an hypoxic top gradient the remaining half of the aquarium was filled with hypoxic medium.

Hypoxic sterile filtered seawater, for experiments that were run entirely hypoxic or with an hypoxic bottom half, was prepared by bubbling sterile filtered seawater inside the flat aquaria with nitrogen gas through the surgical needle fixed at the 16 cm inlet for at least 30 minutes. Glass beads were added and the aquarium was filled with oxygenated seawater to the top if required. For experiments with hypoxic top half sterile filtered seawater was bubbled with nitrogen in a 60 ml syringe closed with a rubber plug and a surgical needle outlet, for at least 30 minutes. The resulting anoxic water was subsequently injected into the aquarium slowly from the top opening. If substrate was required in the top half of the aquarium it was added to the hypoxic medium prepared in the 60 ml syringe to the desired final concentration. For experiments substrate in the entire aquarium hypoxic medium was prepared as described above and the required amount of substrate added directly by injection via the inlet at 16 cm. The same procedure was applied for experiments with substrate in the bottom half of the aquarium and subsequently toped up with anoxic seawater. For experiments with a substrate zonation a red food dye (Brilliant Scarlet 4R, E124) was added to the bottom half of the aquarium to visually differentiate between the two zones.

Substrate measurements: Substrate concentration was measured at the beginning and end of each experiment. For experiments with a zonation both the top and bottom of the aquarium was sampled. Water samples were extracted immediately from the system via the 4 and 16 cm inlet with a syringe and fixed with 2% $ZnCl_2$. GC-Hg measurements for CO and H_2 were taken using a Reduced Gas Analyser, RGA3, Trace Analytics Inc. Hydrogen sulphide measurements were taken by incubating 1000 µl water sample with 80 µl Diamine for 30 minutes (Cline 1969) followed by photometric analysis at 670 nm (Spectronic GENESYS 6, ThermoScientific, Schwerte, Germany).

Image analysis: Image analysis was carried out in ImageJ64 version 1.48 (Schneider *et al.,* 2012) and / or Fiji (Schindelin *et al.,* 2012) using the following workflow: Raw image files were converted into grey scale, orientated and cropped if necessary. To better visualise worm movement an image subtraction algorithm was written and applied (digital supplementary data of this thesis Chapter_II_ImageJ_Java_Scripts)(copyright N. Leisch). The algorithm visually removes the aquarium, glass beads and optode stripes from all images in each set (SI Figure 2a). Every pixel of a frame that did not change position from the frame before it was zeroed out and set to black leaving only moving elements, namely the worms. The subtracted image files were summed in a Z stack, with ImageJ's ZProject / Sum Slices function, which produced a final image of all worm positions during the entire experiment. To numerically determine the zone in the aquarium with the highest worm occurrence over the course of an experiment a X-axis compression algorithm was written in Python script and applied to the summed image files. Here, we set the image to grey scale and sum up all pixels along the width of the aquarium. This results in a numerical value, which is the sum of all grey scale values on any particular row of pixels along the X-axis. These values are reassigned to a scale from 0 to 100 (with the highest attained value being given

100 and the lowest 0) and given a corresponding grey scale value. For simplification only every 1 cm of the aquarium height was analysed in this manner and plotted on a graph. The image attained shows the distribution of worm occurrence over the entire experiment (SI Figure 2b - i). To monitor worm migration patterns over time and to attain a profile of worm alignment to substrate within the aquarium a 3D Projection of the summed Z-stack image was made was made using ImageJ's 3D Project function (SI Figure 2c - ii). The 3D rendered image stack is turned by 90° on the Y-axis whereby time is now plotted on the X-axis and the height of the aquarium on the Y-axis. In this manner worm positions are seen as a continuous line throughout the experiment and their localisation, movement and adaptation to changing conditions in the aquarium can be analysed in space and time. The same workflow was applied to optode images resulting in an image file that shows the change of oxygen distribution throughout the experiment (SI Figure 2d & SI Figure 3). The profile of worm movement can be placed over the optode profile to show worm distribution at any given oxic condition. All attained data is summed up in a single image set for comparison (Figure 3).

Results

A total of 54 experiments were conducted to cover all conditions and substrates tested. This resulted in raw data of ~ 60,000 images for worm movement, 3,000 optode measurements and 96 GC and photometer measurements. The attained data was used to analyse both chemical and behavioural attributes of worm movement in the aquarium as described in Figure 2. All experiments were repeated at least in triplicate (n=3, listed in SI Table 2). Figure 4 shows example experiments representative for each condition tested. For the entire dataset please see Supplementary Information Figure 4 – 16.

Oxygen: Oxygen gradients were tested to assess worm behaviour based solely on oxygen distribution with no additional substrate introduced to the aquariums. Experimental conditions with an average of 60% air saturation (AS) or above were termed as "oxic all" (Figure 4a). Worms were distributed throughout the aquarium for the course of the experiment with no recognisable zone of preference. During the experiments all worms moved downwards in the aquarium at various rates. This was followed by almost immediate oscillating movements along the height of the aquarium in an erratic non-recognisable pattern, in some cases up to 10 cm amplitude.

Experiments termed as "hypoxic all" were adjusted to < 30% AS. Occasionally small pockets exceeding this concentration formed over time. Comparing all experiments, no clear zone of preference could be determined (Figure 4b). For example, in experiment 1 worms were distributed throughout the aquarium, in experiment 2) preferentially at the bottom of the aquarium. Worms oscillated in a directed sinuous pattern with amplitudes of up to 16 cm.

"Hypoxic bottom" conditions were set with < 30% AS at the bottom of the aquarium and 40 – 60% AS at the top. A split in the worm population was observed between the zones (Figure 4c), however the general trend of worm movement was directed towards the bottom of the aquarium. In two of the three experiments worms reside in and follow the chemocline interface. Occasional "dips" into the hypoxic zones were observed followed by realignment with the interface. Oscillation of worms was generally observed in small frequent vertical movements. Compared to other oxic conditions worms did not move through the height of aquarium as frequently and generally resided in specific regions of the aquarium.

"Hypoxic top" experiments were set to 30% AS in the top part of the aquarium and 60% AS in the bottom (Figure 4d). Of the five experiments two revealed worms

taking preference to the top hypoxic layer, two to the oxic bottom and one with worms distributed throughout the aquarium. Irrelevant of the overall zone of preference however, worms oscillate with amplitudes large enough to bring them into the other corresponding zone of the aquarium. Shuttling between the two zones varies from 5 to 60 min in some cases.

Hydrogen sulphide: To analyse the effect that substrate had on worm migration, whist eliminating the influence of oxygen, H_2S was tested in hypoxic conditions only (< 30 % AS) (Figure 4e). Experiments with hydrogen sulphide distributed uniformly in the aquarium, termed "H_2S all", showed an average substrate concentration of 40336 nM at the start of the run and 6520 nM at the end (a 84% substrate decrease) between all experiments. Worms distributed through the aquarium, on both the vertical and horizontal axis, with no clear zone of preference. Worm activity was very high with frequent erratic oscillations of amplitudes between 4 and 16 cm on times scales between 3 to 15 minutes.

Experiments with hydrogen sulphide on the top of the aquarium (Figure 4f) averaged at 25303 nM H_2S at the start and finished with 1318 nM (a 99.9% substrate decrease) in the top half of the aquarium. On average 203 nM was found in the bottom half of the aquarium (a 0.01% contamination) for all experiments. Oxygen gradients were < 25% AS in the top half and <20% AS in the bottom. Worms were primarily found in the top, H_2S rich, layers of the aquarium with highest occurrence around the chemocline between the two zones. However, over the course of the experiment worms also showed high occurrence at the very bottom of the aquarium. Oscillation was fast and erratic on small vertical scales of only a few centimetres. A shuttling into zones of less H_2S concentrations was observed regularly for short time periods between 5 and 10 minutes.

Hydrogen sulphide in the bottom of the aquarium (Figure 4g) measured an average of 20157 nM at the start and 2449 nM at the end of the experiment (a 88%

substrate decrease) in the bottom of the aquarium and 743 nM in the top half (3.6% contamination). Over the course of the experiments worms resided preferentially in H_2S rich zones at the bottom of the aquarium. In one experiment worms were found to reside in the interface zone. Oscillation occurred regularly, on very short time scales of 5 to 10 minutes, between the two zones with amplitudes ranging from 5 to 10 cm.

Carbon monoxide: all experiments were conducted in hypoxic conditions (< 30% AS) only. Experiments with carbon monoxide distributed evenly throughout the entire aquarium and termed "CO all", measured an average concentration of 1120 nM carbon monoxide at the beginning and 940 nM (a 16% substrate decrease) at the end for all experiments (Figure 4h). Oxygen concentrations within the aquarium were generally around < 20% AS with occasional small patches reaching a maximum of ~ 40% AS. The worm population often split between the top and bottom of the aquarium. Constant oscillation was observed on time scales between 5 and 30 min with amplitudes of 3 to 12 cm.

Experiments with CO on the top half of the aquarium (Figure 4i) averaged with a start concentration of 1278 nM and ended with 774 nM (39% substrate decrease) and 195 nM (15% contamination) in the bottom half of the experiment. Oxygen concentrations were < 20% AS in the bottom of the aquarium and between 20% and 30% AS in the top. Over the course of the run worms primarily resided in the top half of the aquarium with some occasionally moving downward. Regular shuttling with oscillations of amplitudes from 2 to 6 cm are observed into zones with lower CO concentrations.

CO in the bottom of the aquarium (Figure 4j) averaged as 1119 nM at the start of the experiments and 678 nM at the end (39% substrate decrease) with an average of 269 nM (24% contamination) in the top zone. Oxygen concentrations were < 20% AS in the bottom of the aquarium and between 20% and 30% AS in the top. Worms moved

downward and resided either in CO rich zones or in the chemocline between higher and lower oxygen concentrations. Between the two zones movement of worms in a highly regulated sinus oscillation-like manner with amplitudes between 2 and 8 cm were observed.

Hydrogen: all experiments were conducted in hypoxic (< 30% AS) conditions. H_2 distributed thorough the entire aquarium, termed "H_2 all" (Figure 4k) averaged with a start concentration of 5938 nM and an end of 3879 nM (35% substrate decrease). Oxygen concentrations measured < 20% AS in the bottom of the aquarium and ~ 25% AS in the top with occasional pockets of higher oxia forming. A general trend of worms migrating downward was observed whilst avoiding pockets of higher oxia. Vertical oscillations were of low frequency and low amplitude.

H_2 on top (Figure 4l) measured an average start concentration of 4608 nM and an end [c] of 2124 nM (54% substrate decrease) for the top of the aquarium and 961 nM on the bottom (21% contamination). Oxygen concentrations measured < 20% AS in the bottom of the aquarium and ~ 25% AS in the top. In all experiments worms migrated downwards, away from areas of high H_2 concentrations and resided there for the remainder of the experiment. Vertical oscillations were with high frequency and low amplitude that do not reach into high H_2 zones.

H_2 on the bottom of the aquarium (Figure 4m) averaged a start concentration of 5003 nM and an end concentration of 2508 nM on the bottom (50% substrate decrease) and 839 nM (17% contamination) on the top. Oxygen concentrations measured < 20% AS in the bottom of the aquarium and 20 – 30% AS in the top. Worms resided in the top of the aquarium in zones of low H_2 concentration over the entire course of the experiment. One worm moved into the hypoxic, H_2 rich, bottom layer of the aquarium for 60 minutes

before moving back to the top. Oscillation of worms was noted with a frequency of roughly 5 minutes and amplitudes of 3-5 cm.

All GC-MS measurements are shown in SI Table 1.

Discussion

Oxygen: Experiments testing worm distribution along oxic gradients showed preference to the chemocline region and higher preference to hypoxic zones over oxic ones. In all cases shuttling between oxic and hypoxic zones was observed regularly. Worms migrate downward over the course of the experiments in both "oxic all" and "hypoxic all" experiments indicating that geotaxis plays an initial role in their distribution (SI Figure 4 & 5, all experiments). When oxygen gradients are present geotaxis appears to be coupled with chemotaxis in determining the worms position. Worms took preference to zones of higher anoxia, which are actively sought out by immediate geotactile downward migration at the start of the experiment (SI Figure 7, experiment 1, 2 & 4). In some cases however, there is a split of the worm population into different zones after initial residence in the hypoxic region (SI Figure 6, experiment 1 & 5). This is not surprising when considering that no reduced substrates are present in these experiments and that hypoxia alone does not fulfil the nutritional requirements for all symbionts. We interpret this as indication that the oxic gradient alone does not determine the permanent distribution of worms in the sediment. Rather it appears that this behaviour fulfils the worm's own demand for oxygen whilst additionally providing the primary γ1 symbiont with the conditions it requires to oxidise stored sulphur compounds. Further we postulate that the variance in behaviour between individual worms is most likely due to a difference in physiological state at the start of each experiment. For example, in "oxic all"

experiments, worms followed the general trend of downward migration. However, this occurred at different rates for each individual in the experiment. A worm with depleted energy reserves may be more likely to reside in oxic zones for prolonged periods of time as energy can potentially be gained by oxidation of stored sulphur compounds by sulphur oxidising symbionts.

Hydrogen sulphide: In H_2S experiments worms reside primarily in zones with high substrate concentration for prolonged periods of time whilst periodically shuttling into zones with no or less H_2S. Experiments with H_2S in the top half and ~30 % AS showed worms to reside there preferentially over areas of higher anoxia (~10% AS) with no H_2S (SI Figure 9, Experiment 1, 2 and 3). We conclude that indeed H_2S itself drives worm distribution, when and if it is available, rather than the oxic gradient alone. Further, geotaxis does not play a decisive role for worm migration when confronted with a chemical gradient. In experiments with H_2S on the top of the aquarium worms did not migrate downwards, in experiments with H_2S on the bottom worms migrated downwards almost immediately at the start of the experiment (SI Figure 10, experiment 1, 3 & 4).

Whether the worms themselves have the ability to sense H_2S remains unclear at this time. H_2S has however been attributed as a "universal and phylogenetically ancient O_2 sensing mechanism" and it does therefore not seem unreasonable that worms can at least partially detect H_2S (Olson, 2015).

Carbon monoxide: CO experiments showed a similar trend to H_2S experiments, whereby worms reside primarily around the chemocline or in CO enriched zones. Frequent oscillation into anoxic zones with less substrate was observed. The amount of available CO seems to be the key factor in determining worm distribution and not necessarily oxic gradients. Worms preferentially resided in CO rich zones with higher O_2 concentration than in CO poor, anoxic zones. This is of particular interest as the γ3

symbiont was shown to utilise an aerobic carbon monoxide dehydrogenase, which yields more net energy than anaerobic CO oxidation. Similarly to H_2S, the presence of CO seems to be a stronger factor for the influence on worm distribution over oxygen alone (SI Figure 12, Experiment 3). During experiments with CO in the bottom of the aquarium worms level off at the chemocline (SI Figure 13, All experiments) and regularly oscillate into zones with less substrate. Chemotaxis towards CO took preference over geotaxis during our CO top experiments in which worms were not inclined to travel to the bottom of the aquarium. In CO bottom experiments worms do travel downwards until stabilising at the chemocline where CO becomes available.

Long exposure for an animal host to high levels of CO could result in carbon monoxide poisoning, whereby CO substitutes oxygen on the binding site of haemoglobin. The high tolerance to CO can be explained by the high abundance of the oxygen binding protein hemerythrin found in worms (Wippler *et al.,* in prep). Hemerythrin is a non-haemal containing protein onto which bound oxygen is not substituted by carbon monoxide.

Hydrogen: Experiments with hydrogen gradients preferentially show worms to resided in substrate poor zones of the aquarium (SI Figure 15, all experiments. SI Figure16, experiments 1, 2 & 3). Worms levelled off in the anoxic zones above or below the area of substrate enrichment respectively. Geotaxis of worms is not overcome by chemotaxis in experiments with H_2 enrichment on the top of the aquarium (SI Figure 15). In these experiments worms migrated down immediately irrelevant of the high substrate availability provided. This was generally not observed for H_2S or CO experiments. In H_2 bottom experiments worms do not migrate downwards into hypoxic, H_2 enriched zones and generally stay in the top of the aquarium. During these experiments it appeared as though worms avoid H_2 rich zones in the aquaria. This is surprising when considering

that, in contrast to H_2S and CO, H_2 has no known toxic effect for a metazoan host but seems to be avoided all the same. Kleiner *et al.,* 2015 showed that although rates of H_2 consumption by worms were high (11 ± 1 µmol g^{-1} (wet weight) h^{-1}) there was no increase in labelled $^{13}CO_2$ fixation during anaerobic incubation experiments. It was suggested that δ-proteobacteria utilise energy gained by H_2 oxidation to break down and use alternative organic carbon sources, such as fatty acids, by lithoheterotrophy, which would explain why $^{13}CO_2$ was not incorporated into biomass. Further, hydrogenases were shown to be of high affinity, which can utilise very low H_2 concentrations, and are only expressed when hydrogen is available in anaerobic conditions (Kleiner *et al.,* 2012). One could speculate that the hypoxic conditions in the aquaria (< 10% AS in zones of highest H_2 concentration) contained too much oxygen to drive anaerobic hydrogen oxidation optimally and therefore expression of hydrogenases. This does not however, explain the apparent avoidance of these H_2 enriched hypoxic zones because conditions more suitable for anaerobic hydrogen oxidation are still offered over aerobic zones that worms resided in preferentially. In addition, if hydrogen had no influence on worm distribution at all then we would expect to find worms randomly distributed throughout the aquarium as was observed for experiments with hypoxic conditions only and no additional substrate.

Sulphate is ubiquitously available in seawater and required as terminal electron acceptor during anaerobic H_2 oxidation, yielding 36 % (85 ΔG_0 [kJ/rnx]) less energy per reaction than the use of oxygen in aerobic H_2 oxidation (Table 1). Low H_2 concentrations are indeed sufficient for hydrogen oxidation as the hydrogenases of the δ-proteobacterial symbionts are of high affinity. Once the enzyme has reached V_{max} additional hydrogen availability is superfluous because no net energy gain can be achieved as the substrate cannot be utilised. The total hydrogen concentration available is therefore not of relevance once V_{max} has been reached. If higher oxic conditions were available whilst

still offering sufficient hydrogen concentrations for hydrogenases to reach V_{max} then an aerobic hydrogen oxidation pathway would be more profitable for the overall net energy yield of the holobiont. Proteomics studies did not find the presence of aerobic hydrogenases in any of the symbionts of *O. algarvensis* (M. Kleiner personal communication). However, their presence amongst the γ-proteobacteria is not excluded and open to future investigation. If γ-proteobacterial symbionts had the ability to oxidise hydrogen under oxic conditions, then the speculative implication based on our behavioural observation in these experiments would be that aerobic hydrogen oxidation is recognised as energetically more favourable by the holobiont. Anaerobic hydrogen oxidation by the δ-proteobacterial symbionts would therefore be considered a secondary metabolic pathway in the overall net energy gain for the host.

General discussion: As already suggested by Ott *et al*., 1991, the universal strategy of migration between oxidised and reduced sediment layers for marine meiofauna in symbiosis with chemosynthetic bacteria is required to meet the symbionts metabolic demands. The geochemical properties and distribution of the chemocline in marine sediments creates a dynamic "landscape" which is subjected to constant shifts based primarily on hydrodynamic forces but also sediment properties and organic content (Ott and Novak, 1989). Unlike, for example, copepods that rely on geotaxis for migration through the water column to feed on phytoplankton in euphotic zones, migration by chemotaxis along chemical gradients is a more suitable strategy in environments that are subjected to constant chemocline and substrate shifts in a non-directional manner. This also applies to free-living chemosynthetic bacteria, which need to position themselves in the relatively large fraction between oxidised and reduced sediment layers to gain access to the required substrates for their metabolic demands. Adaptation to changing conditions,

such as motility or filamentous morphotypes, is therefore highly advantageous if a free-living bacterial species is to be viable in an ecosystem. For example, the filamentous sulphur oxidising bacteria *Beggiatoa sp.* position themselves in the sediment to access a wide range of microzonations over the length of a single cell (Schwedt *et al.,* 2011). Compared to a free-living strategy, the association with motile animal hosts ensures active transport between oxidised, reduced and chemocline sediment layers on short times scales and increases substrate availability to the associated bacteria. The time scale that transport occurs on has however been unclear for the gutless oligochaete symbiosis so far.

In our experiments shuttling of worms between oxic gradients took place on short time scales. When oxygen is available, worms "dip" into oxygen rich zones regularly presumably to fulfil their own oxygen demands but also to provide conditions for γ-proteobacterial symbionts to oxidise sulphur storage compounds. In reduced zones worms were able to tolerate hypoxic conditions for prolonged periods of time. The expression of proteins for anaerobic metabolism of the host and the high oxygen carrying capacity of oxygen binding molecules in its circulatory system presumably facilitate this (Kleiner *et al.,* 2012) (Wippler in prep.). Unlike symbiotic meiofaunal species that only harbour sulphide oxidising symbionts, the utilisation of an anaerobic sulphate reducer is highly profitable for the net energy gain of *O. algarvensis* which can tolerate anaerobic conditions for prolonged periods of time.

In experiments that tested various reduced substrates, with only hypoxic conditions throughout the aquarium, oscillation of worms was also observed between chemical gradients. This indicates that oxygen is not the only factor for determining worm migratory behaviour and that indeed substrates themselves play an important role for worm distribution. Alignment to H_2S, CO and H_2 chemical gradients occurred very rapidly, which may suggest an underlying detection mechanism for reduced substrates by

one of the two partners. We currently have no data to suggest how such a mechanism may work and three possibilities are presented for discussion. i) although unknown in the animal kingdom, the host may have evolved a sensory organ for the detection of CO and H_2 resulting from an adaptation to the symbiosis. ii) sensory organs that originally had a different substrate specificity cross-detect CO and H_2 and the host has evolved a behavioural response to signals detected from pre-existing receptors. iii) the symbiont consortium acts as a chemoreceptor for the holobiont by detecting CO and H_2 and through release of an as of yet unknown signal which triggers a motile response in the host. Albeit true that without direct evidence for the signalling molecules involved the assumption of host regulation by its symbionts may be premature we have begun to tease apart the influence of individual substrates on the behaviour of the worms and gained insight into their ecology.

Hypothetical aspects

The following mechanistic hypothesis is proposed to expand on the speculation that a signal transduction pathway between host and symbiont is in place to determine worm distribution; A recent study shows that electrical signals are used in bacterial biofilms for communication through K^+ initiated ion channel activity, much the same as the action potential in neurons (Prindle *et al.,* 2015). The release of K^+ by a bacterial cell, after receiving a metabolic trigger, depolarises a neighbouring cell, and transmits a signal through the biofilm community. The nervous system of gutless oligochaetes extends into the epidermis, and brings neurons and sensory cells into the proximity of the bacterial consortium (A. Gruhl unpublished data). It is therefore not unreasonable to speculate that the release of K^+ ions from bacterial cells of the symbiotic consortium may cause an action potential in a host neuron. Differences in outer ion concentrations result in a

change of membrane potential, which can open ion channels depolarising a host cell. In this manner the host has the potential to recognise metabolic triggers of relevance to the bacterial community such as, for example, the presence of reduced substrate. Further indication for this hypothesis may also come from Hydra, a cnidarian basal to all metazoans. Recent findings indicate the possibility that the evolution of the nervous system in these animals has its origins in a communicative role between the animal and its associated microbiota (T.C.G. Bosch personal communication). Whether active signalling via the neural network, transfer of carbohydrates between host and symbiont or the use of other signalling molecules lies behind a potential signal transduction pathway is open to further investigation. In any case the presence of such pathways between symbiont and host are hypothesised to be present and may play a crucial role in the ecological regulation of worm distribution.

In conclusion, we speculate that in addition to fulfilling the hosts nutritional demands and waste disposal, symbionts also play a role in the chemotactic capability of the host and act as a nutritionally based chemical sensory organ for the holobiont.

Acknowledgments: We thank Miriam Weber and Christian Lott at the HYDRA field station on Elba, Italy, for help with sample collection and experiments. Georg Herz at the Max-Planck-Institute for marine microbiology for technical assistance and construction of aquaria. This work was funded by European Union (EU) Marie Curie Actions Initial Training Network (ITN) SYMBIOMICS (contract number 264774) and the Max Planck Society.

2.1 Further aspects to Chapter II

The method for analysis of substrate dependant worm distribution presented in this Chapter has a potential broad applicability. The analysis of chemotactic behaviour related to chemical substrate gradients in other biological systems can be tested using this workflow. Such systems could include chemosynthetic symbiotic systems such as

nematodes, ciliates and lucinidae bivalves as well as chemotactic response of non-symbiotic organism such as *Caenorhabditis elegans.* The non-invasive use of planar optodes for real-time measurements of oxygen can be expanded to monitor other analytes such as pH and CO_2. Further, the potential is given to include microsensors, via the inlets on the side of the aquarium, for real-time measurement of an additional array of chemical parameters such as H_2S, CO, H_2, NO_3^- and SO_4^- amongst others.

The presented method for data analysis shown provides both visual and numerical data on worm distribution in aquaria during our experiments. Statements on worm behaviour and their preference to chemical gradients were made based on combinatorial analysis of both these data sets. However, some technical hurdles still need to be overcome to optimise data representation as it is shown in this thesis. For example, the image Z-stack summation (Figure 3c) shows large dark areas caused by condensation of water on the aquarium wall and the refraction of light from the excitation flash on the MOLLIE system (e.g. SI Figure 13, experiment 2). These disturbance events are also seen in in the worm 3D projection Y-axis rotation (Figure 3d). For data analysis and statements made in this thesis the worm and optode 3D projection Y-axis rotation image sets were used. All other data representation (Figure 3a, b and c) was included to show the reader the analytical possibilities with the tools that were developed, even if additional optimisation is required to make conclusive, statistically valid, statements. Indeed work on optimisation has already been conducted, whereby worms themselves are recognised and tracked through an entire image set. All other pixels not recognised as worms are removed from each frame and in this manner disturbance events are eliminated and a clean data set produced. The developed Python script used to achieve this, and an example .gif of its functioning, is included in the attached digital files to this thesis

(Chapter_II_Phython_script.gif & Chapter_II_Phython_Scripts) (copyright with, and courtesy of, A. Kreutzmann).

References

Dubilier N, Bergin C, Lott C. (2008). Symbiotic diversity in marine animals: the art of harnessing chemosynthesis. *Microbiol* **6**: 725–740.

Dubilier N, Mulders C, Ferdelman T, de Beer D, Pernthaler A, Klein M, *et al.,* (2001). Endosymbiotic sulphate-reducing and sulphide-oxidizing bacteria in an oligochaete worm. *Nature* **411**: 298–302.

Felbeck H. (1981). Chemoautotrophic Potential of the Hydrothermal Vent Tube Worm, Riftia pachyptila Jones (Vestimentifera). *Science* **213**: 336–338.

Giere O, Conway NM, Gastrock G, Schmidt C. (1991). "Regulation" of gutless annelid ecology by endosymbiotic bacteria. *Mar Ecol Prog Ser*. **68:** 287-299

Gordon J, Knowlton N, Relman DA, Rohwer F. (2010). Superorganisms and holobionts. *Issues*. http://www.microbemagazine.org/index.php?option=com_content&view=article&id=6300:superorganisms-and-holobionts&Itemid=1464

Hay ME. (2009). Marine chemical ecology: chemical signals and cues structure marine populations, communities, and ecosystems. *Ann Rev Mar Sci* **1**: 193–212.

Holst G, Grunwald B. (2014). Luminescence lifetime imaging with transparent oxygen optodes. *Sensor Actuat B-Chem* **74**: 1–13.

Holst G, Kohls O, Klimant I, König B, Kühl M. (1998). A modular luminescence lifetime imaging system for mapping oxygen distribution in biological samples. *Sensor Actuat B-Chem*. **51:**163-170

Kleiner M. (2012). Metabolism and Evolutionary Ecology of Chemosynthetic Symbionts from Marine Invertebrates. Deutsche Nationalbibliothek. Doctoral Thesis - University of Bremen, Bremen.

Kleiner M, Wentrup C, Holler T, Lavik G, Harder J, Lott C, *et al.,* (2015). Use of carbon monoxide and hydrogen by a bacteria-animal symbiosis from seagrass sediments. *Environ Microbiol*. doi:10.1111/1462-2920.12912.

Kleiner M, Wentrup C, Lott C. (2012). Metaproteomics of a gutless marine worm and its symbiotic microbial community reveal unusual pathways for carbon and energy use. PNAS **109**: E1173–E1182.

Kleiner M, Young JC, Shah M, VerBerkmoes NC, Dubilier N. (2013). Metaproteomics reveals abundant transposase expression in mutualistic endosymbionts. *MBio* **4**: e00223–13.

Levin LA, Ekau W, Gooday AJ, Jorissen F, Middelburg JJ, Naqvi SWA, *et al.,* (2009). Effects of natural and human-induced hypoxia on coastal benthos. *Biogeosciences* **6**: 1–36.

Meyers MB, Fossing H, Powell EN. (1987). Microdistribution of Interstitial Meiofauna, Oxygen and Sulfide Gradients, and the Tubes of Macro-Infauna. *Mar Ecol Prog Ser* **35**: 223–241.

Morse D, Sethi J, Choi AMK. (2002). Carbon monoxide-dependent signaling. *Crit Care Med* **30**: S12–7.

Naqvi SWA, Bange HW, Farías L, Monteiro PMS, Scranton MI, Zhang J. (2010). Marine hypoxia/anoxia as a source of CH_4 and N_2O. *Biogeosciences* **7**: 2159–2190.

Olson KR. (2015). Hydrogen sulfide as an oxygen sensor. *Antioxid Redox Signal* **22**: 377–397.

Ott JA, Novak R. (1989). Living at an interface: Meiofauna at the oxygen/sulfide boundary of marine sediments. Reproduction, genetics and distributions of marine organisms. 23rd European Marine Biology Symposium. P415-422

Ott JA, Novak R, Schiemer F, Hentschel U. (1991). Tackling the sulfide gradient: a novel strategy involving marine nematodes and chemoautotrophic ectosymbionts. *Mar Ecol* **12:** 261-279

Petersen JM, Zielinski FU, Pape T, Seifert R, Moraru C, Amann R, *et al.,* (2011). Hydrogen is an energy source for hydrothermal vent symbioses. *Nature* **476**: 176–180.

Prindle A, Liu J, Asally M, Ly S, Garcia-Ojalvo J, Süel GM. (2015). Ion channels enable electrical communication in bacterial communities. *Nature* **527**: 59–63.

Rohwer F, Seguritan V, Azam F, Knowlton N. (2002). Diversity and distribution of coral-associated bacteria. *Mar Ecol Prog Ser* **243**: 1–10.

Schindelin J, Arganda-Carreras I, Frise E, Kaynig V, Longair M, Pietzsch T, *et al.,* (2012). Fiji: an open-source platform for biological-image analysis. *Nat Meth* **9**: 676–682.

Schneider CA, Rasband WS, Eliceiri KW. (2012). NIH Image to ImageJ: 25 years of image analysis. *Nat Meth* **9**: 671–675.

Schwedt A, Kreutzmann AC, Polerecky L. (2011). Sulfur respiration in a marine chemolithoautotrophic Beggiatoa strain. *Front Microbiol* **2**: 276.

Wadhams GH, Armitage JP. (2004). Making sense of it all: bacterial chemotaxis. *Nat Rev Mol Cell Biol* **5**: 1024–1037.

Wentrup C. (2012). Acquisition and activity of bacterial symbionts in marine invertebrates. Deutsche Nationalbibliothek. Doctoral Thesis - University of Bremen, Bremen.

Tables and Figures

Table 1: Energy yield (ΔG_0 [kJ/rnx]) of redox reaction for one mol substrate used by symbionts of the *O. algarvensis* symbiosis (Wentrup, 2012)

Substrate	e^- donor	e^- acceptor	Redox reaction	ΔG_0 [kJ/rnx]
aerobic				
Sulphide	H_2S	O_2	$H_2S + 2O_2 \rightarrow SO_4^{-2} + 2H^+$	-796
Carbon monoxide	CO	O_2	$CO + 0.5O_2 \rightarrow CO_2$	-257
hydrogen	H_2	O_2	$H_2 + 0.5O_2 \rightarrow H2O$	-237
anaerobic				
Carbon monoxide oxidation / sulphate reduction	CO	SO_4^{-3}	$4CO + SO_4^{-2} + 2H^+ \rightarrow H_2S + 4\ CO_2$	-272
Hydrogen oxidation / sulphate reduction	H_2	SO_4^{-3}	$4H_2 + SO_4^{-2} + H^+ \rightarrow HS- + 4H_2O$	-152

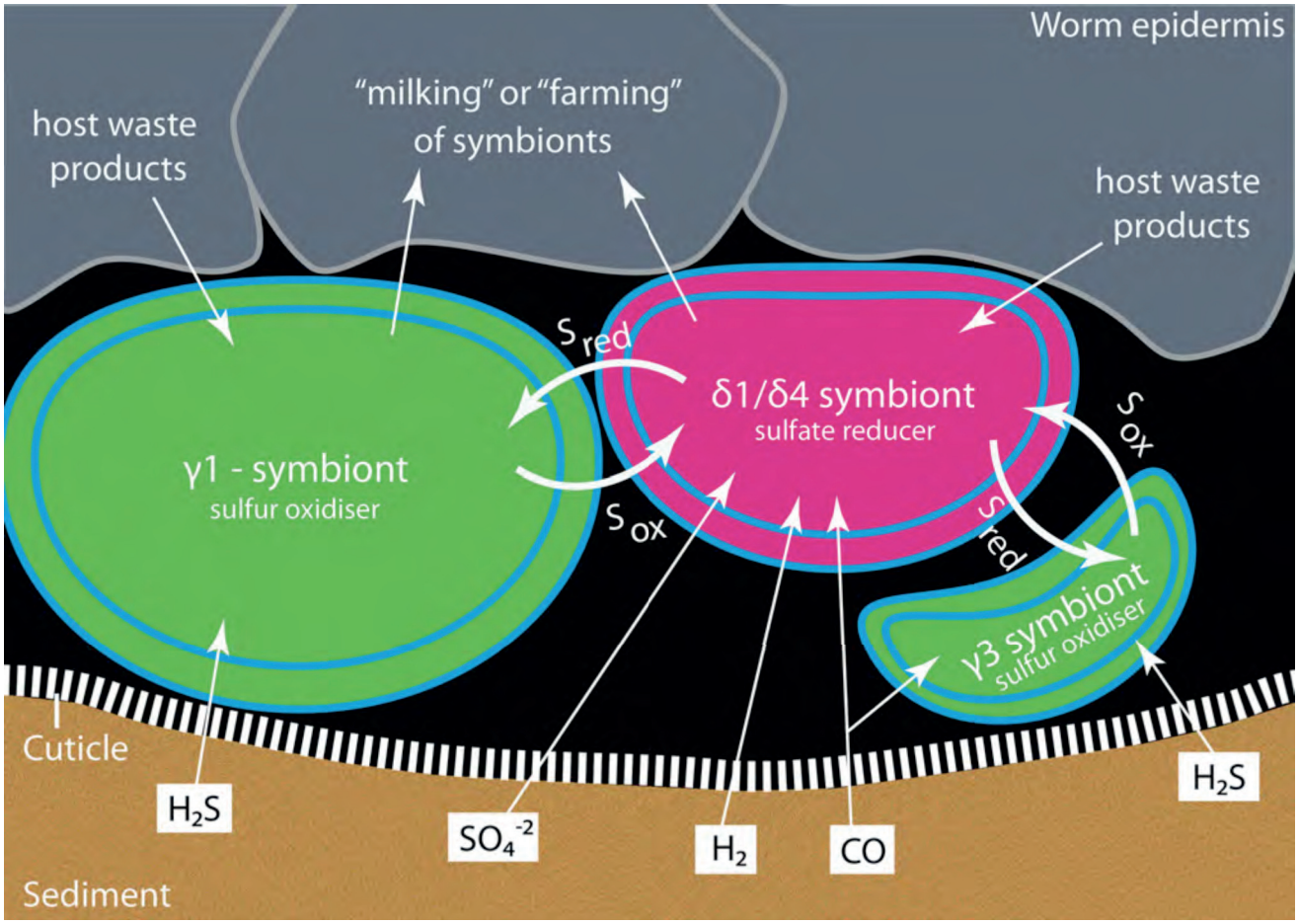

Figure 1: Simplified schematic depicting the symbiotic consortium of *Olavius algarvensis* and its metabolic potential (after Kleiner *et al.,* 2012). Reduced substrates from the sediment are accessed by the symbionts through the worms porous cuticle. Sulphide (H_2S) is oxidised by the sulphur oxidising γ1 & γ3-proteobacterial symbionts. Sulphate is (SO_4^{-2}) reduced by sulphate reducing δ1 & δ4-proteobacterial symbionts. Carbon monoxide (CO) can be used as energy source by both δ -symbionts and by the γ3-symbiont. Hydrogen (H_2) is utilised by the δ-symbionts only. Host waste products such as acetate, propionate or succinate can be metabolised by symbionts. How symbionts transfer fixed carbon to the host is unclear at this stage but two strategies are possible and not mutually exclusive: 1) "milking" – the active transfer of carbon compounds. 2) "farming" phago- or pinocytosis of symbiont cells by host epidermis.

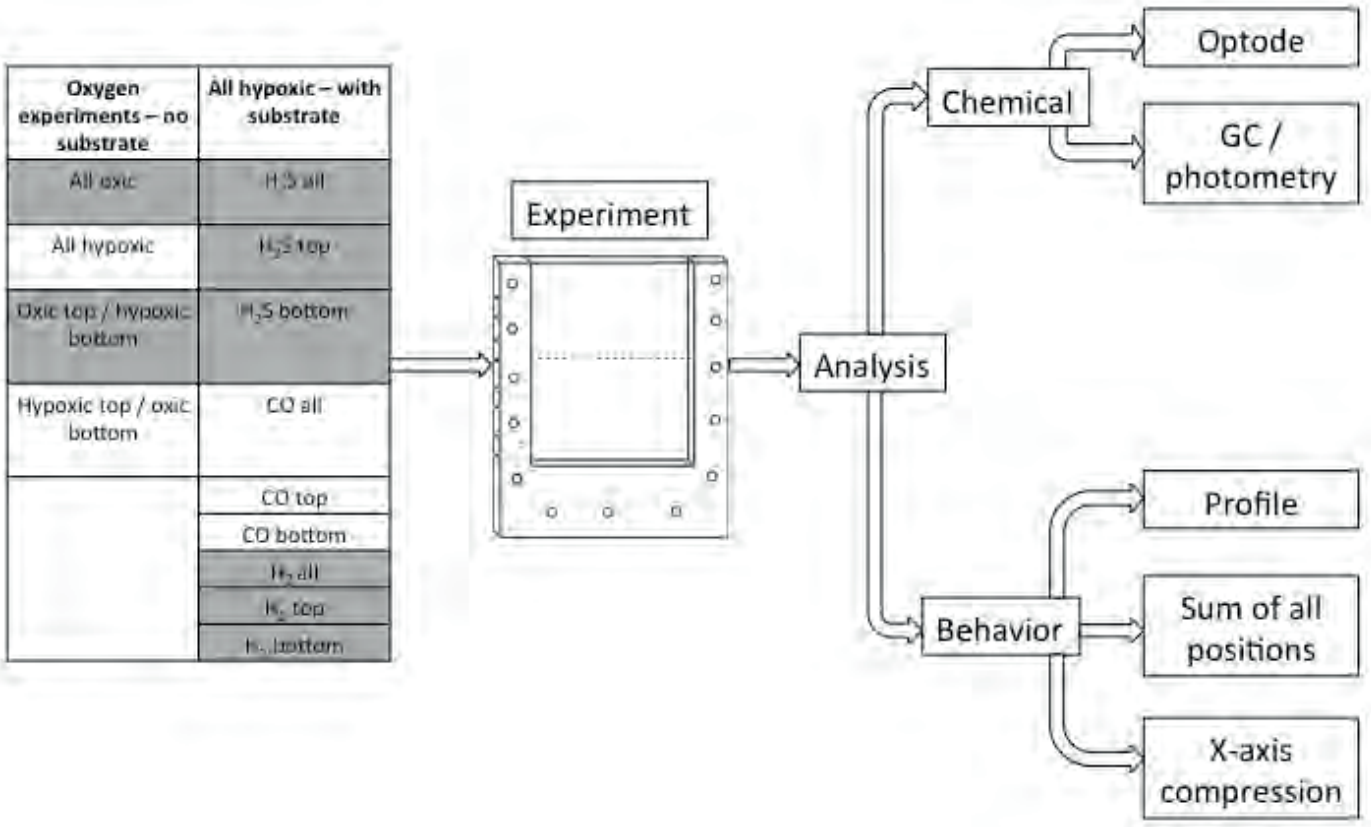

Figure 2: Workflow diagram showing the experimental conditions that were tested and the analytical output gained. During each experiment micrographs were taken every 15 seconds to monitor worm movement in the aquarium and to subsequently analyse behavioural patterns with use of novel imaging algorithms (Figure 3). Chemical conditions were monitored by planar optodes for oxygen distribution within the aquarium every 5 minutes during all experiments. At the start and end of each experiment with added substrate CO and H_2 concentration were measured by Gas chromatography (GC) and H_2S concentration by Diamine photometric analysis.

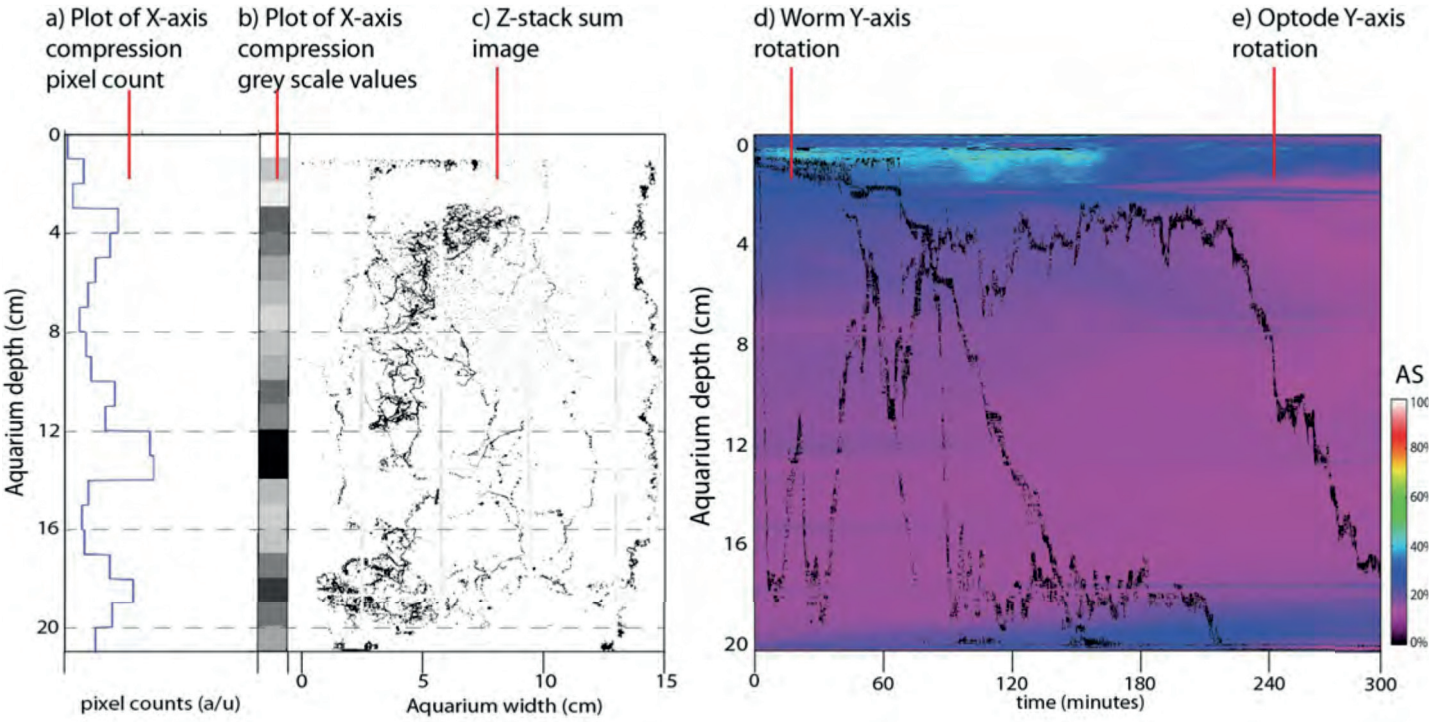

Figure 3: An example of the image set produced for each experiment after the application of all imaging algorithms to the raw image data. a) The pixel counts of all worm positions during the experiment plotted in 1 cm increments along the height of the aquarium. b) Grey scale plot representation of a). c) summed z-stack image file of all worm positions during the experiment. d) profile of worm movement in the aquarium over the course of an experiment. The image is produced by a 90° rotation on the Y-axis of a 3D rendered Z-stack. e) oxygen change and distribution over the course of the experiment produced by a 90° rotation along the Y-axis of a 3D rendered optode Z-stack. Optode scale bar: White = 100% AS, Black = 0 % AS.

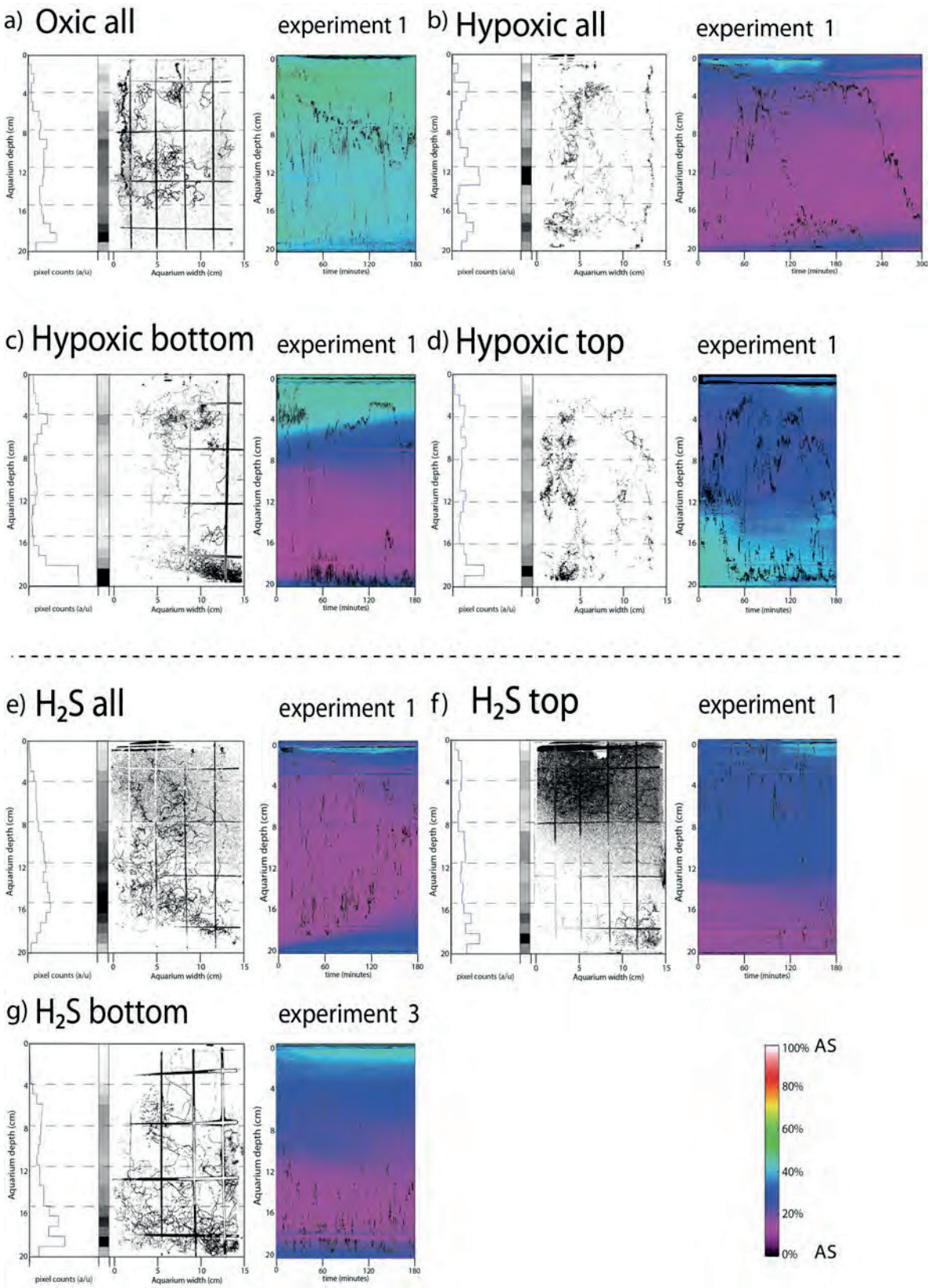
a) Oxic all
experiment 1
b) Hypoxic all
experiment 1
c) Hypoxic bottom
experiment 1
d) Hypoxic top
experiment 1
e) H2S all
experiment 1
f) H2S top
experiment 1
g) H2S bottom
experiment 3
Aquarium depth (cm)
pixel counts (a/u)
Aquarium width (cm)
time (minutes)
100% AS
80%
60%
40%
20%
0% AS

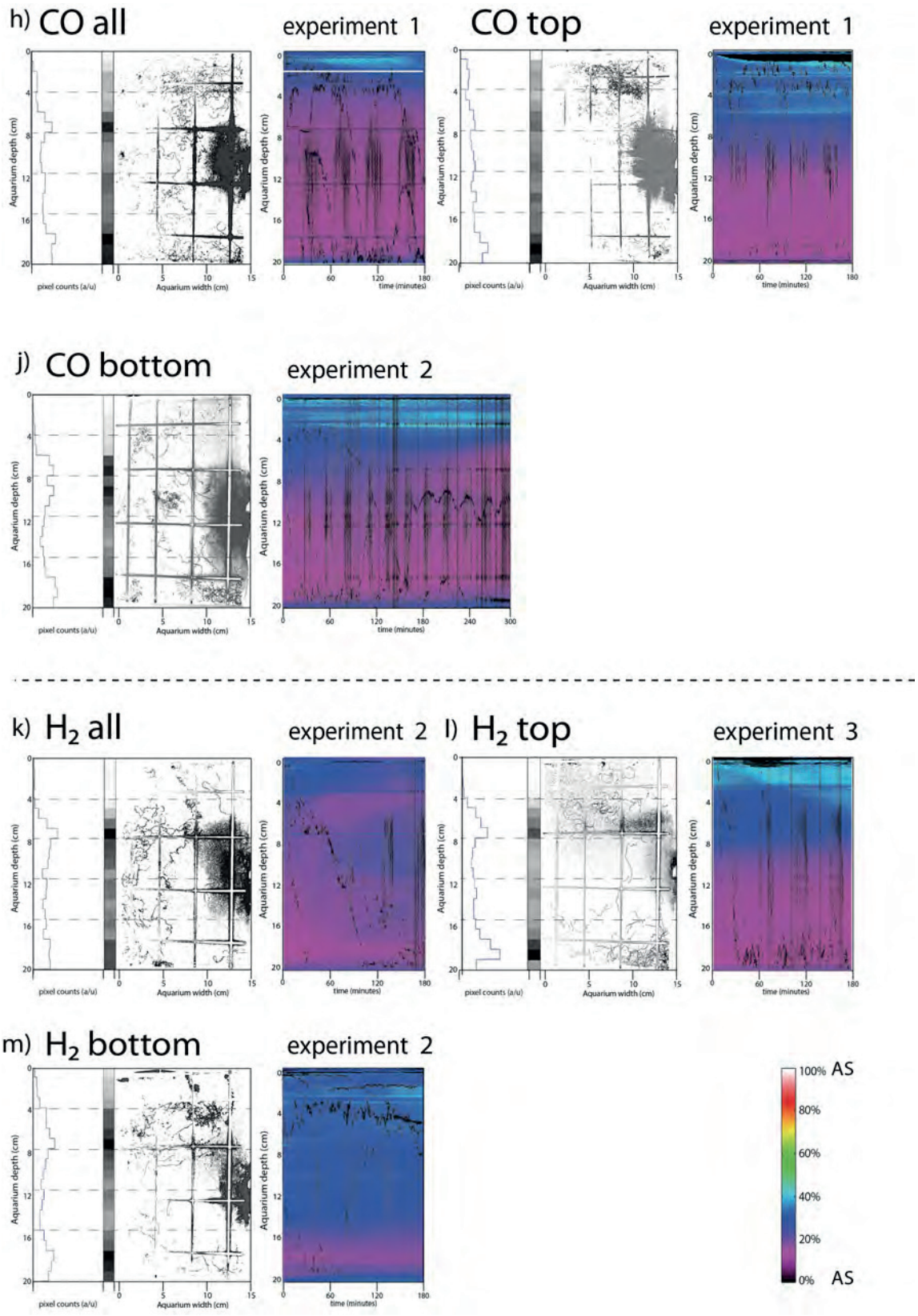

Figure 4: Examples for each incubation condition as described in Figure 2. All experiments were replicated at least n = 3. For individual experiments per condition please refer to SI Figure 4 – 16. GC-MS and photometry measurements are listed in SI Table 1.

Supplementary Information

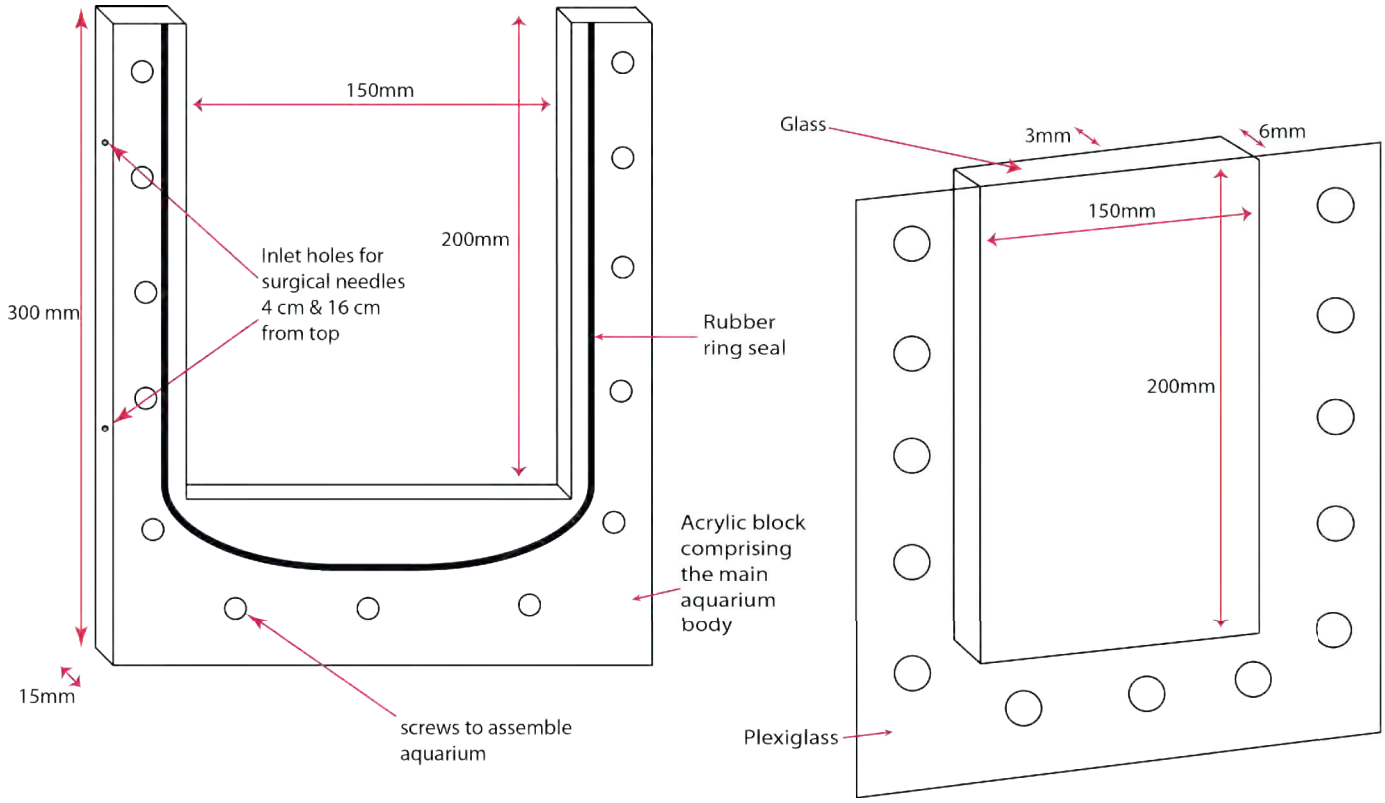

SI Figure 1: Schematic of flat aquaria used in the study. The removable front plate enables fast and easy access to the inside of the aquarium. After assembly the experimental chamber is comprised of a 3 mm spacing between the two glass panes and a total of 20 cm high and 15 cm wide. Surgical needle inlets at 4 cm and 16 cm from the top of the aquarium allows for pore water exchange of substrate-enriched seawater as well as for removal of samples for GC measurements at the end of each experiment.

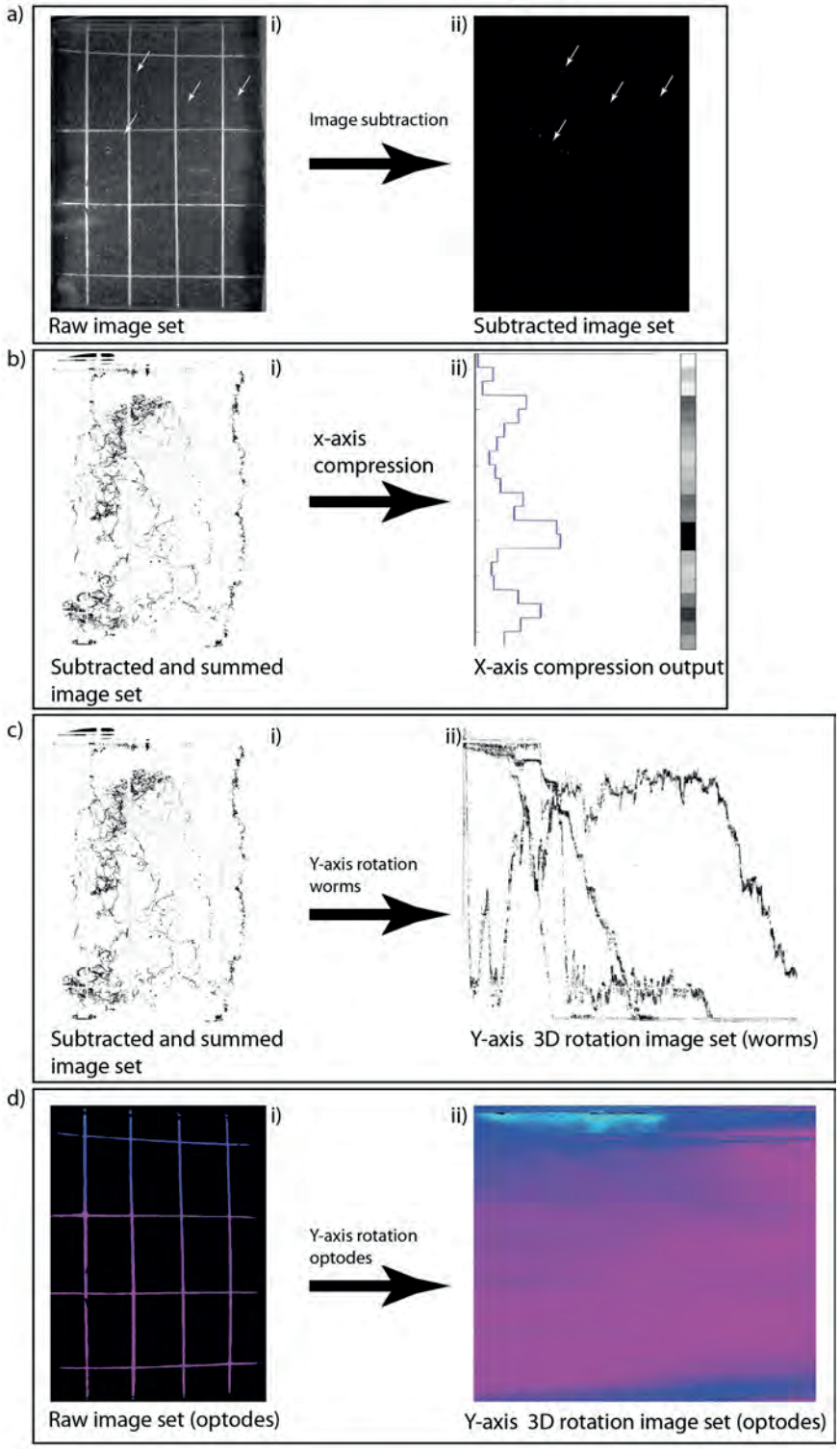

SI Figure 2: application of image editing algorithms used in this study. a) image subtraction algorithm (a-ii) on raw image files (a-i). Arrows indicate worm positions b) after "cleaning" of images by application of the subtraction algorithm a summation of all positions worms occupied during the experiment is made (b-i). This is subsequently used for pixel counts along the x-axis, which are plotted in a bar chart (b-ii) and visualized in a grey scale plot (b-iii). c) rotating the summed image of all worm positions by 90° along the Y-axis (c-ii) results in a profile of worm movement over time. d) the same principal as in c) applied to the optode data.

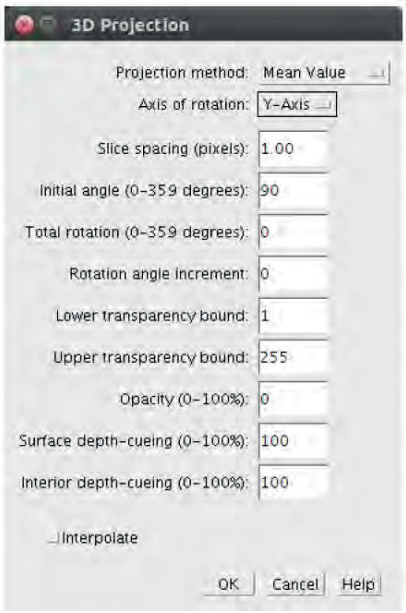

SI Figure 3: ImageJ settings for y-axis rotation parameters to produce a 3D model of optode data. Included in this thesis for reproducibility.

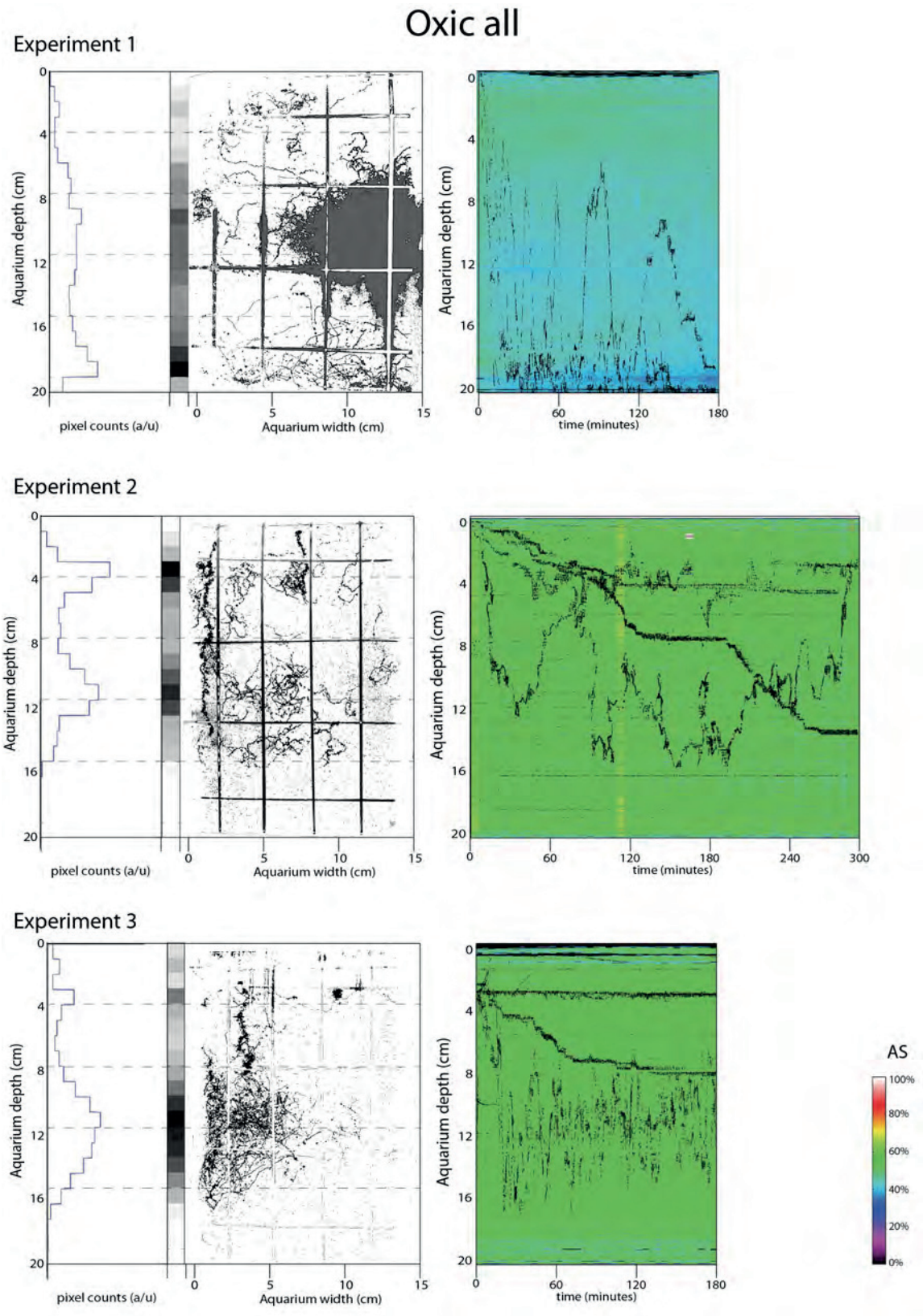

SI Figure 4: n=3 experiments with "oxic all" conditions in the aquaria and an average air saturation of 60%. Two experiments were run for 180 minutes and one for 300 minutes.

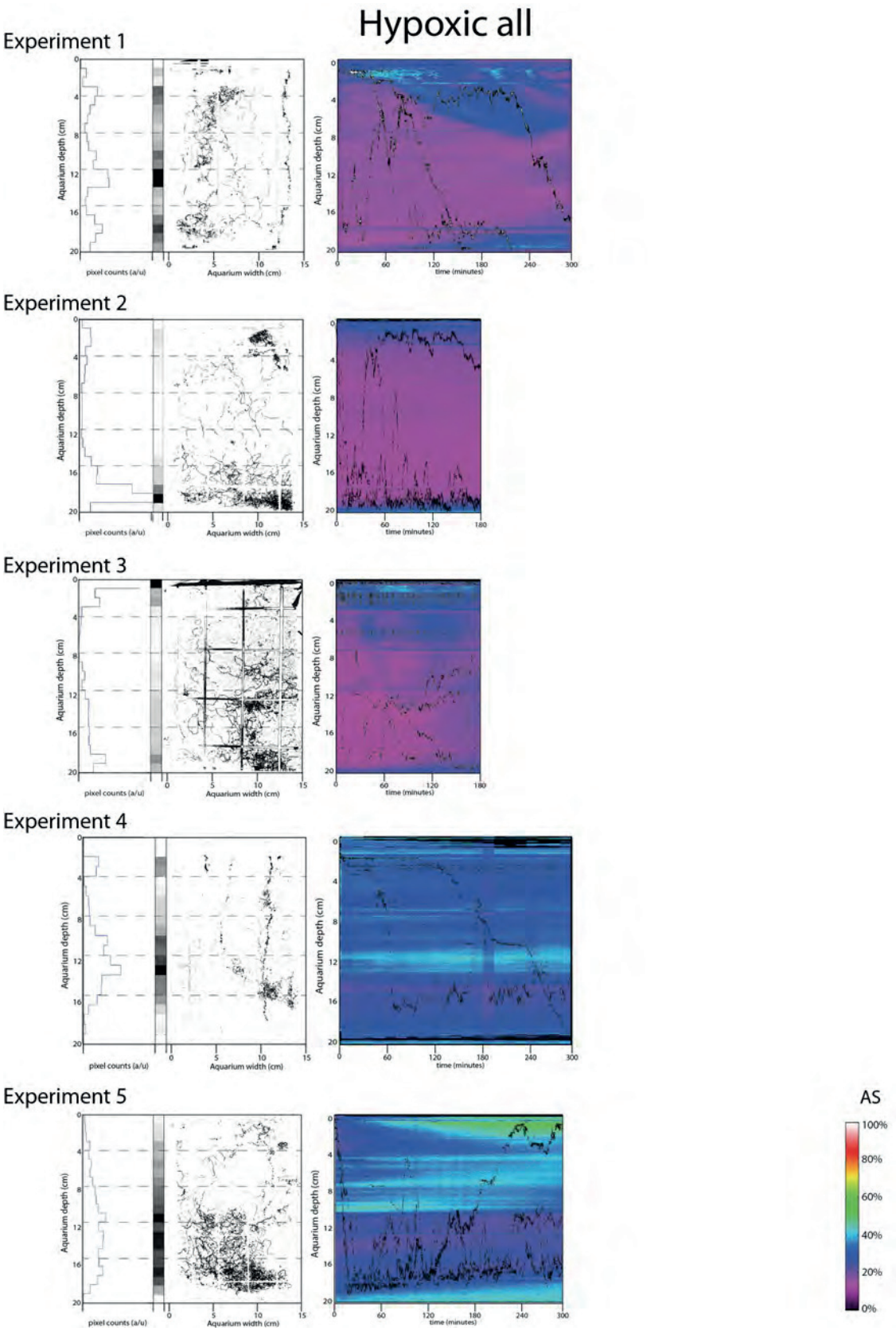

SI Figure 5: n=5 experiments with "Hypoxic all" conditions in the aquaria and an average air saturation of < 30%. Two experiments were run for 180 minutes and three for 300 minutes.

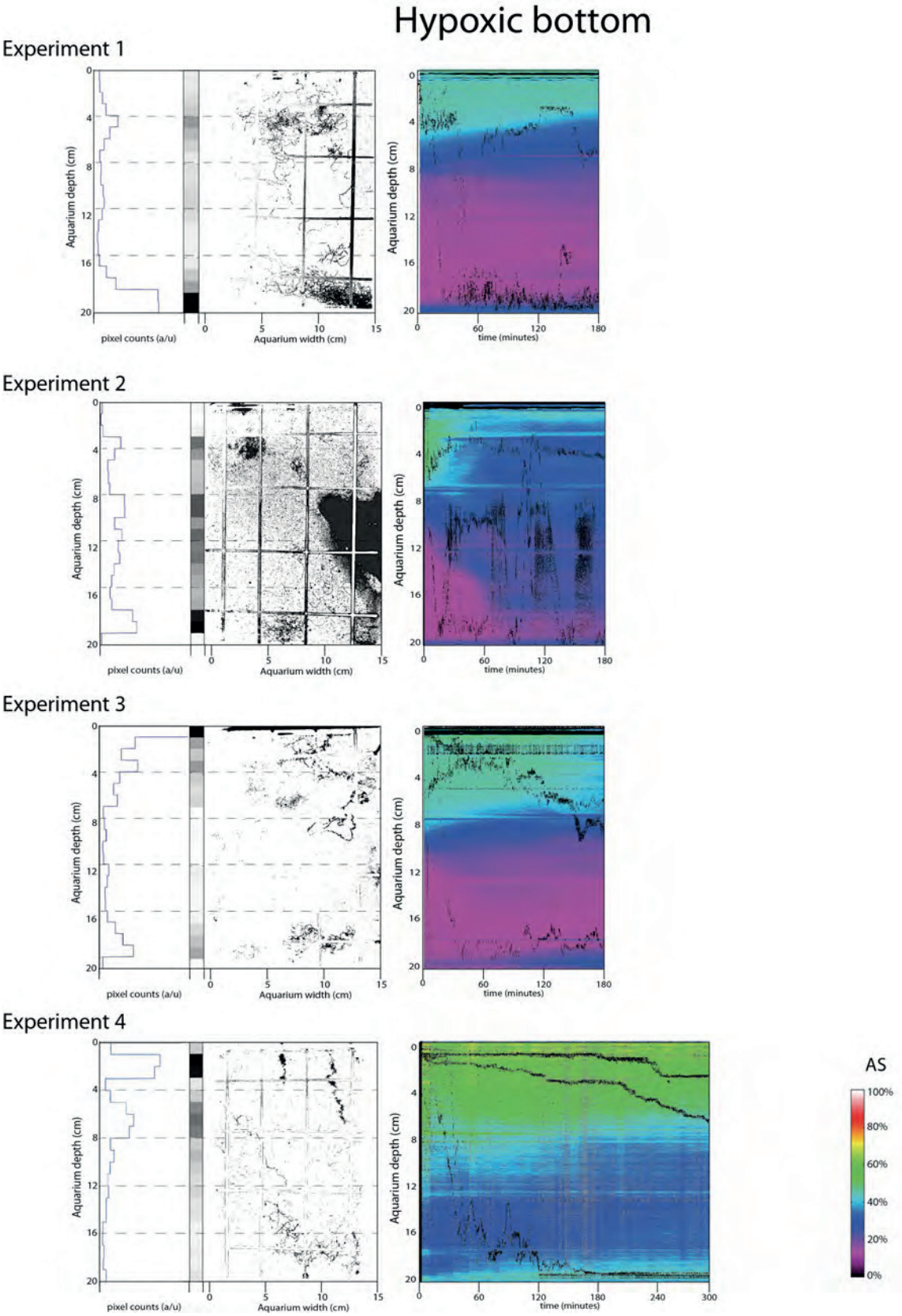

SI Figure 6: n=4 experiments with "Hypoxic bottom" conditions in the aquaria and an average air saturation of 40 - 60% on the top and < 30% on the bottom. Three experiments were run for 180 minutes and one for 300 minutes.

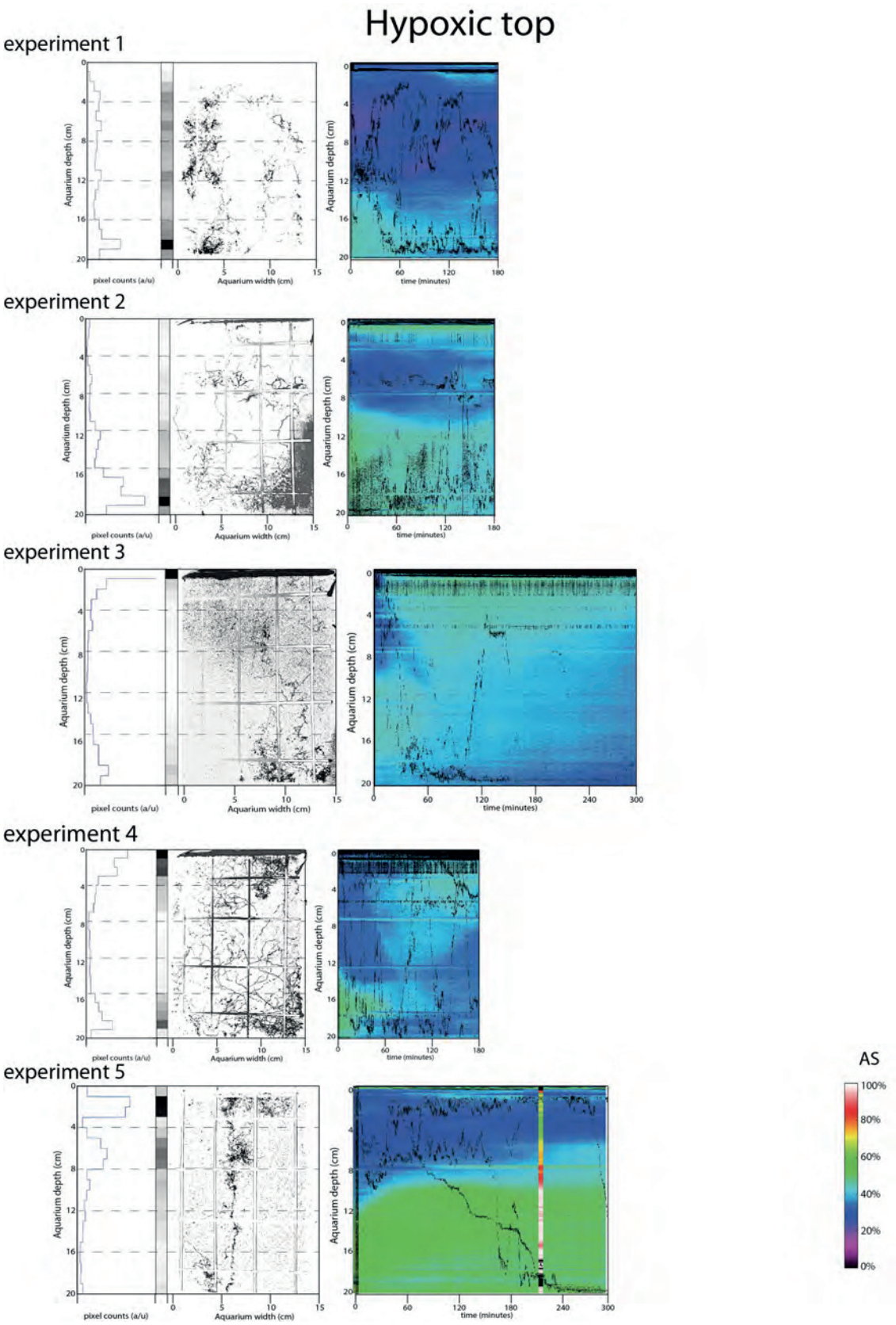

SI Figure 7: n=5 experiments with "Hypoxic top" conditions in the aquaria and an average air saturation of < 30% on the top and > 40% on the bottom. Three experiments were run for 180 minutes and two for 300 minutes.

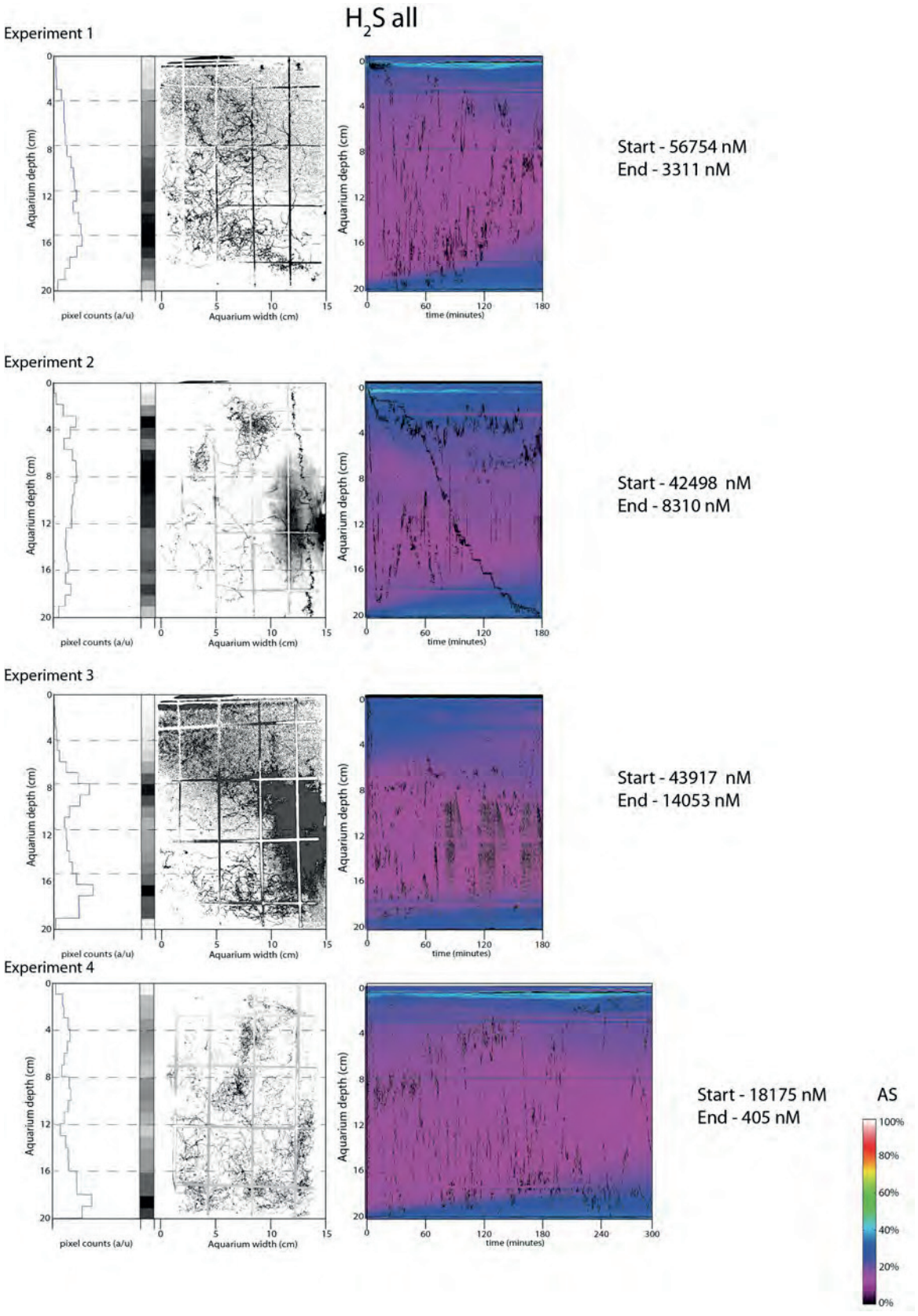

SI Figure 8: n=4 experiments with "H_2S all" conditions in the aquaria and an average air saturation of < 30%. Three experiments were run for 180 minutes and one for 300 minutes.

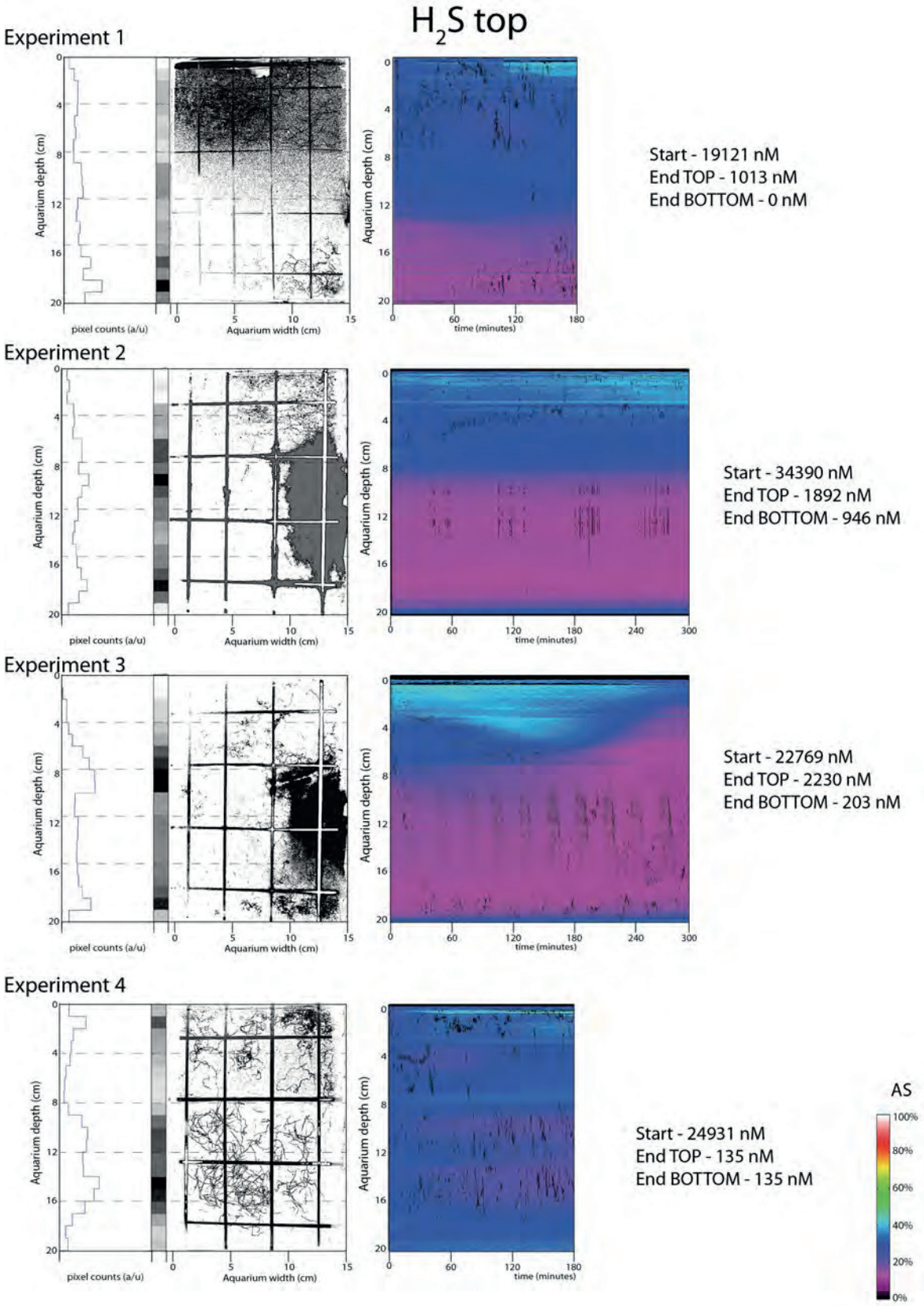

SI Figure 9: n=4 experiments with "H_2S top" conditions in the aquaria and an average air saturation of < 20% in the bottom and < 40% in the top. Two experiments were run for 180 minutes and two for 300 minutes.

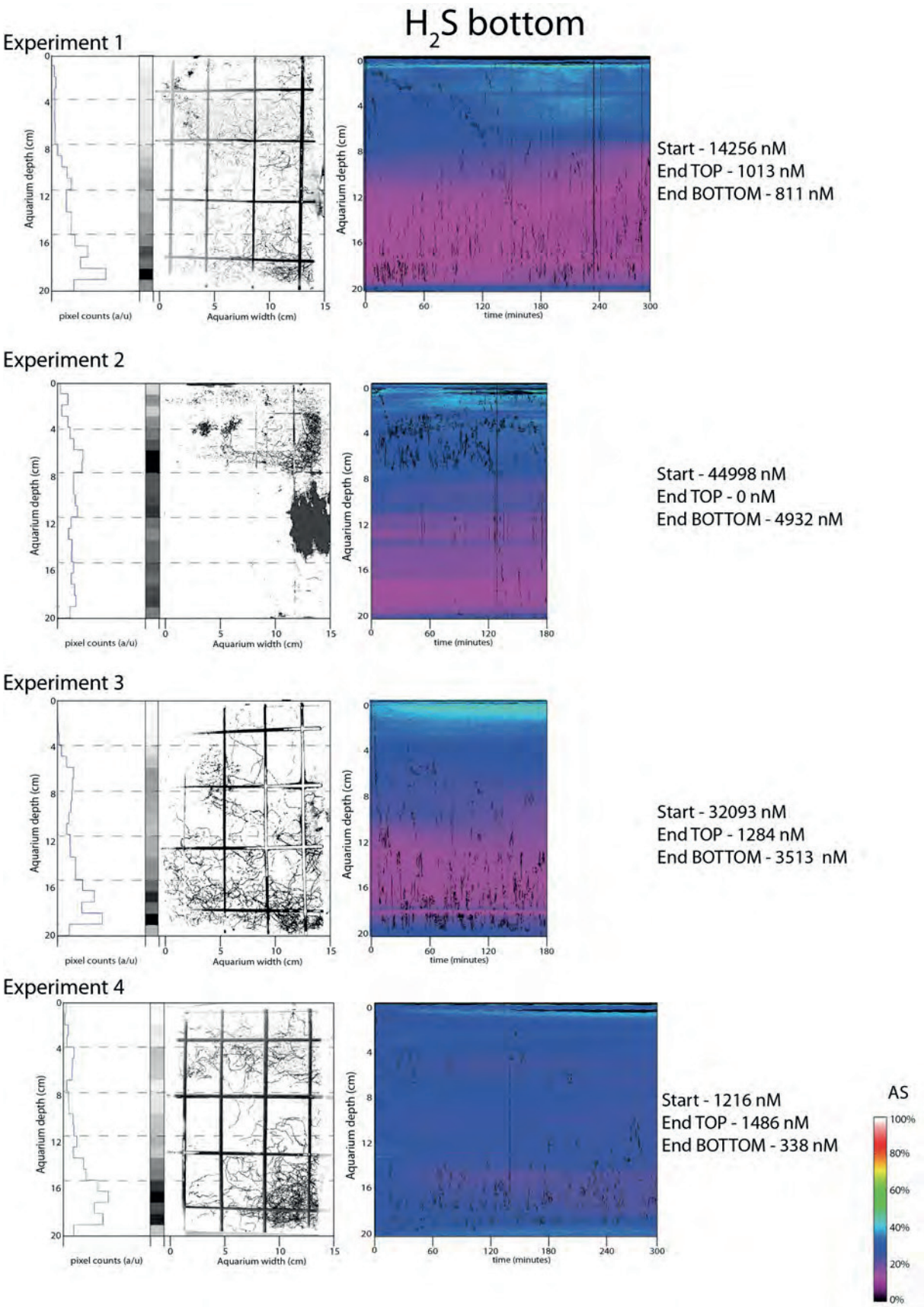

SI Figure 10: n=4 experiments with "H_2S bottom" conditions in the aquaria and an average air saturation of < 20% in the bottom and < 40% in the top. Two experiments were run for 180 minutes and two for 300 minutes.

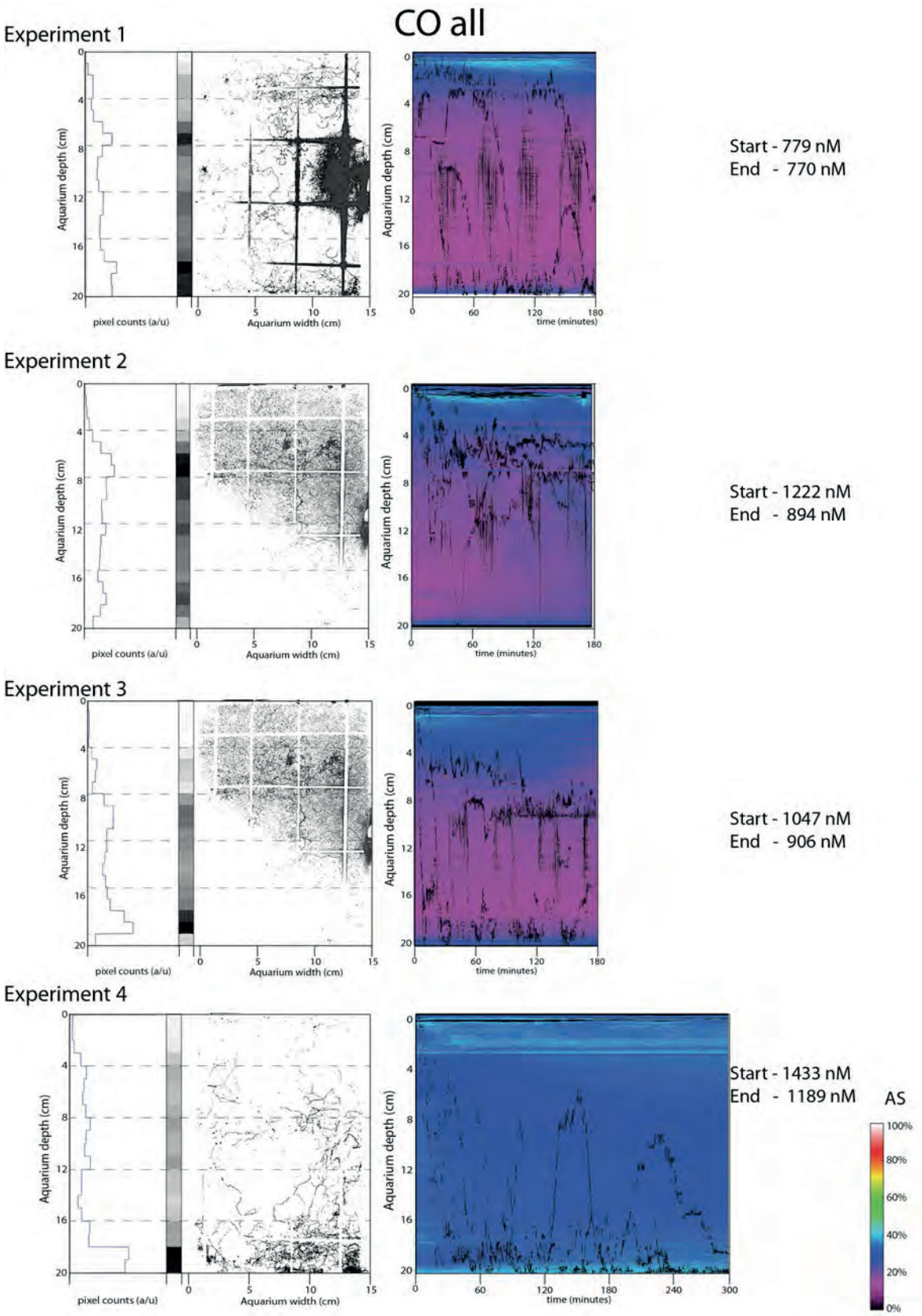

SI Figure 11: n=4 experiments with "CO all" conditions in the aquaria and an average air saturation of < 20%. Three experiments were run for 180 minutes and one for 300 minutes.

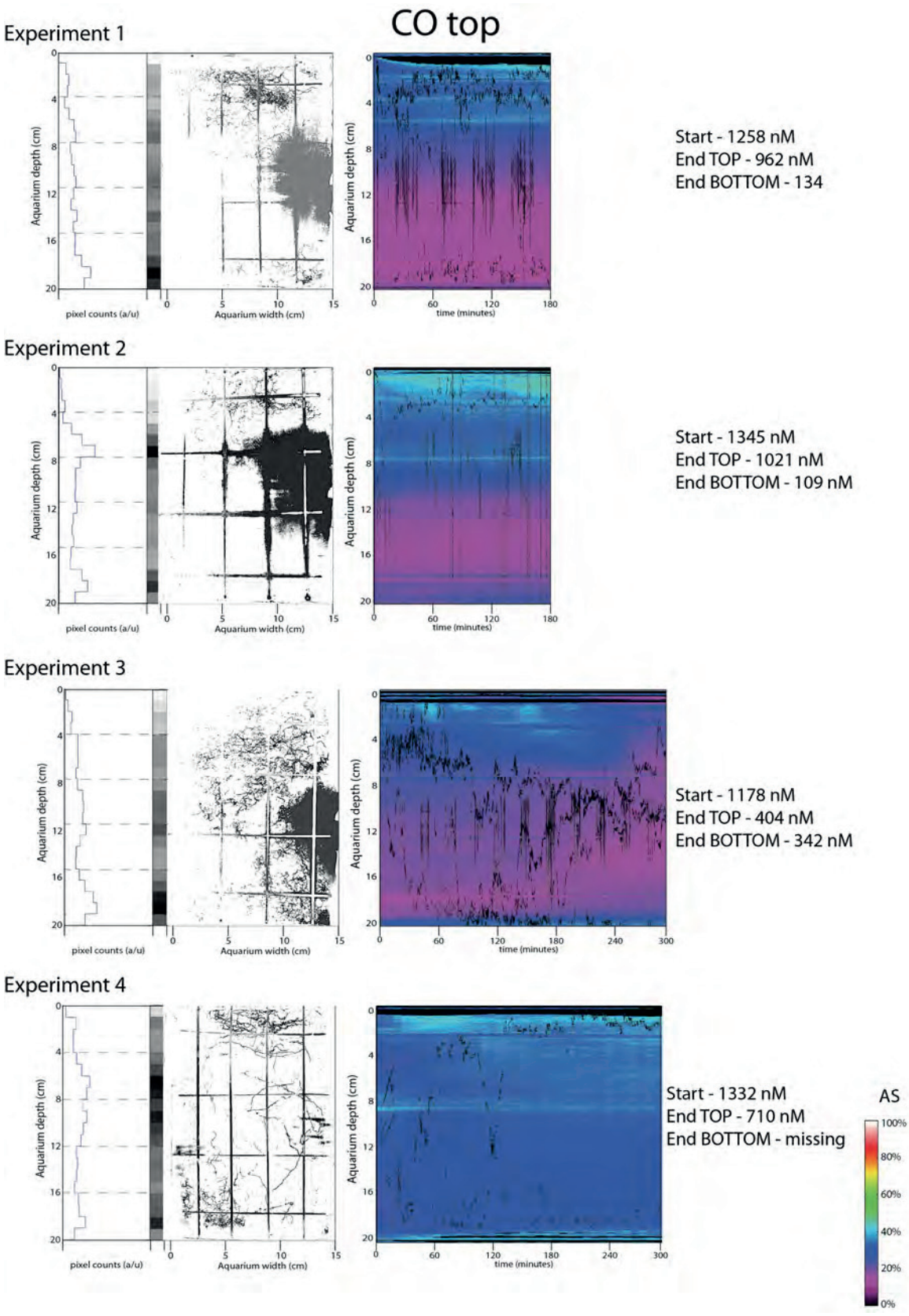

SI Figure 12: n=4 experiments with "CO top" conditions in the aquaria and an average air saturation of < 20% in the bottom and < 40% in the top. Two experiments were run for 180 minutes and two for 300 minutes.

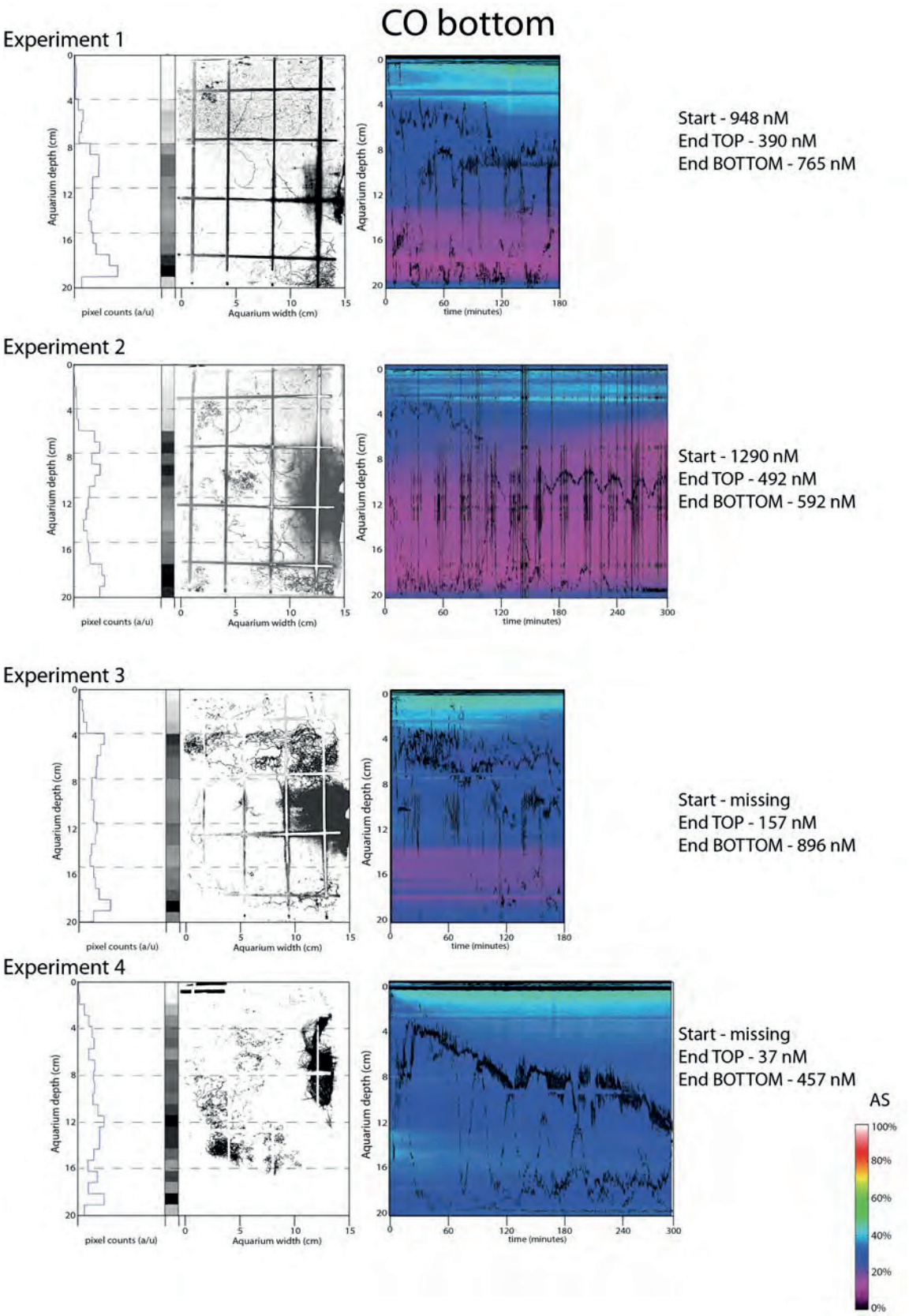

SI Figure 13: n=4 experiments with "CO bottom" conditions in the aquaria and an average air saturation of < 20% in the bottom and < 40% in the top. Two experiments were run for 180 minutes and two for 300 minutes.

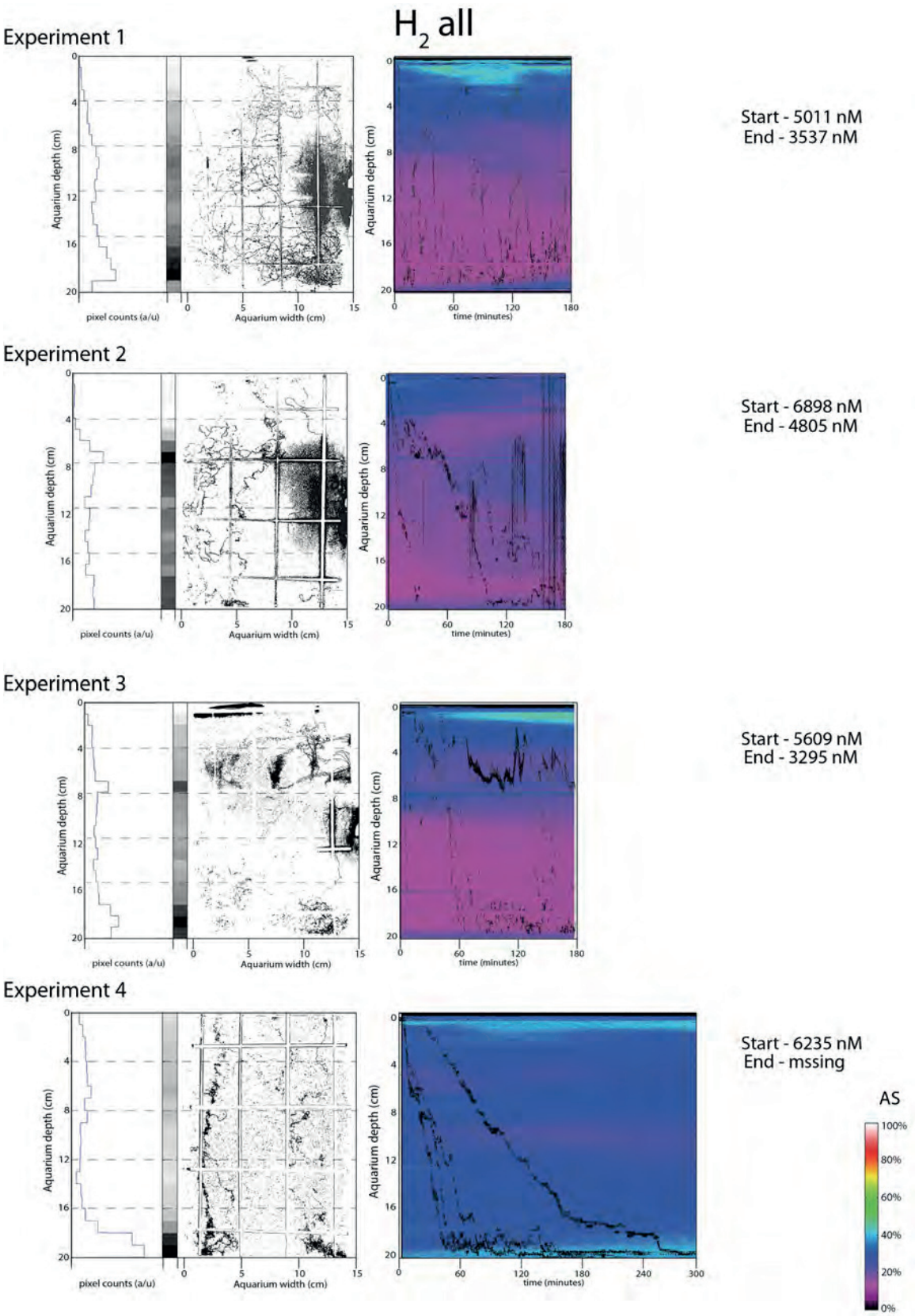

SI Figure 14: n=4 experiments with "H_2 all" conditions in the aquaria and an average air saturation of < 30%. Three experiments were run for 180 minutes and one for 300 minutes.

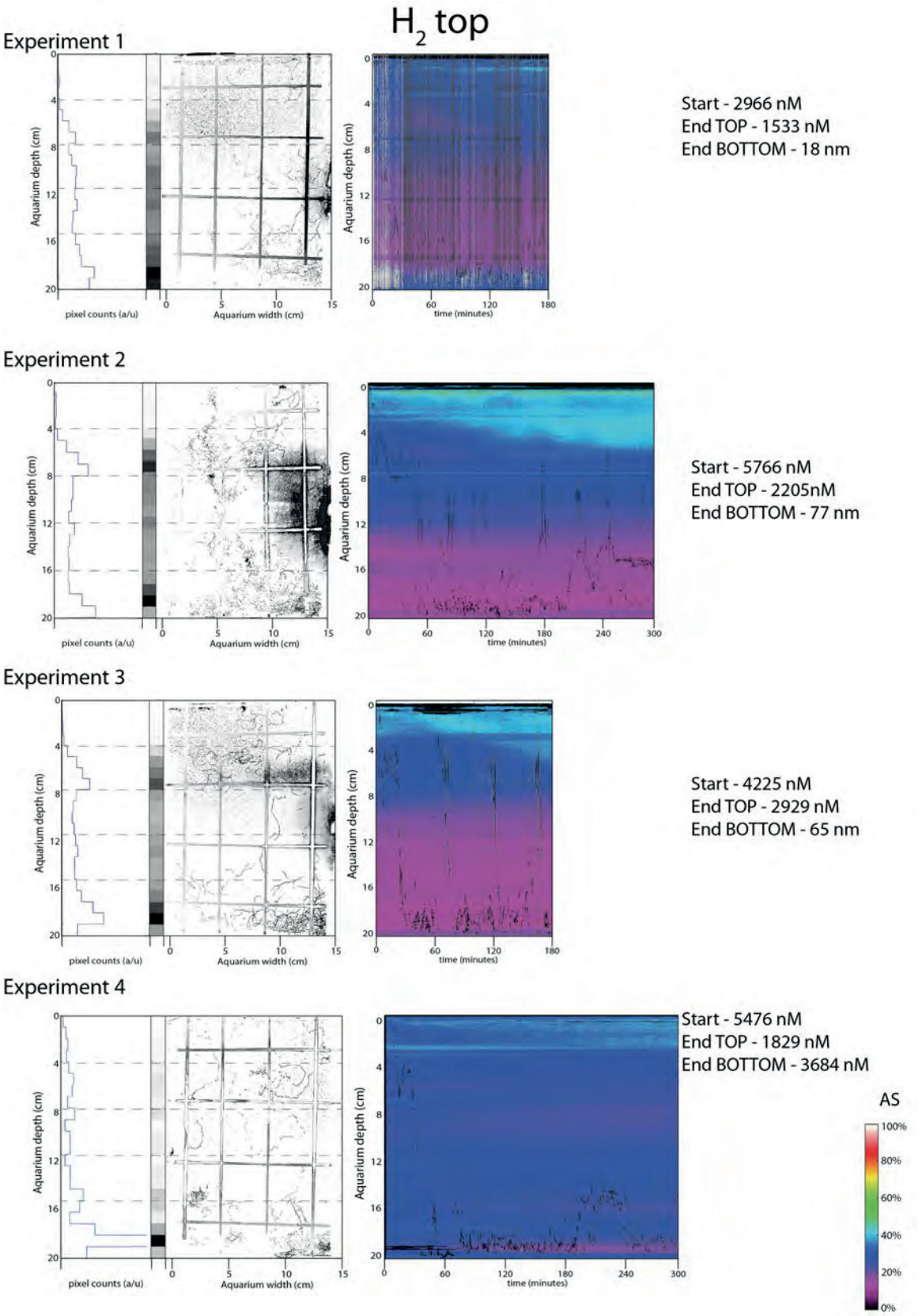

SI Figure 15: n=4 experiments with "H_2 top" conditions in the aquaria and an average air saturation of < 20% in the bottom and < 40% in the top. Two experiments were run for 180 minutes and two for 300 minutes.

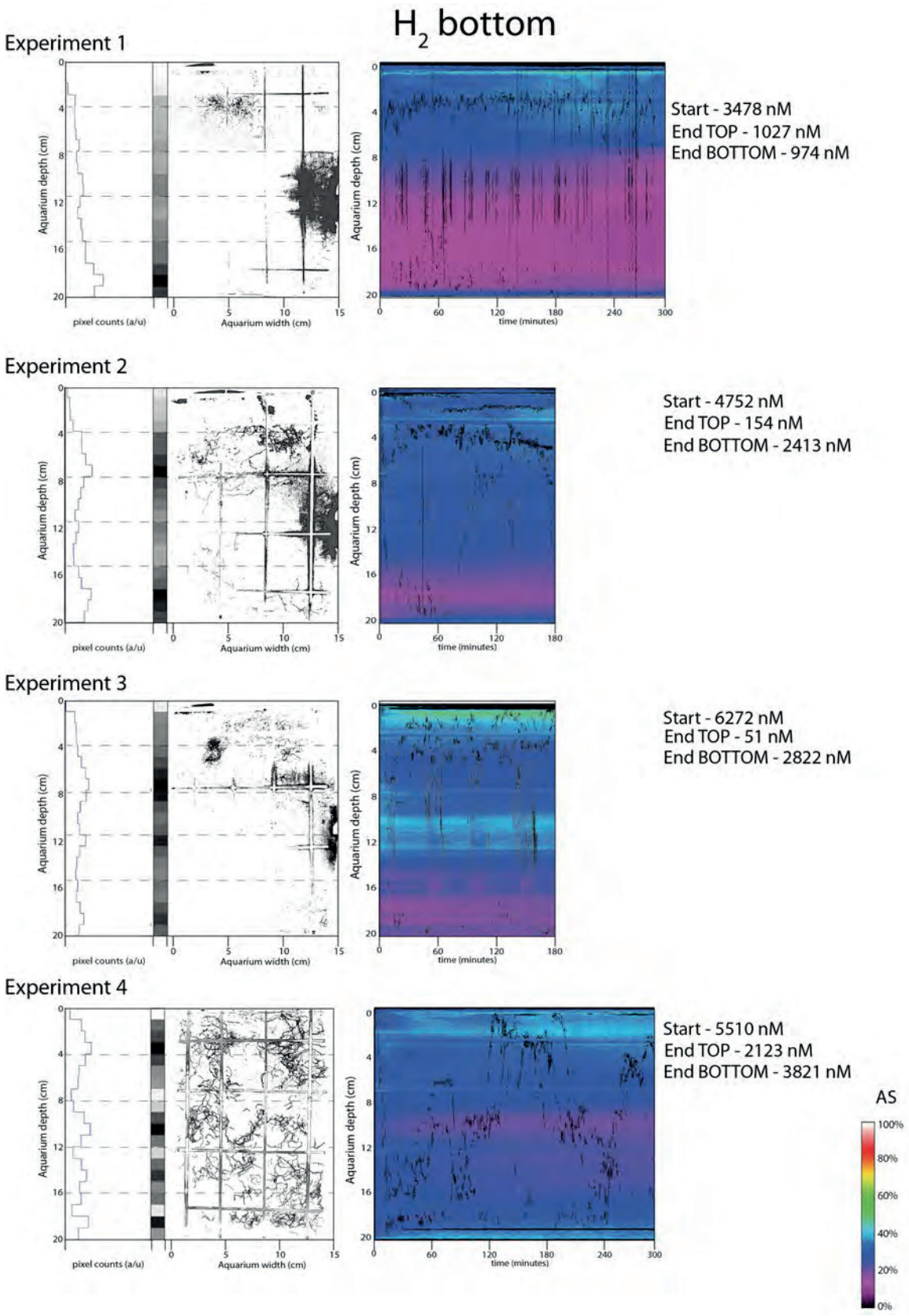

SI Figure 16: n=4 experiments with "H_2 bottom" conditions in the aquaria and an average air saturation of < 20% in the bottom and < 40% in the top. Two experiments were run for 180 minutes and two for 300 minutes.

SI Table 1: GC-MS & photometer measurements for each experiment conducted. Measurements. Listed are 1) substrate tested and measured, 2) experimental setup and zonation within the aquarium. 3) experimental condition repeat number. 4) When during the experiment t the measurement was taken. 5) from where pore water was taken for the measurement. 6) resulting measurement in nM.

Substrate	experimental condition	Experiment number	start / end	zonation	concentration in nM
H_2S	H_2S bottom	17	Start	from syringe	1216
H_2S	H_2S bottom	17	end	Top 4 cm inlet	1486
H_2S	H_2S bottom	17	end	Bottom 16 cm inlet	337
H_2S	All H_2S	18	start	Middle ~ 10cm	18174
H_2S	All H_2S	18	end	Middle ~ 10cm	405
H_2S	H_2S top	19	start	from syringe	24931
H_2S	H_2S top	19	end	Top 4 cm inlet	135
H_2S	H_2S top	19	end	Bottom 16 cm inlet	1351
H_2S	H_2S bottom	1	start	Middle ~ 10cm	14256
H_2S	H_2S bottom	1	end	Top 4 cm inlet	810
H_2S	H_2S bottom	1	end	Bottom 16 cm inlet	1013
H_2S	H_2S Top	1	start	Middle ~ 10cm	19120
H_2S	H_2S Top	1	end	Top 4 cm inlet	1013
H_2S	H_2S Top	1	end	Bottom 16 cm inlet	472
H_2S	H_2S All	1	start	Middle ~ 10cm	56753
H_2S	H_2S All	1	end	Middle ~ 10cm	3310
H_2S	H_2S bottom	2	start	Middle ~ 10cm	44997
H_2S	H_2S bottom	2	end	Top 4 cm inlet	608
H_2S	H_2S bottom	2	end	Bottom 16 cm inlet	4932
H_2S	H_2S Top	2	start	Middle ~ 10cm	34390
H_2S	H_2S Top	2	end	Top 4 cm inlet	1891
H_2S	H_2S Top	2	end	Bottom 16 cm inlet	0945
H_2S	H_2S All	2	start	Middle ~ 10cm	42497
H_2S	H_2S All	2	end	Middle ~ 10cm	8310
H_2S	H_2S Top	3	start	Middle ~ 10cm	22769
H_2S	H_2S Top	3	end	Top 4 cm inlet	2229
H_2S	H_2S Top	3	end	Bottom 16 cm inlet	0202
H_2S	H_2S All	3	start	Middle ~ 10cm	43916
H_2S	H_2S All	3	end	Middle ~ 10cm	14053
H_2S	H_2S bottom	3	start	Middle ~ 10cm	32092
H_2S	H_2S bottom	3	end	Top 4 cm inlet	12837
H_2S	H_2S bottom	3	end	Bottom 16 cm inlet	3513
CO	CO All	10	Start	from syringe	1433
CO	CO All	10	end	Middle ~ 10cm	1189
CO	CO Bottom	9	Start	from syringe	missing
CO	CO Bottom	9	end	Top of aquarium	37

CO	CO Bottom	9	end	bottom of aquarium	457
CO	CO Top	11	Start	from syringe	1332
CO	CO Top	11	end	Top 4 cm inlet	710
CO	CO Top	11	end	Bottom 16 cm inlet	missing
CO	CO All	1	Start	from syringe	779
CO	CO All	1	end	Middle ~ 10cm	770
CO	CO All	2	Start	from syringe	1222
CO	CO All	2	end	Middle ~ 10cm	894
CO	CO All	3	Start	from syringe	1047
CO	CO All	3	end	Middle ~ 10cm	906
CO	CO Bottom	1	Start	from syringe	948
CO	CO Bottom	1	end	Top 4 cm inlet	390
CO	CO Bottom	1	end	Bottom 16 cm inlet	765
CO	CO Bottom	2	Start	from syringe	1290
CO	CO Bottom	2	end	Top 4 cm inlet	492
CO	CO Bottom	2	end	Bottom 16 cm inlet	592
CO	CO Bottom	3	Start	from syringe	missing
CO	CO Bottom	3	end	Top 4 cm inlet	157
CO	CO Bottom	3	end	Bottom 16 cm inlet	896
CO	CO Top	1	Start	from syringe	1258
CO	CO Top	1	end	Top 4 cm inlet	962
CO	CO Top	1	end	Bottom 16 cm inlet	134
CO	CO Top	2	Start	from syringe	1345
CO	CO Top	2	end	Top 4 cm inlet	1021
CO	CO Top	2	end	Bottom 16 cm inlet	109
CO	CO Top	3	Start	from syringe	1178
CO	CO Top	3	end	Top 4 cm inlet	404
CO	CO Top	3	end	Bottom 16 cm inlet	342
H_2	H_2 All	12	Start	from syringe	6235
H_2	H_2 All	12	end	Middle ~ 10cm	
H_2	H_2 Bottom	13	Start	from syringe	5510
H_2	H_2 Bottom	13	end	Top 4 cm inlet	2123
H_2	H_2 Bottom	13	end	Bottom 16 cm inlet	3821
H_2	H_2 Top	14	Start	from syringe	5476
H_2	H_2 Top	14	end	Top 4 cm inlet	1829
H_2	H_2 Top	14	end	Bottom 16 cm inlet	3684
H_2	H_2 All	1	Start	from syringe	5011
H_2	H_2 All	1	end	Middle ~ 10cm	3537
H_2	H_2 All	2	Start	from syringe	6897
H_2	H_2 All	2	end	Middle ~ 10cm	4805
H_2	H_2 All	3	Start	from syringe	5609
H_2	H_2 All	3	end	Middle ~ 10cm	3295
H_2	H_2 Bottom	1	Start	from syringe	3478

H_2	H_2 Bottom	1	end	Top 4 cm inlet	1027
H_2	H_2 Bottom	1	end	Bottom 16 cm inlet	974
H_2	H_2 Bottom	2	Start	from syringe	4752
H_2	H_2 Bottom	2	end	Top 4 cm inlet	154
H_2	H_2 Bottom	2	end	Bottom 16 cm inlet	2413
H_2	H_2 Bottom	3	Start	from syringe	6272
H_2	H_2 Bottom	3	end	Top 4 cm inlet	51
H_2	H_2 Bottom	3	end	Bottom 16 cm inlet	2822
H_2	H_2 Top	1	Start	from syringe	2966
H_2	H_2 Top	1	end	Top 4 cm inlet	1533
H_2	H_2 Top	1	end	Bottom 16 cm inlet	18
H_2	H_2 Top	2	Start	from syringe	5766
H_2	H_2 Top	2	end	Top 4 cm inlet	2205
H_2	H_2 Top	2	end	Bottom 16 cm inlet	77
H_2	H_2 Top	3	Start	from syringe	4225
H_2	H_2 Top	3	end	Top 4 cm inlet	2929
H_2	H_2 Top	3	end	Bottom 16 cm inlet	65

SI Table 2: Conditions tested in the experimental migration setup. A total of 13 different setup conditions, with at least three replicates each, were tested. Experiments containing H_2S, CO or H_2 zones were conducted with hypoxic conditions throughout the aquarium.

Substrate	**Set up**	**Replicates**
Oxygen (O_2)	all oxic	n=3
	all anoxic	n=5
	oxic top half	n=5
	anoxic top half	n=3
Hydrogen sulphide (H_2S)	all H_2S	n=4
	H_2S top	n=4
	H_2S bottom	n=4
Carbon monoxide (CO)	all CO	n=4
	CO top	n=4
	CO bottom	n=4
Hydrogen (H_2)	all H_2	n=4
	H_2 top	n=4

Chapter III

MiL-FISH: Multi-labelled Oligonucleotides for Fluorescence *In situ* Hybridisation Improve Visualisation of Bacterial Cells

Mario P. Schimak[1*], Manuel Kleiner[1, 2], Silke Wetzel[1], Manuel Liebeke[1], Nicole Dubilier[1], Bernhard M. Fuchs[1*]

[1]Max Planck Institute for Marine Microbiology, Celsiusstrasse 1, D-28359 Bremen, Germany
[2]Energy Bioengineering and Geomicrobiology Research Group, University of Calgary, 2500 University Drive, Calgary, Alberta T2N 1N4

Manuscript published in Applied and Environmental Microbiology

Author contributions:

M.P.S. & B.F. designed research and conceived the project; M.K. conducted FACS sorting; N.D. & M.L. co-supervised the research; S.W. provided contextual input and technical assistance; M.P.S. conducted the experiments and wrote the manuscript. All co-authors reviewed and revised the paper.

Accepted Manuscript Posted Online
AEM
Applied and Environmental Microbiology

AEM Accepted Manuscript Posted Online 16 October 2015
Appl. Environ. Microbiol. doi:10.1128/AEM.02776-15
Copyright © 2015, Schimak et al.
This is an open-access article distributed under the terms of the Creative Commons Attribution 4.0 International license.

MiL-FISH: Multi-labelled oligonucleotides for fluorescence *in situ* hybridisation improve visualization of bacterial cells

Running title: Click-synthesised oligonucleotides for FISH

Mario P. Schimak[1*], Manuel Kleiner[1, 2], Silke Wetzel[1], Manuel Liebeke[1], Nicole Dubilier[1], Bernhard M. Fuchs[1*]

[1]Max Planck Institute for Marine Microbiology, Celsiusstrasse 1, D-28359 Bremen, Germany

[2]Energy Bioengineering and Geomicrobiology Research Group, University of Calgary, 2500 University Drive, Calgary, Alberta T2N 1N4

Key Words: fluorescence activated cell sorting, CuAAC oligonucleotides, multi-labelled FISH, LR-White, CLASI-FISH

*** Corresponding authors**

mschimak@mpi-bremen.de

bfuchs@mpi-bremen.de

Co-author emails:

Manuel Kleiner: manuel.kleiner@ucalgary.ca, Silke Wetzel: swetzel@mpi-bremen.de, Manuel Liebeke: mliebeke@mpi-bremen.de, Nicole Dubilier: ndubilie@mpi-bremen.de

Accepted Manuscript Posted Online
AEM Applied and Environmental Microbiology
Applied and Environmental Microbiology

Abstract

Fluorescence *in situ* hybridisation (FISH) has become a vital tool for environmental and medical microbiology and is commonly used for the identification, localisation and isolation of defined microbial taxa. However, fluorescence signal strength is often a limiting factor for targeting all members in a microbial community. Here we present the application of a multi-labelled FISH approach (MiL-FISH) that: 1) enables the targeting of up to seven microbial groups simultaneously using multi-spectral labelling of a single oligonucleotide probe, 2) is applicable for the isolation of unfixed environmental microorganisms via fluorescence activated cell sorting (FACS), and 3) improves signal and imaging quality of tissue sections in acrylic resin for precise localisation of individual microbial cells. We show the ability of MiL-FISH to distinguish between seven microbial groups using a mock community of marine organisms, and its applicability for the localisation of bacteria associated with animal tissue as well as their isolation from host tissues using FACS. To further increase the number of potential target organisms a streamlined "combinatorial labelling and spectral imaging-FISH (CLASI-FISH)" concept with MiL-FISH probes is presented. Through the combination of increased probe signal, the possibility to target hard-to-detect taxa and isolate these from an environmental sample, the identification and precise localisation of microbiota in host tissues and the simultaneous multi-labelling of up to seven microbial groups, we show here that MiL-FISH is a multi-faceted alternative to standard mono-labelled FISH that can be used for a wide range of biological and medical applications.

Accepted Manuscript Posted Online
AEM
Applied and Environmental Microbiology
Applied and Environmental Microbiology

Introduction

Fluorescence *in situ* hybridisation (FISH) is a well established tool in environmental and medical microbiology **(1)**. Standard FISH involves the hybridisation of fluorescently labelled oligonucleotide probes to the ribosomal RNA (rRNA) of whole fixed cells, which can subsequently be visualised under an epifluorescence microscope or isolated from a sample by fluorescence activated cell sorting (FACS) for further analysis such as single cell genomics **(2) (3) (4)**.

Accurate detection of microbial cells in environmental samples greatly depends on probe signal strength, which correlates to the number of rRNA molecules in a target cell **(5)**. Consequently, many environmental cells with low rRNA copy numbers, such as those of the SAR11 clade, are often close to, or below, detection limits **(6)**. Additionally, the identification of bacterial cells associated to plant or animal tissue may be challenging due to high autofluorescence of extracellular matrixes or cellular components such as cuticle, chitin or egg yolk.

Catalysed reporter deposition-FISH (CARD-FISH) was developed to overcome signal limitations via the immobilisation of multiple radicalised fluorescent tyramids by the enzyme horseradish peroxidase (HRP) conjugated to oligonucleotide probes **(7)**. The resulting fluorescence signal is 26 - 41 times higher than mono-labelled FISH making the visualisation of hard to detect cells possible **(5)**. However, the use of CARD-FISH to target several groups of interest from a single sample is very time consuming as consecutive hybridisations for each target group need to be made.

Standard FISH approaches have also undergone development to increase signal through a variety of probe synthesis advancements. A previous study

Accepted Manuscript Posted Online
AEM
Applied and Environmental Microbiology

conjugated a 3x labelled fluorescence tail at one end of the probe **(8)**. The use of these probes, however, increased non-specific binding considerably, presumably due to dye moieties binding to cell components, and was therefore not practical for environmental samples. Another approach called DOPE-FISH, uses double labelled oligonucleotide probes at the 5' and 3' end to increase probe signal twofold and is not compromised by non-specific binding of dye moieties **(9)**. In addition to signal increase, probes for DOPE-FISH can be multilabeled, allowing multicolour probe combinations. Behnam and co-workers showed that DOPE oligonucleotides can be used to target up to six organisms in a single FISH experiment by conjugating various combinations of the standard fluoresceine, Cy3 and Cy5 fluorochromes to a probe **(10)**. Multicolour labelling is also commonly used in human cytogenetics and can be achieved in a number of ways by either: 1) a combinatorial approach whereby the number of available fluorochrome labels determine the number of targets (2^n - 1) **(11)**, 2) ratio labelling whereby the proportion of each dye used determines a ratio code which is allocated to a target molecule **(12)** or 3) a combination of both combinatorial and ratio labelling, such as combined binary ratio labelling (COBRA-FISH) **(13)** (for review see **(14)**). To further increase the number of environmental organisms one can target in microbial ecology studies, combinatorial labelling and spectral imaging (CLASI-FISH) can be employed **(15)**. Here, a target group is allocated a unique spectral tag by hybridising a repertoire of mono-labelled oligonucleotide probes carrying fluorochromes of closely overlapping spectra to several sites on the 16S rRNA. The combination of emitted wavelengths is revealed by linear un-mixing and spectral imaging with modern confocal laser scanning microscopes (CLSM). However, approaches that rely on the targeting of several sites on a target molecule, such as the 16S rRNA, are generally negatively influenced by binding sensitivity and

Accepted Manuscript Posted Online
AEM
Applied and Environmental Microbiology

specificity biases.

The preservation of microbial community composition in, for example, biofilms or within eukaryotic tissue is critical for understanding these systems as a whole. In particular, FISH compatible acrylic resins, such as LR-White, preserve specimen structure and enable semi-thin sectioning (1 µm), without risking cell displacement, which allows the identification and localisation of individual microbial cells within a community **(16) (17) (18)**. In animals and plants, however, high autofluorescence of some tissues, extracellular matrixes or cellular components such as muscle, cuticle, chitin or egg yolk can quench probe signal, making the visualisation of microbial cells challenging. The development of a FISH approach that targets multiple bacterial phylotypes simultaneously and reliably, yields strong probe signals over high background autofluorescence, and preserves cell morphology optimally on specimens embedded in acrylic resins is therefore highly desirable for studies of beneficial and pathogenic microbiota associated with plants and animals.

In this study we demonstrate the application of multi-labelled oligonucleotide probes synthesised by copper catalysed alkyne azide 1,3-dipolar cyclo-addition (CuAAC) or "click" reaction **(19)** on complex microbial populations and term this procedure "**M**ulti-**L**abelled – FISH (MiL-FISH)". We investigated signals and melting behaviour of probes labelled with up to four fluorochromes and show that signal strength was sufficient for the isolation of unfixed environmental microbes via FACS. For optimal localisation of microorganisms in their natural environment, differences between mono-, MiL- and CARD-FISH were evaluated on bacteria associated with animal tissue embedded in FISH compatible acrylic resin. For these analyses we used the well-studied symbiosis in the gutless oligochaete *Olavius algarvensis* **(20)**. This marine worm is nutritionally dependant on a consortium of two gamma- and two

Accepted Manuscript Posted Online
AEM Applied and Environmental Microbiology
Applied and Environmental Microbiology

125 deltaproteobacterial symbionts **(21)**. Attempts at tracing the transmission mode and
126 the association of symbionts to the developing worm embryo using mono-labelled
127 FISH have been challenging due to the high autofluorescence of egg yolk. Finally, to
128 demonstrate the ability of MiL-FISH to target up to seven members of a microbial
129 community, we hybridised a mock consortium of marine microorganisms with probes
130 carrying a variety of combinations of the most commonly used fluorochromes,
131 fluoresceine, Cy3 and Cy5.
132

Accepted Manuscript Posted Online
Applied and Environmental Microbiology
AEM
Applied and Environmental Microbiology

Materials and Methods

Sample material. Seven bacteria: *Escherichia coli* DSM498, *Gramella forsetii*, *Beggiatoa sp.*, *Desulfococcus biacutus*, *Roseobacter sp.* AK 199, *Sulfurimonas denitrificans* and *Rhodopirellula sp.* SH1^T, and one archaeon, *Metallosphaera sedula*, were used in this study (for culture preparation and fixation see Supplementary Data).

For isolation of environmental microorganisms by FACS we used the symbiotic bacteria of the gutless marine worm *Inanidrilus leukodermatus* **(22)**. Roughly 1000 worms were sampled in November 2009 from shallow water sediments (1 m water depth) in Harrington Sound on Bermuda, next to the Bermuda Aquarium (32° 19' 26.52"N, 64° 44' 18.78"W). Worms were homogenized and symbionts partially separated from host tissue via a Histodenz density gradient centrifugation according to the protocol described in **(23)**. Symbiont fraction pellets were kept frozen at -80 °C until further analysis.

The gutless marine oligochaete *Olavius algarvensis*, was retrieved from sediments collected at 7 meters water depth by SCUBA diving in the bay of Sant' Andrea (42° 48' 29.80" N, 10° 8' 34.07" E), Elba, Italy. Worms were sorted from the sediment by hand at the HYDRA field station (Fetovaia, Elba, Italy) and fixed in Carnoy's fixative (6 parts 96% ethanol, 3 parts chloroform, 1 part glacial acetic acid) and 4% PFA for 4 h each at 4 °C and stored in 50% ethanol:seawater or preserved in 96% ethanol directly. Eggs were obtained by incubating worms in sediment filled 78 µm porous vials (Plano GmbH, Wetzlar, Germany) which were subsequently buried in the sediment of an aquarium of 39 ‰ salinity kept at 25 °C with a cooling aggregate (Titan 150 - Aquamedic GmbH, Bissendorf, Germany). Vials were sampled every week and manually screened for eggs. Eggs at different developmental stages were retrieved and fixed as described above.

Accepted Manuscript Posted Online
AEM
Applied and Environmental Microbiology

158 **Oligonucleotide probes.** Sequences for previously published general probes used in
159 this study were obtained from probebase **(24)** (SI Table 1). All probes in this study,
160 including multi-labelled probes, were donated by or purchased from Biomers
161 (Biomers.net GmbH, Ulm, Germany) and synthesised with up to four "click-
162 compatible" nucleotides (either A, T, C or G). Multi-coloured probes were synthesised
163 with two internal "click compatible" nucleotides and two fluorochromes on the 5' and
164 3' end (DOPE) of a different species (see SI Table 1 for positions and dyes used).
165 Probes subsequently underwent a "click" reaction with the respective dye and purified
166 before use.
167
168 **LR-White embedding.** *Olavius algarvensis* worms and eggs were embedded by
169 gradual ethanol dehydration starting at 50% for 10 min followed by 10% increases for
170 10 min each until the final dehydration step at 100% ethanol was repeated three times.
171 Infiltration of resin into dehydrated samples followed on a shaker with an LR-White:
172 ethanol mix of 1:3, 1:2, 1:1, 2:1, 3:1 for 30 min each followed by pure LR-White four
173 times for 1 h each with the last change left overnight. Samples were orientated in
174 gelatine capsules with fresh LR-White, placed into a desiccator, flushed with argon
175 three times followed by the application of a 1000 mBar vacuum before polymerisation
176 at 50 °C in an oven for 3 days. Semi-thin (1 µm) sectioning of embedded specimens
177 was done on an ultra-microtome (UC7, Leica Microsystems, Vienna, Austria).
178 Sections were placed on a drop of 20% acetone on gelatine / chromalaun ($KCr(SO_4)_2 12H_2O$) coated glass slides and dried on a hotplate at 50 °C.
180
181 **FISH.** Hybridisation of cells with multi-labelled oligonucleotide probes followed a
182 slight alteration of the standard FISH protocol as described by Manz et al. **(25)**.

Accepted Manuscript Posted Online
AEM
Applied and Environmental Microbiology

Hybridisation buffer (900 mM NaCl, 20 mM Tris-HCl (pH 7.5), 0.02% sodium dodecyl sulphate (SDS)) with a formamide concentration optimised for individual probes used in each respective experiment (Refer to SI Table 1) was mixed with 8.4 pmol μl^{-1} oligonucleotide working solution at a ratio of 15:1. The effect of CARD-FISH buffer on multi-labelled probes was tested with the addition of 10% dextran sulphate (wt/vol) and 1% (wt/vol) Blocking Reagent (Boehringer, Mannheim, Germany). All hybridisations were conducted at 46 °C in a humid chamber for 3 h (unless otherwise stated) followed by a 10 min wash at 48 °C with washing buffer according to Manz et al. 1992 (14-900 mM NaCl, 20 mM Tris/HCl, pH 8, 5 mM EDTA, pH 8 and 0.01% SDS) adjusted to the stringency of the formamide concentration used. Hybridisation of re-suspended *I. leukodermatus* symbiont pellets was done as described above with the addition that cells were pelleted for each buffer exchange for 15 min at 1500 g centrifugation. This step was necessary because cells for FACS were required to be in aqueous solution and could therefore not be immobilized on filters during the FISH procedure.

CARD-FISH experiments were conduced based on the protocol described in Pernthaler et al. 2002 with slight modifications. Hybridisation buffer (900 mM NaCl, 20 mM Tris-HCl (pH 7.5), 0.02% sodium dodecyl sulphate (SDS), 10% dextran sulphate (wt/vol) and 1% (wt/vol) Blocking Reagent) with 8.4 pmol μl^{-1} probe at a ratio of 150:1 was applied. Hybridisation at 46 °C for 3 h and a subsequent 10 min wash step at 48 °C with the adjusted washing buffer (14-900 mM NaCl, 20 mM Tris/HCl, pH 8, 5 mM EDTA, pH 8 and 0.01% SDS) followed. Amplification buffer (1x PBS [pH 7.3], 0.0015% [vol/vol] H_2O_2, 1% Alexa Fluor 488 or 594 dye [Thermo Fisher Scientific, Waltham, MA, USA]) was prepared and cells incubated for 1 h at 46 °C in a humid chamber until a final wash for 10 min in 1x PBS.

Accepted Manuscript Posted Online
AEM
Applied and Environmental Microbiology
Applied and Environmental Microbiology

For mono-, MiL- and CARD-FISH performed on LR-White embedded *O. algarvensis* specimens, a PAP pen (Science Services, Munich, Germany) was used to draw rings around 1 µm sections mounted on glass slides. Sections were pre-treated in 200 mM HCl for 10 min, washed in 200 mM Tris/HCl for 10 min, incubated in 1 µg/ml proteinase K for 5 min at 46 °C and finally washed again in 200 mM Tris/HCl for 10 min before the protocols above were applied.

Microscopy. Fluorescence images were taken with an AxioCam Mrm camera mounted on an Axioscope2 epifluorescence microscope (Carl Zeiss AG, Oberkochen, Germany) equipped with Fluos Zeiss 09 (ex 470/40 nm, em 515LP), AHF (AHF analysentechnik AK, Tübingen, Germany), F36-525 Alexa488 (ex 472/30, em 520/35), AHF F46-004 Cy3 (ex 545/25, em 605/70) and AHF F46006 Cy5 (ex 620/60, em 700/75) filter sets. Images were recorded with the PC based Axiovision (Release 4.6.3 SP1) imaging software and any image level adjustments made therein.

FACS. Unfixed hybridised microbial cells of *I. leukodermatus* were sorted into a 1.5 ml Eppendorf tube by use of a MoFlow flow cytometer (DAKO Cytomation, Hamburg, Germany). The laser was set to λ 488 nm at 400 mWatt and used with a 488/6 filter cube for side scatter (SSC) and 531/40 for Atto488 fluorescence in dual trigger mode.

Label-dependent intensity. To assess probe-conferred signals of 1x, 2x, 3x and 4x labelled EUB338 oligonucleotide probes (MiL-FISH probes) three reference strains, *E. coli*, *G. forsetii* and *Roseobacter sp. AK199* were each hybridised in triplicate. Fluorochrome positions on the probes are listed in SI Table 1. Cells were re-

Accepted Manuscript Posted Online
Applied and Environmental Microbiology
AEM
Applied and Environmental Microbiology

suspended in 10 ml 1x PBS and filtered onto 42 mm GTTP filters of 0.22 µm pore size (Millipore, Darmstadt, Germany). Filters were cut into eighths and placed on a piece of parafilm (Brand, Wertheim, Germany) on a glass slide. FISH was conducted on each filter piece with the addition of 56 µl hybridisation buffer and 4 µl probe. After washing, filter pieces were placed onto new glass slides with a mounting media mix consisting of 11 parts Citifluor™ (CitiFluor Ltd, London, England), two parts VectaShield® (Vector Laboratories, Burlingame, CA, USA) and one part 1x PBS (pH 9), to prevent bleaching of pH sensitive dyes, and sealed with a cover slip before microscope analysis. To avoid over-saturation of signal by strong fluorescence of multi-labelled probes, images were recorded at exposure times optimal for each label type and later correlated to each other. Recorded images were evaluated with ACMEtool version 2 build 1.0.0.42 (available for download at http://www.technobiology.ch/?id=main)

Melting curves. Melting behaviour of multi-labelled probes was determined in triplicate with 1x, 2x and 4x fluorescine labelled CF319a probe targeting *Gramella forsetii*. Filters were prepared as above with hybridisation conditions ranging from 20 – 70% formamide in 10% step increases. Epifluorescence microscopy followed and images were analysed with the diame 2.0 software package **(26)**.

MiL-FISH for multi-colour detection of seven micr obial groups. For detection of multiple microbial cells probes were labelled with fluoresceine, Cy3 and Cy5 only, as well as a combination of fluoresceine & Cy3, fluoresceine & Cy5, Cy3 & Cy5 and Cy3 & Cy5 & fluoresceine. Recording signals in the respective channels, and overlaying all channels of an image, results in the visualisation of mixed colours. For

Accepted Manuscript Posted Online
AEM Applied and Environmental Microbiology
Applied and Environmental Microbiology

example, a fluoresceine and Cy3 labelled probe yields a yellow overlay signal in positively hybridised cells, whereas a Cy3 & Cy5 labelled probe produces magenta when Cy5 is set to blue. Strains, probes and fluorochrome combinations are listed in SI Table 1 and shown in SI Figure 3. For optimal stringency two sequential hybridisations were performed, the first at 60% formamide for DSS658, the second at 35% formamide for the remaining six probes.

Accepted Manuscript Posted Online
AEM
Applied and Environmental Microbiology
Applied and Environmental Microbiology

281 Results

282 **Label-dependent intensity of MiL-FISH.** The 2x, 3x and 4x labelled
283 EUB338 probe yielded an average of 1.8, 2.3 and 2.9 fold signal increase,
284 respectively, over a 1x labelled probe with standard FISH hybridisation buffer (Figure
285 1). The *G. forsetii* hybridisation yielded the strongest signal, followed by *Roseobacter*
286 *sp.* AK199 and then *E. coli*. For all labels and organisms an average linear increase
287 proportional to the number of labels was measured ($R^2 = 0.99$). The use of CARD-
288 FISH buffer during hybridisation yielded a 20% increase in signal for all labels and
289 reference strains (Figure 1). This indicates that CARD-FISH buffer increases signal
290 by the same factor independent of the number of labels added to a probe.
291 For all experiments a 4x labelled NON-EUB negative control was included that
292 yielded no visible signals in cells. In our experiments the S/N (signal to noise) ratios
293 between negative controls and *Gramella forsetii* cells hybridised with the CF319a
294 probe carrying various label numbers were as follows: 1x labelled probe – 4.3, 2x
295 labelled probe – 13.2, 3x labelled probe 23.6 and 4x labelled probe – 34.7 (SI Table
296 2).

297 To demonstrate efficiency of multi-labelled probes for fluorescence activated
298 cell sorting in a flow cytometer, microbial symbionts of the gutless oligochaete *I.*
299 *leukodermatus* were hybridised unfixed directly after worm homogenisation.
300 Separation from host tissues was evident by a clear cluster of labelled microbial cells
301 above background fluorescence that were distinct from negative controls hybridised
302 with a 4x Atto488 labelled NON338 probe (Figure 2). Visual inspection under an
303 epifluorescence microscope confirmed that sorted cells were free of host tissues, cells
304 and other visible host components.
305

Accepted Manuscript Posted Online
AEM Applied and Environmental Microbiology
Applied and Environmental Microbiology

306 **Melting behaviour of MiL-FISH probes.** Melting curves for the probe CF319a
307 labelled with a 1x, 2x and 4x fluoresceine were generated with *G. forsetii* cells and
308 standard hybridisation buffer. All fluoresceine labelled probes showed a characteristic
309 decrease of signal between 30% and 40% formamide as previously described for
310 CF319a with mono-FISH **(27)** (SI Figure 1).
311
312 **LR-White FISH:** Differences between FISH with mono-, multiple- and HRP-labelled
313 probes of resin embedded material were evaluated by hybridising
314 gammaproteobacterial sulphur-oxidising and deltaproteobacterial sulphate-reducing
315 microbial symbionts of *O. algarvensis*.
316 For standard FISH with mono-labelled probes, two hybridisation times were
317 tested on LR-White embedded worms fixed with Carnoy's / PFA and stored in 50%
318 ethanol as well as worms conserved in 96% ethanol directly. None of the PFA fixed
319 individuals showed positive signals with mono-labelled oligonucleotides. In contrast,
320 a 19-hour hybridisation of a 96% ethanol preserved specimens based on Schimak et
321 al. 2012 yielded clearly visible signals of bacterial cells using the standard FISH
322 protocol with CARD-FISH buffer (Figure 3B). A three-hour hybridisation of ethanol
323 preserved material yielded signal for the DSS658 probe but none for the Gam42a
324 probe (Figure 3C). For both hybridisation times long exposure during image
325 acquisition was required, increasing the signal to noise ratio and dampening overall
326 probe signals.
327 CARD-FISH on LR-White sections yielded strong signals at hybridisation
328 times of 3 hours on formalin-fixed individuals (Figure 3D). However, microbial cell
329 morphology was compromised by a "patchy" distribution of probe signal making
330 identification of individual cells within the bacterial consortia difficult.

Accepted Manuscript Posted Online
AEM
Applied and Environmental Microbiology
Applied and Environmental Microbiology

MiL-FISH with hybridisation times of 3 hours overcame problems with image quality and cell integrity (Figure 3E). Single microbial cells were clearly visible within the consortia and could be differentiated from each other easily. Reduced exposure times, compared to mono-labelled probes (< 25 %), were sufficient during imaging, increasing the S/N ratio by 53% over mono-FISH.

Further, probe signals were high enough to overcome tissue autofluorescence, enabling the accurate localisation and identification of individual microbial cells. MiL-FISH on eggs embedded in LR-white resulted in clear signals of gamma- and deltaproteobacteria around high auto-fluorescence regions such as egg yolk (Figure 5b). Gamma 1 symbiont phylotypes in close proximity to both egg yolk and cuticle were clearly visible in a juvenile worm by use of a specific 16S rRNA probe dual labelled with 2x FITZ and 2x Cy3 producing a yellow overlay (Figure 5d & listed in SI Table 1).

MiL-FISH: for multi-colour detection of seven microbial groups. A mock mix of seven marine microbial groups of different size and morphology was hybridised with MiL-FISH probes labelled with different fluorochrome combinations. Our experiments showed that each member of the mix could be distinguished based on the specific colour spectrum emitted by the combination of fluorochromes allocated to the probes as shown in Figure 4 and SI Figure 3 and listed in SI Table 1. A comparison of cell morphology and signal of the respective probe was used to confirm positive hybridisation of bacterial cells. Further, visual control for positive hybridisation was compared with the other six organisms in the mix that acted as negative controls. Exposure times for each channel in the final overlay image were set to accommodate

Accepted Manuscript Posted Online
AEM Applied and Environmental Microbiology
Applied and Environmental Microbiology

all wavelengths and signal intensities for fluorochromes used in the experiment: fluoresceine - 213 ms, Atto488 – 1197 ms, Cy5 – 435 ms and Cy3 - 123 ms.

Hybridisation of *Gramella forsetii* with a 4x fluoresceine labelled CF319a probe yielded signals optimal at exposure times of ~ 100 ms. This was, however, not sufficient to visualise the 2x fluoresceine component of mixed probes containing two types of fluorochromes, such as Ros537, causing incorrect colour representation of these cells in the final overlay image. Therefore, a 2x fluoresceine labelled CF319a probe was used in the final probe mix and a ~ 200 ms exposure time applied (Figure 4H, SI Table 1). This observation was not made for probes labelled with a Cy3 dye. Adding a 4x Cy3 labelled DSS658 probe, that targeted *Desulfococcus biactus*, to the probe mix did not negatively influence the 2x Cy3 component of mixed probes.

Accepted Manuscript Posted Online
AEM
Applied and Environmental Microbiology

Discussion

In our study a maximum of four fluorochromes per probe were tested yielding an average of 2.9 fold signal increase over a 1x labelled probe. Standard FISH on most environmental cells yields a signal to noise ratio (S/N ratio) of around 4. In our experiment S/N ratio was improved by a factor of 8.5, and a quarter shorter exposure times were required to visualise cells with a 4x labelled probe. Photochemical quenching may have influenced the overall signal yield, however, we assume that by placing dye moieties along the entire length of the probe quenching was minimised. Theoretically probes can be labelled with at least twice the number of labels. However, the point at which additional labelling yields no further signal increase is still open to investigation. The results from our negative controls indicate that dye moieties did not adhere to cellular components, as shown in past studies **(8)**, making non-specific binding a negligible factor for MiL-FISH probes. To further increase probe signal hybridisation buffer that contains dextran sulphate (like for CARD-FISH), a known crowding reagent that reduces the time required for probe annealing **(28),** can be used. Unlike HRP labelled probes that are used for CARD-FISH multi-labelled probes did not significantly affect melting behaviour (SI Figure 1). Specific testing of additional probes and organisms may be advisable but based on our experience we expect no differences in optimal hybridisation conditions for already published probes from sources such as probebase **(29)**.

In mono-FISH a minimum of ~ 400 probe - rRNA hybrids are necessary for a detectable signal of cells using modern epifluorescence microscopes **(5)**. This implies that with a four times labelled MiL-FISH probe a minimum of only ~ 130 probe – rRNA hybrids result in the same signal yield. Thus MiL-FISH probes have the potential to increase the detection of organisms with low ribosomal content in

Accepted Manuscript Posted Online
Applied and Environmental Microbiology
AEM
Applied and Environmental Microbiology

environmental samples, such as members of the SAR11 clade **(30)**. Additionally, unfixed environmental bacteria hybridised with MiL-FISH probes were detectable and isolated by flow cytometric sorting. Flow cytometers are lower in sensitivity compared to epifluorescence microscopes and require stronger probe signals for a positive detection of hybridised cells.

MiL-FISH on LR-White sections yielded stronger signals than mono-labelled probes and clearer bacterial cell morphology than CARD-FISH for symbionts of adult *O. algarvensis*. CARD-FISH signals were strong, but individual microbial cells could not be clearly distinguished from each other. As there is no probe penetration into LR-White sections **(31)** access to cellular components requires chemical etching, usually with hydrochloric acid, to expose target rRNA on the section surface onto which probes can bind. The amplification process in CARD-FISH radicalises tyramides, which bind to intracellular proteins. We speculate that target molecules for tyramids are not homogenously accessible after etching, resulting in the observed patchy signal and suboptimal visualisation of bacterial cell morphology. Analysis of O. algarvensis eggs revealed that both gamma- and deltaproteobacterial symbionts occur on the blastomeres of the developing embryo from as early as the first cleavage. This could indicate that they play an important role in the developmental processes of their host, as shown for other symbiotic associations (i.e. **(32)**). The distribution of individual symbiont cells was clearly visible and a distinction between bacterial phylotypes within the consortia could be easily made (Figure 5b). The MiL-FISH combinatorial labelling concept identified the primary gammaproteobacterial symbiont (Gamma 1) in the juvenile host using a 6-FAM and Cy3 labelled probe. As with the multi-colour detection of seven bacteria in our mock mix we are now able to identify and visualise all four symbiont phylotypes simultaneously, and can overcome limitations such as

Accepted Manuscript Posted Online
AEM
Applied and Environmental Microbiology
Applied and Environmental Microbiology

417 background autofluorescence. These findings pave the way for a more detailed
418 analysis of the roles that individual microbes play in the establishment of this
419 symbiosis. Our results show that MiL-FISH can be used in combination with acrylic
420 resins to identify and localize host-associated bacteria, making this approach useful
421 for many biological and medical applications.

422 A past study targeted seven closely related β-proteobacteria with three probes
423 carrying individual label types targeting three sites on the 16S rRNA **(33)**. However,
424 difficulties may arise in probe design of highly conserved 16S rRNA regions of
425 closely related species as well as the targeting of phylogenetically distant groups.
426 MiL-FISH enabled the visualisation of seven microbial groups by combinatorial
427 labelling of probes and eliminated sensitivity biases, as only one site on the 16s rRNA
428 was targeted. Probe signal strength depends on rRNA content of a target cell and
429 differences between organisms must be considered in multi-colour hybridisation of a
430 large bacterial community. To account for rRNA variation, we suggest first
431 hybridising with individual probes and carefully monitoring exposure times before a
432 multi-coloured MiL-FISH approach is applied to environmental samples. Large
433 differences between cell signals can subsequently be adjusted by reduction or addition
434 of the corresponding fluorochrome label on probes used for multicolour imaging.

435 CLASI-FISH can be employed to target even more than seven species in
436 environmental samples and relies heavily on an even accessibility of probes to
437 multiple sites on the 16S rRNA. The variability in binding efficiency and
438 accessibility to different 16S rRNA target sites **(34)** **(35)** can result in false
439 negative binding of probes and / or false and incomplete spectral allocation to a
440 target group. A solution has been described to overcome this by using a mix of
441 mono-labelled probes carrying a variety of label types. However, because in this

Accepted Manuscript Posted Online
AEM
Applied and Environmental Microbiology
Applied and Environmental Microbiology

case only a single site is targeted, probe-probe competition and a linear reduction of fluorescence correlating to the number of dyes added is expected **(36)**. The use of MiL-FISH probes in CLASI-FISH would greatly streamline this concept and reduce the time needed for probe design and testing of multiple target sites on the 16S rRNA while offering high probe signals. Several strategies can be employed in combining MiL- and CLASI-FISH: 1) A single site is targeted by a 4x multi-labelled probe resulting in the same spectral identity as four mono-labelled probes targeting four sites on the 16S rRNA. This greatly increases specificity and sensitivity as only one target site is used and by placing dye moieties along the length of the probe several dozen label combinations can be utilised (SI Figure 2, A1. & A2.). Indeed, this concept can be expanded to ratio labelling or combined combinatorial and ratio labelling approaches such as COBRA – FISH **(13)**, which could also greatly benefit from the use of MiL-FISH probes by allocating ratio combinations to the probe itself. 2) If several sites on the 16S rRNA are available, a signal increase can be achieved by the addition of 4x labelled probes carrying the same fluorochrome combination for each target site. This potentially allows the inclusion of environmental cells with low ribosomal content in future CLASI-FISH studies (SI Figure 2, B). 3) The targeting of multiple 16S rRNA sites using MiL-FISH probes with a large variety of fluorochrome combinations can increase available spectral identities fourfold (SI Figure 2, C).

Acknowledgements

We thank Matthias Resmini and Barbara Pohl from Biomers for coordinating probe synthesis, excellent product support, initial donation of test probes and dealing with special requests. We thank Rudolf Amann for intellectual input and critical

Accepted Manuscript Posted Online
Applied and Environmental Microbiology
AEM
Applied and Environmental Microbiology

467 reading of the manuscript. We are grateful to Jörg Wulf and Andreas Ellrott for
468 excellent technical support, Cecilia Wentrup for help with sample preparation for
469 FACS and probe design, as well as Miriam Weber and Christian Lott, at the HYDRA
470 field station, for support with sample collection. We are grateful to Jens Harder for
471 providing *Rhodopirellula baltica* SH1^T cultures and Anne-Christin Kreutzmann for
472 *Beggiatoa sp.* cultures. Further, we would like to thank Meghan Chafee for input into
473 the manuscript and Alejandro Manzano-Marín and Daniel Tamarit for intellectual
474 input. This work was funded by the Max Planck Society, a Gordon and Betty Moore
475 Foundation Marine Microbiology Initiative Investigator Award (ND), and the
476 European Union (EU) Marie Curie Actions Initial Training Network (ITN)
477 SYMBIOMICS (contract number 264774).
478
479
480
481
482
483
484
485
486
487
488
489
490
491

Accepted Manuscript Posted Online
AEM
Applied and Environmental Microbiology
Applied and Environmental Microbiology

492

493 **References**

494 1. **Amann R, Fuchs BM**. 2008. Single-cell identification in microbial
495 communities by improved fluorescence in situ hybridization techniques.
496 Microbiol **6**:339–348.

497 2. **Amann RI, Krumholz L, Stahl DA**. 1990. Fluorescent-oligonucleotide
498 probing of whole cells for determinative, phylogenetic, and environmental
499 studies in microbiology. J Bacteriol **172**:762–770.

500 3. **Stepanauskas R**. 2012. Single cell genomics: an individual look at microbes.
501 Curr Opin Microbiol **15**:613–620.

502 4. **Yilmaz S, Haroon MF, Rabkin BA, Tyson GW, Hugenholtz P**. 2010.
503 Fixation-free fluorescence in situ hybridization for targeted enrichment of
504 microbial populations. ISME J **4**:1352–1356.

505 5. **Hoshino T, Yilmaz LS, Noguera DR, Daims H, Wagner M**. 2008.
506 Quantification of target molecules needed to detect microorganisms by
507 fluorescence in situ hybridization (FISH) and catalyzed reporter deposition-
508 FISH. Appl Environ Microbiol **74**:5068–5077.

509 6. **Mary I, Heywood JL, Fuchs BM, Amann R, Tarran GA, Burkill PH,**
510 **Zubkov MV**. 2006. SAR11 dominance among metabolically active low
511 nucleic acid bacterioplankton in surface waters along an Atlantic meridional
512 transect. Aquat Microb Ecol **45**:107–113.

513 7. **Pernthaler A, Pernthaler J, Amann R**. 2002. Fluorescence in situ
514 hybridization and catalyzed reporter deposition for the identification of marine
515 bacteria. Appl Environ Microbiol **68**:3094–3101.

516 8. **Spear RN, Li S, Nordheim EV, Andrews JH**. 1999. Quantitative imaging and
517 statistical analysis of fluorescence in situ hybridization (FISH) of
518 Aureobasidium pullulans. J Microbiol Meth **35**:101–110.

519 9. **Stoecker K, Dorninger C, Daims H, Wagner M**. 2010. Double labeling of
520 oligonucleotide probes for fluorescence in situ hybridization (DOPE-FISH)
521 improves signal intensity and increases rRNA accessibility. Appl Environ
522 Microbiol **76**:922–926.

523 10. **Behnam F, Vilcinskas A, Wagner M, Stoecker K**. 2012. A straightforward
524 DOPE (Double labeling of oligonucleotide probes)-FISH (Fluorescence in situ
525 hybridization) method for simultaneous multicolor detection of six microbial
526 populations. Appl Environ Microbiol **78**:5138–5142.

527 11. **Nederlof PM, Van der Flier S, Wiegant J, Raap AK, Tanke HJ, Ploem JS,**
528 **van der Ploeg M**. 1990. Multiple fluorescence in situ hybridization. Cytometry
529 **11**:126–131.

Accepted Manuscript Posted Online
Applied and Environmental Microbiology
AEM
Applied and Environmental Microbiology

12. **Nederlof PM, Van der Flier S, Vrolijk J, Tanke HJ, Raap AK**. 1992. Fluorescence ratio measurements of double-labeled probes for multiple in situ hybridization by digital imaging microscopy. Cytometry **13**:839–845.

13. **Szuhai K, Tanke HJ**. 2006. COBRA: combined binary ratio labeling of nucleic-acid probes for multi-color fluorescence in situ hybridization karyotyping. Nat Protoc **1**:264–275.

14. **Liehr T, Starke H, Weise A, Lehrer H, Claussen U**. 2004. Multicolor FISH probe sets and their applications. Histol Histopathol **19**:229–237.

15. **Valm AM, Welch J, Rieken CW**. 2011. Systems-level analysis of microbial community organization through combinatorial labeling and spectral imaging. PNAS **108**:4152–4157.

16. **Moter A, Leist G, Rudolph R, Schrank K, Choi B-K, Wagner M, Göbel UB**. 1998. Fluorescence in situ hybridization shows spatial distribution of as yet uncultured treponemes in biopsies from digital dermatitis lesions. Microbiology (Reading, Engl) **144**:2459–2467.

17. **Schimak MP, Toenshoff ER, Bright M**. 2012. Simultaneous 16S and 18S rRNA fluorescence in situ hybridization (FISH) on LR White sections demonstrated in Vestimentifera (Siboglinidae) tubeworms. Acta Histochem **114**:122–130.

18. **Sweet M, Bulling M, Cerrano C**. A novel sponge disease caused by a consortium of micro-organisms. Coral Reefs **34**:871–883.

19. **Morvan F, Meyer A, Pourceau G, Vidal S, Chevolot Y, Souteyrand E, Vasseur JJ**. 2008. Click chemistry and oligonucleotides: How a simple reaction can do so much. Nucl Acid S **52**:47–48.

20. **Giere O, Erseus C**. 2002. Taxonomy and new bacterial symbioses of gutless marine Tubificidae (Annelida, Oligochaeta) from the Island of Elba (Italy). Org Divers Evol **2**:289–297.

21. **Dubilier N, Mulders C, Ferdelman T, de Beer D, Pernthaler A, Klein M, Wagner M, Erseus C, Thiermann F, Krieger J, Giere O, Amann R**. 2001. Endosymbiotic sulphate-reducing and sulphide-oxidizing bacteria in an oligochaete worm. Nature **411**:298–302.

22. **Giere O, Felbeck H, Dawson R, Liebezeit G**. 1984. The gutless oligochaete *Phallodrilus leukodermatus* Giere, a tubificid of structural, ecological and physiological relevance. Hydrobiologia **115**:83–89.

23. **Kleiner M, Wentrup C, Lott C**. 2012. Metaproteomics of a gutless marine worm and its symbiotic microbial community reveal unusual pathways for carbon and energy use. PNAS **109 (19)**:E1173–E1182.

24. **Loy A, Maixner F, Wagner M, Horn M**. 2007. probeBase--an online resource for rRNA-targeted oligonucleotide probes: new features 2007. Nucleic Acids Res **35**:D800–4.

Accepted Manuscript Posted Online
AEM
Applied and Environmental Microbiology

25. **Manz W, Amann R, Ludwig W, Wagner M, Schleifer K-H**. 1992. Phylogenetic oligodeoxynucleotide probes for the major subclasses of proteobacteria: Problems and solutions. Syst Appl Microbiol **15**:593–600.

26. **Daims H, Lücker S, Wagner M**. 2006. daime, a novel image analysis program for microbial ecology and biofilm research. Environ Microbiol **8**:200–213.

27. **Manz W, Amann R, Ludwig W, Vancanneyt M**. 1996. Application of a suite of 16S rRNA-specific oligonucleotide probes designed to investigate bacteria of the phylum cytophaga-flavobacter-bacteroides in the natural environment. Microbiol **142**:1097–1106.

28. **Wetmur JG**. 1975. Acceleration of DNA renaturation rates. Biopolymers **14**:2517–2524.

29. **Loy A, Horn M, Wagner M**. 2003. probeBase: an online resource for rRNA-targeted oligonucleotide probes. Nucleic Acids Res **31**:514–516.

30. **Morris RM, Rappé MS, Connon SA, Vergin KL, Siebold WA, Carlson CA, Giovannoni SJ**. 2002. SAR11 clade dominates ocean surface bacterioplankton communities. Nature **420**:806–810.

31. **Brorson SH, Roos N, Skj F**. 1994. Antibody penetration into LR-White sections. Micron **25**:453–460.

32. **McFall-Ngai MJ**. 2002. Unseen forces: the influence of bacteria on animal development. Dev Biol **242**:1–14.

33. **Amann R, Snaidr J, Wagner M, Ludwig W, Schleifer KH**. 1996. In situ visualization of high genetic diversity in a natural microbial community. J Bacteriol **178**:3496–3500.

34. **Yilmaz LS, Noguera DR**. 2004. Mechanistic approach to the problem of hybridization efficiency in fluorescent in situ hybridization. Appl Environ Microbiol **70**:7126–7139.

35. **Behrens S, Ruhland C, Inacio J, Huber H, Fonseca A, Spencer-Martins I, Fuchs BM, Amann R**. 2003. In situ accessibility of small-subunit rRNA of members of the domains Bacteria, Archaea, and Eucarya to Cy3-labeled oligonucleotide probes. Appl Environ Microbiol **69**:1748–1758.

36. **Valm AM, Welch JLM, Borisy GG**. 2012. CLASI-FISH: Principles of combinatorial labeling and spectral imaging. Syst Appl Microbiol **35**:496–502.

Accepted Manuscript Posted Online
Applied and Environmental Microbiology
AEM
Applied and Environmental Microbiology

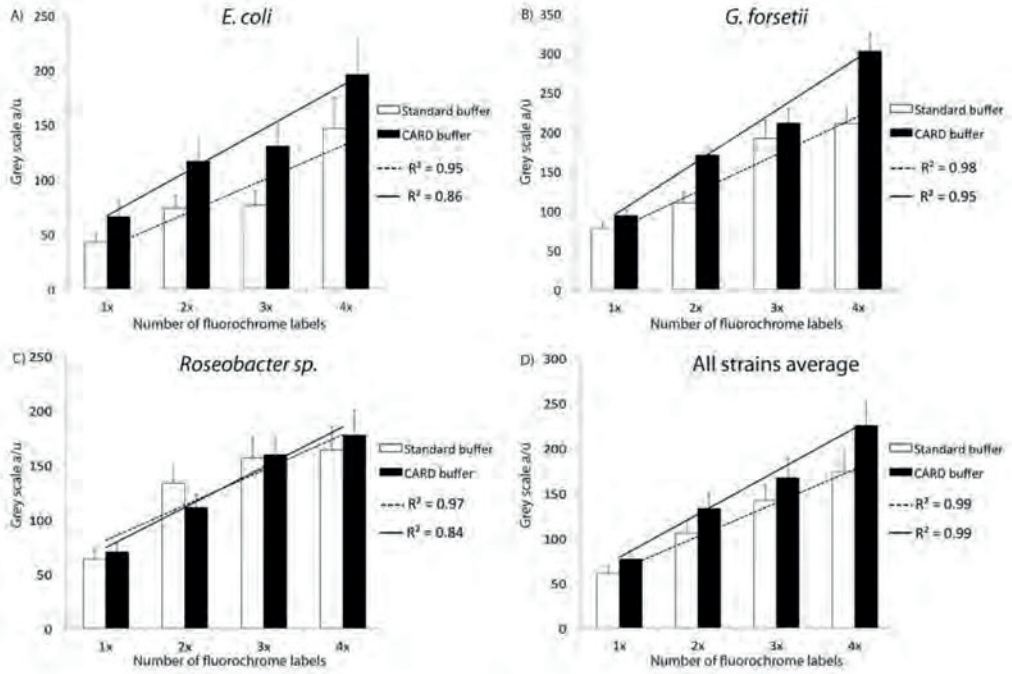

Figure 1: Signal intensities of MiL-FISH probes with 1 – 4 fluorescent labels. Three reference strains, A) *Escherichia coli*, B) *Gramella forsteii* and C) *Roseobacter sp.* AK199 were hybridised in triplicate with a 1x, 2x, 3x and 4x 6-FAM labelled EUB338 MiL-probe using both standard (white bars) and CARD-FISH (black bars) hybridisation buffer. D) Average signal increase in all three reference strains. Dark line shows linear regression of CARD-FISH buffer on cells, dashed line shows linear regression of standard FISH buffer. a/u = arbitrary units

Accepted Manuscript Posted Online
Applied and Environmental Microbiology
AEM
Applied and Environmental Microbiology

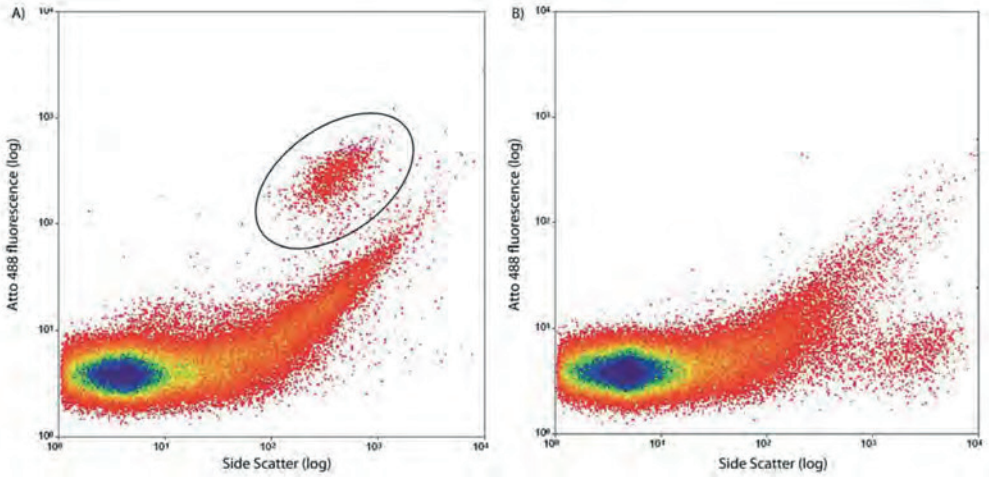

Figure 2: FACS plot of A) 4x Atto488 multi-labelled EUB338 probe targeting symbionts of *Inanidrilus leukodermatus*. B) Corresponding negative control with 4x Atto488 multi-labelled NON338 probe. The marked region in plot A shows the fraction of labelled bacterial cells.

Accepted Manuscript Posted Online
Applied and Environmental Microbiology
AEM
Applied and Environmental Microbiology

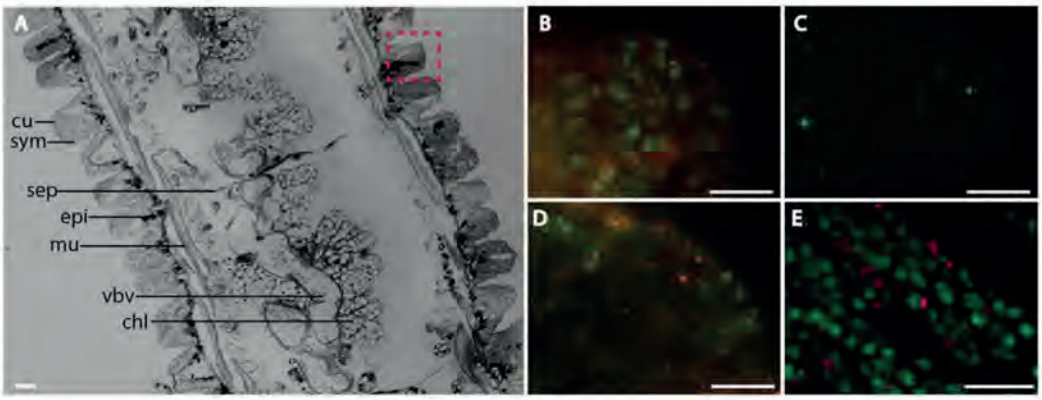

Figure 3: Comparison of mono-, MiL-and CARD-FISH on LR-White embedded *O. algarvensis* cross sections A: Ethanol preserved specimen, cu = cuticle, sym = symbionts, sep = septum, epi = epidermis, mu = muscle, vbv = ventral blood vessel & nerve chord, chl = chloragogen tissue, grid square = example of region shown in images B, C, D and E.

Gam42a (green) & DSS658 (red) on B) mono-FISH on ethanol preserved specimen, 19 hour hybridisation. C) mono-FISH on ethanol preserved specimen, 3 hour hybridisation and D) CARD-FISH on Carnoy's / PFA fixed specimen, 3-hour hybridisation. E) MiL-FISH on Carnoy's / PFA fixed specimen, 3 hour hybridisation. Scale Bar = 5 µM

Accepted Manuscript Posted Online
Applied and Environmental Microbiology
AEM
Applied and Environmental Microbiology

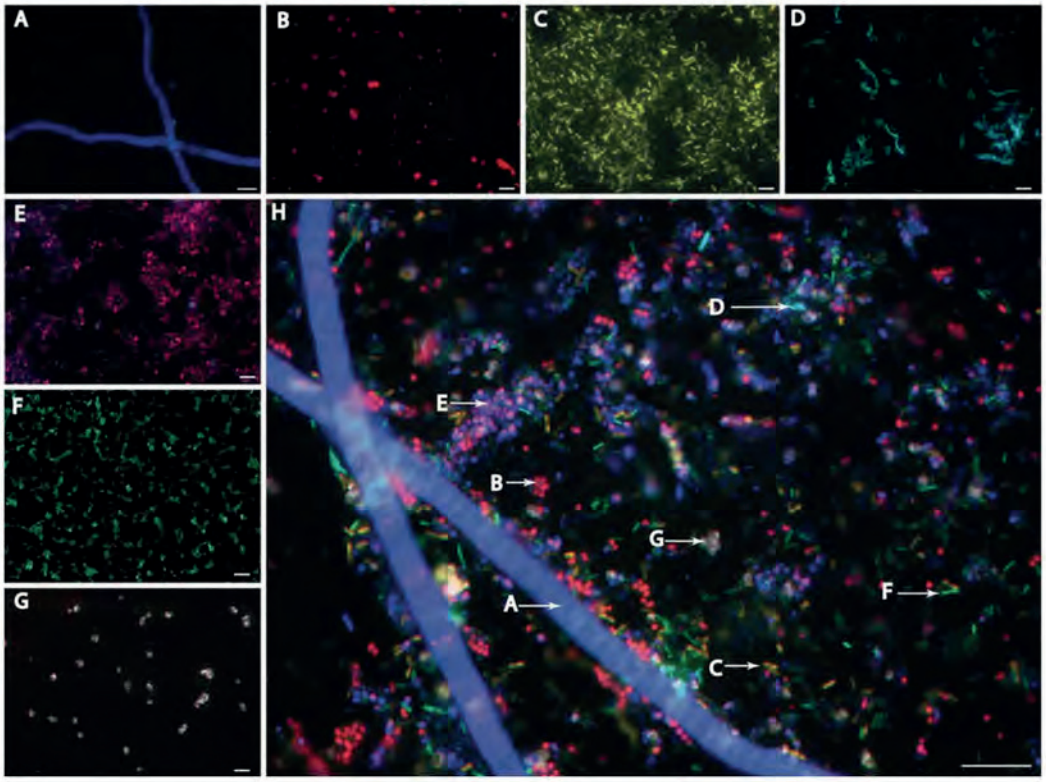

Figure 4: Epifluorescence images of MiL-FISH labelled microorganisms as listed in SI Table 1 and shown in Figure 4: A) *Beggiatoa sp.* hybridised with Gam42a, B) *Desulfococcus biacutus* with DSS658, C) *Roseobacter sp.* with Ros537, D) *Sulfurimonas denitrificans* with EPSY914, E) *Rhodopirellula sp.* SH1 ^{T} with PLA46, F) *Gramella forsetii* with CF319a, G) *Metallosphaera sedula* with Arch915, H) Composite image of all seven microbial partners in an artificial mix. Letters correlate to images of individual organisms A-G. Scale bar: A & H = 10 µm, B-G = 5 µm

Accepted Manuscript Posted Online
Applied and Environmental Microbiology
AEM
Applied and Environmental Microbiology

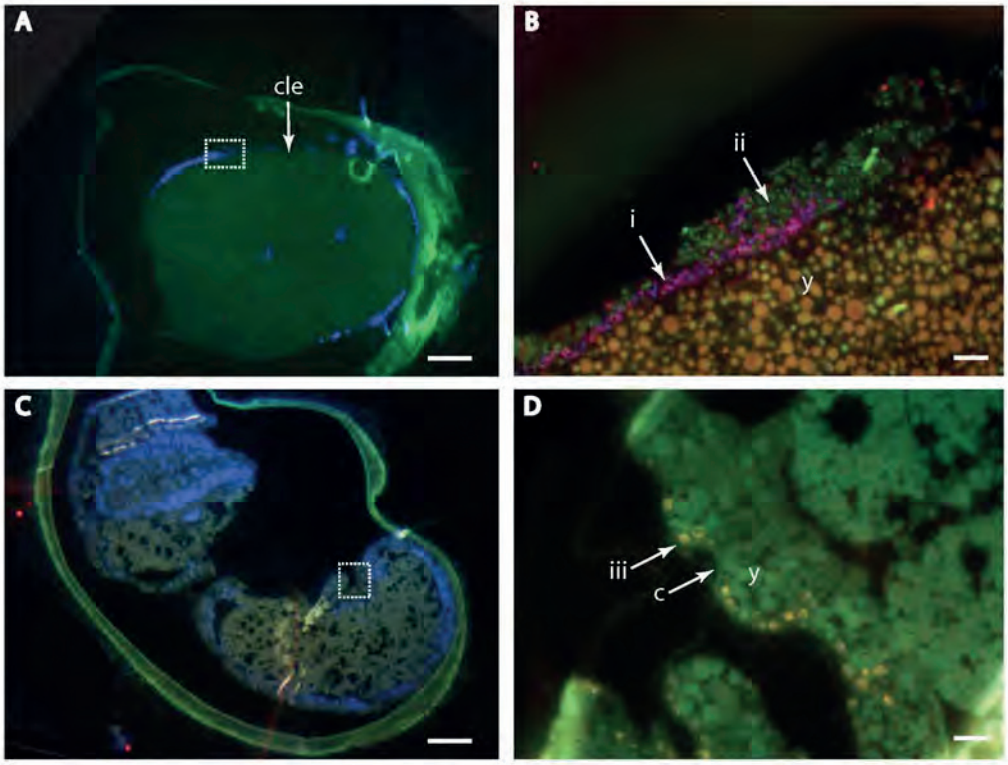

Figure 5: 1 µm sections of LR-White embedded *O. algarvensis* eggs. A) DAPI stained overview of egg after first cleavage, grid square = region in B, cle = cleavage. B) Gamma- (ii) and Delta- (i) proteobacteria hybridised with 4x labelled Gam42a & 4x labelled DSS658 probe respectively. Autofluorescence of egg yolk is overcome and bacteria are seen to closely associate to the developing embryo. y = egg yolk C) DAPI stained overview of juvenile worm in egg, grid square = region in D. D) Gamma 1 symbiont phylotype (iii) hybridised with 16S rRNA specific probe labelled with 2x FITC and 2x Cy3 to produce yellow in the overlay. Symbiont cells are incorporated between cuticle and epidermis and in close proximity to egg yolk. y = egg yolk, c = cuticle. Scale: A & C = 50 µm, B & D = 5 µm.

Supplementary Information:

Bacterial cultures and sample material:

The gammagroteobacteria, *Escherichia coli* DSM498, was grown in Luria-Bertani medium for 4h 20 at 37°C. At the end-log phase and an optical density of 0.468 (600nm) cells were harvested at 1500g for 10 min., fixed in 2% formaldehyde (v/v) for 1h at RT, washed three times in 1xPBS and pelleted at 1500g for 5 min. Fixed cells were re-suspended in 1xPBS / ethanol (50%) and stored at -20°C until further analysis.

The flavobacteria, *Gramella forsetii* KT0803, was grown on SY-medium containing 40g/L sea salt (Sigma-Aldrich, St. Louis, MO, USA) and 0.1% yeast extract. To avoid cell clumping and after growth at RT for 60h to an optical density of 0.146 (600 nm), 1ml was used as an inoculant in 100ml SY-medium and re-grown to an optical density of 0,065 (600nm). Cells were harvested by centrifugation at 1500 g for 10 min, fixed in 2% formaldehyde for 1h at RT, washed 3 times in 1x PBS and pelleted at 1500g for 10 min. Cells were re-suspended in 50% 1xPBS / ethanol (50%) and stored at -20°C until further analysis.

The planctomycetes, *Rhodopirellula baltica* SH1^{T}, was grown in medium M9 as previously described by Schlesner et al. 1986 **(1)**. Cells were harvested at 1500g for 10 min, fixed in 2% formaldehyde (v/v) for 1h at RT, washed three times in 1xPBS and pelleted at 1500g for 5 min. Fixed cells were re-suspended in 1xPBS / ethanol (50%) and stored at -20°C until further analysis.

The alphaproteobacteria, *Roseobacter sp.* AK 199, plate cultures were picked and grown in 300 ml Difco™ Marine Broth 2216 (Beckton, Dickinson and Company,

New Jersey, USA) for 5 days on a shaker at 28 °C. 10ml of the culture stock was taken and centrifuged at 4000g for 10 minutes and re-suspended in 800 µl 1x PBS. Cells were fixed in 4% PFA for 1 hour at room temperature washed three times in 1x PBS and re-suspended in 50% EtOH / PBS.

The deltaproteobacteria, *Desulfococcus biacutus* DSM5651, were cultured after the guidelines for anaerobic cultivation at 30°C as described on www.dsmz.de for the given reference number DSM5651. Cells were harvested at 1500g for 10 min., fixed in 2% formaldehyde (v/v) for 1h at RT, washed three times in 1xPBS and pelleted at 1500g for 5 min. Fixed cells were re-suspended in 1xPBS / ethanol (50%) and stored at -20°C until further analysis.

The gammaproteobacteria, *Beggiatoa sp.*, were grown with 4 mMol H_2S final concentration after Schwedt et al. 2012 **(2)**, in the presence of *Pseudovibrio sp.* Cells were hand picked, washed three times in 1x PBS and transferred onto 10 well Diagnostika (Thermo Fisher Scientific, MA, USA) gelatine / chromalaune ($KCr(SO_4)_2 \cdot 12H_2O$) coated glass slides. Fixation followed with 4% PFA at room temperature for 1 hour and washed three times in 1 x PBS.

The epsilonproteobacteria, *Sulfurimonas denitrificans*, was grown as described for DSMZ strain DSM1251 (http://www.dsmz.de/catalogues/details/culture/DSM-1251.html). 10ml of the culture stock was taken and centrifuged at 4000g for 10 minutes and re-suspended in 800 µl 1x PBS. Cells were fixed in 4% PFA for 1 hour at room temperature washed three times in 1x PBS and re-suspended in 50% EtOH / PBS.

The sulfolobales (Archaea), *Metallosphaera sedula* DSM 5348^T, was grown as described by Huber *et al.* 1989 **(3)** without sulfur particles in the media as previously described by Behrens *et al.* 2003 **(4)**. Cells were harvested at 1500g for 10 min., fixed in 2% formaldehyde (v/v) for 1h at RT, washed three times in 1xPBS and pelleted at 1500g for 5 min. Fixed cells were re-suspended in 1xPBS / ethanol (50%) and stored at -20°C until further analysis.

91 References

92 1. **Schlesner H**. 1986. Pirella marina sp. nov., a budding, peptidoglycan-less
93 bacterium from brackish water. Syst Appl Microbiol **8**:177–180.

94 2. **Schwedt A, Kreutzmann AC, Polerecky L**. 2011. Sulfur respiration in a
95 marine chemolithoautotrophic Beggiatoa strain. Front Microbiol **2**:276.

96 3. **Huber G, Spinnler C, Gambacorta A, Stetter KO**. 1989. Metallosphaera
97 sedula gen. and sp. nov. Represents a New Genus of Aerobic, Metal-Mobilizing,
98 Thermoacidophilic Archaebacteria. Syst Appl Microbiol **12**:38–47.

99 4. **Behrens S, Ruhland C, Inacio J, Huber H, Fonseca A, Spencer-Martins I,**
100 **Fuchs BM, Amann R**. 2003. In Situ Accessibility of Small-Subunit rRNA of
101 Members of the Domains Bacteria, Archaea, and Eucarya to Cy3-Labeled
102 Oligonucleotide Probes. Appl Environ Microbiol **69**:1748–1758.

103

Probe	Sequence 5' - 3' (reverse complementary)	Target gene	Label	Synthesis	Taxon	Target Species	FA %	Colour
DSS658	TCC ACT TCC CTC TCC CAT	16S rRNA	4x Cy3	Click chemistry	Delta-proteobacteria	*Desulfococcus biacutus*	60%	Red
Gam42a	GCC TTC CCA CAT CGT TT	23S rRNA	4x Cy5	Click chemistry	Gamma-proteobacteria	*Beggiatoa sp.*	35%	Blue
CF319a	TGG TCC GTG TCT CAG TAC	16S rRNA	4x 6-FAM	Click chemistry	Flavobacteria	*Gramella forsetii*	35%	Green
CF319a	TGG TCC GTG TCT CAG TAC	16S rRNA	5' & 3' 6-FAM	DOPE	Flavobacteria	*Gramella forsetii*	35%	Green
CF319a	TGG TCC GTG TCT CAG TAC	16S rRNA	5' 6-FAM	mono	Flavobacteria	*Gramella forsetii*	35%	Green
Ros537	CAA CGC TAA CCC CCT CC	16S rRNA	5' & 3' end 6-FAM, 2x Cy3 intern	DOPE & Click chemistry	Alpha-proteobacteria	*Roseobacter sp.* AK 199	35%	Yellow
EPSY914	GGT CCC CGT CTA TTC CTT	16S rRNA	5' & 3' end 6-FAM, 2x Cy5 intern	DOPE & Click chemistry	Epsilon-proteobacteria	*Sulfurimonas denitrificans*	35%	Cyan
PLA46	GAC TTG CAT GCC TAA TCC	16S rRNA	5' & 3' Cy3, Cy5 intern	DOPE & Click chemistry	Planctomycetes	*Rhodopirellula sp.* SH^{1} T	35%	Magenta

Arch915	GTG CTC CCC CGC CAA TTC CT	16S rRNA	2x Cy5 intern, 5' Cy3, 3' Atto 488	DOPE & Click chemistry	Archaea	*Metallosphaera sedula*	35%	White
Oalg_G1_644_20mer	TAC CAC ACT CTA GCC GGA CA	16S rRNA	5' & 3' 6-FAM, Cy3 intern	DOPE & Click chemistry	Gamma-proteobacteria	gamma 1 symbiont of *O. algarvensis*	35%	Yellow
EUB338	GCT GCC TCC CGT AGG AGT	16S rRNA	1x 6-FAM	Click chemistry	Bacteria	Most Bacteria	35%	Green
EUB338	GCT GCC TCC CGT AGG AGT	16S rRNA	2x 6-FAM	Click chemistry	Bacteria	Most Bacteria	35%	Green
EUB338	GCT GCC TCC CGT AGG AGT	16S rRNA	3x 6-FAM	Click chemistry	Bacteria	Most Bacteria	35%	Green
EUB338	GCT GCC TCC CGT AGG AGT	16S rRNA	4x 6-FAM	Click chemistry	Bacteria	Most Bacteria	35%	Green
EUB338	GCT GCC TCC CGT AGG AGT	16S rRNA	4x Atto488	Click chemistry	Bacteria	Most Bacteria	35%	Green
NON338	ACT CCT ACG GGA GGC AGC	16S rRNA	4x 6-FAM	Click chemistry	Non-sense	none	n/a	Green
NON338	ACT CCT ACG GGA GGC AGC	16S rRNA	4x Atto488	Click chemistry	Non-sense	none	n/a	Green
DSS658	TCC ACT TCC CTC TCC CAT	16S rRNA	Alexa 594 Tyramide	HRP - label	Delta-proteobacteria	delta 1 & 4 symbiont of *O. algarvensis*	60%	Red
Gam42a	GCC TTC CCA CAT CGT TT	23S rRNA	Alexa 488 Tyramide	HRP - label	Gamma-proteobacteria	gamma 1 & 3 symbiont of *O. algarvensis*	35%	Green

SI Table 1: Oligonucleotide probes used in this study. Probe name, nucleotide sequence – modified nucleotide-fluorochrome complexes are indicated by an underscore for MiL-FISH probes, target gene, label type, label synthesis, target taxon or higher, target species and probe colour during imaging

Label	EUB338 Probe signal	NON338 probe signal	S/N ratio
1x EUB338	60.8	14.0	4.3
2x EUB338	105.6	8.0	13.2
3x EUB338	141.3	6.0	23.6
4x EUB338	173.3	5.0	34.7
LR-White mono-FISH, 3h	21.3	4.6	4.6
LR-White mono-FISH, 19h	69.3	14.9	4.7
LR-White 4x labelled MiL-FISH, 3h	70.9	10.0	7.1

SI Table 2: Signal to noise ratio (S/N) for 1x, 2x, 3x and 4x 6-FAM labelled EUB338 probe to the 4x labelled nonsense probe NON338 with mono-FISH hybridisation buffer on *Gramella forsetii*. For imaging with 4x labelled probes lower exposure times resulted in higher S/N ratio. LR-White sections of *O. algarvensis* targeting bacterial symbionts with EUB338 for hybridisation times of both 3 and 19 hours resulted in lower S/N ratio than MiL-FISH on LR-White sections.

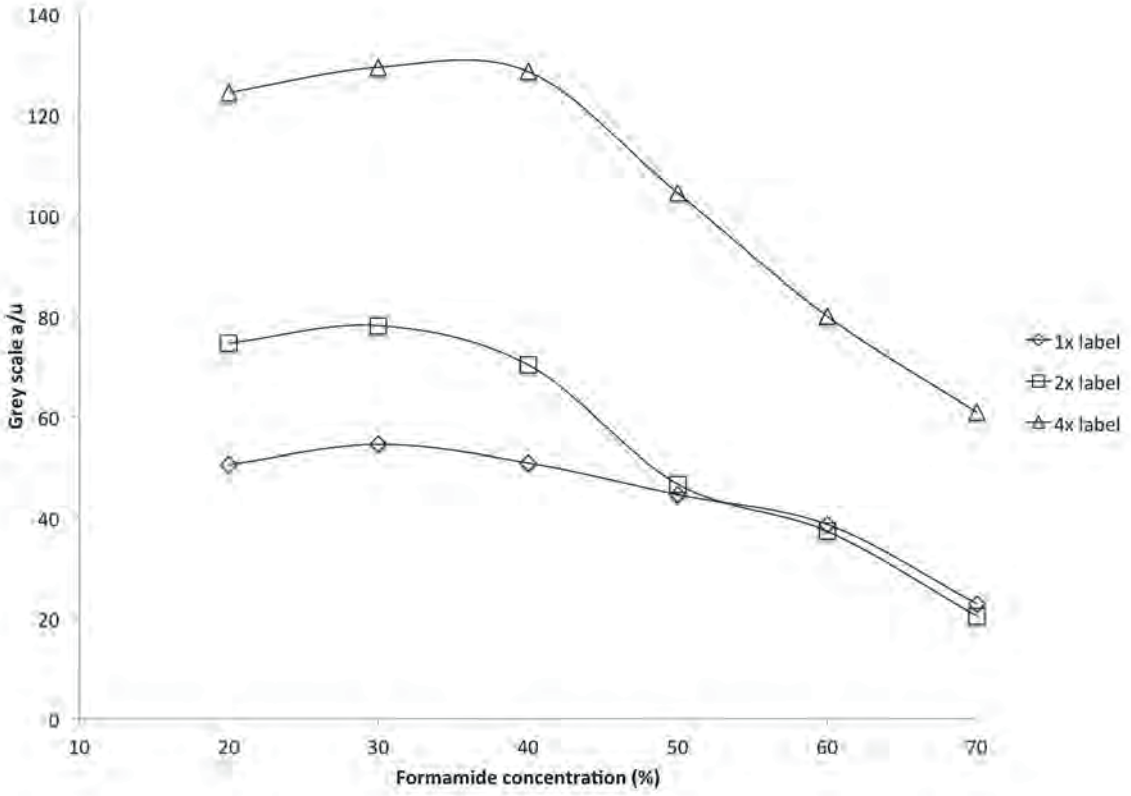

SI Figure 1: Melting curve in grey scale (a/u) of 1x. 2x and 4x times 6-FAM labelled CF319a on *Gramella forsetii* hybridised under increasing denaturing conditions with standard FISH buffer in triplicate. Signals for all label types decrease between 30 and 40 % formamide as previously described for CF319a.

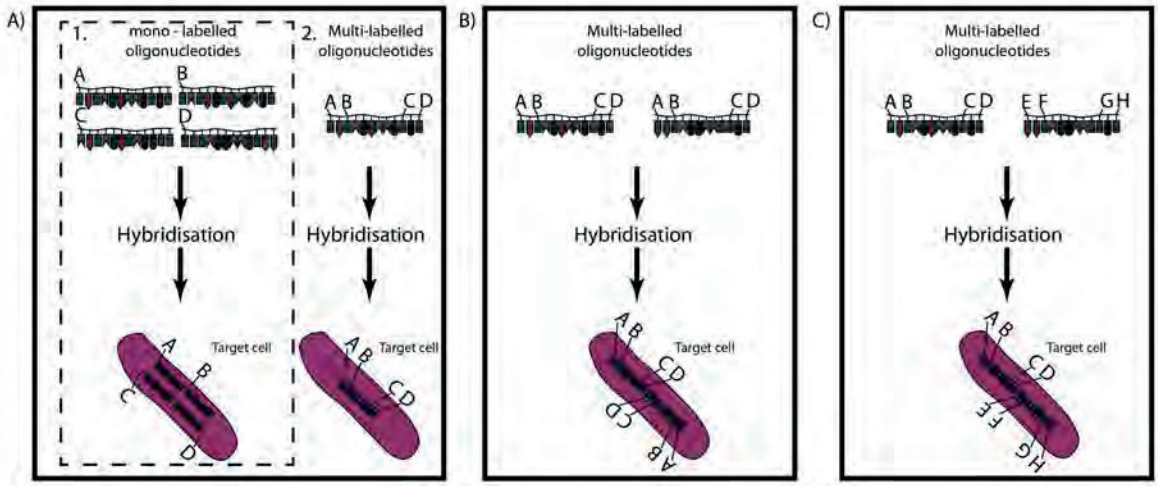

SI Figure 2: Three optimisation approaches for CLASI-FISH using MiL-FISH probes. A1.) CLASI-FISH with a repertoire of four probes targeting four sites on the 16S rRNA labelled with various fluorochromes A, B, C & D. A2.) MiL-FISH probe targeting only one site on the 16S rRNA labelled with the same repertoire of fluorochromes A, B, C, & D. B) Two MiL-FISH probes targeting two sites on the 16S rRNA carrying the same label combination for an increase in probe-conferred signal. C) Two MiL-FISH probes carrying a repertoire of eight fluorochromes, A-H, for an increase of label combinations.

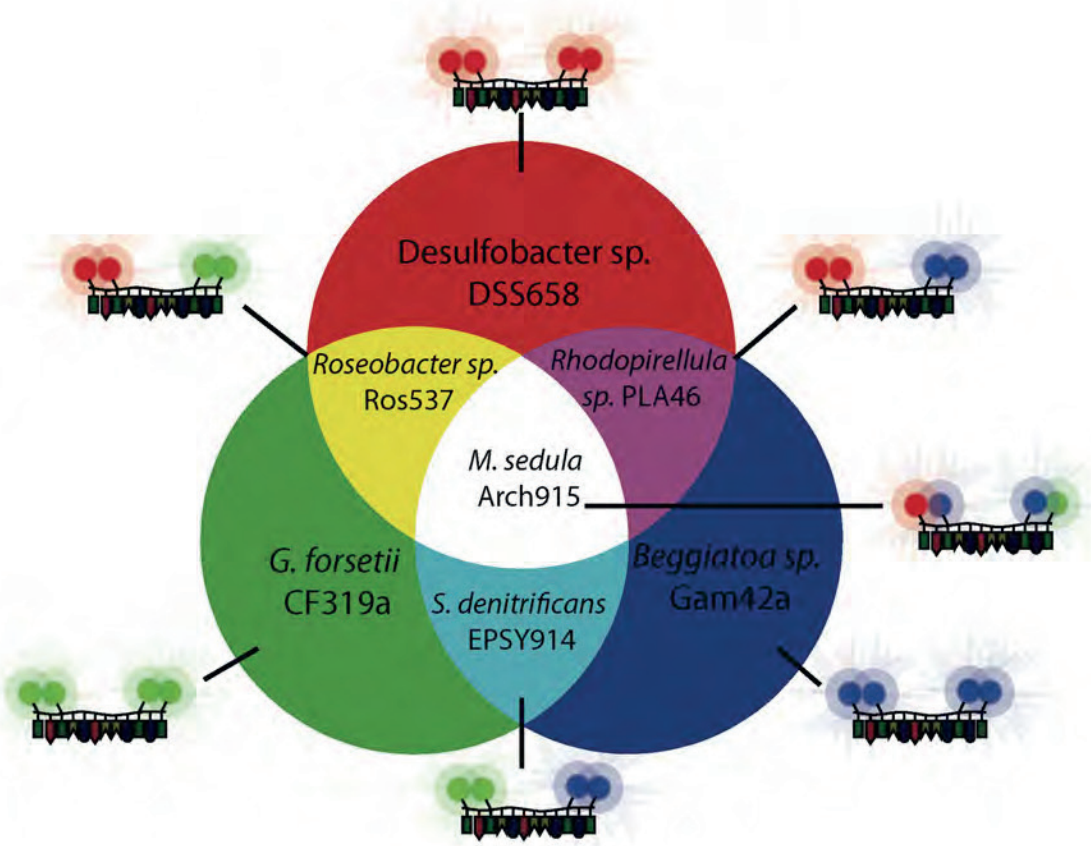

SI Figure 3: Schematic of multi-labelled oligonucleotide probes and target organisms for the hybridisation of seven marine microbial groups. The RGB colours red, blue and green are combined by mixing of fluorochrome dye moieties on probes to create magenta, cyan, yellow and white.

Chapter IV

MiL-FISH: for preservation of microbial genomic DNA post-hybridisation

Mario P. Schimak[1], Halina E. Tegetmeyer[2], Adrien Assie[1], Bernhard M. Fuchs[1], Nicole Dubilier[1]

[1]Max Planck Institute for Marine Microbiology, Celsiusstr. 1, D-28359 Bremen, Germany
[2]Centre for Biotechnology (CeBiTec), Bielefeld University, 33615 Bielefeld, Germany

Manuscript in preparation – short communication

Journal requirements: Abstract, Max. 250 words. Main text, Max. 1000 words. Images, Max. 2.

Corresponding author

Mario Schimak: mschimak@mpi-bremen.de

Author contributions:

M.P.S., B.F. & N.D. designed research and conceived the project; H.E.T. conducted library preparation and sequencing, A.A. conducted coverage and genome assembly, M.P.S. conducted FISH experiments and wrote the manuscript. All co-authors reviewed and revised the manuscript.

Abstract

To understand the roles of individual cells within a metacommunity several methodological approaches need to be successfully combined. In combination these methods allow for a more targeted testing of hypotheses regarding individual cell niche partitioning compared to mass meta-omic approach. The isolation of phylogenetically defined groups from an environmental sample can be achieved by fluorescence *in situ* hybridisation (FISH) and fluorescence activated cell sorting (FACS). However, the effect of FISH on genomic DNA, and therefore its influence in single cell genomics, has not been investigated to date. Here we compare two FISH approaches, multi-labelled-FISH (MiL-FISH) and catalysed reporter deposition (CARD) – FISH, and show their effects on the sequence quality of *E. coli* genomic DNA. In contrast to CARD-FISH, MiL-FISH yielded pair-end reads comparable to non-FISH control cells after Illumina sequencing. Subsequent genome assembly of the attained reads was unproblematic. We propose MiL-FISH for improved DNA preservation in single cell genomics.

Article text

Using single cell genomics to understand the role of individual cells in multiplex communities such as those of a developing embryo, tumours or environmental microbial population involves the combination of several methodical approaches (for review see (Kalisky *et al.,* 2011)). The technical challenges involved include the simultaneous visualisation of key cells, the isolation of partners from the metacommunity and the downstream -omic analyses of diversity and function to determine niche partitioning within a given community.

Fluorescence *in situ* hybridisation (FISH) is a vital tool for both environmental microbial ecology and medical microbiology. In combination with fluorescence activated cell sorting (FACS) and subsequent genomic analysis one can tease apart the roles of individuals or consortia within the larger metacommunity (de Jager & Siezen, 2011). The sorting of phylogenetically distinct environmental cells by FACS requires high probe-conferred fluorescence signal, which correlates to the number of rRNA molecules in a target cell during FISH (Sekar *et al.,* 2004). Standard FISH approaches may therefore potentially miss groups of low rRNA content, such as those of the SAR11 clade for example (Amann *et al.,* 1990) (Stoecker *et al.,* 2010). To resolve this CARD-FISH is commonly used, yielding a 26 – 41 fold amplified signal (A Pernthaler, J Pernthaler & Amann, 2002a) (Hoshino, Yilmaz, Noguera, Daims & Wagner, 2008a). Although high fluorescence signal is given, the chemistry employed during CARD-FISH may inhibit reliable downstream genomic analyses such as genome sequencing and assembly. Further, it was shown recently that standard fixation techniques employed in FISH protocols can negatively affect genomic DNA recovered from microbial cells (Clingenpeel *et al.,* 2014). Chemical influence on DNA during fixation and hybridisation of cells must therefore be considered and accounted for in single cell genomics especially as sequencing

technologies begin to include platforms for large DNA fragments in the Kbp range (i.e. PacBio). In this study we compare the influence of CARD-FISH with Multi-labelled-FISH (MiL-FISH) (Schimak *et al.,* 2015) on genomic DNA. By combinatorial labelling of probes, MiL-FISH can target seven phylogenetically distinct groups simultaneously and yields strong enough probe signals to isolate unfixed environmental cells via FACS. This makes MiL-FISH a valuable tool for environmental single cell genomics.

Escherichia coli K12 S17-1 cells were hybridized in triplicate with the EUB338 oligonucleotide probe, labelled with horseradish peroxidase (HRP) for CARD-FISH and a 4x Atto488 for MiL-FISH (SI Table 1). To eliminate fixation biases and to solely test the effect that FISH protocols have on genomic DNA, cells were hybridized unfixed. A reference triplicate control of non-FISH cells was included. To avoid biases that could be introduced by multi-displacement amplification (MDA), DNA was extracted directly from cells after hybridization following Zhou *et al.,* 1996 (Zhou *et al.,* 1996) and subsequently prepared for whole genome shotgun sequencing.

TruSeq PCR free libraries with insert sizes of approximately 700-800 bp were generated. Bioanalyser data of the finished libraries showed mean library fragment lengths clearly lower for CARD -FISH than for MiL - FISH and control DNA (SI Figure 1). Quantitative PCR revealed that for CARD-FISH DNA, correct ligation of adapters was less than 0.2 % compared to 10 – 17 % for MiL-FISH and control DNA. Adapter ligation for MiL-FISH and controls was lower than usually observed for TruSeq PCR free libraries (25 – 40 %). This was most likely due to the use of longer insert sizes in our experiments compared to the 350 – 500 bp of standard protocols (personal observation H.E.T.). The poor ligation efficiency during library preparation for CARD-FISH products could be an indication of chemically modified or damaged DNA (i.e. Gründemann & Schömig, 1996). The cause of this is most likely the inhibition of one, or several, of the

three enzymatic reactions, namely end repair, the generation of a ligation site ('A-tailing'), or the adapter ligation itself.

The number of sequencing reads obtained from CARD-FISH libraries was only 8,268 read-pairs per fmol of DNA loaded onto the MiSeq, which is less than 1% of the 1,216,401 read-pairs obtained from MiL-FISH libraries (Table 1A). Accordingly, genome coverage depth from CARD-FISH cells was only five to ten fold compared to 50 to 100 fold for MiL-FISH cells and controls (SI Figure 2). Alignment over the reference genome of the closely related *E. coli* strain K-12 W3110 averaged at 92.64% for sequence data from CARD-FISH cells and 95.93% and 95.99% for MiL-FISH and controls respectively (SI Table 2). General statistics of *de novo* assemblies showed an N_{50} of 1500 bp for CARD-FISH cells, whereas both MiL-FISH cells and controls cells showed an N_{50} of 130,000 bp. Deeper sequencing of CARD-FISH cells might resolve this issue, provided enough DNA is available, however the costs associated in doing so would make this a sub-optimal solution and not applicable for single cell genomics.

A possible explanation for the poor sequence quality after CARD-FISH may be the exposure of cells to hydrogen peroxide (H_2O_2), which is required for the inactivation of endogenous peroxidase and during the amplification process. H_2O_2 can cause oxidation of DNA by mediating the highly reactive oxidant OH- (Imlay *et al.,* 1988) and break DNA strands (Balasubramanian *et al.,* 1998). Furthermore, DNA and DNA associated proteins may be affected by radicalized tyramides during the amplification process potentially causing covalent crosslinking and preventing denaturation of the DNA double helix.

MiL-FISH probes provide signals strengths sufficient for the detection of unfixed cells by FACS (Schimak *et al.,* 2015). In addition, the quality and quantity of DNA isolated from cells after MiL-FISH was comparable to DNA extracted from untreated

control cells. Based on a combination of our results and the previously published inferred negative influence of fixation on genomic DNA we propose unfixed cell identification by MiL-FISH followed by FACS and subsequent DNA recovery via MDA for an optimal single cell genomic workflow (Figure 1). We conclude that the application of such a workflow will enable more targeted testing of individual cells diversity and function in multiplex environmental samples.

Acknowledgements

We thank Silke Wetzel for excellent technical support and Meghan Chafee for reading of the manuscript. This work was funded by the Max Planck Society and the European Union (EU) Marie Curie Actions Initial Training Network (ITN) SYMBIOMICS (contract number 264774).

References

Amann RI, Krumholz L, Stahl DA. (1990). Fluorescent-oligonucleotide probing of whole cells for determinative, phylogenetic, and environmental studies in microbiology. *J Bacteriol* **172**:762–770.

Balasubramanian B, Pogozelski WK, Tullius TD. (1998). DNA strand breaking by the hydroxyl radical is governed by the accessible surface areas of the hydrogen atoms of theDNA backbone. *PNAS* **95**:1–6.

Clingenpeel S, Schwientek P, Hugenholtz P, Woyke T. (2014). Effects of sample treatments on genome recovery via single-cell genomics. *ISME J* **8**:2546–2549.

de Jager V, Siezen RJ. (2011). Single-cell genomics: unraveling the genomes of unculturable microorganisms. *Microb Biotechnol* **4**:431–437.

Gründemann D, Schömig E. (1996). Protection of DNA during preparative agarose gel electrophoresis against damage induced by ultraviolet light. *BioTechniques* **21**:898–903.

Hoshino T, Yilmaz LS, Noguera DR, Daims H, Wagner M. (2008a). Quantification of target molecules needed to detect microorganisms by fluorescence in situ hybridization (FISH) and catalyzed reporter deposition-FISH. *Appl Environ Microbiol* **74**:5068–5077.

Hoshino T, Yilmaz LS, Noguera DR, Daims H, Wagner M. (2008b). Quantification of target molecules needed to detect microorganisms by fluorescence in situ hybridization (FISH) and catalyzed reporter deposition-FISH. *Appl Environ Microbiol* **74**:5068–5077.

Imlay JA, Chin SM, Linn S. (1988). Toxic DNA damage by hydrogen peroxide through the Fenton reaction in vivo and in vitro. *Science* **240**:640–642.

Kalisky T, Blainey P, Quake SR. (2011). Genomic analysis at the single-cell level. *Annu Rev Genet* **45**:431–445.

Pernthaler A, Pernthaler J, Amann R. (2002a). Fluorescence in situ hybridization and catalyzed reporter deposition for the identification of marine bacteria. *Appl Environ Microbiol* **68**:3094–3101.

Pernthaler A, Pernthaler J, Amann R. (2002b). Fluorescence in situ hybridization and catalyzed reporter deposition for the identification of marine bacteria. *Appl Environ Microbiol* **68**:3094–3101.

Schimak MP, Kleiner M, Wetzel S, Liebeke M, Dubilier N, Fuchs BM. (2015). MiL-FISH: Multi-labelled oligonucleotides for fluorescence in situ hybridisation improve visualization of bacterial cells. *Appl Environ Microbiol*. doi:10.1128/AEM.02776-15.

Sekar R, Fuchs BM, Amann R, Pernthaler J. (2004). Flow sorting of marine bacterioplankton after fluorescence in situ hybridization. *Appl Environ Microbiol* **70**:6210–6219.

Stoecker K, Dorninger C, Daims H, Wagner M. (2010). Double labeling of oligonucleotide probes for fluorescence in situ hybridization (DOPE-FISH) improves signal intensity and increases rRNA accessibility. *Appl Environ Microbiol* **76**:922–926.

Zhou JZ, Bruns MA, Tiedje JM. (1996). DNA recovery from soils of diverse composition. *Appl Environ Microbiol* **62**:316–322.

Table 1: Number of read pairs attained by Illumina sequencing of extracted DNA from *E. coli* K-12 S17-1 cells post MiL- and CARD-FISH hybridisations. Note that the addition of DNA to the sequencing run of CARD-FISH cells 2 and 3 did not yield significantly more attained read pairs.

sample number	percent of fragments with correct adapters*	total DNA in seq run [pg]	total DNA in seq run [fmol]	total read pairs in output	read pairs in output per fmol loaded DNA
CARD-FISH 1	0.18	699	1.20	20,009	16,669
CARD-FISH 2	0.05	2,207	3.97	21,243	5,351
CARD-FISH 3	0.03	4,214	7.24	20,146	2,783
MiL-FISH 4	12.99	896	1.54	1,707,110	1,109,251
MiL-FISH 5	15.96	696	1.25	1,813,436	1,447,710
MiL-FISH 6	13.99	832	1.43	1,560,485	1,092,243
Control 7	13.52	861	1.48	1,753,534	1,185,797
Control 8	16.27	683	1.23	1,580,684	1,286,288
Control 9	14.76	788	1.35	1,181,510	872,408

* determined by qPCR

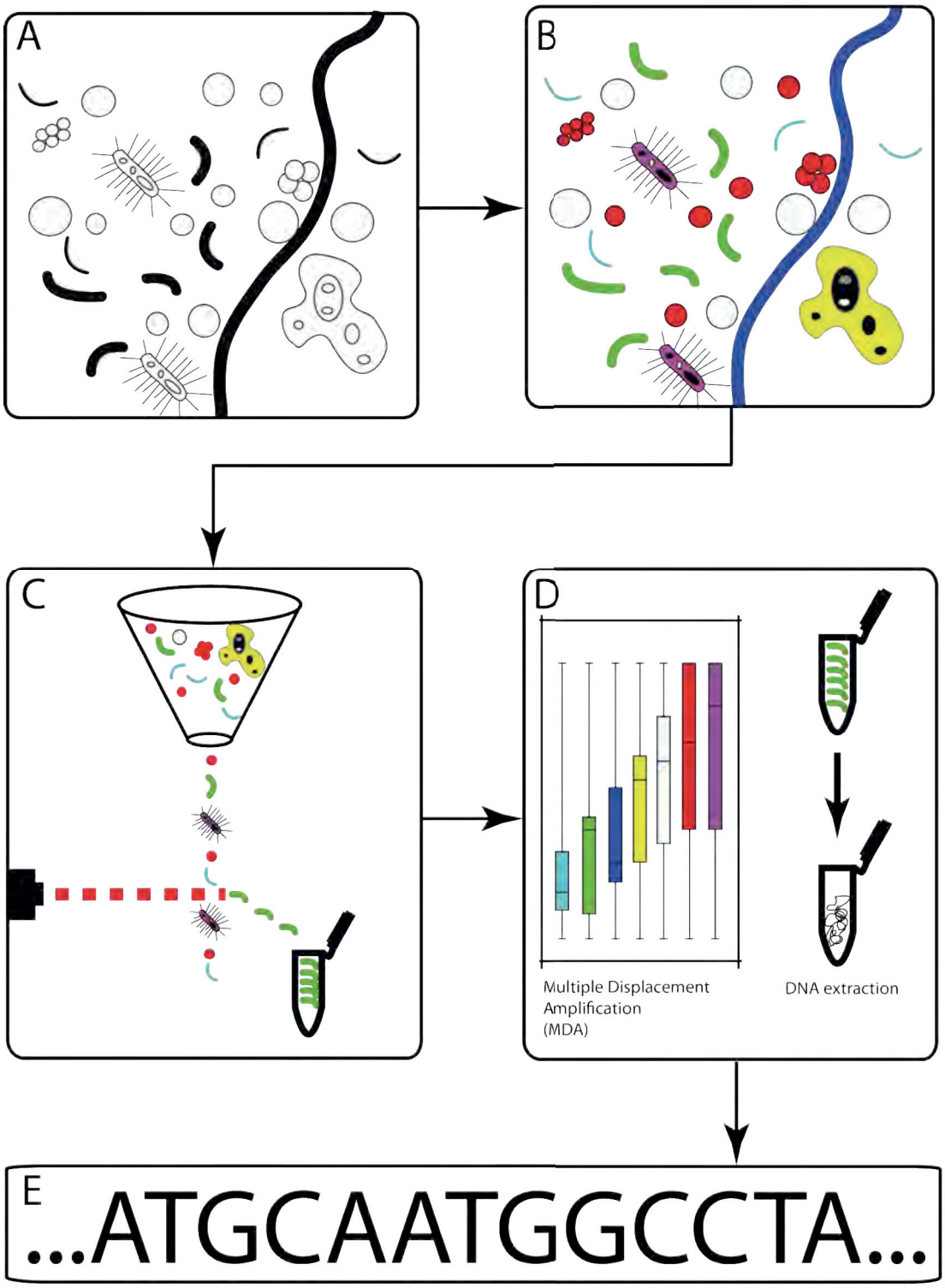

Figure 1: Proposed workflow for the isolation of environmental microorganisms with MiL-FISH followed by FACS and DNA recovery. 1) Environmental community, 2) MiL-FISH for targeting of up to seven members of the community, 3) isolation of desired community members via FACS, 4) DNA recovered by MDA or direct extraction, 5) sequencing.

Supplementary information

Material and Methods

Cultures. The γ-proteobacteria, *Escherichia coli* K12 S17-1, was grown in Luria-Beltane medium for 14 hours at 37°C. At an optical density of 0.323 (600nm) cells were harvested by centrifugation at 1500 g for 10 minutes. To solely evaluate the influence FISH procedures have on genomic DNA cells were not fixed and subsequent protocols were conducted directly after harvesting of cells. Cells were divided into nine 2 ml Eppendorf tubes (Eppendorf AG, Hamburg, Germany), three for CARD-FISH, three for MiL-FISH and three non-FISH controls. Control cells were frozen at -80 °C directly after harvesting until DNA extraction (see bellow).

Fluorescence *in situ* hybridisation. MiL-FISH. Hybridisation of cells with click-synthesised multi-labelled oligonucleotides (MiL-probes) followed the standard FISH protocol found at http://www.arb-silva.de/fish-probes/fish-protocols/ in triplicates. Hybridisation buffer (900 mM NaCl, 20 mM Tris-HCl (pH 7.5), 0.02% sodium dodecyl sulphate (SDS)) with 30% formamide (Sigma-Aldrich, St. Louis, MO, USA), was mixed with 8,42 pmol μl^{-1} 4 x FITZ labelled EUB338 oligonucleotide probe at a ratio of 15:1. 500 µl hybridisation buffer / probe mix were added to cells in the Eppendorf tube. **CARD-FISH.** Followed after Pernthaler *et al*., 2002 with slight modifications (Pernthaler *et al.,* 2002). Endogenous peroxidase was inactivated with methanol (Sigma-Aldrich, St. Louis, MO, USA) and 0.5% H_2O_2 for 30 minutes at room temperature followed by washing in 1x phosphate buffer saline (PBS) for 10 minutes. 500 µl hybridisation buffer (900 mM NaCl, 20 mM Tris-HCl (pH 7.5), 0.02% sodium dodecyl sulphate (SDS), 10% dextran sulphate (wt./vol) and 1% (wt/vol) Blocking Reagent) with 30% formamide and 8.42 pmol μl^{-1} horseradish peroxidase (HRP) labelled EUB338 probe, at a ratio of 150:1, was added to cells in the Eppendorf tube.

Hybridisation followed at 46 °C on a rotor (six revolution per minute) for 3 hours. Eppendorf tubes were centrifuged for 20 minutes at 1500 g, hybridisation buffer discarded, followed by a 10 minute wash at 48 °C with washing buffer (112 mM NaCl, 20 mM Tries/HCl, pH 8, 5 mM EDTA, pH 8 and 0.01% SDS). A final wash in 1x PBS was conducted for all samples, after which, cells that underwent the MiL-FISH protocol were stored at -20 °C until DNA extraction. CARD-FISH samples were amplified with buffer (1x PBS [pH 7.3], 0.0015% [vol/vol] H_2O_2, 1% Alexa Fluor 488 [Thermo Fisher Scientific, Waltham, MA, USA]) for 1 hour at 46 °C in the Eppendorf tubes until a final wash for 10 minutes in 1x PBS.

All changes of solution were conducted by centrifugation of tubes for 10 minutes at 1500 g, unless otherwise stated. Sub-sample of each repeat were taken and mounted onto 10 well Diagnostica slides (ThermoFischer Scientific Inc. Waltham, MA, USA) for visual conformation of positive hybridisation. Fluorescent images were taken with a Axioscope2 Epi-fluorescence microscope (Carl Zeiss AG, Oberkochen, Germany) equipped with Fluos Zeiss 09 (ex 470/40 nm, em 515LP) filter cube and an AxioCam Mrm connected to a Windows based PC running the Axiovision (Release 4.6.3 SP1) imaging software.

DNA extraction. DNA extraction followed Zhou *et al*., 1996 (Zhou *et al.,* 1996) with the modification of cells being incubated at 55 °C overnight in 400 µl extraction buffer. Final DNA concentration was measured with a Qubit® 2.0 fluorometer (Invitrogen, Life Technologies, Thermo Fisher Scientific, MA, USA) and samples were stored at -80 °C until being sent for sequencing on dry ice (CeBiTec, Bielefeld University). RNase digestion (37 °C, 30 min, RNase, A, Fermentas) was applied to extracted DNA, purified (Genomic DNA clean and concentration kit, Zymo) and eluted in TE buffer, before 2 µl were loaded on a 0.8% agarose gel as an initial quality control.

Sequencing library generation. TruSeq PCR-free libraries with an insert size of approx. 750-800 bp were generated for Illumina sequencing. For each of the nine samples, 2.5 µg of extracted and purified DNA were mechanically fragmented in 500 µl ice-cold nebulization buffer (50% Glycerin v/v, 35 mM Tris-HCl, 5 mM EDTA) to a mean size of 750-800 bp in a Nebulizer (Roche), by applying 30 psi air pressure for 1.5 min. The fragments were purified using the MinElute PCR purification kit (Quiagen), and end repair was performed according to the Illumina TruSeq DNA PCR-free sample preparation guide (Revision B). To generate long insert libraries, the first size selection step was performed with a modified diluted bead mixture as follows: 100 µl PCR grade water were mixed with 80 µl sample purification bead solution (Illumina), 160 µl of the mixture were added to the end repaired DNA sample. The second size selection step and the remaining procedure was performed according to the library preparation guide. For library quantification, qPCR was done with dilutions of the generated libraries (PerfeCta® NGS Library Quantification Kit for Illumina® Sequencing Platforms, Quanta Biosciences). In order to reduce processing bias, all nine samples were treated in parallel for each of the steps in the library generation. As the three libraries generated from DNA of the CARD-FISH treated cells showed very low efficiency of adaptation (high Ct in qPCR), these three libraries were concentrated in a vacuum concentrator prior to pooling and sequencing of all libraries.

Illumina sequencing. The pooled libraries were sequenced on a MiSeq flow cell, in a 2 x 300 cycles paired end run (v3 chemistry).

Genome assembly. Draft genomes were assembled using the software package SPAdes (Nurk *et al*., 2013) with default parameters and error correction. Resulting draft genome statistics were calculated with Quast (Gurevich *et al.,* 2013). Original reads were

mapped to the largest contig from the control assemblies using bbmap script (http://bbmap.sourceforge.net). The .sam file was converted to .bam format and sorted with the samtools package (Li *et al*., 2009). With the qualview software (Garcia-Alcalde *et al.,* 2012) the average coverage value of every 1000 bp was calculated for each assembly. Heat maps where generated with Microsoft Excel© and overview picture were edited with Photoshop© CS5.

SI Table 1: Oligonucleotide probes used in this study. Probe name, nucleotide sequence – nucleotide-fluorochrome complexes are indicated by an underscore in the probe sequence, target gene, label type, label synthesis, target species and formamide concentration used.

Probe	Sequence 5' - 3' (reverse complementary)	Target gene	Label	Synthesis	Target Species	FA %
EUB338	GCT GCC TCC CGT AGG AGT	16S rRNA	4x Atto488	Click chemistry	Most Bacteria	30%
EUB338	GCT GCC TCC CGT AGG AGT	16S rRNA	HRP	CARD	Most Bacteria	30%

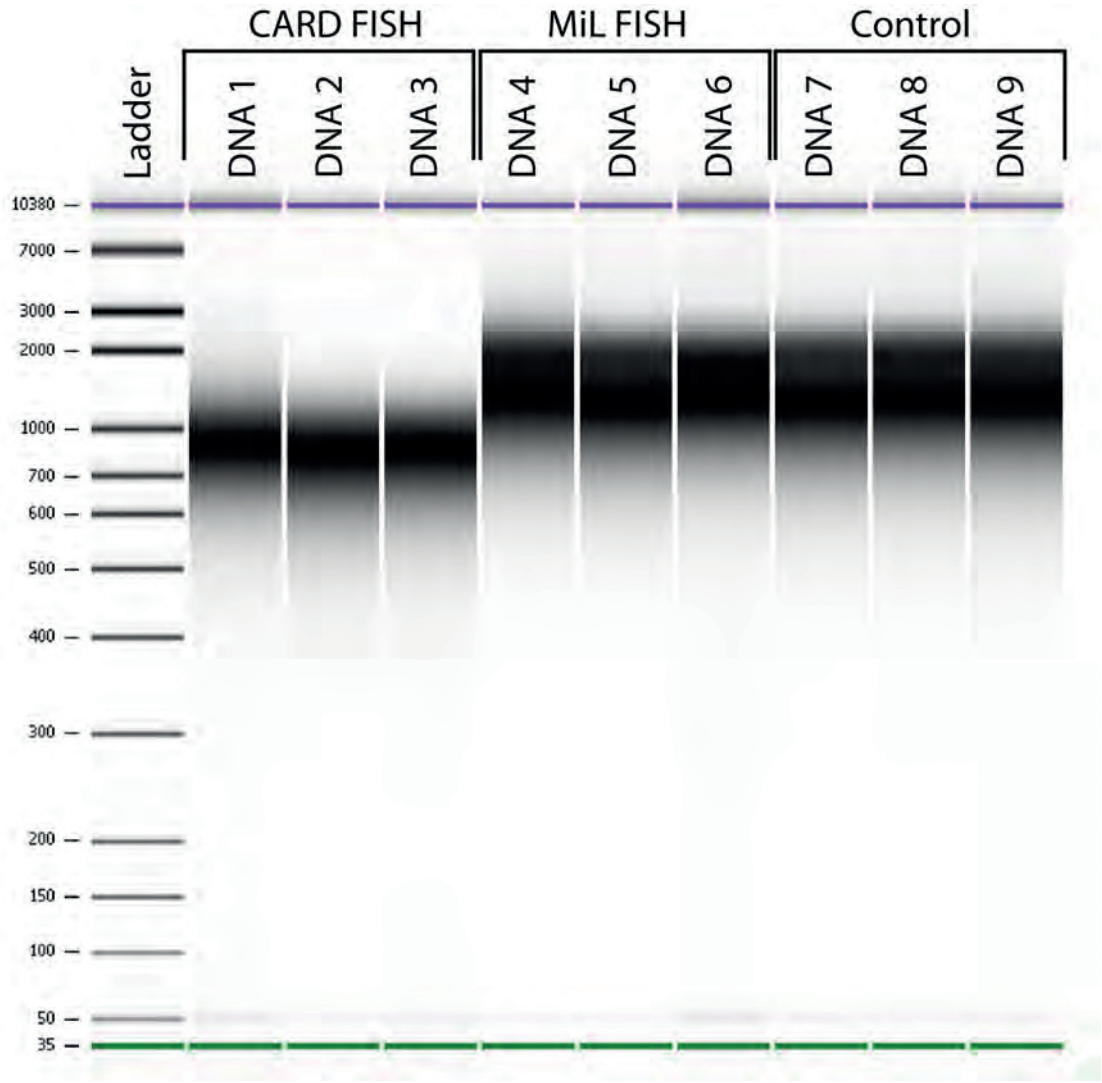

SI Figure 1: Bioanalyser assay of *E.* coli DNA, post CARD - and MiL - FISH. DNA 1-3 CARD-FISH cells, DNA 4-6 MiL-FISH cells and DNA 7-9 non-FISH, non-fixed controls.

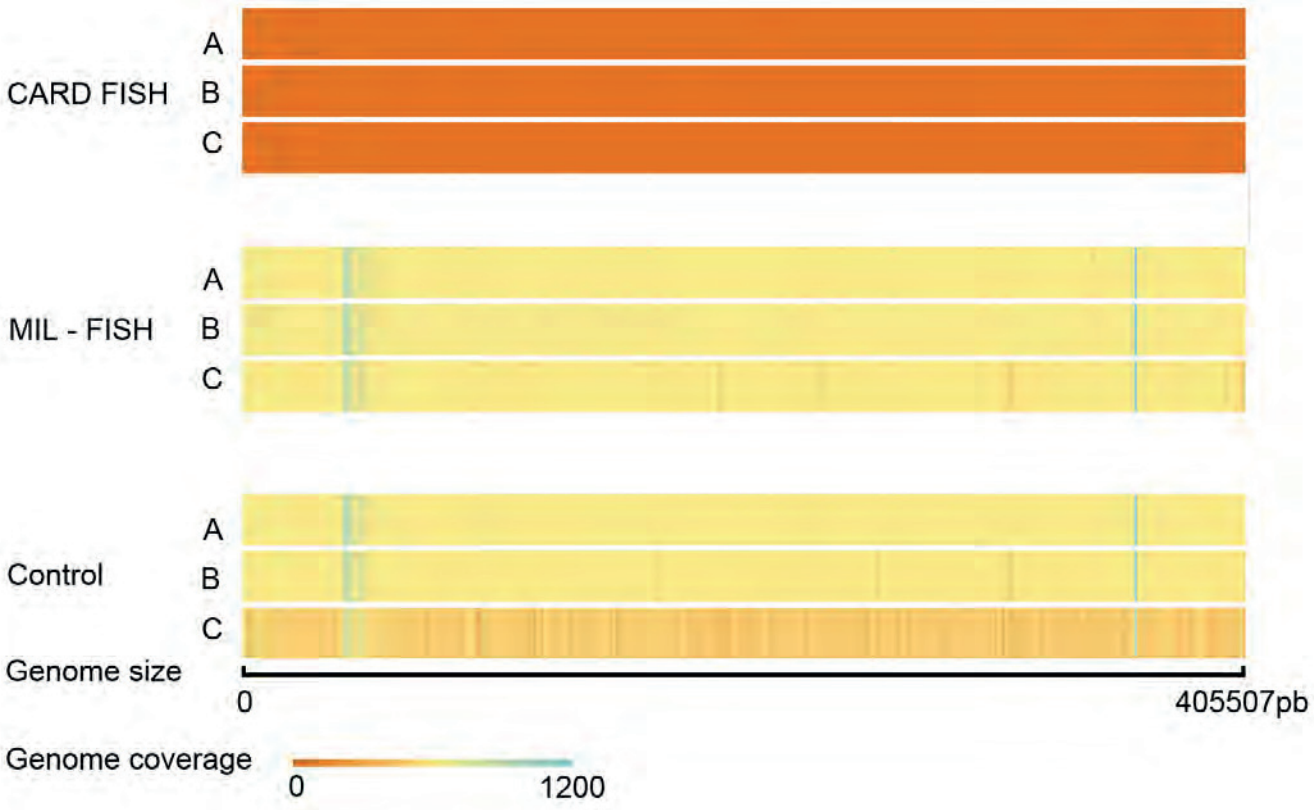

SI Figure 2: a) coverage over the largest contig of *de novo* assembled control sequence. CARD-FISH cells yield low pair end reads and therefor show low coverage even in high repeat regions (shown in blue for MiL-FISH and controls).

SI Table 2: Alignment over the reference genome of the closely related *E. coli* strain K-12 W3110. MiL-FISH cells show a 3.3 % better alignment over CARD-FISH cells.

	CARD-FISH cells			**MiL-FISH Cells**			**Control cells**		
	DNA 1	DNA 2	DNA 3	DNA 4	DNA 5	DNA 6	DNA 7	DNA 8	DNA 9
Alignment in %	93.09	90.49	94.34	96.10	96.08	95.62	96.20	96.12	95.67
Average Alignment	92.64			95.93			96.00		
Standard deviation	1.96			0.27			0.29		

References:

Garcia-Alcalde F, Okonechnikov K, Carbonell J, Cruz LM, Gotz S, Tarazona S, *et al.,* (2012). Qualimap: evaluating next-generation sequencing alignment data. *Bioinformatics* **28**:2678–2679.

Gurevich A, Saveliev V, Vyahhi N, Tesler G. (2013). QUAST: quality assessment tool for genome assemblies. *Bioinformatics* **29**:1072–1075.

Li H, Handsaker B, Wysoker A, Fennell T, Ruan J, Homer N, *et al.,* (2009). The Sequence Alignment/Map format and SAMtools. *Bioinformatics* **25**:2078–2079.

Nurk S, Bankevich A, Antipov D, Gurevich A. (2013). Assembling genomes and mini-metagenomes from highly chimeric reads. *J Comput Biol* **20(10)**:714–737.

Pernthaler A, Pernthaler J, Amann R. (2002). Fluorescence In situ Hybridization and Catalyzed Reporter Deposition for the Identification of Marine Bacteria. *Appl Environ Microbiol* **68**:3094–3101.

Zhou JZ, Bruns MA, Tiedje JM. (1996). DNA recovery from soils of diverse composition. *Appl Environ Microbiol* **62**:316–322.

Chapter V

Transmission of bacterial symbionts by smearing in the gutless marine oligochaete *Olavius algarvensis*

Mario P. Schimak[1], Niels J. Schoffelen[1], Alexander Gruhl[1], Nicole Dubilier[1]

[1]Max Planck Institute for Marine Microbiology, Celsiusstr. 1, D-28359 Bremen, Germany

Manuscript in preparation

Corresponding author

Mario Schimak: mschimak@mpi-bremen.de

Author contributions:

N.D was project supervisor, A.G. gave assistance in image analysis and scientific input into the project. N. J. S. operated the nanoSIMS and assisted in data interpretation. M. P. S. conceived the project, designed experiments, performed experiments and wrote the manuscript.

Abstract

The gutless oligochaete *Olavius algarvensis* from the island of Elba, Italy, lives in an obligate symbiosis with a consortium of sulphide oxidizing γ-proteobacteria, sulphate reducing δ-proteobacteria and a spirochaete. The nutritional dependency of the host to its symbionts has led to the reduction of the digestive tract and excretory system. To date, however, it is unclear how symbionts are passed into the next host generation. In contrast to other oligochaetes, eggs of gutless oligochaetes initially lack a rigid cocoon. Free-living symbiont stages provided these exist, could potentially therefore be transmitted horizontally from the environment. Vertical transmission during the egg laying process through smearing of symbionts from the worm's genital pads is another possibility, and has been described in a gutless oligochaete from Bermuda. To trace the transmission mode of this non-cultivatable organism we employ the use of ^{15}N-ammonium as a stable isotope tracer. After label incubation of sexually mature worms during the reproductive period collected cocoons were analysed by MiL-FISH to determine bacterial cell identity and localisation to the developing embryo. Cell enrichment was determined by secondary-ion-mass-spectrometry (nanoSIMS) and based on our experimental setup any enriched symbionts cells inside the cocoons should have originated from the parent worm. Both γ- and δ-proteobacteria showed ^{15}N enrichment for all analysed specimens. We conclude that vertical transmission via the worm's genital pad is the principle mode of transmission in *O. algarvensis*. There is however indication that horizontal transmission does occasionally take place, which gives grounds for discussion at the end of this chapter.

Introduction

Mutualistic association between bacteria and animal hosts is recognised as a key factor in driving evolution for both partners (Brucker and Bordenstein, 2012). Through association, the sum of all partners, the holobiont, effectively creates a "new" organism that can utilise alternate physiological and ecological niches. Salient examples of this are the pivotal roles that bacterial symbioses play for the distribution of earths primary producers, such as the photoautotrophic plant – rhizobia symbiosis in which N_2 fixing bacteria enable plant growth in nitrogen poor soils (van der Heijden *et al.,* 2008). Further, the deep-sea hydrothermal vent symbiosis between chemosynthetic sulphur-oxidising bacteria and annelid worms build ecosystems with some of the highest known biomass on earth (Lutz and Kennish, 1993) (Felbeck, 1981). Chemosynthetic symbioses, in particular, are nutritionally based, whereby most commonly a chemoautotrophic proteobacterial symbiont fixes CO_2 for its host by energy from sulphur oxidation (Krueger *et al.,* 2002). The utilisation of other electron donors by symbionts, such as carbon monoxide and hydrogen, have also been documented but are generally less common (Kleiner, Wentrup and Lott, 2012a), (Petersen *et al.,* 2011). This nutritional dependency has in some cases lead to extreme morphological adaptations of the host, such as the complete reduction of the digestive tract. Particularly in annelids morphological adaptation of gut reduction has occurred a number of times. The deep sea vestimentiferan polychaetes have reduced their digestive tract and house a visceral mesoderm derived symbiont containing organ – the trophosome (Nussbaumer *et al.,* 2006). The gutless oligochaetes (Phallodrilinae) have not only completely reduced their digestive tract but also their excretory organs, the nephridia, and rely solely on a consortium of bacterial symbionts for both nutrition uptake and, presumably, waste disposal (Dubilier *et al.,* 2001) (Kleiner, Wentrup and Lott, 2012b).

Obligate symbiotic associations between animals and bacteria, and in particular obligate nutritional ones, are presented with the challenge of reliably transmitting microbial partners over successive host generations if survival of the host species is to be insured. Two main modes of symbiont transfer have been described; horizontal transmission – whereby environmental symbionts infect the host with each generation anew and vertical transmission - whereby symbionts are passed on from the host to its progeny, most commonly through the gametes. Both modes of transmission are not mutually exclusive and mixed strategies are generally the rule in nature (for review see (Bright and Bulgheresi, 2010) & (Ebert, 2013). Vertical transmission strategies that do not run through the germ line may include symbiont infection of juveniles whilst still inside their mother, such as in the "beneficial" nematode species *Heterorhabditis bacteriophora* (Ciche *et al.,* 2006) or alternatively, infection of juveniles or eggs after birth or oviposition by bacterial smearing. To date a smearing strategy has only been documented twice for invertebrate phyla: within the arthropods - Heteroptera family of the Pentatomidae and the Hymenopteran family of the Crabronidae ((Prado and Almeida, 2009) & (Kaltenpoth *et al.,* 2005)) - and within the gutless oligochaete annelids (Phallodrilinae) (Giere and Langheld, 1987). The Phallodrilinae bear dense bacterial "pockets" located ventrally at the posterior end of the clitellum in segment XII. These so-called "genital pads" only become visible in reproductive adults. A transmission electron microscopy (TEM) study on the Caribbean species, *Inanidrilus leukodermatus,* showed that the infection of eggs occurs by smearing of symbionts from the genital pads during oviposition (Giere and Langheld, 1987) (for schematic of the egg laying process see Figure 1). This is followed shortly after by the clitellum secreting the materials needed for cocoon formation in which the zygote later develops. Which of the symbiont classes

found in *I. leukodermatus* are passed on the next host generation during the smearing process could not be resolved using TEM alone.

The gutless oligochaete *Olavius algarvensis* (Giere and Erseus, 2002) from the island of Elba, Italy, lives in symbiosis with two primary sulphur-oxidising γ -proteobacteria, two secondary sulphate-reducing δ -proteobacteria and a spirochaete (Dubilier *et al.,* 2001). To date, two γ -proteobacterial, γ1 and γ3, and four δ-proteobacterial, δ1, 3, 4 and 6, phylotypes have been identified from Metagenomic data and clone banks of adult worms (Wippler *et al*., in prep). The primary γ1 symbiont oxidises sulphur aerobically, sulphate reduction by δ -proteobacterial symbionts is an anaerobic process which has resulted in the need for adult worms to shuttle between sediment layers to provide both symbiont groups with the substrates and conditions required to drive their metabolism ((Giere *et al.,* 1991) (Schimak *et al.,* in prep – Chapter II of this thesis). Additionally it was shown that carbon monoxide and hydrogen could also be respired by the symbiotic consortium (Kleiner *et al.,* 2012) (Kleiner *et al.,* 2015).

All oligochaetes undergo spiral cleavage and direct development, however, unlike those of terrestrial oligochaetes, the mucus encased zygote of gutless oligochaetes initially lacks a rigid chitinous cocoon after deposition ((Giere and Langheld, 1987) & personal observation). This leaves a potential timeframe for the infection of eggs by environmental symbiotic bacteria, provided these exist, from the sediment in which they are deposited. To date however no free-living symbiont phylotypes have been found in the environment. Gutless oligochaete eggs have also never been found in the environment and currently there are no possibilities to cultivate worms in the laboratory. All studies have therefore been limited to fieldwork during the short reproductive period from mid June to mid August (other seasonal reproductive periods are not excluded but currently unknown to us). Past studies were able to retrieve only a few eggs from *ex situ* conditions

during this two month timeframe (~ 40 per season). The majority of theses specimens were either not fertilized or did not development past the first few cell cleavages and no late developmental stages could therefore attained. It was concluded that *ex situ* incubation conditions were suboptimal for rearing eggs and obtaining of late developmental stages.

Typically adult specimens are collected from open shallow water siliceous sediments around *Posidonia oceanica* sea grass meadows. Although metazoan embryos have high oxygen demands during development (Flewelling and Parker, 2015) (Fernández *et al.,* 2003) (Simon and Keith, 2008), it would seem unlikely that gutless oligochaetes deposit eggs in the oxygenated upper few centimetres of the open sediments where they are exposed to extreme mechanical stress by wave movement and sediment shifts as well as high levels of epibenthic macrofauna predation (Wilson, 1991). In addition eggs are immotile and can only be deposited in either oxygenated, reduced or the chemocline sediment region. Sediments chemical properties are not stable however, and subjected to constant irregular shifts by pore water movement (Ott and Novak, 1989). Correspondingly, for the stationary egg, conditions can quickly turn unfavourable and inhibit oxygen availability to the developing embryo with no guarantee that they will change favourable again. The open sediment is therefore surely a suboptimal environment for egg deposition of animals that appears to only have a low number of offspring per reproductive season (Chapter 1.4.2 of this thesis). An alternative location for egg deposition could therefore be the other dominant feature of the natural habitat, the sea grass meadow itself. Sea grasses actively pump O_2 into the surrounding sediment through their roots in a photosynthesis dependant diurnal pattern, to protect their own tissue from reduced substances (for review see (Ogden, 2006)). Cocoons attached to the

roots of a seagrasses would not only be protected from mechanical stress but also regularly supplied with oxygen for development of the embryo.

In this study we ask which members of the *Olavius algarvensis* symbiont consortium are passed on to the next host generation from the parent worm and which, if any, are taken up from the environment. We devised novel sampling methods for egg acquisition of various developmental stages and apply Multi-labelled-fluorescence *in situ* hybridisation (MiL-FISH) (Schimak *et al.,* 2015) to document symbiont association at various ontogenetic stages of the developing embryo. The transmission of symbionts is determined by ^{15}N-ammonium stable isotope tracing and nanoSIMS analysis. Further, we shed light on oligochaete reproductive ecology and discuss the role that symbionts have in the developmental process of the host as well as the evolutionary implications that our finding have for gutless oligochaetes and for symbiosis on the whole.

Material & Methods

Sample Collection. Specimens of the gutless oligochaete *O. algarvensis,* were retrieved on the island of Elba, Italy, by collecting sediment from a water depth of 7 meters by SCUBA diving in the bay of Sant' Andrea (42° 48' 29.80" N, 10° 8' 34.07" E) during the months of June, July and August 2013. Worms were picked from the sediment at the Hydra field station (Fetovaia, Elba, Italy) and visually separated into three groups of *O. algarvensis*, the co-occurring *O. ilvae* and unidentifiable worms lacking the identification criterion of the genital pad (Giere, 2002).

Egg retrieval and incubation. *O. algarvensis* worms were kept in glass bowls filled with sediment of grain sizes between 400 and 600 µm at a constant temperature of 25 °C in an aquarium filled with natural seawater of 39 ‰ salinity. Sediment was

changed every week and passed through a 600 µm sieve. After deposition, eggs attach to sand grains, forming clumps larger than 600 µm, which are retained in the sieve.

To attain late developmental stages we exposed eggs to fluctuating oxic / hypoxic conditions in a 12 hour cycle to emulate O_2 conditions as would be expected in sea grass roots systems (Ogden, 2006). Eggs were collected and placed into 78 µm porous CPD vials (Plano GmbH, Wetzlar, Germany), which in turn were placed into 250 ml Schott flasks closed with a rubber cap. A peristaltic pump (Ismatec, Wertheim, Germany) was used to introduce a water flow through the rubber cap by hypodermic needles into the Schott flask. Oxygenated seawater was produced by aeration with an air stone; hypoxic, substrate rich, seawater was prepared by setting up three sediments filled flasks with a dead rhizome bottom layer. The flasks were left to stand for three days until a characteristic black sediment layer for reduced substrates was observed before being used for one 12 hour cycle in the setup. In this manner hypoxic seawater containing reduced substrates (H_2S, CO and H_2) was introduced by the peristaltic pump into Schott flasks containing eggs. As a control, some CPD vials containing eggs were incubated in a setup using only oxygenated seawater and some were buried in the anoxic zone of a flask containing dead rhizome and sediment.

^{15}N incubation. Sexually mature adult *O. algarvensis* worms were incubated in a 15ml Eppendorf tube (Eppendorf, Hamburg, Germany) filled with sterilised sediment and 426 µMol ^{15}N-Ammonium Sulphate ($(^{15}NH_4)_2SO_4$) (Sigma-Aldrich, St. Louis, MO, U.S.A.) enriched sterile filtered seawater for 18 hours. Worms were picked out of the sediment and washed thoroughly three times in sterile filtered seawater. Pairs of worms were placed into 78 µm porous CPD vials (Plano GmbH, Wetzlar, Germany) filled with freshly collected sediment from the sampling site. An incubation aquarium was prepared consisting of a ~ 3 cm bottom sediment layer, ~ 3 cm *Posidonia oceanica* rhizome layer

followed by a ~ 18 cm top sediment layer and filled with sea-water of 39 ‰ salinity kept at constant temperature of 25 °C with a Titan 150 cooling aggregate (Aquamedic GmbH, Bissendorf, Germany). A standard air stone and aquarium pump was used to oxygenate and circulate water. All material used in the aquarium was collected from the sampling site. The CPD vials containing worms were subsequently buried in the top sediment layer of the aquarium in such a manner that worms could potentially access both oxic and hypoxic sediment layers within them. As it was not possible to determine the time of egg deposition inside the vials, and a range of developmental stages were desired, vials were retrieved in time intervals ranging from 7 to 35 days (SI Table 2). The content of vials was carefully sorted after retrieval under a dissecting microscope and any worm and / or egg specimens found were fixed (SI Figure 2).

Fixation. Worms and eggs were fixed in Carnoy's fixative (6 parts 96% EtOH, 3 parts chloroform, 1 part glacial acetic acid) for 1 hour, washed three times in 1x phosphate buffer saline (PBS) followed by fixation in 2% PFA overnight (14 hours) at 4 °C and washed again 3 times in PBS before storage in 50% ethanol:PBS.

LR-White embedding and sectioning. Egg specimens were embedded by gradual ethanol dehydration starting at 50% Ethanol:PBS for 10 min followed by 10% increases for 10 min each until the final dehydration step with 100% ethanol was repeated three times. Infiltration of resin into dehydrated samples followed on a shaker with an LR-White:ethanol mix of 1:3, 1:2, 1:1, 2:1, 3:1 for 30 min each followed by pure LR-White three times for 1 h each with the last change being left overnight. Samples were orientated in gelatine capsules with fresh LR-White, placed into a desiccator, flushed with Nitrogen gas three times followed by a 1000 mBar vacuum being applied before polymerisation at 50 °C in an oven for 3 days. Semi-thin (1 µm) sectioning of embedded specimens followed on an Ultra-microtome (UC7, Leica microsystems, Vienna, Austria).

Sections were placed on a drop of 20 % acetone on Gold / Palladium sputtered 42 mm GTTP filters of 0.22 μm pore size (Millipore, Darmstadt, Germany) or on glass slides and dried on a hotplate at 50 °C for analysis in a nano-scale secondary ion mass spectrometer (nanoSIMS).

FISH. Sections of LR-White embedded specimens were pre-treated in 200 mM HCl for 10 min, washed in 200 mM Tris/HCl for 10 min, incubated in 1 μg/ml Proteinase K for 5 min at 46 °C and finally washed again in 200 mM Tris/HCl for 10 min. For nanoSIMS specimens, filters were placed on a piece of Parafilm (Brand, Wertheim, Germany) on a glass slide and FISH conducted directly on them. Multi-labelled FISH (MiL-FISH) (Schimak *et al*., 2015) followed the standard FISH protocol found at http://www.arb-silva.de/fish-probes/fish-protocols/. Hybridisation buffer (900 mM NaCl, 20 mM Tris-HCl (pH 7.5), 0.02% sodium dodecyl sulphate (SDS)) with a formamide concentration optimised for probes used in each respective experiment (Refer to SI Table 1) was mixed with 8.42 pmol μl^{-1} oligonucleotide working solution at a ratio of 15:1. All hybridisations were conducted at 46 °C in a humid chamber for 4 hours followed by a 10 min wash at 48 °C with washing buffer (14-900 mM NaCl, 20 mM Tris/HCl, pH 8, 5 mM EDTA, pH 8 and 0.01% SDS) adjusted to the stringency of the formamide concentration used. Filters were washed for 10 minutes in distilled water for 1 minute followed by a 10 minute DAPI staining.

Microscopy. Fluorescence images were taken on an Axioscope2 epifluorescence microscope (Carl Zeiss AG, Oberkochen, Germany) equipped with a Fluos Zeiss 09 (ex 470/40 nm, em 515LP), an AHF (AHF analysentechnik AK, Tübingen, Germany) F36-525 Alexa488 (ex 472/30, em 520/35), an AHF F46-004 Cy3 (ex 545/25, em 605/70) and an AHF F46006 Cy5 (ex 620/60, em 700/75) filter cubes and an AxioCam Mrm. Images

were recorded with the PC based Axiovision (Release 4.6.3 SP1) imaging software and any image level adjustments made therein.

Nanoscale secondary ion mass spectrometry (nanoSIMS). Sections of LR-White embedded specimens were sputtered with 6 nm Gold / Palladium and analysed on a NanoSIMS 50L (Cameca, Gennevilliers Cedex-France) at the Max-Planck-Institute for Marine Microbiology in Bremen, Germany. Areas of interest were pre-sputtered with a Cs^+ primary ion beam of 300 pA to remove surface contamination, to implant Cs^+ ions in the sample and to achieve an approximately stable ion emission rate. A primary Cs^+ ion beam with a beam current between 0.8 and 1 pA and a beam diameter between 50 and 100 nm was rastered across the section for analysis. For each individual cell secondary ion images of $^{12}C^-$, $^{13}C^-$, $^{19}F^-$, $^{12}C^{14}N^-$, $^{12}C^{15}N^-$, $^{31}P^-$ and $^{32}S^-$ were simultaneously recorded using seven electron multipliers. The Analysis areas were 15x15 µm in size and an image size of 256 x 256 or 512x512 pixels with a dwell time of 1 ms per pixel. To minimize interferences for $^{12}C^{15}N^-$ the instrument was tuned for high mass resolution (around 7000 MRP). Images and data were processed using the matlab based software "Look@nanosims" (Polerecky *et al.,* 2012)

Results

Egg retrieval and incubation: Roughly one thousand eggs of various developmental stages were retrieved from glass bowls containing *O. algarvensis* worms between mid June to mid August 2013. It was initially noted that eggs retrieved from glass bowls did not develop past the blastula stage. Several of these eggs were monitored daily under a dissecting microscope for up to 11 days. No further development of the embryo inside the cocoons could be visually determined during this time period. Instead, a rotating blastula like stage was observed (Digital supplementary data on attached CD,

File name: Chapter_V_ SI_Video_1_Rotating_Blastula). After exposing the same set of 11 day old blastula like specimens to fluctuating oxic / anoxic conditions with pore water from reduced sediment layers, vermiform juveniles had developed inside the cocoon after a time period of only 3 days (Digital supplementary data on attached CD, File name: Chapter_V_SI_Video_2 _Juvenile_Worm). If eggs were kept for a period of roughly two weeks without incubation in fluctuating conditions the majority of embryos were observed to decease. Death of an embryo was determined by a lack of rotation of the embryo, which eventually resulted an empty cocoon (personal observation). Based on these initial findings all newly collected eggs were incubated in fluctuating oxic / anoxic incubations to ensure the rearing of collected sample material to late developmental stages.

Egg morphology & embryonic development. Retrieved eggs were between 200 – 300 μm in width and 350 – 450 μm in length. It was noted that freshly deposited eggs were encased in a transparent, soft and fragile sticky egg casing surrounded by mucus onto which sand grains adhered (Figure 2). After roughly two days cocoons congealed and turned opaque in appearance whilst tolerating higher levels of mechanical stress during sample manipulation.

Of the obtained specimens, 30 were visually selected under a dissection microscope to cover a range of developmental stages. These were subsequently embedded and sectioned for further analysis. Of these, 16 eggs were selected to cover the 10 chosen developmental stages described in this study (Figure 3 & SI Figure 1). The γ- and δ-proteobacterial general 16S rRNA probes, Gam42a and DSS658 respectively, were used to localise and identify bacterial symbionts within the cocoons. The following observations were made:

After egg deposition and prior to first embryonic cleavage bacteria were found accumulated on the inside of the egg at the operculum (SI Figure 1-1). A membrane like structure surrounding the embryo separated the zygote from the bacterial aggregate (not seen in shown image). DAPI staining revealed several bacteria in the matrix of the mucus filament attached to the operculum of the egg (SI Figure 1-1, ii). The following stage showed the bacterial aggregate associated directly to the developing embryo and bacteria were observed inside the wall of the egg casing (SI Figure 1-2 & 1-2 ii). Specific 16S rRNA probes were used and identified cells inside the cocoon wall and revealed the γ1 & γ3 and δ- 1 phylotypes (Figure 4). In a later stage but still before first embryonic cleavage both γ- and δ-proteobacterial cells were found attached to the inside of the cocoon wall and surrounding the zygote in a thin layer (SI Figure 1-3). From this stage on and for the rest of the developmental process symbionts were always seen to closely associate to the embryo. After first cleavage symbionts surrounding the embryo were found to aggregate at the cleavage site in large numbers (SI Figure 1-4). At an embryonic stage of pole differentiation symbionts were found to aggregating between blastomeres, at both the yolk rich vegetal pole and the animal pole (SI Figure 1-5). During the blastula, and subsequent documented gastrula like stages, a bacterial aggregate is present and associates to a specific regions on the developing embryo, whilst a thin layer of symbiont cells continuously surrounds the developing embryo (SI Figure 2-6 & 7). With onset of cephalisation, symbionts are seen to accumulate on the anterior end of the developing embryo in the region that would through differentiation of ectoderm form into the mouth opening in other protostomes (SI Figure 2–8) (for reference please compare with (Bergter *et al.,* 2004)). The symbiosis between bacteria and worm is permanently established after epidermal cells secrete the cuticle entrapping symbionts that are associated to the developing worm in the interstitial space. At this stage the coelomic cavity has begun

formation, but still contains much egg yolk (SI Figure 2-9). The final stage of a fully formed juvenile worm, determined by the complete formation of a coelomate cavity, was not present in our dataset (SI Figure 2-10).

^{15}N experiments. ^{15}N-ammonium incubated adult worms deposited a total of 14 eggs in porous CPD vials during incubations (SI Table2). By nature of the experimental design (SI Figure 2), we propose that any ^{15}N enriched bacteria found within an egg originated from the parent worm, whereas non-enriched bacteria originate from the environmental sediment. After fixation, embedding and sectioning eggs were analysed for their developmental stages and three were selected for further nanoSIMS analysis: 1) a zygote, pre first cleavage (early) 2) a 32 cell stage, for which pole differentiation is given (mid) and 3) a late stage, juvenile worm (late) (Figure 5).

MiL-FISH on egg sections with the general γ - and δ -proteobacterial probe, Gam42a and DSS658 respectively, localised and identified bacteria at all analysed stages. Interestingly, in the 32-cell stage (mid), symbionts targeted by a γ1 specific 16S rRNA probe were found to aggregate in high numbers on the D quadrant of macromeres that later goes on to develop into the teloblasts which give rise to ectoderm (N, O, P and Q), mesoderm (M) and endoderm (E) in a closely related oligochaete *Tubifex tubifex* (Figure 5, 2a) (Nakamoto *et al.,* 2000) & (Bergter *et al.,* 2004)). In other oligochaetes, the cells from this region, which differentiate into ectodermal tissue, go on to form the for- and hindgut and cells that differentiate into endoderm the midgut. No indication of digestive tract development was ever observed in any of the analysed specimens during this study.

Sections were subsequently measured by nanoSIMS and regions of interest (ROI's) selected for correlative identification of cells with the MiL-FISH images. We found all γ -proteobacterial cells, identified by MiL-FISH or γ1 symbiont cell morphology, to contain ^{15}N label in all analysed developmental stages (Figure 6). Natural

^{15}N abundance lies at a $^{12}C^{15}N/^{12}C^{14}N$ ratio of 0.0036 and all analysed γ-proteobacterial cells measured a $^{12}C^{15}N/^{12}C^{14}N$ ratio between 0.015 and 0.035 enrichment (Figure 6 b – 3 & 4). Cells in cocoons identified as δ-proteobacteria were enriched by a $^{12}C^{15}N/^{12}C^{14}N$ ratio of between 0.008 and 0.015 (Figure 6 a & c – 3 & 4). For controls, adult worms were fixed directly after ^{15}N-ammonium incubation and analysed by correlative MiL-FISH and nanoSIMS. The measured control specimen came from a repeated incubation experiment because the parent worms of the eggs analysed in this study were required for elemental-analysis-isotopic-ratio-mass-spectrometry (EA-IRMS) to confirmation ^{15}N uptake before nanoSIMS analysis. Cells identified as δ-proteobacteria in the control worm were enriched by a $^{12}C^{15}N/^{12}C^{14}N$ ratio between 0.0075 and 0.012 (Figure 6d – 3&4). Cells that showed ^{15}N enrichment and did not hybridised with the general δ-proteobacterial probe DSS658 were classed as γ-proteobacteria and showed $^{12}C^{15}N/^{12}C^{14}N$ ratio between 0.011 and 0.013.

Discussion

Egg morphology. As worms reach sexual maturity, and several days before egg deposition, the clitellum swells and increase in volume due to glandular cells starting the production of mucus required for copulation. The large bacteria filled genital pads are also noted to increase in size, presumably coupled with the proliferation of symbiont cells to increase cell numbers before an upcoming smearing event (Giere and Erseus, 2002), (Giere and Langheld, 1987). In both sexually immature worms and worms that have recently deposited eggs the genital pads are not observed (personal observation A. Gruhl & M. P. Schimak). This indicates that an anatomical adaptation to a reproduction event has the sole purpose of transmission of symbionts to the next host generation and appears to be an intrinsic part of the worm's reproductive process.

Additionally, and as discussed in section 1.4.1 of this thesis, other oligochaetes, such as the earthworms of the family *Lumbricidae*, produce a hard cocoon to ensures offspring survival rates necessary after the high investment of energy into the production of the eggs. In contrast, gutless oligochaetes initially lack a rigid chitinous cocoon and until congealment of the outer mucus layer occurs, bacteria smeared from the worm's genital pads can potentially pass into the egg albumen (Figure 4). The sticky property of the secreted mucus adheres the egg to sand grains forming a sand-egg complex that adds resistance to environmental mechanical stress and potentially to macro-fauna predation. The adherence to sand grains brings the eggs into direct contact with a diverse environmental bacterial community. It is know from several other invertebrate systems that symbionts can play a protective role for a developing embryo by either outcompeting other bacterial taxa or producing antibiotics (Fraune *et al.,* 2010) (Nyholm and McFall-Ngai, 2003) (Kaltenpoth *et al.,* 2005). In all positively hybridised specimens of our study no cells were observed inside the cocoons that did not hybridise with either the γ- and δ-proteobacterial 16S rRNA probe. Additionally, symbiont specific 16S rRNA probes revealed γ1, γ3 and δ1 phylotypes within the cocoon casing. Although we cannot exclude the possibility of non-symbiotic environmental bacteria entering cocoons we hypothesize a protective role of symbionts for the developing embryo.

Embryo development. The nature of our experimental design did not allow monitoring of the precise time point of egg deposition. It was therefore not possible to clearly document how long embryos take to develop into juveniles. However, if directly after collection eggs are kept in fluctuating oxic / hypoxic conditions an approximate 7 days passed until a vermiform juvenile worms was recognised within the cocoon. Developmental processes from initial cell cleavage up to the blastula stage are generally very stable and hold much resistance to unfavourable conditions (Hamdoun and Epel,

2007). Indeed, it was observed that the majority of eggs collected from glass bowls only developed to the blastula like stage and ceased development for a time period of up to roughly two weeks. When eggs were exposed to fluctuating conditions, and pore water from reduced rhizome sediment, development commenced. By providing both reduced substrate and oxic conditions for sulphur oxidation and sulphate reduction we were able to attain late developmental stages of *O. algarvensis*. However, to determine the exact parameters that influence embryo development more concise experiments will have to be conducted. In nature fluctuating oxic conditions and simultaneous access to reduced substrates are provided in the root system of seagrass meadows. I propose that indeed the sea grass meadow offers a more optimal habitat for oviposition over the open sediment. A model is presented for how development of embryos may occur in the seagrass root system with SI Figure 3 and further discussed in Chapter 6.1.

The close association of symbionts to the developing embryo through all documented ontogenetic stages gives further indication of their potential influence during the developmental process. Of particular interest is the aggregation of symbionts during cephalisation at the anterior of the developing worm. As documented for other oligochaete protostomes the initial development of the mouth opening at the anterior of the worm was never observed in *O. algarvensis* (Bergter *et al.,* 2004) (Wanninger, 2015). Indeed, none of the ontogenetic stages in our analysed specimens showed any indication for the development of a digestive tract. The lack of a functioning digestive tract is known from other bacteria – annelid associations such as the deep-sea giant tubeworm, *Riftia pachyptila* (Nussbaumer *et al.,* 2006). Here, a digestive tract initially develops in the planktotrophic trochophore, which is later presumably reduced after infection of bacterial symbionts as the trophosome develops. The development of a digestive tract was never observed in *O. algarvensis* and although only speculative it cannot be excluded

that processes disrupting differential gene expression for gut development may play a role for the gutless oligochaetes (further discussed in Chapter 6.2 iii).

Transmission - ^{15}N tracing. All nanoSIMS analysed eggs of ^{15}N-incubated worms showed enrichment for sulphur oxidising γ-proteobacteria contained within them. Only parent worms and their symbionts were exposed to ^{15}N-ammonium during the incubation and we therefore conclude a vertical transmission from the parent worm via smearing from the genital pad for γ-proteobacteria. The primary γ1 and γ3 symbionts do not show typical genome characteristics that are often found in obligate intracellular symbionts, namely genome reduction and an AT bias (Woyke *et al.,* 2006). The γ1 symbiont does however have a high abundance of transposable elements and it is suggested that this is a key factor in many host-restricted bacteria during their transition to an obligate symbiotic life-style and a prerequisite before reduction of their genome (Kleiner *et al.,* 2013). The high expression of transposes was stated to increases the likelihood for deleterious mutations by genome rearrangements. Further it has been suggested that genome reduction in obligate symbionts is primarily due to the fixation of mildly deleterious mutations in small population sizes, which persist due to single infection events by vertical transmission over host generations (Moran and Wernegreen, 2000). In combination with data from our study it is therefore plausible that at the γ1 symbiont has been transmitted for many consecutive host generations without regular environmental uptake intermediates. Further, the γ1 symbiont of *O. algarvensis* falls into the *Candidatus* Thiosymbion clade (H. Gruber-Vodicka in prep.) and occurs in all other gutless oligochaetes with one exception. There is therefore a high degree of conservation of the γ1 symbiont within the Phallodrilinae, indicating a common ancestry and a lack of symbiont switching throughout the host genus.

All δ-proteobacteria in the cocoons identified with the 16S rRNA general probe, DSS658, also show ^{15}N enrichment. We conclude a vertical transmission mode for the δ-proteobacteria by smearing from the parent worm. Recent single nucleotide polymorphism (SNP's) analysis however indicates that at least one of the two δ-proteobacterial symbionts phylotypes is transmitted horizontally. In contrast to the γ1 symbiont, δ-symbionts SNP's phylogeny is not congruent with that of the host mitochondria which is inherited only through the female germline (J. Wippler in prep). In addition, a sulphate reducing δ-proteobacterial environmental strain, *Candidatus* Desulfoproteus, isolated from sediments along the European Atlantic coast, shows 97% 16s rRNA similarity to the δ1 symbiont of *O. algarvensis* (M. Mussmann in prep.). Although δ1 symbiont phylotypes have never been found in the environment we do not exclude their presence or indeed the possibility for vertical transmission of these cells to the host.

The argument has been put forward that non-enriched horizontally transmitted δ-proteobacterial symbionts may have been missed during our experiments. It cannot be excluded that cross feeding of metabolites from enriched vertically transmitted cells may accumulate in non-enriched δ-proteobacteria. The argument is plausible, however, there was no significant difference of enrichment between cells found in any of the examined egg stages or the controls. If cross feeding between bacterial cells would have occurred then: 1) cells with much lower enrichment and / or no enrichment at all and identified as δ-proteobacteria by MiL-FISH would be present in the early analysed developmental stage and the controls, and 2) cross feeding between symbionts within cocoons would result in higher $^{12}C^{15}N/^{12}C^{14}N$ ratio for δ-proteobacterial cells found in late developmental stages than in early ones due to an accumulation of label over time. This was not the case and a $^{12}C^{15}N/^{12}C^{14}N$ ratio between 0.008 and 0.015 were measured for

all analysed developmental stages and controls. We therefore exclude the possibility to miss non-enriched cells due to cross feeding of ^{15}N labelled metabolites and conclude that δ-proteobacteria were indeed transmitted vertically during our experiments.

Based on our data we conclude that the primary mode of transmission for all bacterial symbionts of *Olavius algarvensis* is vertical by bacterial smearing from the parent worms genital pad. We do not exclude horizontal transmission as a secondary environmental transmission mode however as several indications for this are given: 1) the initial soft casing of the eggs after oviposition potentially allows bacteria to enter cocoons, 2) SNP's analysis of δ-proteobacteria indicate a horizontal transmission mode, and 3) there is a large variance in δ-proteobacterial phylotypes within and between gutless oligochaete species indicating several switching events since the establishment of the symbiosis across the genus.

Acknowledgments:

We thank Miriam Weber and Christian Lott at the HYDRA field station on Elba, Italy, for help with sample collection and on site experiments. Cecilia Wentrup and Beatriz Elizabeth Noriega Ortega for preliminary experiments. Sten Littmann for nanoSIMS assistance. This work was funded by European Union (EU) Marie Curie Actions Initial Training Network (ITN) SYMBIOMICS (contract number 264774) and the Max Planck Society.

5.1 Further aspects to Chapter V

Our experiments in this Chapter indicate vertical transmission as the typical pathway for symbionts to pass into the next host generation of *Olavius algarvensis*. However, as discussed, horizontal transmission is not excluded and likely to occur occasionally in the environment. Several questions remain open from the study and some approaches are suggested to experimentally test these hypothesis.

i) To improve the analytical resolution of the current study further specimens should be analysed to verify the trend that we currently observe. Further, 16S rRNA oligonucleotide probes specific to each symbiont phylotype should be applied and nanoSIMS analysis conduced. The presented multi-coloured MiL-FISH approach, presented in Chapter III, can be used to simultaneously identify and visualise each symbiont phylotype and co-localisation of signal with nanoSIMS data can be applied (Chapter VII – Appendix – A – 7.5). In this manner we can test if all symbiont phylotypes found within the cocoons are transmitted vertically. Additional insight with species-specific probes would enhance our understanding of the current transmission mode and help support our arguments regarding the evolutionary theories presented in this thesis.

The potential for cocoons to take up environmental bacteria by horizontal transmission can be tested with additional ^{15}N-ammonium incubation experiments. A "reverse" labelling approach to the one presented in this Chapter can be applied. In contrast to ^{15}N enrichment of parent worms environmental sediment could be incubated with ^{15}N-ammonium. This would enrich the environmental bacterial community associated to the sediment. With correlative MiL-FISH and nanoSIMS eggs deposited in ^{15}N enriched sediment can be analysed and potential detection of enriched bacteria within the cocoons determined. For such an approach I propose the use of natural sediment that originates from seagrass roots as discussed in Chapter 6.1.

References:

Bergter A, Beck LA, Paululat A. (2004). Embryonic development of the oligochaete Enchytraeus coronatus: an SEM and histological study of embryogenesis from one-cell stage to hatching. *J Morphol* **261**: 26–42.

Bosch TCG, Adamska M, Augustin R, Domazet-Loso T, Foret S, Fraune S, *et al.,* (2014). How do environmental factors influence life cycles and development? An experimental framework for early-diverging metazoans. *Bioessays* **36**: 1185–1194.

Bright M, Bulgheresi S. (2010). A complex journey: transmission of microbial symbionts. *Microbiol* **8**: 218–230.

Brucker RM, Bordenstein SR. (2012). Speciation by symbiosis. *Trends Ecol Evol* **27**: 1–9.

Ciche TA, Darby C, Ehlers RU, Forst S. (2006). Dangerous liaisons: the symbiosis of entomopathogenic nematodes and bacteria. *Biol Control* **38**: 22–46.

Dubilier N, Mulders C, Ferdelman T, de Beer D, Pernthaler A, Klein M, *et al.,* (2001). Endosymbiotic sulphate-reducing and sulphide-oxidizing bacteria in an oligochaete worm. *Nature* **411**: 298–302.

Ebert D. (2013). The epidemiology and evolution of symbionts with mixed-mode transmission. *Annu Rev Ecol* **44**: 623–643.

Erseus C. (2003). The gutless Tubificidae (Annelida: Oligochaeta) of the Bahamas. *Meiofauna Marina*. **12:** 59-84.

Felbeck H. (1981). Chemoautotrophic Potential of the Hydrothermal Vent Tube Worm, Riftia pachyptila Jones (Vestimentifera). *Science* **213**: 336–338.

Fernández M, Ruiz-Tagle N, Cifuentes S, Pörtner HO. (2003). Oxygen-dependent asynchrony of embryonic development in embryo masses of brachyuran crabs. *Mar Biol* **142**: 559–565.

Flewelling S, Parker SL. (2015). Effects of temperature and oxygen on growth and differentiation of embryos of the ground skink, Scincella lateralis. *J Exp Zool A Ecol Genet Physiol* **323**: 445–455.

Fraune S, Augustin R, Anton-Erxleben F, Wittlieb J, Gelhaus C, Klimovich VB, *et al.,* (2010). In an early branching metazoan, bacterial colonization of the embryo is controlled by maternal antimicrobial peptides. *PNAS* **107**: 18067–18072.

Giere O. (2002). Taxonomy and new bacterial symbioses of gutless marine Tubificidae (Annelida, Oligochaeta) from the island of Elba (Italy). *Org Divers Evol* **2**: 289–297.

Giere O, Conway NM, Gastrock G, Schmidt C. (1991). Regulation" of gutless annelid ecology by endosymbiotic bacteria. *Mar Ecol Prog Ser* **68**: 287–299.

Giere O, Erseus C. (2002). Taxonomy and new bacterial symbioses of gutless marine Tubificidae (Annelida, Oligochaeta) from the Island of Elba (Italy). *Org Divers Evol*. **2:** 289-297.

Giere O, Langheld C. (1987). Structural organisation, transfer and biological fate of endosymbiotic bacteria in gutless oligochaetes. *Mar Biol*. **93:** 641-650.

Gilbert SF. (2001). Ecological Developmental Biology: Developmental Biology Meets the Real World. *Dev Biol* **233**: 1–12.

Hamdoun A, Epel D. (2007). Embryo stability and vulnerability in an always changing world. *PNAS* **104**: 1745–1750.

Kaltenpoth M, Göttler W, Herzner G, Strohm E. (2005). Symbiotic bacteria protect wasp larvae from fungal infestation. *Curbio* **15**: 475–479.

Kleiner M, Wentrup C, Lott C. (2012a & b). Metaproteomics of a gutless marine worm and its symbiotic microbial community reveal unusual pathways for carbon and energy use. *PNAS* **109 (19)**: E1173–E1182.

Kleiner M, Wentrup C, Holler T, Lavik G, Harder J, Lott C, *et al.,* (2015). Use of carbon monoxide and hydrogen by a bacteria-animal symbiosis from seagrass sediments. *Environ Microbiol*. doi:10.1111/1462-2920.12912.

Kleiner M, Young JC, Shah M, VerBerkmoes NC, Dubilier N. (2013). Metaproteomics reveals abundant transposase expression in mutualistic endosymbionts. *MBio* **4**: e00223–13.

Krueger DM, Gustafson RG, Cavanaugh CM. (2002). Vertical Transmission of Chemoautotrophic Symbionts in the Bivalve Solemya velum (Bivalvia: Protobranchia). *Biol Bull* **190**: 1–8.

Lutz RA, Kennish MJ. (1993). Ecology of deep-sea hydrothermal vent communities: A review. *Rev Geophys* **31**: 211–242.

McFall-Ngai MJ. (2002). Unseen forces: the influence of bacteria on animal development. *Dev Biol* **242**: 1–14.

Moran NA, Wernegreen JJ. (2000). Lifestyle evolution in symbiotic bacteria: insights from genomics. *Trends Ecol Evol* **15**: 321–326.

Nakamoto A, Arai A, Shimizu T. (2000). Cell lineage analysis of pattern formation in the Tubifex embryo. II. Segmentation in the ectoderm. *Int J Dev Biol* **44**: 797–805.

Nussbaumer AD, Fisher CR, Bright M. (2006). Horizontal endosymbiont transmission in hydrothermal vent tubeworms. *Nature* **441**: 345–348.

Nyholm SV, McFall-Ngai MJ. (2003). Dominance of Vibrio fischeri in secreted mucus outside the light organ of Euprymna scolopes: the first site of symbiont specificity. *Appl Environ Microb* **69**: 3932–3937.

Ogden J. (2006). Seagrasses: Biology, Ecology and Conservation. Springer Netherlands doi:10.1007/springerreference_205924.

Ott JA, Novak R. (1989). Living at an interface: Meiofauna at the oxygen/sulfide boundary of marine sediments. Reproduction, genetics and distributions of marine organisms. 23rd European Marine Biology Symposium. 415-422.

Petersen JM, Zielinski FU, Pape T, Seifert R, Moraru C, Amann R, *et al.,* (2011). Hydrogen is an energy source for hydrothermal vent symbioses. *Nature* **476**: 176–180.

Polerecky L, Adam B, Milucka J, Musat N, Vagner T, Kuypers MMM. (2012). Look@NanoSIMS--a tool for the analysis of nanoSIMS data in environmental microbiology. *Environ Microbiol* **14**: 1009–1023.

Prado SS, Almeida R. (2009). Role of symbiotic gut bacteria in the development of Acrosternum hilare and Murgantia histrionica. *Entomol Exp Appl*. doi:10.1111/j.1570-7458.2009.00863.x.

Schimak MP, Kleiner M, Wetzel S, Liebeke M, Dubilier N, Fuchs BM. (2015). MiL-FISH: Multi-labelled oligonucleotides for fluorescence in situ hybridisation improve visualization of bacterial cells. *Appl Environ Microbiol*. doi:10.1128/AEM.02776-15.

Simon MC, Keith B. (2008). The role of oxygen availability in embryonic development and stem cell function. *Nat Rev Mol Cell Biol* **9**: 285–296.

van der Heide T, Govers LL, de Fouw J, Olff H, van der Geest M, van Katwijk MM, *et al.,* (2012). A Three-Stage Symbiosis Forms the Foundation of Seagrass Ecosystems. *Science* **336**: 1432–1434.

van der Heijden MGA, Bardgett RD, van Straalen NM. (2008). The unseen majority: soil microbes as drivers of plant diversity and productivity in terrestrial ecosystems. *Ecol Letters* **11**: 296–310.

Wanninger A. (2015). Evolutionary Developmental Biology of Invertebrates 6. Springer-Verlag, Wien.

Wilson WH. (1991). Competition and Predation in Marine Soft-Sediment Communities. *Annu Rev Ecol Syst* **21**: 221–241.

Woyke T, Teeling H, Ivanova NN, Huntemann M, Richter M, Gloeckner FO, *et al.,* (2006). Symbiosis insights through metagenomic analysis of a microbial consortium. *Nature* **443**: 950–955.

Tables and Figures

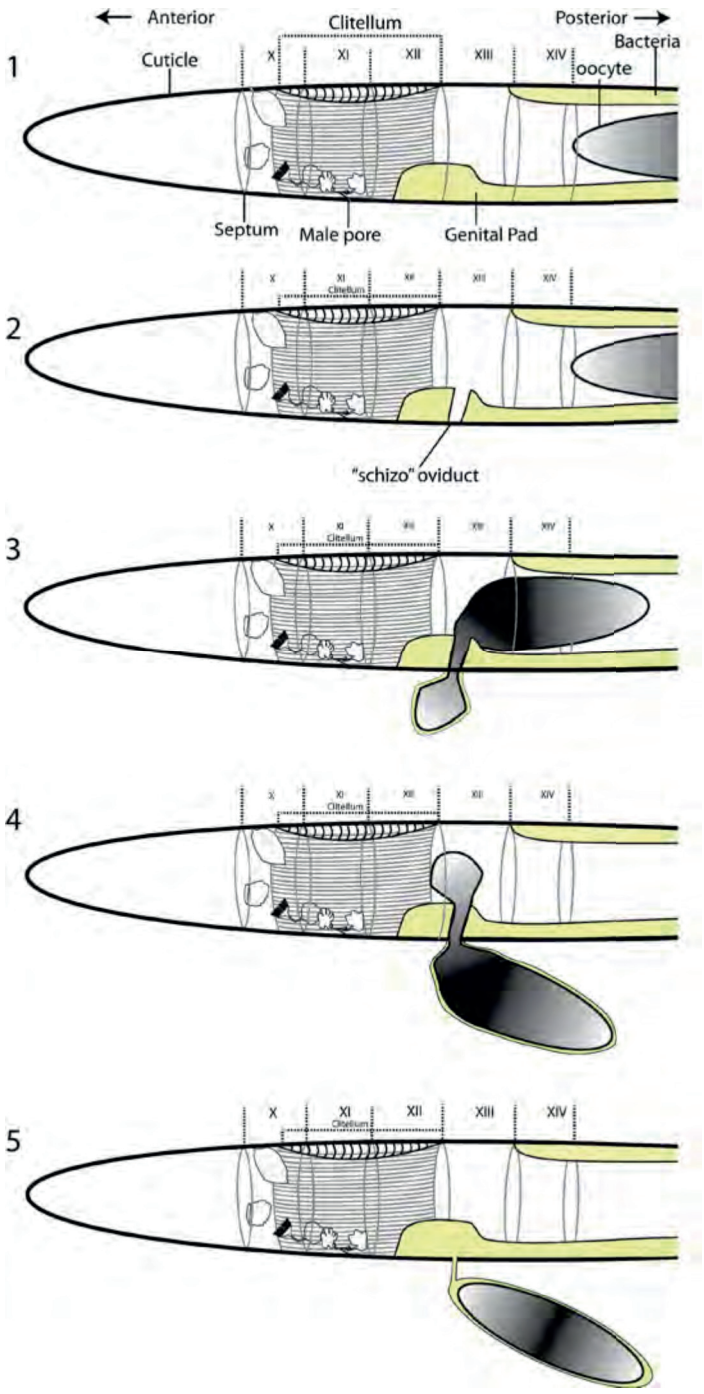

Figure 1: Schematic representation of oviposition in the gutless oligochaetes. 1) Male reproductive organs are found in segment X to XI, the Clitellum in segment ½ X to XII. The genital pad is located on the ventral side of the worm around segment XII. 1) The oocyte moves internally in an anterior direction to segment XIV. 2) A "schizo-oviduct" opens in the genital pad region of segment XII. 3 & 4) The unfertilised oocyte is pressed through the schizo-oviduct and smeared with symbionts from the genital pad. Sperm is released from the male pore to fertilise the oocyte. Mucus and albumen is secreted from the clitellum to later form the cocoon. 5) The mucus encased zygote is attached to the worm for a short period of time by filament that later congeals to form the cocoons operculum.

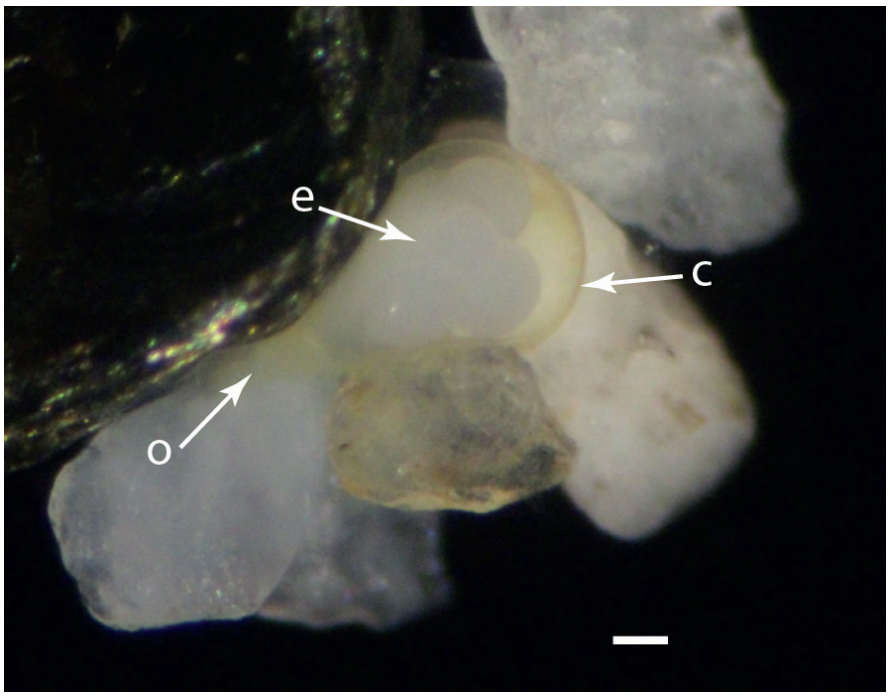

Figure 2: *O. algarvensis* egg attached to sand grains. Several blastomeres are visible through the translucent egg casing before it congeals and takes on a milky white appearance. Attached sand grains build a "casing" around the egg, which provides additional mechanical stability form the environment and potential protection from predation. o = operculum, c = cocoon, e = embryo. Scale bar: 50 µm

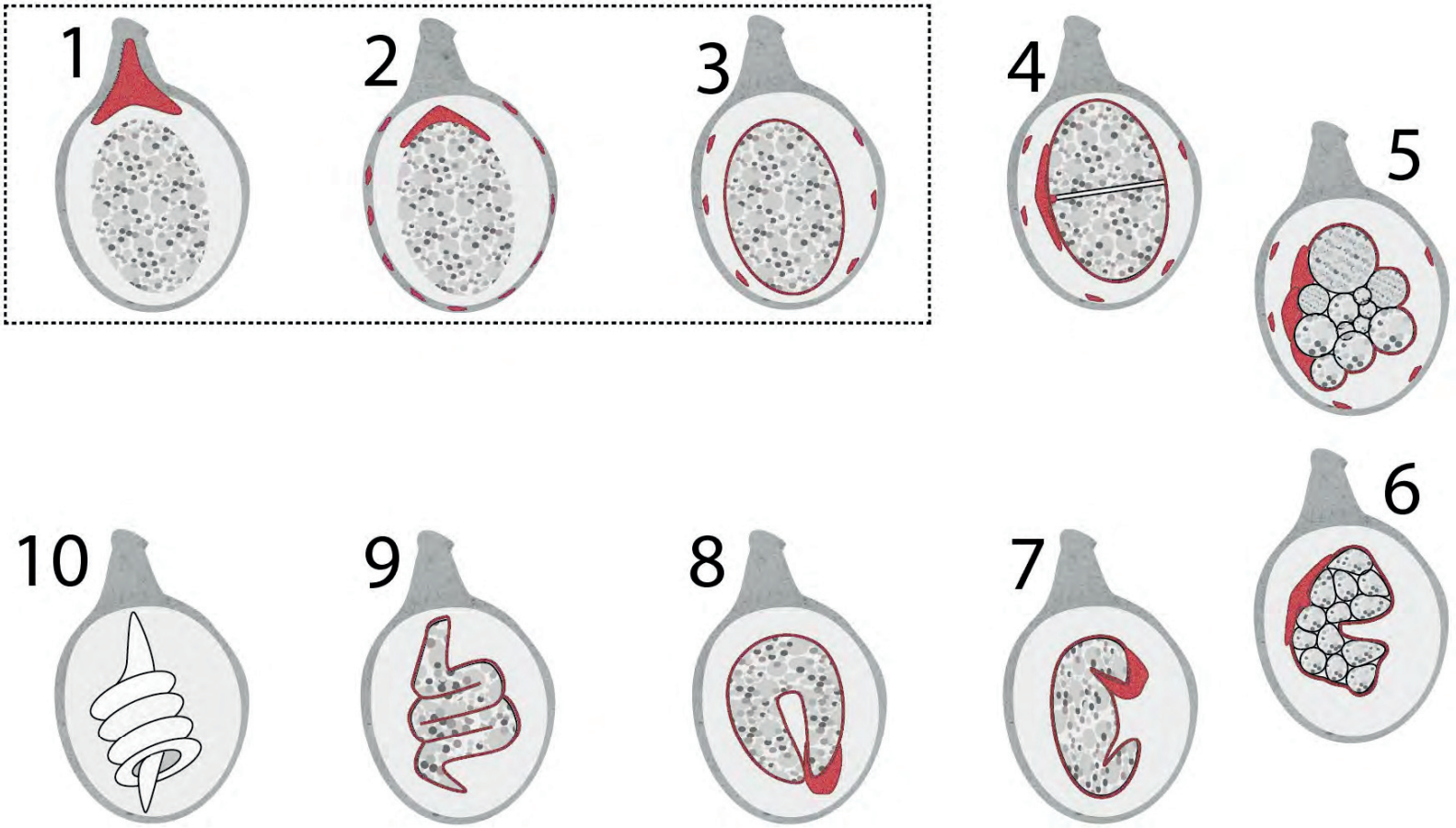

Figure 3: Schematic representation of egg developmental stages analysed in this study and symbiont localisation (red) on the developing embryos. Grid box (Stage 1, 2 & 3) pre first cleavage. 4) first cleavage, 2-cell stage. 5) embryo pole differentiation. The yolk rich vegetal pole is situated at the operculum. 6) early blastula like stage. 7 & 8) onset of development by teloblast differentiation and subsequent development into a juvenile worm. Note: bacteria associated to the anterior of the developing worm. 9) The establishment of the symbiosis: symbionts surrounding the early juvenile are entrapped between worm epidermis and the freshly secreted cuticle. 10) the fully formed juvenile worm inside the cocoon prior to hatching.

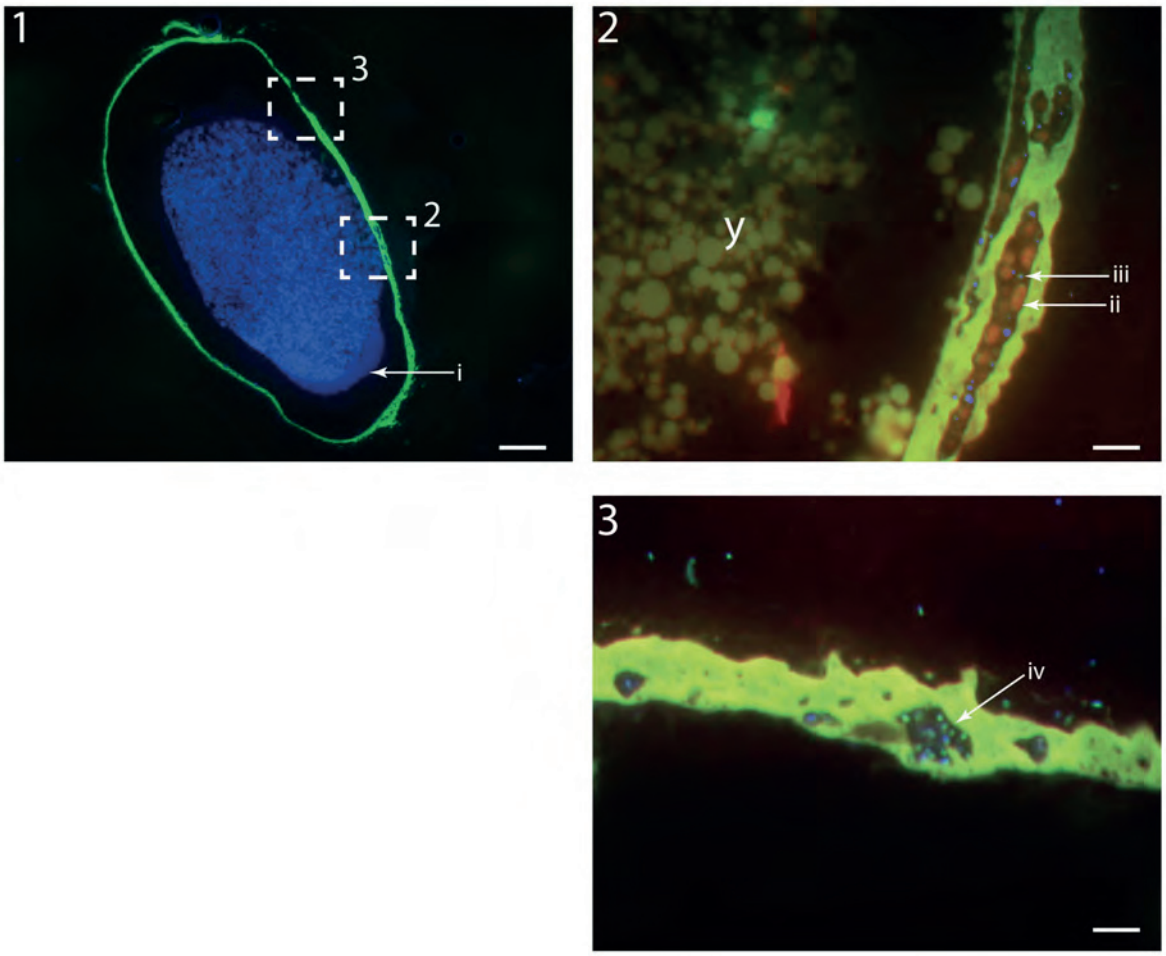

Figure 4: FISH of developmental stage 2 from Figure 3. 1) Overview of DAPI stained egg. i) Bacterial aggregate closely associated to the embryo at the operculum pole. Grid square shows area of interest in panel 2 and 3. Scale bar 50 µm. 2) MiL-FISH with phylotype specific 16S rRNA probes (see SI Table 1) targeting γ1 (ii – red cells) and γ3 (iii – green cells) symbionts inside the egg wall. DAPI stain in blue. 3) MiL-FISH targeting δ1 symbiont in the egg wall with phylotype specific 16S rRNA probe (iv – green). Scale bar 5 µm.

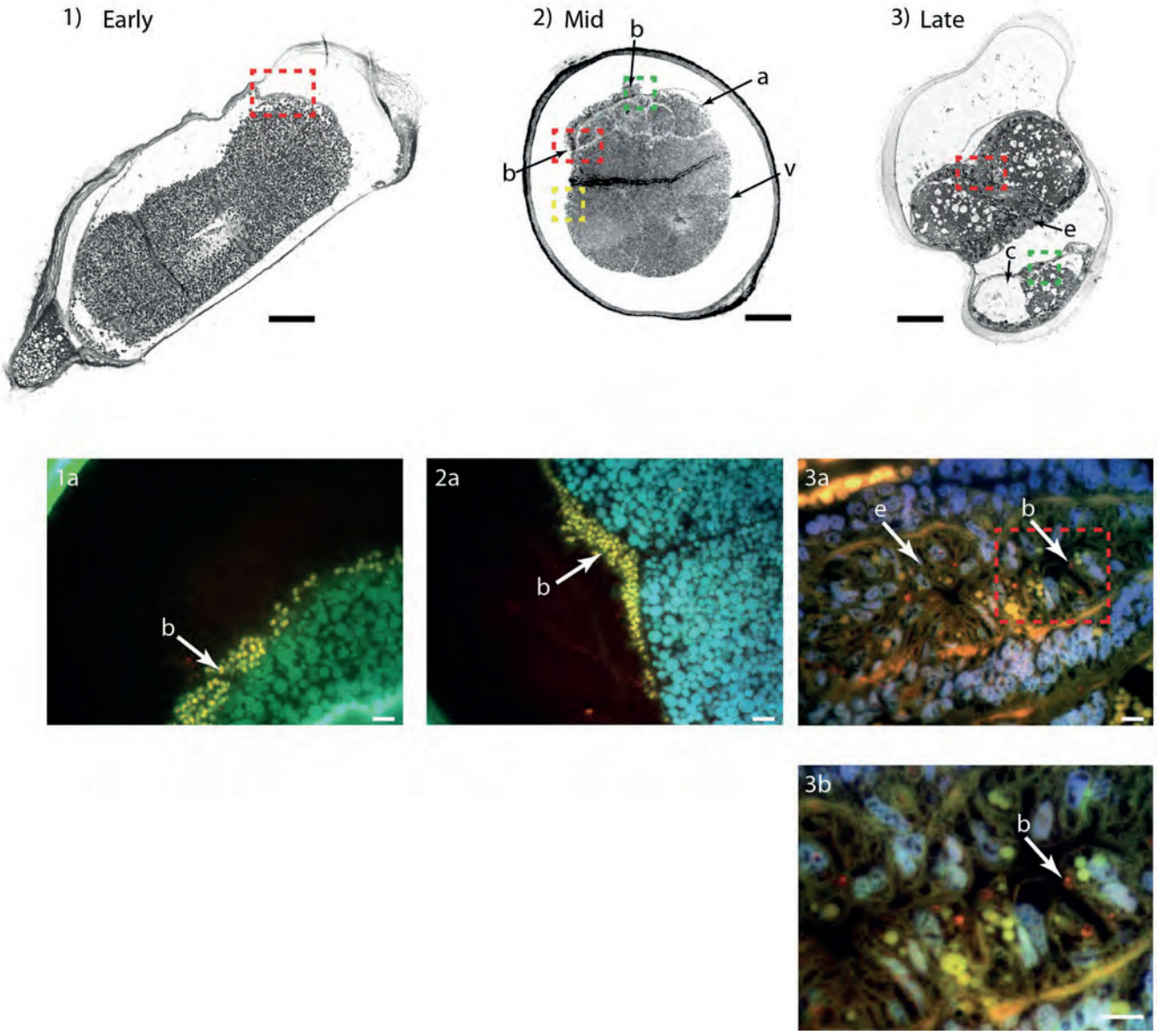

Figure 5: Eggs selected for nanoSIMS analysis deposited by worms after ^{15}N-ammonium incubation. 1) Longitudinal section of early egg pre-first cell cleavage. Bacteria are found in a thin layer around the embryo. This stage represents stage 3 from Figure 3 (nanoSIMS analysis of this stage is not shown in this Thesis). 2) Cross-section of 32-cell stage embryo (a = animal pole, v = vegetal pole). Bacteria surround the embryo and accumulate between blastomeres. This stage represents stage 5 in Figure 3. 3) Cross-section of juvenile worm in egg. Glandular epidermal cells (e) have secreted cuticle and symbionts are found in the interstitial space between cuticle and epidermis. Coelomic cavity has partially formed with egg yolk still present (c). Grid squares for all three panels: red – area shown in panel 1a, 2a and 3a. Green - shows region of MiL-FISH & nanoSIMS analysis for the δ-proteobacteria (Figure 6 – a & c). Yellow - shows region of MiL-FISH & nanoSIMS for the γ-proteobacteria (Figure 6 – b). Scale bar for all images: 50 µm. Panels 1a, 2a, 3a & 3b show Mil-FISH targeting the γ1 symbiont phylotype (SI Table 1) with 16S rRNA specific probes (yellow cells in 1a and 2a, red cells in 3a and 3b). b = bacteria (γ1 phylotype). 3a) e = epidermis, red square grid in 3a shows region depicted in 3b. Scale bar = 5 µm.

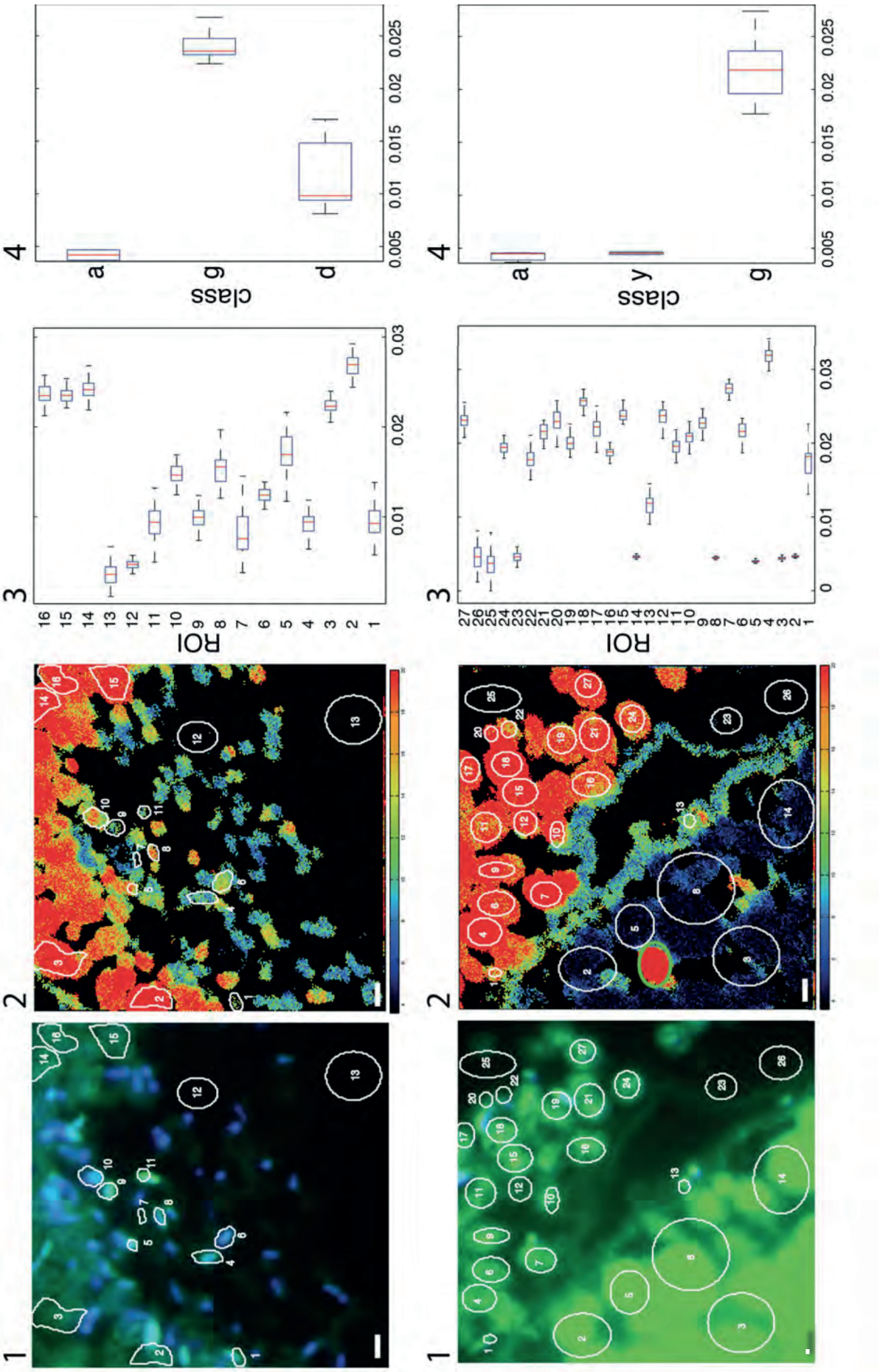
a
b
1
2
3
4
ROI
class
a
g
d
y
0.005
0.01
0.015
0.02
0.025
0.03

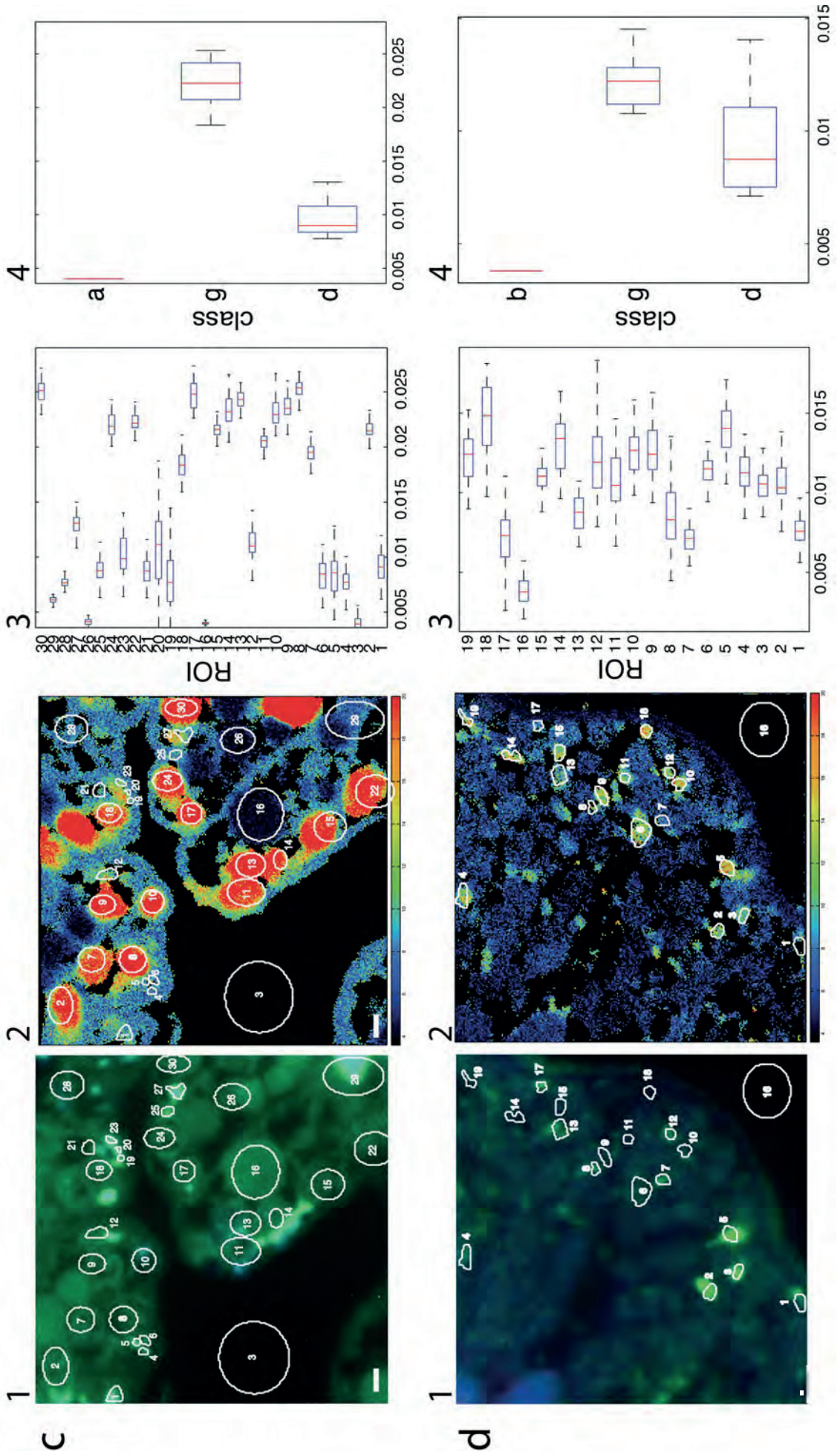
c
d
1
2
3
4
ROI
class
a
g
d
b
0.005
0.01
0.015
0.02
0.025

Figure 6: MiL-FISH and nanoSIMS of eggs from ^{15}N-ammonium incubated worms. For all panels (a, b, c and d): image 1) = FISH & DAPI with ROI's corresponding to image 2, scale bar 1 µm 2) = $^{12}C^{15}N/^{12}C^{14}N$ nanoSIMS image, scale bar = 1 µm 3) = enrichment of each ROI as labelled in 1 & 2, 4) = ROI $^{12}C^{15}N/^{12}C^{14}N$ enrichment grouped into classes, a = egg albumen, g = γ-proteobacteria, d = δ-proteobacteria, y = egg yolk, b = background.
a) Egg of mid developmental stage hybridised with the δ-proteobacterial general probe DSS658 (green signal) (Figure 5 – 2, region of nanoSIMS measurement green grid square). b) Egg of mid developmental stage hybridised with the γ-proteobacterial general probe Gam42a (Figure 5 – 2, region of nanoSIMS measurement yellow grid square). c) Egg of late developmental stage (juvenile worm in egg) hybridised with the δ-proteobacterial general probe DSS658 (green signal) (Figure 5 – 3, region of nanoSIMS measurement green grid square). Symbiont cells are located underneath the cuticle of the juvenile worm. d) Control of adult ^{15}N incubated worm hybridised with the δ-proteobacterial general probe DSS658 (green signal)

_SI Table 1: MiL-FISH oligonucleotide probes used in this study. Probe name, nucleotide sequence – for MiL-FISH probes modified nucleotide-fluorochrome complexes are indicated by an underscore, target gene, label type, label synthesis, target taxon or higher, target species and probe colour imaging.

Probe	Sequence 5' - 3' (reverse complementary)	Target gene	Label	Synthesis	Taxon	Target Species	FA %	Colour
DSS658	TCC ACT TCC CTC TCC CAT	16S rRNA	4x Cy3	Click chemistry	δ-proteobacteria	δ-symbionts of *O. algarvensis*	60%	Red
Gam42a	GCC TTC CCA CAT CGT TT	23S rRNA	4x Cy5	Click chemistry	γ-proteobacteria	γ-symbionts of *O. algarvensis*	35%	Blue
Oalg_G1_644	TAC CAC ACT CTA GCC GGA CA	16S rRNA	5' & 3' end 6-FAM, 2x Cy3 intern	DOPE & Click chemistry	γ-proteobacteria	γ1 symbiont of *O. algarvensis*	35%	Yellow
Oalg_G1_644	TAC CAC ACT CTA GCC GGA CA	16S rRNA	4x Cy3	DOPE & Click chemistry	γ-proteobacteria	γ1 symbiont of *O. algarvensis*	35%	Red
Oalg_G3_268	TAT AGA GCG TTG CCT TGG TAG	16S rRNA	4x Cy5	Click chemistry	γ-proteobacteria	γ3 symbiont of *O. algarvensis*	35%	Blue
Oalg_D1_129	CCG ACT CGG GGG AAG ATT A	16S rRNA	4x 6-FAM	Click chemistry	δ -proteobacteria	δ1 symbiont of *O. algarvensis*	20%	Green
Oalg_D4_468	CCG TCA ATA CCC GAA CGT	16S rRNA	4x Cy3	Click chemistry	δ -proteobacteria	δ4 symbiont of *O. algarvensis*	35%	Red
EUB338	GCT GCC TCC CGT AGG AGT	16S rRNA	4x 6-FAM	Click chemistry	Bacteria	Most Bacteria	35%	Green
NON338	ACT CCT ACG GGA GGC AGC	16S rRNA	4x 6-FAM	Click chemistry	Non-sense	none	n/a	Green

SI Table 2: Egg specimens attained from worms incubated in ^{15}N-ammonum. Sample name, time that worms were incubated in porous CPD vials before they were opened for egg retrieval , time of 15N-ammonium incubation.

Sample name	Aquarium Incubation time	N^{15} incubation time
Egg 20	7 days	19.30 h
Egg 23	7 days	19.30 h
Egg 24	9 days	19.30 h
Egg 25	9 days	19.30 h
Egg 43	5 days	22 h
Egg 44	5 days	22 h
Egg 60	10 days	22 h
Egg 75	15 days	22h
Egg 76	15 days	22 h
Egg 86	20 days	22 h
Egg 87	20 days	22 h
Egg 94	25 days	22 h
Egg 97	30 days	22 h
Egg 99	35 days	22 h

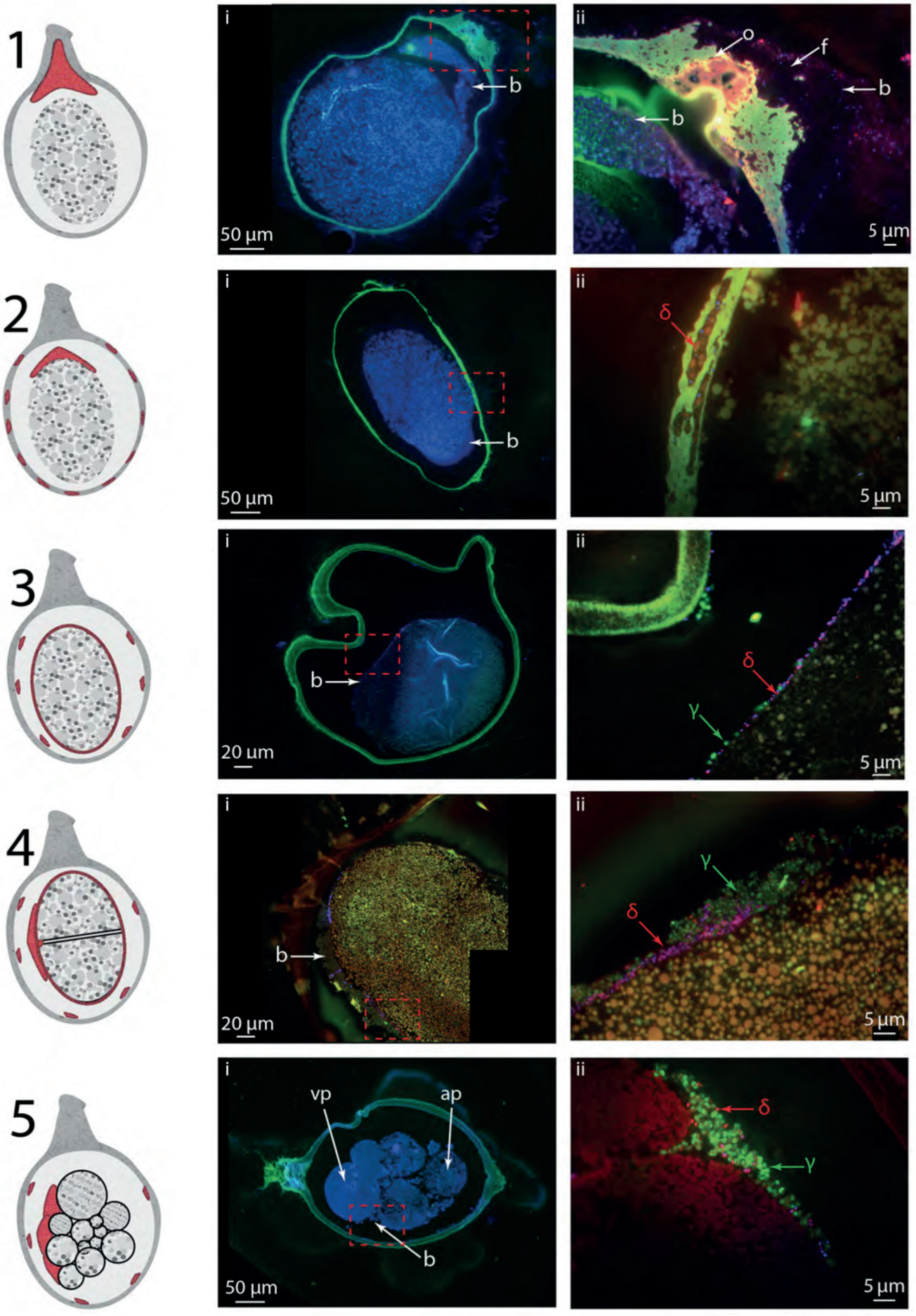
1
2
3
4
5
i
ii
b
o
f
δ
γ
vp
ap
50 µm
20 µm
5 µm

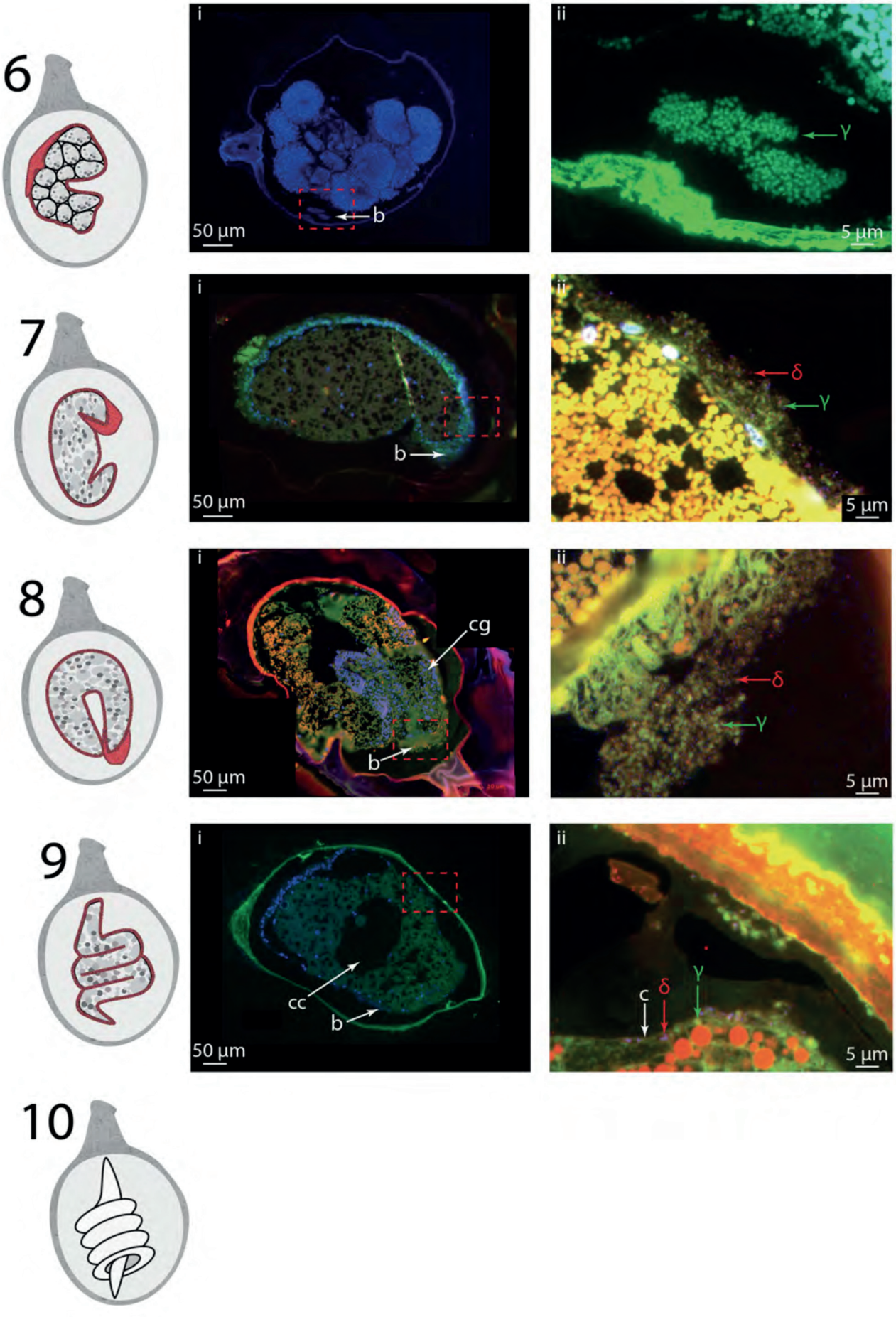
6
i
ii
b
γ
50 µm
5 µm
7
i
ii
δ
γ
b
50 µm
5 µm
8
i
ii
cg
δ
γ
b
50 µm
5 µm
9
i
ii
cc
b
c
δ
γ
50 µm
5 µm
10

SI Figure 1: The ten developmental stages analysed in this study depicting bacteria associated to the developing embryo. For all image sets from left to right. 1-10 Schematic of developmental stage generated by analysis of ~20 % of the semi-thin sections (1 µm) attained from each specimen. i) overview image of a single semi-thin section for each stage. b = bacteria. Panel 5: bp = vegetal pole, ap = animal pole. Overview images 1, 2, 3, 5 and 9 were DAPI stained and recorded in both blue (DAPI) and green (autofluorescence) channels of the microscope. Stage 6 was recorded in the blue channel only and no DAPI staining. Stages 4, 7 and 8 are overview images compiled by stitching together of several images after MiL-FISH and DAPI staining. Stage 8: cg = cerebral ganglion developing at the anterior of the worm determined by a high number host nuclei (for reference see Berger *et al.,* 2004). Stage 9: cc = coelomic cavity. Images were recorded in blue, green and red channels. Red Grid Square shows area of panel ii. ii) MiL-FISH of bacteria in the eggs (except stage 1 – DAPI stain only). Stage 1 panel ii) b = bacteria, f = filament attaching egg to worm, o = operculum. Stage 9 panel ii) c = cuticle. For all other panels γ = γ-proteobacteria hybridised with Gam42a 23S rRNA probe (Green), δ = δ-proteobacteria hybridised with DSS658 16S rRNA probe (Red). Stage 10) a juvenile with a fully formed coelomic cavity was not present in the data set and only represented here by a schematic.

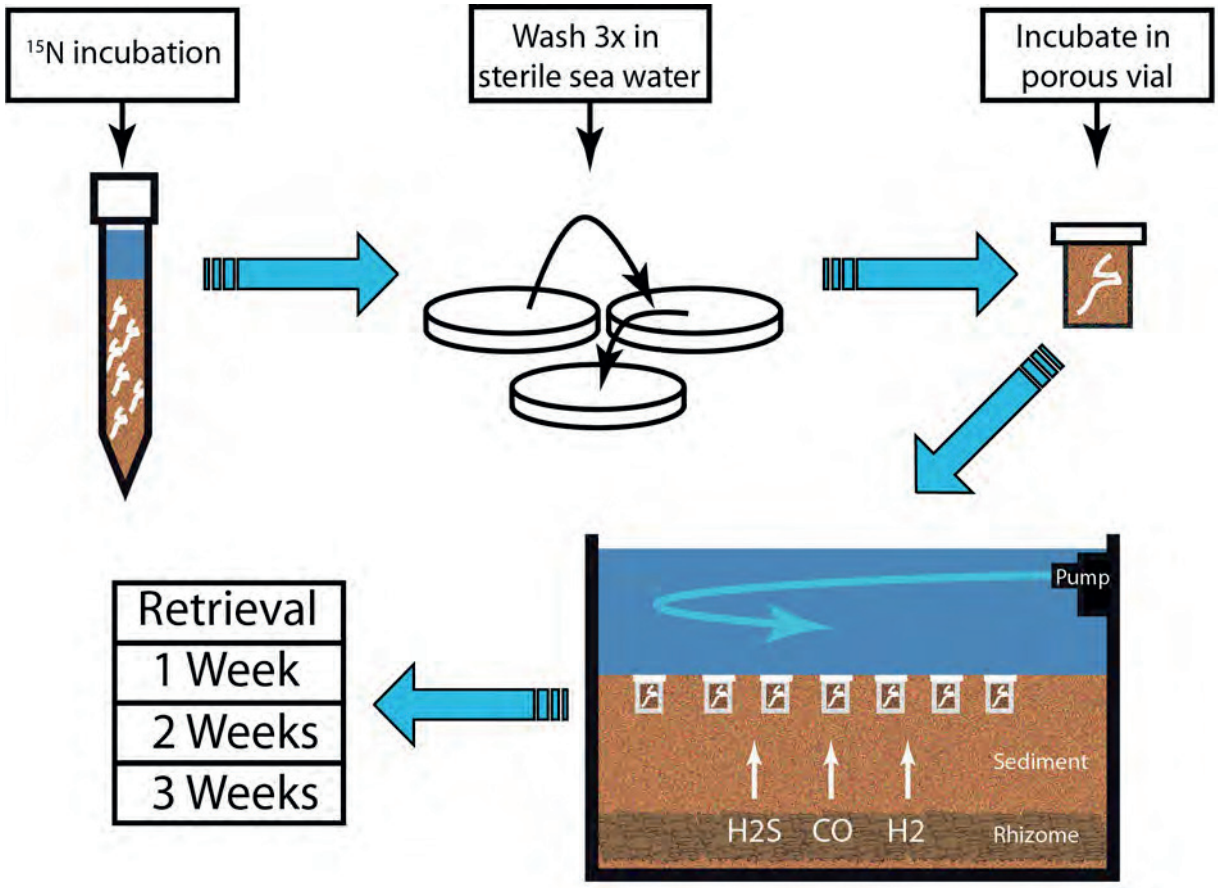

SI Figure 2: Experimental setup for ^{15}N-ammonium incubations. Sexually mature adult *O. algarvensis* worms were incubated ^{15}N-ammonium, washed three times in sterile filtered seawater and reintroduced to aquaria in sediment filled 78 µm porous vials. The incubation aquarium was kept at 25° C and contained a rhizome bottom layer to provide reduced substances. A subset of vials was sampled every week in an attempt to attain a variety of developmental stages.

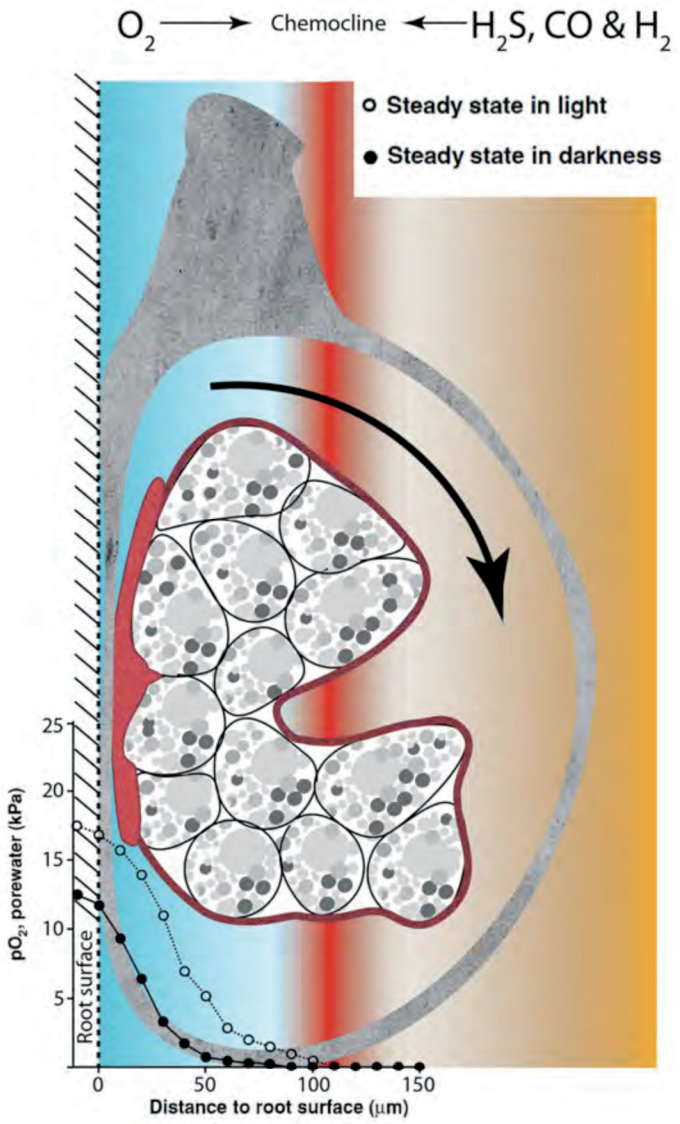

SI Figure 3: Adapted from Borum 2006 in (Ogden, 2006). Measurements from the study of Borum, 2006 show the concentration (y-axis) and distance (x-axis) that oxygen moves into the sediment as it is released from the roots of the seagrass *Zostera marina*. Unfortunately, no such data is available for *Posidonia oceanica.* Oxygen concentrations fluctuate in a diurnal pattern with day (steady state in light) and night (steady state in darkness) photosynthesis of the seagrass. I propose that a ~ 250 µm *Olavius algarvensis* egg attached to the root surface would be exposed to a range of oxygen concentrations (blue background). As the embryo rotates inside the cocoon bacteria associated to it are exposed to O_2 gradients ranging from oxic, hypoxic to anoxic. In this manner both aerobic and anaerobic symbiont groups are supplied with the conditions they required to fuel sulphate reduction and sulphur oxidation. Reduced substrates such as H_2S, CO and H_2 are available from the surrounding reduced sediments (orange background). In the transition zone between oxidised and reduced sediment layers, a vertical chemocline is formed (red line). The developing embryo is supplied with oxygen required for development. In non-photosynthetic periods (steady state in darkness) the embryo may go into arrested development or tolerate low oxygen concentrations until conditions turn favourable again.

Chapter VI

General Discussion and outlook

6 General discussion

Using the symbiotic system *Olavius algarvensis,* this thesis offers new insight into ecology, zoology, developmental biology, symbiosis theory and microbiology in the following ways: 1) the ecology and substrate dependant distribution of the holobiont in the environment is experimentally determined, 2) novel insights into the reproductive biology and morphology of the host, 3) documentation of oviposition, various developmental stages and the conditions required for development of embryos, 4) the transmission of symbionts into the next host generation and the evolutionary implications that this may have for the holobiont and 5) MiL-FISH a novel fluorescent *in situ* hybridisation method which is applicable for future studies in symbiosis research, microbial ecology and medical microbiology. The specific aspects to each of the presented manuscripts have been discussed in the corresponding chapters and will not be summarised here. Instead, several questions have arisen, which pave the way for future research and give grounds for hypothetical and speculative discussion. These, as well as additional technical aspects, will be presented and discussed in the following chapter.

6.1 Life and reproduction in the seagrass meadow

The decay of dead seagrass rhizome provides H_2S, CO and H_2 as discussed in Chapter II. This has been argued as the biogeochemical basis that enables *O. algarvensis* to colonise an otherwise oligotrophic habitat (Kleiner *et al.,* 2012) & (Kleiner *et al.,* 2015). During sampling worms are found to closely associate with the seagrass meadow itself and as discussed in Chapter V it would seem plausible that egg deposition primarily occurs in the seagrass root system because, compared to the open sediment, mechanical stability and reduced predation pressure is given. Further, seagrasses shield their own tissue from highly toxic reduced substrates by active radial oxygen release through roots to build a protective layer around them (Hasler-Sheetal and Holmer, 2015) (Ogden, 2006). Release of oxygen into reduced sediments builds a redox potential discontinuity layer resulting in the formation of a chemocline around the root surface. Compared to the open sediment this chemocline is very stable and offers both the oxic conditions and reduced substrates needed for sulphur oxidation and sulphate reduction. A higher concentration of these substrates is expected in the seagrass meadows compared to the open sediment because i) more fresh organic matter is "trapped" in the root and rhizome system and ii) the reduced influence of wave dynamics ensures that less oxidised seawater penetrates into the sediment which would otherwise disperse substrate rich water (Calleja *et al.,* 2007). This does however present a potential conflict for CO_2 fixation by CO oxidation for the γ3 symbionts. pH increases with high rates of organic matter decomposition (Andersson *et al.,* 2001), however CO_2 saturation in seawater decreases with high pH, which results in lower carbon availability for autotrophic CO_2 fixing organisms. A hypothetical solution for this is the shuttling of CO_2 from the δ-proteobacteria. Kleiner *et al.,* 2015 suggested that the energy gained by CO oxidation of the δ -proteobacteria originates from fatty acids derived from the host under anoxic

conditions. It is therefore lithoheterotrophy and not autotrophy that provides carbon for cellular growth (Kleiner *et al.,* 2015). I suggest that δ-proteobacteria oxidise CO, to gain energy for carbon fixation from fatty acids, producing CO_2 as a waste product thus making it available to the closely associated γ3 symbionts for autotrophic anaerobic CO_2 fixation by CO oxidation. In organic matter rich habitats like the seagrass meadow such a metabolic strategy may be of particular advantage to compensate for pH dependent reduced CO_2 availability. Unfortunately no *in situ* substrate measurements from within the seagrass meadows on Elba have been taken to date.

Free-living symbiont phylotypes, provided these exist, have never been found in the open sediment. As discussed in Chapter V, closely related free-living sulphate reducing δ-proteobacteria are known from coastal sediments. Based on the presented arguments in this thesis the chemocline around the seagrass roots could support free-living sulphur oxidising and sulphate reducing bacterial communities up to roughly 100 µm around the root surface (Chapter V - SI Figure 3). Gutless oligochaete cocoons attached to seagrass roots would therefore be in close proximity to environmental bacteria that oxidise and reduce sulphur species. As discussed horizontal transmission does not appear to be the common transmission mode, however it is still a plausible strategy amongst the gutless oligochaetes. The close association of eggs to such a free-living environmental bacterial community could increase the number of horizontal transmission events and help explain the high number of δ-proteobacteria phylotypes found in the *O. algarvensis* symbiosis. To experimentally test the ideas proposed in this model both *in situ* measurements of chemical parameters and Metagenomic sequence analysis of sediments from seagrass root systems could be conducted in an attempt to better understand the ecology and environmental transmission potential of *O. algarvensis*.

Van der Heide *et al.,* 2012 proposed a three-way symbiosis between seagrasses, bivalves and their sulphur oxidising gill symbionts as the foundation for reducing sulphide stress on seagrasses, attributing to their worldwide success (Van der Heidi *et al.,* 2012). Indeed, this argument holds true not only for bivalves and their chemosynthetic symbionts but for all chemosynthetic animal-bacterial symbioses and free-living chemosynthetic communities in the seagrass ecosystem. Similarly, the oxidation of reduced substances by chemosynthetic symbionts may not only help protect seagrasses but host tissue itself. In our experiments *O. algarvensis* tolerated prolonged exposure to toxic hydrogen sulphide exceeding tenfold the concentrations found in the environment (Chapter II). Several meiofaunal species have been shown to possess sulphide detoxification mechanisms (Powell *et al.,* 1980) and recent work on *O. algarvensis* has confirmed the presence of haemoglobin capable of binding H_2S (Wippler in prep.). This can help explain tolerance to high H_2S concentrations in our experiments. However, once all H_2S haemoglobin-binding sites are occupied as would be expected when exposed to high concentrations, host tissue damage may still occur. In any case, the symbiont mantel around the worm is postulated to at least partially protect the host tissue from sulphide damage.

6.2 Host reproductive morphology, oviposition, embryogenesis and the reduction of the digestive tract

Prior to the start of this thesis the collection of gutless oligochaete eggs in various developmental stages had not been achieved. This was indeed the major constraint in trying to resolve the transmission mode and the establishment of the symbiosis in this non-cultivatable biological system. A workflow was designed with the primary goal of attaining sample material to resolve some of the questions posed in this thesis. During the

two months of July and August 2013 just over 1000 eggs were successfully retrieved. The possibility of reliably attaining eggs of various developmental stages paves the way for future developmental studies. Based on preliminary results and observations, discussed in Chapter II & V, various hypothesis and open questions that have arisen will be discussed:

i) Oviposition

In the common earthworm *Lumbricus terrestris* (Clitellata, Lumbricidae), the ovaries and ovisac are situated in segment XIII anterior to the clitellum. Here, oocytes mature until they are laid via the oviduct opening in segment XIV (Figure 7A). In the gutless oligochaete *Olavius algarvensis* oocytes are found posterior to the clitellum spanning through several segments of the worm. During oviposition, oocytes move forward and are expelled via an oviduct around segment XII (see Chapter V, Figure 1). Similar to the common earthworm however, the ovaries in *O. algarvensis* are also situated anterior in segment XI (Chapter 1.3.7.2, Figure 8B). Oocytes produced in segment XI must therefore travel posterior past the clitellum through several worm segments where they mature (Figure 8C & D). Subsequently, during oviposition oocytes travel anterior again before leaving the worm in segment XII. The internal shuttling of oocytes to a posterior position and back to segment XII seems highly unusual and is to the author's knowledge unique in gutless oligochaetes amongst the Clitellata. The symbiont bacterial coat starts posterior to the clitellum in the same region where oocytes mature. Oocytes of the Tubificidae are generally large and yolk rich, coupled with high-energy investment and a low production number per reproductive season. It is to be expected that symbionts provide the energy required for oocytes maturation in the gutless oligochaetes because they are the sole nutritional provider for the worms. However, the placing of the oocytes directly into the vicinity of the nutrient providing symbionts may

actively support their maturation process even further. Although not conclusive and based on observations made during nanoSIMS measurements symbionts could energetically contribute to the production of yolk during oocyte maturation directly. In Chapter V, Figure 6 b2 highly ^{15}N enriched yolk globules are found randomly distributed within the zygote (not in ROI statistics and situated to the left of ROI 5, marked as a green ellipse). We exclude the possibility that these are bacteria within the zygote based on their size (e.g. Chapter V, Figure 6 c2 above ROI 29) and a high label content of 0.07 $^{12}C^{15}N/^{12}C^{14}N$ ratio. Further, the possibility that ^{15}N-ammonium adhered to the oocyte during the incubation phase is excluded because no other worm tissue, such as muscle and epidermal cells, showed enrichment in control worms. Rather, we conclude that when ^{15}N-ammonium was readily available during incubation it was assimilated by symbionts and subsequently transferred and incorporated by the oocyte during maturation via an as of yet unknown energy transfer pathway. Indeed, the region in which oocytes mature becomes translucent even in otherwise white worms during the reproductive period. This indicates elevated γ1 symbiont metabolism as storage compounds are depleted (compare Figure 6b with Figure 8C). The energy produced by oxidation of sulphur storage compounds in this region of the worm only could be required to compensate for the high-energy investment associated with oocyte maturation.

In conclusion I hypothesise that the unusual oocyte positioning within the worms is a morphological adaptation to an obligate symbiotic lifestyle which ensures: i) localised energy and nutrient transfer by symbionts for oocyte maturation during the host's reproductive period and ii) positioning of the oocyte for smearing of symbionts during oviposition. Morphological analysis by transmission electron microscopy (TEM) and stable isotope tracing for energy transfer by nanoSIMS will need to be conducted to elucidate on this hypothesis.

ii) Symbiont influence on the development of the zygote

It is known from several other obligate symbiotic systems that bacteria can play a crucial role in the development of their host (see Chapter 1.1.6). During the initial incubation of freshly collected *Olavius algarvensis* eggs an exceptionally high mortality was recorded. The presumed causality was the depletion of readily available oxygen in the small 0,5 ml incubation vials that eggs were kept in. No additional reduced substrate was introduced into the vials and therefore no nutritional source for any symbionts that may be inside the cocoons was provided. This presented suboptimal conditions and eggs appeared to enter a diapause until death, as suggested in Chapter V. Fluctuating oxic / hypoxic incubation conditions were developed for incubation of cocoons with the result that several hundred embryos developed to late ontogenetic stages. As control, eggs were incubated in hypoxic conditions only, which resulted in a high level of mortality, and oxic conditions only resulting in the development of some juveniles but overall less than in fluctuating conditions (observation M. P. Schimak).

Detrimental effect for embryo development by absence of symbiotic partners has been demonstrated a number of times for Arthropods. Females of the Japanese stinkbug *Megacopta punctatissima* for example, attach small bacteria-filled capsules to their egg masses, from which nymphs acquire their symbionts by vertical transmission, immediately after hatching. If the bacteria are removed retarded growth, mortality and sterility of the insects will result (Prado and Almeida, 2009) (Fukatsu and Hosokawa, 2002) (Hosokawa *et al.,* 2006). Similarly Abe *et al*., 1995 showed that sterilized eggs of the green bug *Plauti stali* did not reach an adult stage (Abe *et al.,* 1995). Unlike these studies, during our experiments symbionts were not removed from *O. algarvensis* cocoons. However, if incubation conditions are suboptimal and no reduced substrate and /

or oxygen is provided then we can assume that at least one of the symbiotic partner groups is deemed metabolically inactive. This, in the context of the developing embryo, is analogous to the removal of the symbiont because no active energy contribution during the developmental process can take place, provided of course symbionts do so. Based on observation from incubation in various oxic conditions I hypothesize that at least the primary γ -proteobacterial symbiont, is required to be metabolically active for regular development of the host. Experiments will need to be repeated with particular focus on the number of eggs that develop into fully formed juveniles, precise monitoring of chemical incubation parameters and adequate morphological analysis of eggs to better understand the conditions required for development and the influence that symbionts may have in this process.

iii) Reduction of the digestive tract

As protostomes the mouth opening develops first in all oligochaetes during embryogenesis (i.e. (Bergter *et al.,* 2004)). This was however, never observed for any of the analysed developmental stages in *Olavius algarvensis.* Unlike the reduction of the digestive tract in the deep-sea polychaete *Riftia pachyptila*, after formation of the trophosome it appears that the digestive tract of *O. algarvensis* does not develop during host ontogeny at all. The lack of full differentiation for two of the three germ layers that build the digestive tract, namely endoderm for midgut development and ectoderm for fore- and hindgut development, seems highly unusual. Homeobox genes (*Hox*) are said to tightly regulate the differentiation of germ layers during the developmental process that builds the digestive tract (Beck, 2002). For example: i) ParaHox genes such as cdx appear to be highly conserved in the development of the hindgut in all bilateria (Hejnol and Martín-Durán, 2015), ii) homeobox proteins, such a *brachyury,* are expressed as transcription factors and involved in the development of the foregut in all bilaterians

(Arendt *et al.,* 2001) and iii) specific gene expression of endoderm and ectoderm precursors which go on to develop the mid gut and oral cavity, such as *Ct-ozx* or *Ct-foxAB* respectively, was demonstrated in several bilaterian sub-clades including the annelids (Boyle *et al.,* 2014).

Although not excluded entirely it does seem unlikely that only two genus within the Phallodrilinae do not express genes for gut development which are otherwise highly conserved amongst all bilateria. In fact ectoderm does differentiate in *O. algarvensis* and goes on to form the epidermis. Gutless oligochaetes are the only lophotrochozoans currently known, with chemoautotrophic symbionts closely associated to the developing embryo during the whole developmental process and with a reduced digestive track. Interestingly, during the differentiation of macromeres, γ1 symbionts were found to aggregate on the D quadrant of cells that develop into the teloblasts which give rise to ectodermal stem cells (NOPQ) and endodermal cells (E^D) in another closely related Tubificidae, *Tubifex tubifex* (Nakamoto *et al.,* 2000) (Chapter V – Figure 5). Endo- and ectoderm precursor genes, such as *Gt-otx* and *Ct-foxAB,* are expressed in these macromeres (Boyle *et al.,* 2014). Based on the arguments presented, it seems plausible that the inhibition of specific gene expression may therefore be due to the presence of symbionts. Speculation lies on gene silencing by phenomena such as environmental RNAi, which causes disturbances in differential gene expression through interaction with exogenous RNAs that may originate from bacterial symbionts inside the cocoons (for review see (Meng *et al.,* 2013)). In any case the active influence of symbionts in the core developmental processes of an animal host has large-scale implications for the evolution of all metazoans and should be grounds for future research in this system.

Within the bacterial market theory presented in chapter 1.1.2 the control of benefits gained by the bacterial microbe over the animal macrobe raises many questions

regarding the investment of resources to keep a mutualistic association viable in evolutionary terms. Further, the fundamental question arises if the influence of symbionts and the associated processes are reversible, provided of course these processes exist. Removal of a bacterial partner from the consortium may result in retarded growth as was documented for *Megacopta punctatissima* or reversely provide developmental conditions for proliferation of at least part of the digestive tract in the host. I propose experiments with antibiotic treatments and / or sterilisation of eggs shortly after oviposition to gain further insight into these hypotheses. Further, comparative transcriptomics of eggs from various incubation conditions and of different ontogenetic stages would shed light on the processes that may inhibit gut development (i.e. (Rosso *et al.,* 2009)).

6.3 Hypothetical evolutionary aspects of the *Olavius algarvensis* symbiosis

The evolution of stable vertical transmission modes is the result of both partners gaining a net benefit from each other (Kaltenpoth, 2009). The Hymenopteran European beewolf *Philanthus triangulum,* has developed a morphological and behavioural adaptation to bacterial smearing, whereby the parent wasps "coat" eggs with a *Streptomyces spp.* species from specialised glands in the antenna (Kaltenpoth *et al.,* 2005). Indeed behavioural adaptation for transmission appears to occur a number of times within the arthropods. For example, the Pentatomidae exhibit behaviour by which females excrete symbiont containing material during oviposition that is later fed upon by offspring to establish vertical transmission (Hosokawa *et al.,* 2013). The annelid gutless oligochaetes display an anatomical adaptation in the form of the genital pad to facilitate smearing. We hypothesise that this specialised anatomical feature may have been favoured by directional selection pressure, which evolved after the initial contact and establishment of the symbiosis.

The implications are that prior to the appearance of the genital pad the symbiosis was established with each generation anew by horizontal environmental uptake of symbionts. Individuals in a population that developed a genital pad, or a precursor of it, had selective advantages over worms that didn't. These individuals could ensure that symbionts were always transmitted to the next generation, irrelevant of potential environmental disturbance events or shifts in sediment bacterial communities. A strategy that provides additional nutritional benefits to the host increases overall fitness by providing more energy to increase the number of progeny that can be produced over a reproductive lifetime. For a species that has adopted an obligate nutritional dependency to its symbionts, a stable transmission mechanism must be in place to ensure that the next host generation is provided with the life essential nutrient providers. Further, transporting and successfully passing on a "package" of these life essential nutrient provides to each new host generation will facilitate colonization of habitats in which beneficial symbionts may not otherwise be present in the environment or posses the molecular tools required to establish the symbiosis.

If, however, a new potential symbiont is available in the environment that offers more benefit to the holobiont than an already established member, switching of microbial partners may result, as discussed in Chapter 1.1.2 of this thesis. Symbiont switching appears to have occurred on several occasions within the gutless oligochaetes and may help explain the large variance of symbiotic partners across the genus. Theory would predict that in combination with our results from Chapter V, symbiont switching is only possible during the reproductive cycle of the host, for once the symbiosis has been established the cuticle presents a formidable barrier for uptake of environmental bacteria. Indeed, other obligate symbiosis such as the catenulate flatworm genus *Paracatenula,* for example, do not display symbiont phylotype switching. On the contrary co-evolution

between host and symbiont was shown for this ancient symbiosis and the asexual reproductive strategy of worms may at least partially inhibit symbiont switching with the environment (Gruber-Vodicka *et al.,* 2011; Dirks *et al.,* 2012).

In the gutless oligochaetes vertically transmitted symbionts may play a regulative role for the horizontal transmission strategy by preventing infection of opportunistic, pathogenic or cheating environmental bacteria (Pradeu, 2011). Within the holobiont, competition between bacterial partners selects for the most optimised phylotypes for any given environment because individuals too removed from the Pareto-optimal, such as cheaters or pathogens, act antagonistic and will be removed by the community. As discussed in Chapter 1.1.2, individuals act in self-interest and not for the "greater good" per se. However, if a reduction of benefits is detected by the holobiont through the presence of an antagonistic element then exclusion strategies, if they are available, will be employed to regain benefits lost. On the contrary a new element that contributes positively to the overall net benefit will escape selection pressure because a Pareto-improvement will have been made providing increased benefit for every member of the holobiont in the trading relationship (chapter 1.1.2 – Figure 2).

O. algarvensis is nutritionally dependent on its symbiotic consortium and considering the presented model for Pareto-improvement will continuously strives to attain the most beneficial partners based on a self-interest for optimal exploitation of available nutrients. If for example an environmental bacterium possesses pathways to exploit a resource novel to the holobiont then it will readily be accepted into the symbiotic consortium because benefits are offered that increase net energy production over a partner that cannot exploit such a pathway. For an already established symbiont of the consortium the Red Queen hypothesis applies, whereby "it takes all the running you can do to keep in the same place", if it is not to be outcompeted. Mechanisms such as

horizontal gene transfer may help already established members of the symbiotic consortium keep their place in the holobiont by offering novel genetic potential, such as carbon monoxide or hydrogen oxidation pathway genes for example (Jain *et al.,* 2003).

This has long-term evolutionary implications because due to constant natural selection within the holobiont a host will be provided with a highly adapted symbiontic consortium for any given environment. Compared to strictly vertical transmitted bacteria, environmental bacteria carry a larger array of genetic potential to cope with higher selection pressure from competition and to better adapted to environmental change (see Chapter 1.1.5). The combination of horizontal uptake with symbiont switching therefore provides this genetic potential to the holobiont by "cherry-picking" the most profitable symbiont partners. A mixed strategy, as postulated for *O. algarvensis,* which primarily consists of vertical transmission events with occasional horizontal ones offers permanent nutrient providers and an adaptive capability to environmental changes or resource availability by switching of symbiotic partners. Once such an adaptive mechanism is in place a global radiation of the host genus is possible across many environmental conditions (Moran and Wernegreen, 2000).

6.4 Applicability of MiL-FISH for further studies of the *Olavius algarvensis* symbiosis

The application of MiL-FISH (Chapter III) and subsequent single cell genomics workflow (Chapter IV) for the *Olavius algarvensis* symbiosis can give additional hypothesis driven insights into the specific roles that individual symbionts play. Symbionts may express a variety of genetic potential or up-regulate specific metabolic pathways in different regions or life stages of the adult worm. For example, symbionts appear to up-regulate proliferation rates during the worm's reproductive period

to form the genital pad, symbiont metabolism appears to increase in the region of the worm where oocytes mature and symbionts may express genes with defensive potential to increase resistance to environmental bacteria before deposition of eggs into the sediment. To help answer some of these questions the workflow presented in Chapter IV can be applied. Here we present a combination of bacteria cell identification for all symbiont phylotypes, isolation of these cells via FACS, single cell genomics, sequencing and subsequent *in silico* analysis. However, FACS and DNA quality comparison had only been conduced on unfixed material in thus far, which may be impractical for most environmental samples because long-term storage without fixation causes damage to cells and therefore negatively influences DNA integrity. With this in mind additional experiments have been conducted to include Ethanol preserved and paraformaldehyde (PFA) fixed samples. Preliminary results of fixed cells after MiL-FISH indicate that the DNA yield was comparable to non-FISH control cells and that subsequent genome assembly proved unproblematic. These results have however not yet been compared to CARD-FISH cells and leaves room for additional analysis in the near future.

6.6 References - Chapter VI

Anderson S, Nilsson SI. (2001). Influence of pH and temperature on microbial activity, substrate availability of soil-solution bacteria and leaching of dissolved organic carbon in a mor humus. *Soil Biology and Biochemistry* **33**: 1181–1191.

Abe Y, Mishiro K, Takanashi M. (1995). Symbiont of Brown-Winged Green Bug, Plautia-Stali Scott. *Jpn J Appl Entomol Z* **39**: 109–115.

Arendt D, Technau U, Wittbrodt J. (2001). Evolution of the bilaterian larval foregut. *Nature* **409**: 81–85.

Beck F. (2002). Homeobox genes in gut development. *Gut* **51**: 450–454.

Bergter A, Beck LA, Paululat A. (2004). Embryonic development of the oligochaete Enchytraeus coronatus: an SEM and histological study of embryogenesis from one-cell

stage to hatching. *J Morphol* **261**: 26–42.

Boyle MJ, Yamaguchi E, Seaver EC. (2014). Molecular conservation of metazoan gut formation: evidence from expression of endomesoderm genes in Capitella teleta (Annelida). *Evodevo* **5**: 39.

Brusca R. Brusca, 2003: Invertebrates. 2nd Edition. Sinauer Associated, Inc.

Calleja ML, Marbà N, Duarte CM. (2007). The relationship between seagrass (Posidonia oceanica) decline and sulfide porewater concentration in carbonate sediments. *Estuarine* **73**: 583–588.

Dirks U, Gruber-Vodicka HR, Leisch N, Bulgheresi S, Egger B, Ladurner P, *et al.,* (2012). Bacterial Symbiosis Maintenance in the Asexually Reproducing and Regenerating Flatworm Paracatenula galateia Yu, J-KS (ed). *PLoS ONE* **7**: e34709–9.

Fukatsu T, Hosokawa T. (2002). Capsule-transmitted gut symbiotic bacterium of the Japanese common plataspid stinkbug, Megacopta punctatissima. *Appl Environ Microb* **68**: 389–396.

Gruber-Vodicka HR, Dirks U, Leisch N, Baranyi C, Stoecker K, Bulgheresi S, *et al.,* (2011). Paracatenula, an ancient symbiosis between thiotrophic Alphaproteobacteria and catenulid flatworms. *PNAS* **108**: 12078–12083.

Hamdoun A, Epel D. (2007). Embryo stability and vulnerability in an always changing world. *PNAS* **104**: 1745–1750.

Hasler-Sheetal H, Holmer M. (2015). Sulfide Intrusion and Detoxification in the Seagrass Zostera marina. *PLoS ONE* **10**: e0129136.

Hejnol A, Martín-Durán JM. (2015). Getting to the bottom of anal evolution. *Zol Anz* **256**: 61–74.

Hosokawa T, Kikuchi Y, Nikoh N, Shimada M, Fukatsu T. (2006). Strict host-symbiont cospeciation and reductive genome evolution in insect gut bacteria. *Plos Biol* **4**: e337.

Hosokawa T, Hironaka M, Inadomi K, Mukai H, Nikoh N, Fukatsu T. (2013). Diverse strategies for vertical symbiont transmission among subsocial stinkbugs. *PLoS ONE* **8**: e65081.

Jain R, Rivera MC, Moore JE, Lake JA. (2003). Horizontal gene transfer accelerates genome innovation and evolution. *Mol Biol Evol* **20**: 1598–1602.

Kaltenpoth M. (2009). Actinobacteria as mutualists: general healthcare for insects? *Trends Microbiol* **17**: 529–535.

Kaltenpoth M, Göttler W, Herzner G, Strohm E. (2005). Symbiotic bacteria protect wasp larvae from fungal infestation. *Curr Biol* **15**: 475–479.

Kleiner M, Wentrup C, Holler T, Lavik G, Harder J, Lott C, *et al.,* (2015). Use of carbon monoxide and hydrogen by a bacteria-animal symbiosis from seagrass sediments. *Environ Microbiol*. doi:10.1111/1462-2920.12912.

Kleiner M, Wentrup C, Lott C. (2012). Metaproteomics of a gutless marine worm and its symbiotic microbial community reveal unusual pathways for carbon and energy use. *PNAS*. **109:** E1173-E1182.

Meng LF, Chen L, Li ZY, Wu ZX, Shan G. (2013). Environmental RNA interference in animals. *Chinese Sci Bull* **58**: 4418–4425.

Moran NA, Wernegreen JJ. (2000). Lifestyle evolution in symbiotic bacteria: insights from genomics. *Trends Ecol Evol* **15**: 321–326.

Nakamoto A, Arai A, Shimizu T. (2000). Cell lineage analysis of pattern formation in the Tubifex embryo. II. Segmentation in the ectoderm. *Int J Dev Biol* **44**: 797–805.

Ogden J. (2006). Seagrasses: Biology, Ecology and Conservation. Springer Netherlands doi:10.1007/springerreference_205924.

Powell EN, Crenshaw MA, Rieger RM. (1979). Adaptations to sulfide in sulfide-system meiofauna. Endproducts of sulfide detoxification in three turbellarians and a gastrotrich. *Mar Ecol Prog Ser* **2:** 169-177

Pradeu T. (2011). A Mixed Self: The Role of Symbiosis in Development. *Biol Theory* **6**: 80–88.

Prado SS, Almeida R. (2009). Role of symbiotic gut bacteria in the development of Acrosternum hilare and Murgantia histrionica. *Entomol Exp Appl*. doi:10.1111/j.1570-7458.2009.00863.x.

Rosso MN, Jones JT, Abad P. (2009). RNAi and functional genomics in plant parasitic nematodes. *Annu Rev Phytopathol* **47**: 207-232

van der Heide T, Govers LL, de Fouw J, Olff H, van der Geest M, van Katwijk MM, *et al.,* (2012). A Three-Stage Symbiosis Forms the Foundation of Seagrass Ecosystems. *Science* **336**: 1432–1434.

Chapter VII

Appendix - A

Additional projects & collaborations

7.1 The smell of *Olavius algarvensis*

(M. Liebeke & M. Schimak)

During sample collection of the gutless marine oligochaete *Olavius algarvensis* a strong "cucumber" smell had been noticed from freshly collected worms when stressed during retrieval from the sediment (C. Lott, M. Kleiner, C. Wentrup, M. Schimak, M. Liebecke personal observation). To date the function and ecological relevance of emitting volatiles into the surrounding seawater by gutless oligochaetes is unclear. Similar to the response of worms to reduced substrates, as discussed in Chapter II, the strong "cucumber" smell may act as a chemical cue and influence worm distribution and ecology. It would seem likely that a volatile emitted by the holobiont serves as a chemical signal for communication between the environment or within the population. Chemical signals in the marine environment have been attributed to the "language of life in the sea" and act as communication signals between organisms for foraging strategies, feeding choices, commensal associations, selection of mates and habitats, competitive strategies, and transfer of energy within and amongst ecosystems (Hay, 2009). Additionally, signals may act as a warning to other members of a community in the presence of potential predators or as a repellent to predators themselves. A literature search revealed a likely candidate volatile that is commonly perceived as the typical "cucumber" smell and often used in the food industry (Forss *et al.,* 1962). 2-*trans,* 6-*cis*-nonadienal (Figure 1) has

been described to possess several biological functions including genotoxic effects (Dittberner *et al.,* 2002) and function as a sexual pheromone in the invertebrate fruit fly *Anastrepha striata* (Cruz-López *et al.,* 2015). Preliminary attempts to identify the volatile that gives *O. algarvensis* its distinctive smell were conducted with the intent to include the compound in additional experiments for Chapter II.

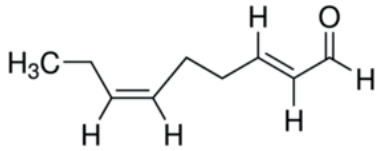

Figure 1: 2-*trans,* 6-*cis*-nonadienal

Experimental procedure and Preliminary results: In January 2014 four hundred freshly collected worms were placed into 0.5 ml seawater in gas chromatograph – mass spectrometer (GC-MS) glass vials. The vials were vortexed gently to stress worms and induce release of the volatile. Worms were removed and chloroform added to the seawater 1:1 and further vortexted. The volatile was released into the gaseous phase, and analysed in a GC-MS for identification. Analysis was performed on an Agilent 7890B gas chromatograph connected to an Agilent 5977A MSD. Samples were injected in splitless mode with an Agilent 7693 auto-sampler injector into deactivated splitless liners. Separation was done on an Agilent 30 m DB5-MS column with a 10 m DuraGuard column. Oven temperatures were set to 40°C for 1 min, then heated with 4°C min^{-1} up to 160°C, followed by 30°C min^{-1} to 280°C and a hold for 1 min at 280°C. As reference and for comparison chemically pure 2-*trans,* 6-*cis*-nonadienal was purchased (Sigma-Aldrich, St. Louis, MO, USA) and analysed by GC-MS as described above. Peaks were attained form both measured volatiles and compared (Figure 2) & (Figure 3).

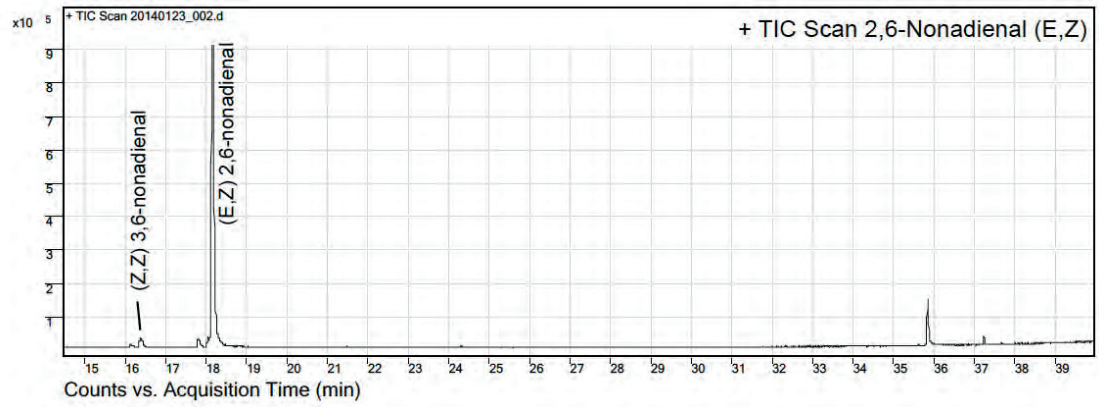

Figure 2: GC-MS measurement of laboratory standard 2-*trans,* 6-*cis*-nonadienal as reference.

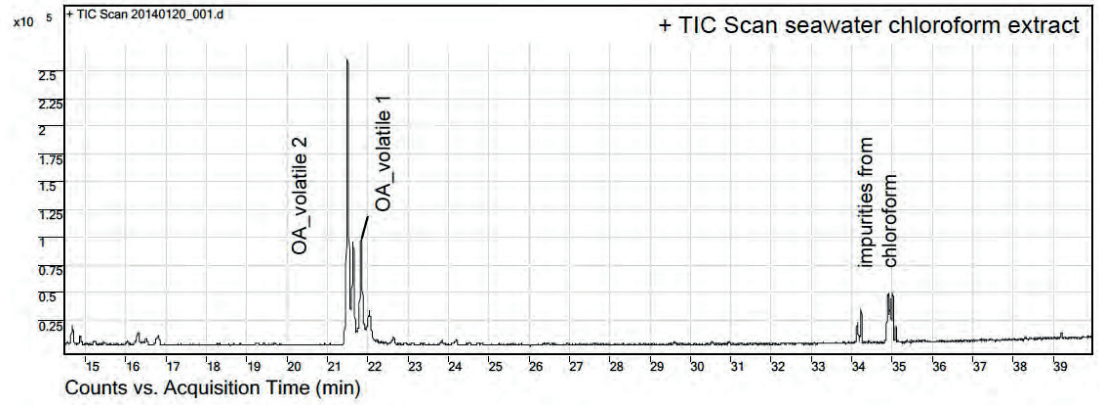

Figure 3: GC-MS measurement of volatile from the headspace of 400 *Olavius algarvensis* after agitation.

Conclusion: Although highly similar in chemical composition the two GC-MS plots do not match fully. The volatile of *Olavius algarvensis* is not the standard 2-*trans,* 6-*cis*-nonadienal. Comparison of the attained peaks to databases of known compounds resulted in two other potential candidate molecules, 2-Octyn-1-ol (Figure 4) and bicycle[6.1.0]non-4-ene-9-carbaldehyde (Figure 5) (GC-MS plots not shown). Both of these molecules however only showed an 80% and 70% coverage similarity respectively and therefore did not match to the volatile either. Our conclusion is that the volatile of *Olavius algarvensis* is most likely a stereoisomer of 2-*trans,* 6-*cis*-nonadienal and not currently available in any known databases.

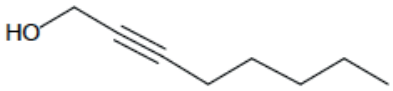

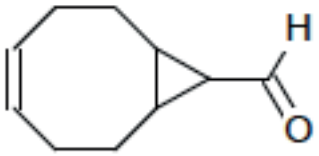

Figure 4: 2-Octyn-1-ol Figure5: bicycle[6.1.0]non-4-ene-9-carbaldehyde

(experiments and GC-MS analysis conducted by M. Liebeke)

7.2 Aquaristic and culturing of *Olavius algarvensis*

To date it has not been possible to culture gutless oligochaetes in aquaria. All experiments thus far have relied on *in situ* sampling of worms form the environment. A live-stock of animals for *ex situ* experiments and for the testing of hypothesis presented in this thesis would therefore be highly advantageous. Worms had been successfully transported and kept in 250 ml glass cylinder (Biometra, Göttingen, Germany) for a period of up to 6 months at room temperature (M. Kleiner unpublished data). Cylinders were filled with *in situ* sediment and seawater and worms introduced to them. Bottom sediment layers in the cylinders discoloured to a dark grey / black typical for reduced sediment layers after a short time period. Survival rates of worms varied and the population size declined over time (visual observation only). Cocoons were never retrieved and it was therefore assumed that worms did not reproduce within this experimental setup.

To ensure more stable conditions and to provide worms with reduced substrates for prolonged periods of time a new aquarium setup was conceived as follows: *In situ* sediment and seawater was transported to Bremen, Germany, to fill a 500 litre aquarium. The aquarium was filled ½ with sediment and ½ water to provide a representative

microbiota and chemical buffer for a seawater aquarium system. Water was oxygenated with standard aquarium air stones and circulated with two standard 50 litre/hour aquarium pumps (Figure 6). Three sealable cylinders, of three-litre volume each (Duran Group GmbH, Wertheim, Germany) were fitted with in- and outlet tubes to provide water exchange as described in Figure 7. In this manner individual cylinders can be connected in series or setup individually depending on the experimental requirements. Each cylinder contained a sediment layer of ~3 cm followed by a ~5 cm dead rhizome layer and toped up ~15 cm sediment. This emulated sediment layers found in the natural habitat and by decay of dead rhizome provided the reduced substrate H_2S, CO and H_2 for chemoautotrophic symbiont metabolism. The cylinders were setup in the 500 litre aquarium in series, connected to each other by silicone tubing, and water pumped through with a standard aquarium pump (Figure 6). Aquarium parameters were set to a constant temperature of 15° C and a salinity of 39 ‰. Roughly 50 worms were introduced into each cylinder on the 23rd of November 2011 and monitored weekly for a period of up to one year. On the 8th of December 2012, two of the three cylinders were opened and worms retrieved. A total of 33 worms were found in each cylinder of which 17 and 26 were white in colour respectively. The white colour of worms indicates that reduced sulphur species are available in the system and that symbionts are provided with conditions required to build up sulphur storage compounds. The remaining 16 and 7 worms, respectively, appeared to have spent prolonged periods of time in oxic zones depleting their sulphur storage compounds giving them a translucent / pale appearance. The discrepancy in physiological state of worms from the same cylinders cannot be explained because every zone in the aquarium was accessible for all individuals. Cocoons were not retrieved and the large volume of sediment in the cylinders made the search a fallible task. The third cylinder was not opened and kept in the aquarium for visual

control of worms for a further 6 months after which their presence could not be detected any longer.

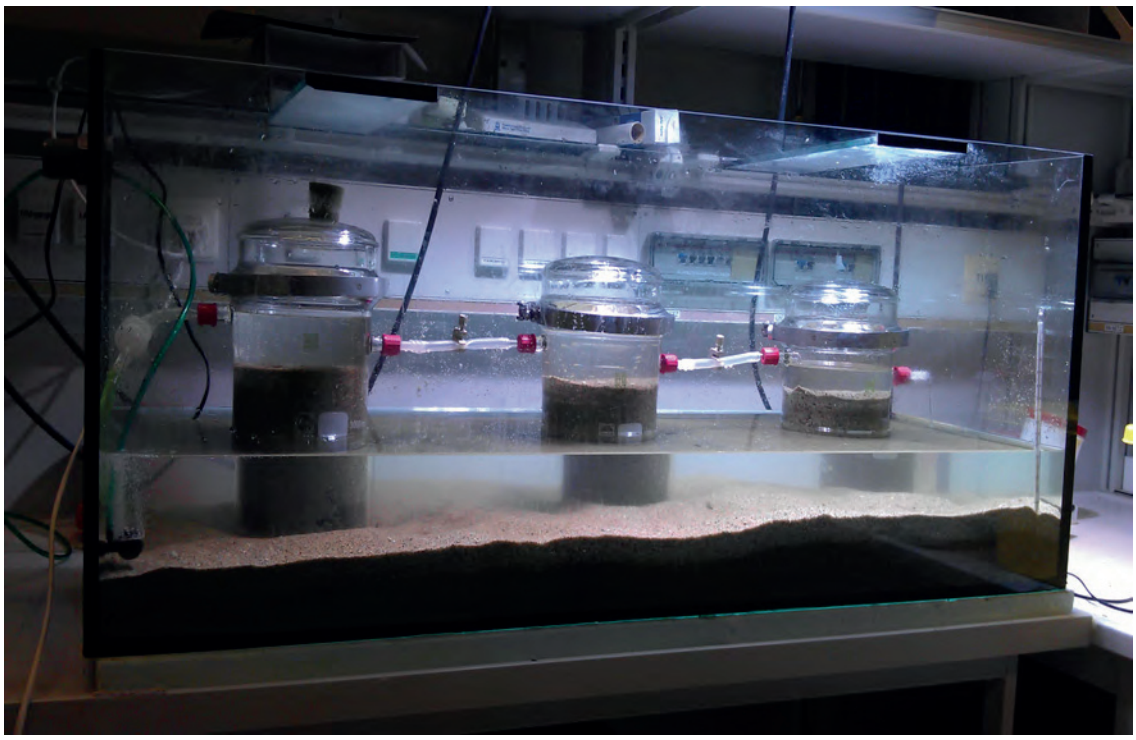

Figure 6: aquarium set up of the 500-litre aquarium with three serial connected modified cylinders as shown in Figure 7.

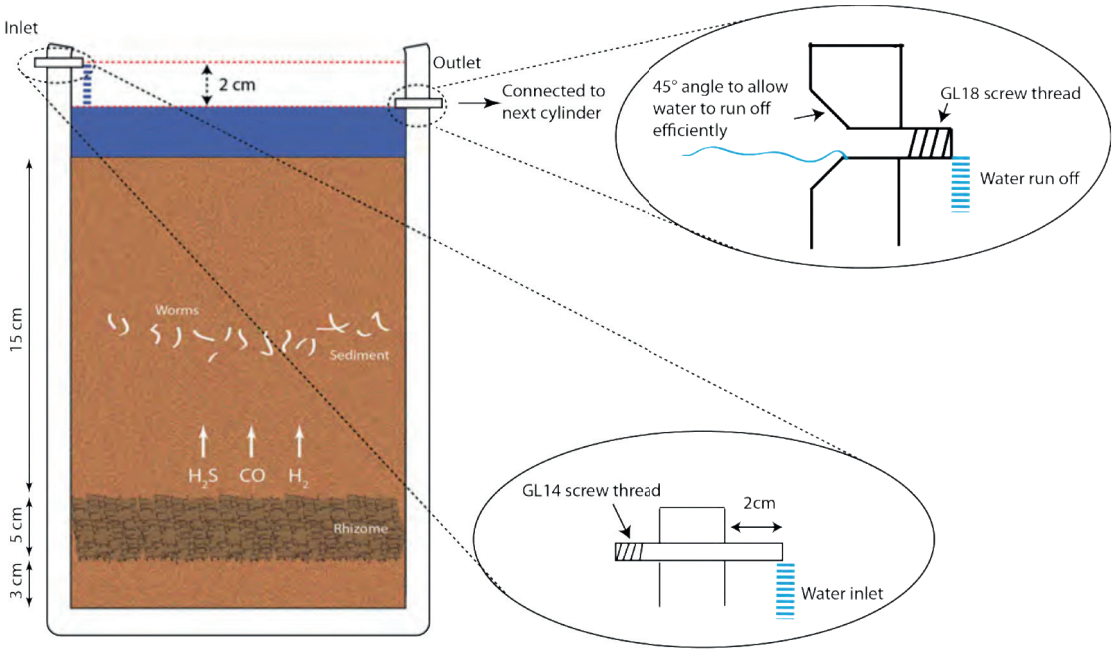

Figure 7: sediment zonation in the three litre flasks used to keep worms for a period up to 18 months.

Including dead rhizome into incubation cylinders to provide reduced substrate proved viable in keeping worms over prolonged periods of time. With this concept an additional setup for worm cultivation and egg retrieval was conceived. The primary aim was to eliminate difficulties associated with egg retrieval in the larger cylinders. Three 250 ml Biometra cylinders, as used by M. Kleiner, were connected in series, filled with rhizome and sediment as described above and kept in the large 500 litre aquarium (Figure 8). Silicone tubing, attached to a water pump, connected the three cylinders in series supplied each one with water from the previous. Roughly 50 worms were introduced into each cylinder and visually controlled for a period of up to 9 months during which worms were observed in the smaller cylinders. Unfortunately however, due to the time constraints during this PhD, cylinders were not opened and analysed for presence of worms or eggs.

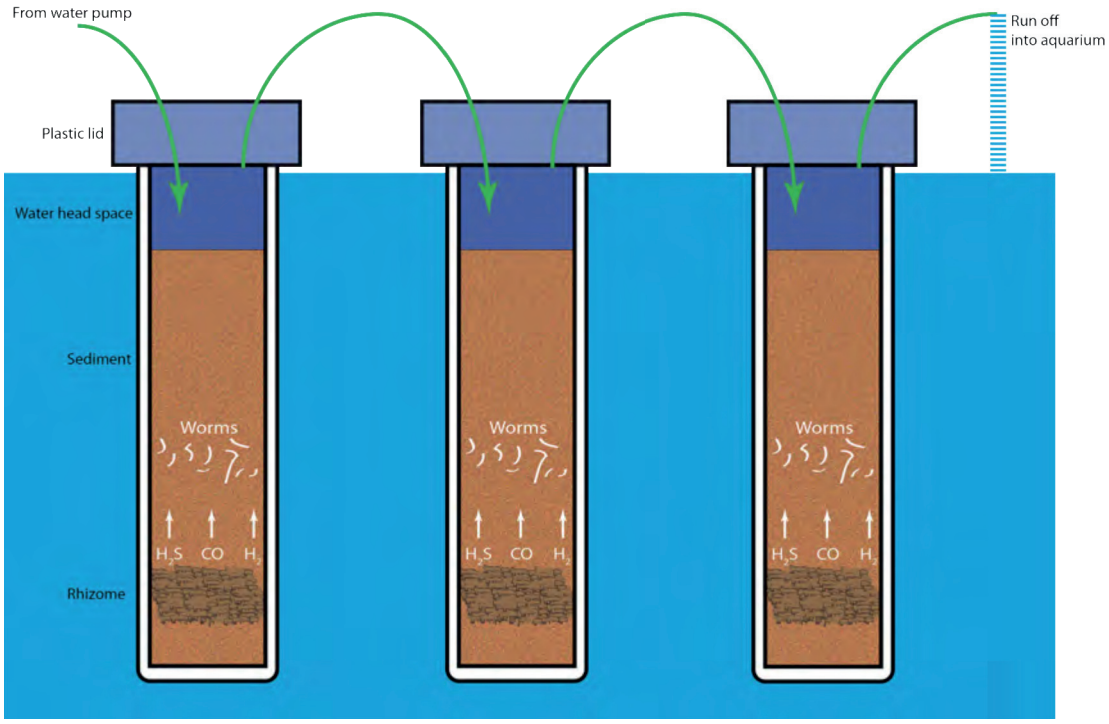

Figure 8: setup of three 250 ml Biometra flasks connected to each other by water flow via silicone tubes.

Conclusion and Outlook: Worms were kept in the presented aquarium setup for a time period of up to 18 months. The life expectancy of worms in the environment is unknown but based on the apparent low number of offspring per reproductive season it would seem plausible that worms live for several years. The age of worms introduced into the aquarium could not be determined and it is therefore difficult to conclude the efficiency of the setup for the overall keeping and potential culturing of worms. Having found white worms after 12 months however, does indicate that at least a large fraction of the introduced population remained in a good physiological condition for this time period. For cultivation of worms and successful cocoon retrieval I propose the second setup using the 250 ml cylinders (Figure 8). In this setup conditions are given to provide the required substrates for symbiont metabolism and in addition, taking lessons learnt from field experiments into consideration (Chapter V), I propose the introduction of a constant water temperature at 25°C to induce mating. It is known from several invertebrates, especially ones that inhabit temperate zones, that reproduction is triggered by temperature cues from the environment (i.e. (Hotchkiss *et al.,* 2008)). As described in this thesis egg retrieval can be simplified by using pre-sieved sand grains between of 400 and 600 µm size.

7.3 Scanning electron microscopy (SEM) of *Olavius algarvensis*

Preliminary scanning electron microscopy (Quanta 250 FEG, FEI, Oregon, USA) analysis of *Olavius algarvensis* revealed highly organized pores situated on only one of the seven annuli that comprise each worm segment at the anterior of the worm. Based on their location and alignment to the male chaetae, these pores may play a role in the reproduction of the worms. The diameter of pores (Figure 9 c) and chaeta (Figure 9 d) measure 2.5 µm. We count 8 penal chaetae and 8 – 9 pore openings arranged longitudinally. I conclude that the pores depicted in Figure 9 c are the openings of the spermatheca. The most likely mechanism for copulation in *O. algarvensis* is therefore an

interlocking of chaetae into the pores followed by release of sperm from the male pore (Figure 9 e) Although not conclusive, these findings pave the way for further transmission electron microscopy (TEM) studies to resolve the identity of the pores and the precise reproductive anatomy of *Olavius algarvensis.*

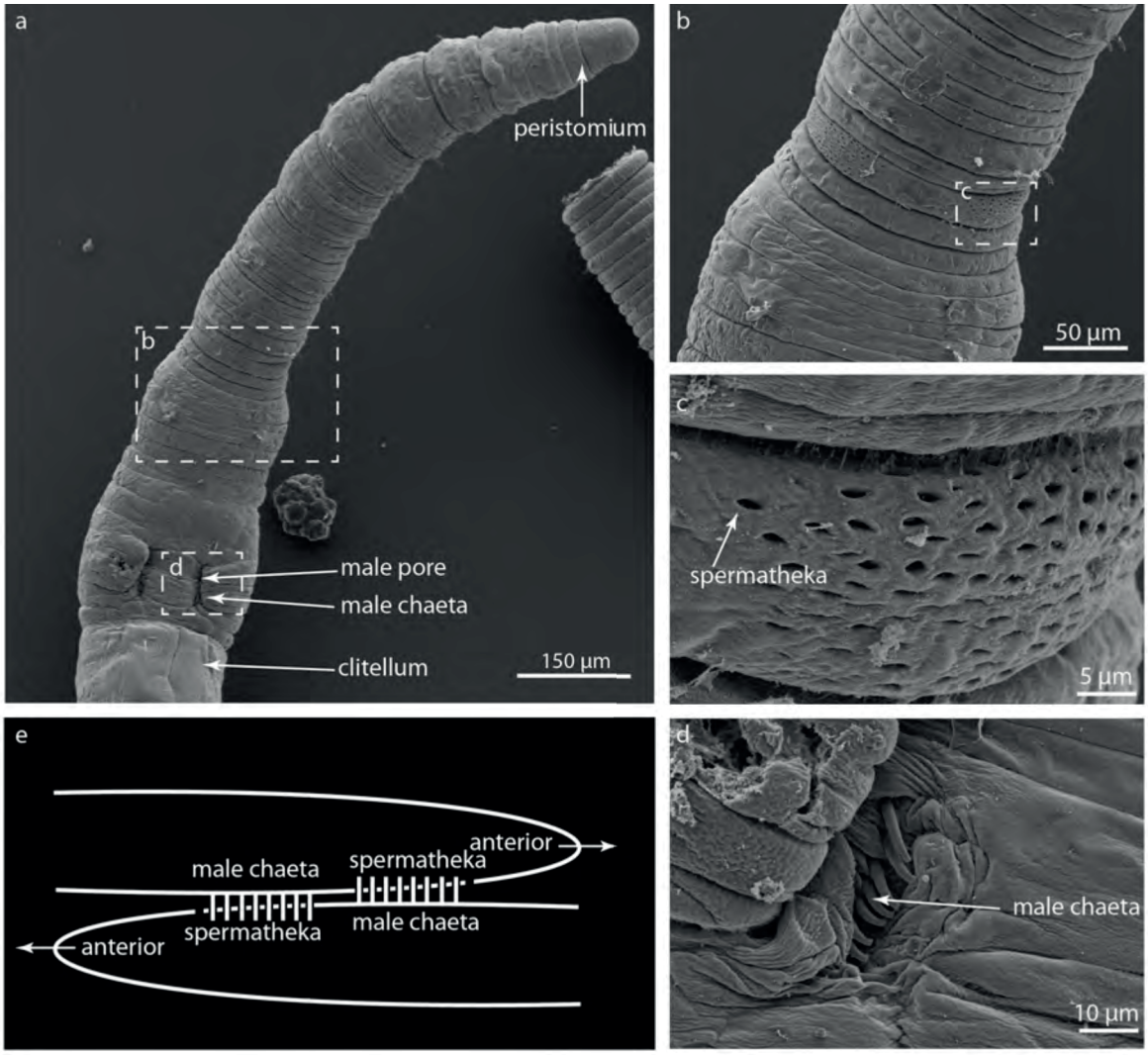

Figure 9: SEM of *Olavius algarvensis* anterior. a) overview of anterior ventral side of the worm, grid square are regions of interest depicted in b & d. b) anterior, ventral side of worm, each worm segment is comprised of 6-7 annuli. Spermatheca opening highly organised to the left and right ventral side of the worm aligned to the location of the male chaeta. Grid square depicts region shown in c. c) spermatheca openings found on a single annual anterior to male chaetae. Width of pore 2.5 µm. 8 – 9 pores are counted in a longitudinally from anterior to posterior. d) male chaeta and male pore. Chaetae protrude during copulation. A total of 8 chaeta are found (also see Chapter 1.3.7.2, Figure 8). e) Schematic of worm copulation. Male chaetae align and penetrate into one of the longitudinal rows of the spermatheca openings interlocking the two copulating worms. This ensures that sperm can pass from the male pore into the receiving spermatheca. Schematic not to scale.

7.4 µCT of *Olavius algarvensis* eggs

To analyse various developmental stages for symbiont localisation to the developing embryo eggs were embedded and sectioned as described in Chapter V. This process is very time consuming however, and the exact developmental stage of a specimen cannot be determined until microscopic analysis of the sections is completed. Working with a large amount of specimens to cover several developmental stages required light microscopy to estimate which stage embryos are in. This is however not very accurate and to further streamline the identification process for pre-selection of eggs a non-destructive analytical method was require. Confocal laser scanning microscopy (CLSM) did not yield the desired results because the laser could not penetrate the cocoon and embryo sufficiently to produce a 3D reconstruction. Computer tomography (CT) uses X-rays to make "optical sections" through an object in a non-invasive manner. Physical density differences of ~1 % can be enough to distinguish between tissues and create an image. In November 2012 early stage eggs were taken to the Max Planck Institute for Evolutionary Anthropology in Leipzig, Germany to be analysed by µCT. The resulting images however were unsatisfactory because embryos could not be clearly defined to a cellular level and early developmental stages not determined. This was due to density differences between embryo and egg albumen being lower than is required for CT imaging. In a second attempt a juvenile worm inside a cocoon was stained with osmium tetroxide (OsO_4) to increase density-based contrast of the specimen (CT scans made at the Technische Universität München, Germany, by Benedikt Geier). Image quality was improved, however not at a resolution that enabled identification of individual cells (Figure 10). Early developmental stages of gutless oligochaete embryos can therefore not be resolved by application of µCT. Further the use of a contrasting agent such as OsO_4

prohibits subsequent FISH analysis, rendering this approach inappropriate for the study presented in Chapter V.

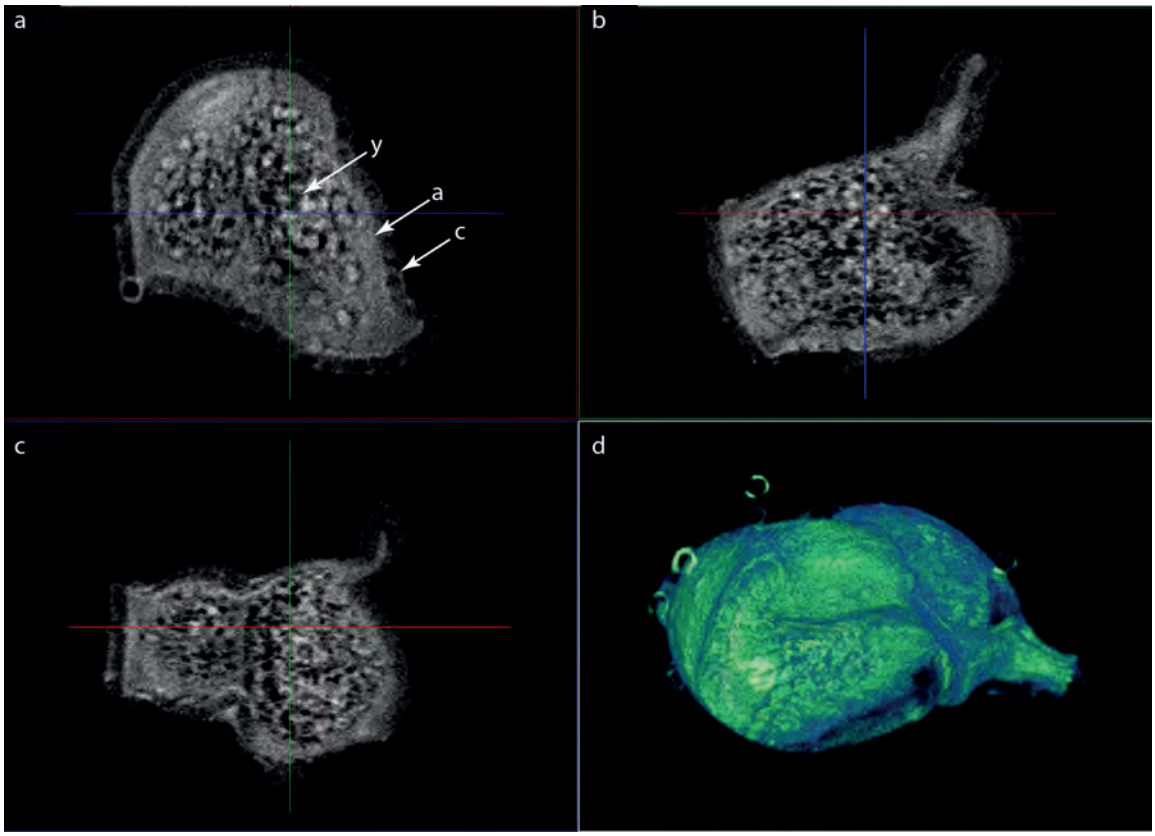

Figure 10: µCT scans of a juvenile worm in its cocoon. Panels a, b and c show single scans of various angles through the egg. Egg yolk in the coelomate cavity (y), egg albumen (a) and the cocoon (c) could be resolved. d) shows a 3D reconstruction of all scans. The crescent shaped juvenile can be seen inside the cocoon.

7.5 Correlative MiL-FISH and nanoSIMS signal co-localisation

During nanoSIMS data analysis in Chapter V difficulty arose in cell identification of MiL-FISH images and correlation to signal from nanoSIMS images. The challenge lies in finding sufficient anchor points for the alignment (registration) of both images to each other because not all cells yield a detectable signal i.e. a γ cell will not be visible in a MiL-FISH image if a δ specific probe was applied, it will however be visible in the nanoSIMS image. A solution was conceived using Fiji (Schindelin *et al.,* 2012) and the RG2B colocalisation plugin (found at

http://rsb.info.nih.gov/ij/plugins/rg2bcolocalization.html). Images are converted to the same pixel aspect ratio, then to RGB so that MiL-FISH signals are allocated one colour, nanoSIMS signals another and the co-localisation signal a third. In this manner any pixel that contains both MiL-FISH and nanoSIMS signal is identified and used to compile a co-localisation image over the data set (Figure 11). This approach proved useful for images on which registration did not work sufficiently and will be applied to the data set presented in Chapter V in the near future.

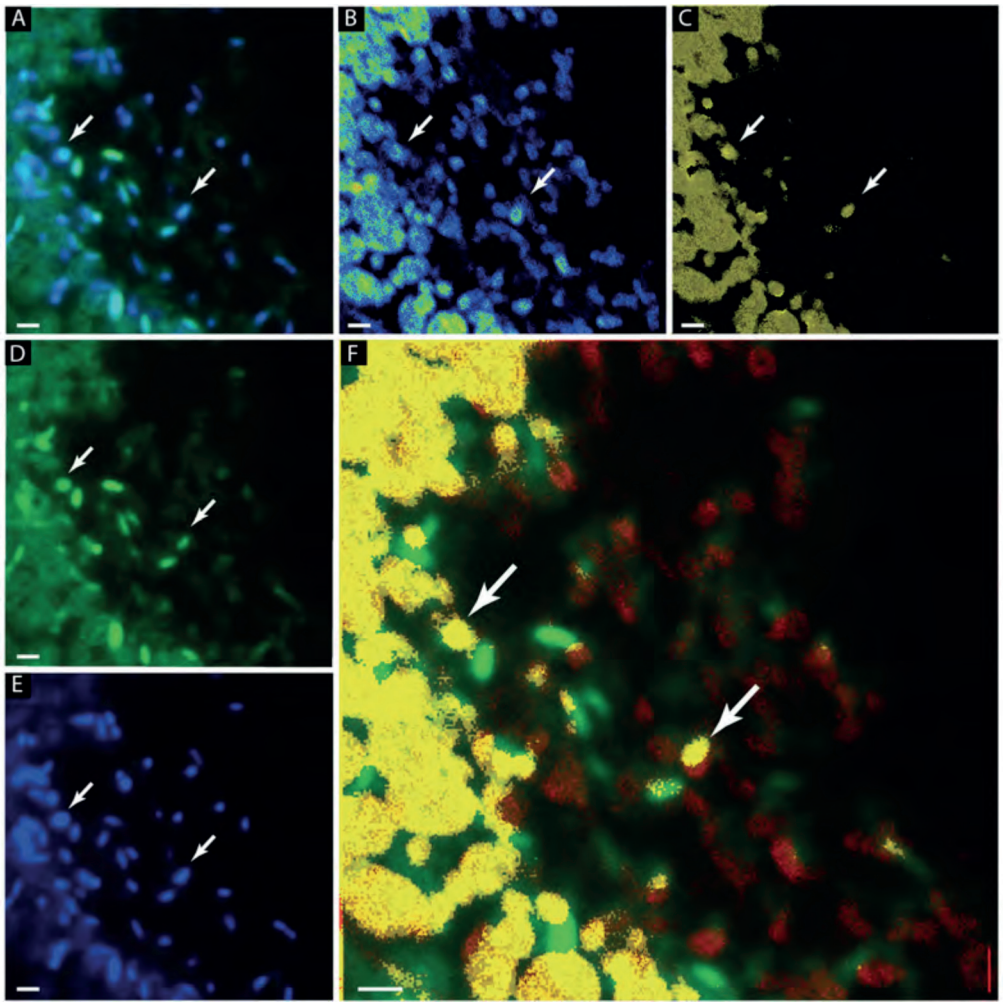

Figure 11: correlative MiL-FISH and nanoSIMS of mid developmental stage egg (chapter V – Figure 6 a) from ^{15}N-ammonium incubation. A) MiL-FISH targeting δ-proteobacteria with the general DSS658 probe & DAPI, B) ^{15}N nanoSIMS signal. Note: this image does not show $^{15}N^{12}C/^{14}N^{12}C$ ratio and does therefore not show enrichment of cells, C) co-localisation of MiL-FISH & nanoSIMS, D) MiL-FISH only, E) DAPI only and F) composite of B, C and D. White arrows indicate positively hybridised cells and co-localisation signal. Scale bar: 1 µm.

Appendix - B

Author contributions

7.6 - (Wentrup *et al.*, 2014)

Forever competent: deep-sea bivalves are colonized by their chemosynthetic symbionts throughout their lifetime.

Cecilia Wentrup[1], Annelie Wendeberg[2], Mario Schimak[1], Christian Borowski[1] and Nicole Dubilier[1]

[1]*Department of Symbiosis, Max Planck Institute for Marine Microbiology, Celsiusstrasse 1, Bremen 28359,Germany.*
[2]*Department of Environmental Microbiology, UFZ, Helmholtz Centre for Environmental Research, Permoserstrasse 15, Leipzig 04318, Germany.*

Abstract:
Symbiotic bivalves at hydrothermal vents and cold seeps host chemosynthetic bacteria intracellularly in gill cells. In bivalves, the gills grow continuously throughout their lifetime by forming new filaments. We examined how newly developed gill tissues are colonized in bivalves with horizontal and vertical symbiont transmission (*Bathymodiolus* mussels versus a vesicoymid clam) using fluorescence in situ hybridization and transmission electron microscopy. Symbiont colonization was similar in mussels and clams and was independent of the transmission modes. Symbionts were absent in the growth zones of the gills, indicating that symbionts colonize newly formed gill filaments *de novo* after they are formed and that gill colonization is a continuous process throughout the host's lifetime. Symbiont abundance and distribution suggested that colonization is shaped by the developmental stage of host cells. Selfinfection, in which new gill cells are colonized by symbionts from ontogenetically older gill tissues, may also play a role. In mussels, symbiont infection led to changes in gill cell structure similar to those described from other epithelial cells infected by intracellular pathogens, such as the loss of microvilli. A better understanding of the factors that affect symbiont colonization of bivalve gills could provide new insights into interactions between intracellular bacteria and epithelial tissues.

Published in: Environmental Microbiology (2014), doi:10.1111/1462-2920.12597

Contribution: transmission electron microscopy

7.7 - (Klose *et al.*, 2015)

Endosymbionts escape dead hydrothermal vent tubeworms to enrich the free-living population

Julia Klose[a], Martin F. Polz[b], Michael Wagner[c], Mario P. Schimak[a,d], Sabine Gollner[a,e,f], and Monika Bright[a,1]

[a]Department of Limnology and Bio-Oceanography, University of Vienna, A-1090 Vienna, Austria; [b]Parsons Laboratory for Environmental Science and Engineering, Department of Civil and Environmental Engineering, Massachusetts Institute of Technology, Cambridge, MA 02139; [c]Department of Microbiology and Ecosystem Science, University of Vienna, A-1090 Vienna, Austria; [d]Max Planck Institute for Marine Microbiology, 28359 Bremen, Germany; [e]Department of Ecosystem Studies, Royal Netherlands Institute for Sea Research (NIOZ), 4401 NT Yerseke, The Netherlands; and [f]German Center for Marine Biodiversity Research, Senckenberg am Meer, 26382 Wilhelmshaven, Germany

Edited by Margaret J. McFall-Ngai, University of Hawaii at Manoa, Honolulu, HI, and approved July 15, 2015 (received for review January 19, 2015)

Theory predicts that horizontal acquisition of symbionts by plants and animals must be coupled to release and limited dispersal of symbionts for intergenerational persistence of mutualisms. For deep-sea hydrothermal vent tubeworms (Vestimentifera, Siboglinidae), it has been demonstrated that a few symbiotic bacteria infect aposymbiotic host larvae and grow in a newly formed organ, the trophosome. However, whether viable symbionts can be released to augment environmental populations has been doubtful, because (i) the adult worms lack obvious openings and (ii) the vast majority of symbionts has been regarded as terminally differentiated. Here we show experimentally that symbionts rapidly escape their hosts upon death and recruit to surfaces where they proliferate. Estimating symbiont release from our experiments taken together with well known tubeworm density ranges, we suggest a few million to 1.5 billion symbionts seeding the environment upon death of a tubeworm clump. In situ observations show that such clumps have rapid turnover, suggesting that release of large numbers of symbionts may ensure effective dispersal to new sites followed by active larval colonization. Moreover, release of symbionts might enable adaptations that evolve within host individuals to spread within host populations and possibly to new environments.

Published in: Proceedings to the National Academy of Science (PNAS). www.pnas.org/cgi/doi/10.1073/pnas.1501160112

Contribution: experimental fieldwork

7.8 References - Chapter VII

Cruz-López L, Malo EA, Rojas JC. (2015). Sex Pheromone of Anastrepha striata. *J Chem Ecol* **41**: 458–464.

Dittberner U, Eisenbrand G, Zankl H. (2002). Genotoxic effects of the alpha, beta-unsaturated aldehydes 2-trans-butenal, 2-trans-hexenal and 2-trans, 6-cis-nonadienal. *Mut Res* **335**: 1–7.

Forss DA, Dunstone EA, Ramshaw EH. (1962). The flavor of cucumbers. *J Food Sci.***27** (1): 90-93.

Hay ME. (2009). Marine chemical ecology: chemical signals and cues structure marine populations, communities, and ecosystems. *Ann Rev Mar Sci* **1**: 193–212.

Hotchkiss AK, Sternberg RM, LeBlanc GA. (2008). Environmental cues trigger seasonal regression of primary and accessory sex organs of the mud snail, Ilyanassa obsoleta. *J Mollus Stud* **74**: 301–303.

Klose J, Polz MF, Wagner M, Schimak MP, Gollner S, Bright M. (2015). Endosymbionts escape dead hydrothermal vent tubeworms to enrich the free-living population. *PNAS* **112**: 11300–11305.

Schindelin J, Arganda-Carreras I, Frise E, Kaynig V, Longair M, Pietzsch T, *et al.,* (2012). Fiji: an open-source platform for biological-image analysis. *Nat Meth* **9**: 676–682.

Wentrup C, Wendeberg A, Schimak M, Borowski C, Dubilier N. (2014). Forever competent: deep‐sea bivalves are colonized by their chemosynthetic symbionts throughout their lifetime. *Environ Microbiol* **16**: 3699–3713.

Appendix – C

Digital Supplement

The digital supplements described here are found on the CD attached to this thesis:

7.9 Digital files to Chapter II

- Folder named Chapter_II_ImageJ_Java_Scripts contains Java scripts for use in ImageJ as described in Chapter II. Scripts were applied to Raw image data sets of worm migratory behaviour and used to produce Z-stack summation and 3D projection images (i.e. Chapter II – Figure 3 c & d)
- Folder named Chapter_II_Phython_Scripts contains Python scripts used to produce statistical analysis data of worm distribution in the aquaria. Scripts were applied to Raw image files of worm migration. The result of the scripts is shown in Chapter II – Figure 3 a & b. Additional algorithms for worm tracking and removal of disturbance events as described in Chapter II are included. Please note several scripts are still under construction and not fully functional at the time of printing this thesis.
- The file Chapter_II_Phython_script demonstrates the application of the included Python scripts on a Raw image data set to produce data analysis as shown in Chapter II – Figure 3 a & b. Please note disturbance events have not been removed from this demonstration. Video has been accelerated and is not in real-time.
- Folder Chapter_II_Figure_Files contains all images form Chapter II in digital format for a higher resolution than the printable version.

7.10 Digital files to Chapter V

- Video file Chapter_V_ SI_Video_1_Rotating_Blastula shows an egg of *Olavius algarvensis* in a blastula like developmental stage. This is one of several specimen that were observed in this developmental stage for up to 11 days prior to incubation in fluctuating oxic / anoxic conditions. Scale bar not available. Video played at double speed.
- Video file Chapter_V_SI_Video_2_Juvenile_Worm shows the same specimen from Chapter_V_ SI_Video_1_Rotating_Blastula after three days in fluctuating oxic / anoxic conditions. A vermiform juvenile worm is seen inside the cocoon. Scale bar not available. Video played at double speed.
- Folder Chapter_V_Figure_Files contains all images form Chapter II in digital format for a higher resolution than the printable version.

Chapter VIII

Acknowledgments

I want to thank a number of people on both a professional and personal level without whom this thesis would not have been possible:

Prof. Dr. Nicole Dubilier - for accepting me in her workgroup and offering me the opportunity to conduct research on this fascinating biological system. The continuing freedom to allow me to follow up on my ideas, no matter how unorthodox these may have been, has over the years made the synthesis of this thesis possible

Prof. Dr. Monika Bright – for kindly accepting to evaluate this thesis and for the continuing support over the years.

Prof. Dr. Michael Friedrich – for kindly accepting to act as a member of my examination board.

Prof. Dr. Andreas Schramm - for kindly accepting to act as a member of my examination board and for the many thought provoking discussions and useful input over the course of this PhD.

Burak Avci & Andreas Sichert – for kindly serving as student representatives of the examining board.

Dr. Bernhard Fuchs – for the exciting collaboration, kind-hearted supervision and for opening up the fascinating world of microbial ecology and molecular methods to me.

Dr. Alexander Gruhl – for great guidance, advice, fruitful discussions and input into my work. Your contribution to the last stages of this thesis was invaluable and made me consider many things in a new light.

Dr. Manuel Liebecke – for offering support, supervision and advice during many stages of this work. Your acceptance of new ideas and hypothesis as well as your advice on how to present and logically argue these gave me confidence and security in knowing that "I was at least doing something right".

Silke Wetzel – for great technical support, indispensible discussions and assistance in both the field and laboratory. Thank you for your great advice over the years and your help in streamlining many of my workflows through your exceptional technical competence.

Dr. Manuel Kleiner – for not only being great advisor and inspiration but also for always taking the time to help and listen both work and non-work related. Your approach to science is something that is energising and admirable.

Dr. Cecilia Wentrup – for being of invaluable help at the beginning of this thesis and continually offering your experiences, insights and support for the remainder of it.

Dr. Miriam Weber & Christian Lott & all at the **HYDRA** institute – for exceptional help with on site field and laboratory work. Your "out of the box thinking" and resolving of technical and experimental challenges was invaluable. Thank you for the hospitable and accommodating atmosphere during my prolonged field trips and for the possibility to test various ideas *in situ*. Your "anything is possible" attitude made this work possible.

Adrien "Frenchie" Assie & Dr. Nicolaus Leisch – for being there from the beginning, through all "the good, the bad and the ugly" times, and always adding a pinch of humour, whisky and bad movies to them.

Juliane "Spotzl" Wippler & Oliver "chewing gum" Jäckle – for being a great office mates, friends and scientific sparing partners. Keep it up and I'll come visit your lab on Hawaii in a few years.

Dimitri, Sa(h)ra, Brandon, Liz, Judith, Rahel, Benedikt, Miriam, Miguel, Jimena, Giorgito, Niels & Cameron – for great times, many laughs and continuing friendship over the years.

Margit Manneh –for the continuing moral support. Thank you for all the encouragement in anything I did over the years.

To all members of the **Symbiosis Department** at the Max Planck Institute for marine Microbiology in Bremen, Germany, and all students of the **Symbiomics** network worldwide. Thank you for all the fun times, valuable input and comradery.

To all the **co-authors and collaborators** who contributed to the projects – thank you for the essential technical and scientific input and extensive help with the various aspects of this work. I was always met with a warm welcome and an open ear.

To the Marie Curie initial training network "**Symbiomics**" and the **Max Planck Society** for funding of this research.

Mario Philip Schimak
Max Planck Institut für Marine Mikrobiologie
Celsiusstr. 1
28359 Bremen

Erklärung

Gemäß § 6 (5) Promotionsordnung erkläre ich hiermit, dass ich die Doktorarbeit mit dem Titel:

Transmission of obligate bacterial symbionts in the gutless oligochaete *Olavius algarvensis*

selbständig verfasst und geschrieben habe und nur die von mir angegebenen Quellen und Hilfsmittel verwendet habe. Die den benutzten Werken wörtlich oder inhaltlich entnommenen Stellen habe ich als solche kenntlich gemacht.

Ebenfalls erkläre ich hiermit, dass es sich bei den von mir abgegebenen Arbeiten um drei identische Exemplare handelt.

Mario Philip Schimak